

GENETICALLY RESTRICTED METABOLIC LABELING IN *DANIO RERIO*,
A SIMPLE VERTEBRATE CAPABLE OF
PROTEIN SYNTHESIS-DEPENDENT MEMORY FORMATION.

Thesis by

Flora Irma Hinz

In Partial Fulfillment of the Requirements

for the Degree of

Doctor of Philosophy



California Institute of Technology

Pasadena, California

2012

(Defended April 5, 2012)

© 2012

Flora Irma Hinz

All Rights Reserved

ACKNOWLEDGEMENTS

First and foremost, I would like to thank my advisor Erin Schuman for her unwavering support over the past five years and two continents. She has inspired me with her infectious enthusiasm for science, and I am extremely grateful for her willingness to support my ambitious project (new model organism and all) and her critical guidance of my thesis work. I couldn't have asked for a better advisor.

Next, I would like to thank the current and past members of my thesis committee, Gilles Laurent, Scott Fraser, David Prober and Michael Dickinson. My meetings with them helped focus my thesis work and I very much appreciate their extra effort to advise me throughout my time on 'detached duty'. Furthermore, I would like to thank David Tirrell and John Ngo for their advice regarding all things 'click chemistry', Sean Megason and Le Trinh for their patience while teaching me the basics of zebrafish genetics and Julian Langer for his efforts to explain the fundamentals of mass spectroscopy and his help running preliminary samples.

The guidance, advice and friendship of Schuman lab members both in Pasadena and in Frankfurt have been absolutely indispensable to my thesis work and my happiness during my graduate career. In particular, I would like to thank Daniela Dieterich and Jennifer Hodas for guiding me through my first BONCAT and FUNCAT experiments, their patience with my repeated questions concerning the details of protocols even from afar and their mentoring during my time at Caltech. Mark Aizenberg, with his dry sense of humor, his creativity and his indefatigable efforts to get those darn larvae to learn something (anything!), is an absolute inspiration without whom Chapter IV of this thesis

would not exist. Furthermore, I am indebted to Georgi Tushev for writing most of the Matlab scripts used to acquire and analyze the behavioral data, usually at a moments' notice, to Iván Cajigas for cloning advice, to Sakshi Garg for software advice and to Susanne tom Dieck for her optimism and for ensuring that the lab keeps running smoothly on a daily basis. The fact that Stefanie Bunse can tell you how transient transgenesis using a UAS::EGFP responder construct injected into a Gal4 driver line embryo can lead to mosaic fluorescence in larval zebrafish without ever having touched a fish indicates just how essential she has been as a sounding board, cheerleader and, most importantly, great friend.

Last, but certainly not least, I would like to thank my family, who have been unbelievably supportive, each in their own way, for as long as I can remember. The unquestioning faith they instilled in me that I can achieve anything I set my mind to gave me the confidence necessary to make it through graduate school. So I would like to conclude by thanking my parents, Henriette and Volker, for gently pushing me by asking every week how my experiments were coming along and James Karnesky, for understanding and not inquiring once.

ABSTRACT

Determining which neural circuits and proteins are involved in encoding memories is a central goal in neuroscience. Protein expression in the nervous system is known to undergo regulated changes in response to changes in behavioral states, in particular long-term memory formation. In this study we developed tools to investigate protein synthesis in an intact organism, the larval zebrafish, capable of simple learning behavior. Methods have recently been developed (BONCAT and FUNCAT), which introduce noncanonical amino acids bearing small bioorthogonal functional groups into proteins using the cells' own translational machinery. Using the selective 'click reaction', this allows for the identification and visualization of newly synthesized proteins *in vitro*.

Here we demonstrate that noncanonical amino acid labeling can be achieved *in vivo* in the larval zebrafish. We show that azidohomoalanine is metabolically incorporated into newly synthesized proteins, in a time- and concentration-dependent manner, but has no apparent toxic effect and does not influence simple behaviors such as spontaneous swimming and escape responses. This enables fluorescent labeling of newly synthesized proteins in whole mount larval zebrafish. Furthermore, we demonstrate that genetically restricted expression of a mutant methionyl-tRNA synthetase permits cell-specific metabolic labeling with the larger noncanonical amino acid, azidonorleucine, both *in vitro* and *in vivo*. Finally, we present an associative conditioning paradigm for larval zebrafish. During a three-hour training period, 6-8dpf larvae learn to associate the social reward of visual access to a group of conspecifics with a dark environment. The memory formed during this place-conditioning paradigm undergoes rapid extinction, but

is extremely stable, lasting for up to 36h. Furthermore, memory formation is both protein synthesis- and partially NMDAR-dependent. Together, the techniques developed in this study will enable the investigation of protein synthesis during long-term memory formation in the larval zebrafish.

TABLE OF CONTENTS

ACKNOWLEDGEMENTS	iii
ABSTRACT	v
TABLE OF CONTENTS	vii
LIST OF ILLUSTRATIONS	x
ABBREVIATIONS USED	xii
<i>Chapter I</i>	1
INTRODUCTION.....	1
The role of protein synthesis in long-term memory formation.....	2
Bioorthogonal chemistry.....	9
The larval zebrafish as a model organism.....	15
<i>Chapter II</i>	24
NONCANONICAL AMINO ACID LABELING <i>IN VIVO</i> TO VISUALIZE AND AFFINITY PURIFY NEWLY SYNTHESIZED PROTEINS IN LARVAL ZEBRAFISH..	24
Introduction.....	25
Application of BONCAT and FUNCAT techniques to larval zebrafish	27
Incubation with AHA is not toxic to larval zebrafish and does not alter simple behaviors.....	29
AHA is metabolically incorporated in larval zebrafish	33
Newly synthesized proteins can be visualized in whole-mount larval zebrafish.....	38
FUNCAT and BONCAT can be used to detect changes in protein synthesis with chemical stimulation in larval zebrafish	43
Discussion.....	45
Methods.....	47

<i>Chapter III</i>	52
LABELING NEWLY SYNTHESIZED PROTEINS IN GENETICALLY SPECIFIED LARVAL ZEBRAFISH CELL POPULATIONS MEDIATED BY SELECTIVE EXPRESSION OF A MUTANT MetRS	52
Introduction.....	53
Cell-specific metabolic labeling of a multicellular organism, the larval zebrafish	56
Zebrafish L13G-MetRS mutant enables metabolic labeling with ANL <i>in vitro</i>	59
Zebrafish L13G-MetRS mutant enables metabolic labeling with ANL <i>in vivo</i>	61
NLL and PLL mutations of the zebrafish MetRS sequence enable ANL incorporation neither <i>in vitro</i> nor <i>in vivo</i>	69
Discussion	72
Methods.....	73
 <i>Chapter IV</i>	 81
PROTEIN SYNTHESIS-DEPENDENT PLACE-CONDITIONING IN LARVAL ZEBRAFISH	81
Introduction.....	82
Associative place-conditioning paradigm for 6-8dpf larval zebrafish.....	84
Memory extinction occurs rapidly, whereas memory retention lasts up to 36h	91
Memory formation is protein synthesis- and NMDAR-dependent.....	95
Exposure to social environment sustains exploratory behavior.....	99
Discussion	102
Methods.....	104
 <i>Chapter V</i>	 109
DISCUSSION AND FUTURE DIRECTIONS	109
Discussion	110
Future directions	113
Chemical screening	113

Proteomics	114
Live labeling.....	115
Visualizing memory formation	117
Work cited	121
APPENDIX	134
A: Vector maps	134
B: Drawings of behavioral chambers.....	178
C: Matlab scripts.....	190
D: Protein identification list.....	193
E: Publications	204
Hinz et al., 2012	205
tom Dieck et al., 2012	215

LIST OF ILLUSTRATIONS

Figure 1.1. Chemical structures and ‘click chemistry’ reaction scheme	11
Figure 1.2. The twelve amino acid residues of MetRS found within 4Å of bound methionine are predicted to be part of the catalytic binding pocket.....	14
Figure 1.3. The binary Gal4-UAS gene expression system	18
Figure 2.1. Labeling of newly synthesized proteins for quantification, affinity purification (BONCAT) and visualization (FUNCAT) in larval zebrafish.....	28
Figure 2.2. At low concentrations, AHA exposure is not toxic and does not significantly alter simple behaviors.....	30
Figure 2.3. Tracks of spontaneous swimming behavior of 7-day-old larval zebrafish	32
Figure 2.4. AHA is metabolically incorporated into larval zebrafish proteins <i>in vivo</i>	34
Figure 2.5. Metabolic labeling is AHA concentration dependent	36
Figure 2.6. AHA incorporation occurs throughout the proteome	37
Figure 2.7. Newly synthesized proteins can be visualized in whole-mount larval zebrafish after <i>in vivo</i> labeling	39
Figure 2.8. FUNCAT can be combined with antibody staining to identify specific cell populations in the whole-mount larval zebrafish	42
Figure 2.9. The GABA antagonist PTZ induces increased protein synthesis in larval zebrafish	44
Figure 3.1. Genetically restricted metabolic labeling.....	57
Figure 3.2. MetRS protein sequence alignment of <i>E. coli</i> , <i>Danio rerio</i> , <i>Mus musculus</i> and <i>Homo sapiens</i>	58
Figure 3.3. Cell-selective labeling with ANL <i>in vitro</i>	61
Figure 3.4. Cell-selective labeling with ANL in transiently L13G-MetRS-expressing larval zebrafish	64
Figure 3.5. Cell-selective labeling with ANL in F1 transgenic larval zebrafish expressing L13G-MetRS.....	67

Figure 3.6. Restricted mutant MetRS expression in the telencephalon of larval zebrafish via FlipTrap gene trapping.....	68
Figure 3.7. NLL and PLL mutations of zebrafish MetRS do not enable metabolic labeling with ANL <i>in vitro</i> or <i>in vivo</i>	71
Figure 4.1. Place-conditioning apparatus and experimental set up	85
Figure 4.2. 6-8dpf larval zebrafish show unconditioned preference for light and social environment	87
Figure 4.3. Associative place-conditioning paradigm for 6-8dpf larval zebrafish.....	89
Figure 4.4. Rapid extinction of the conditioned association	92
Figure 4.5. Memory of association persists for at least 36h	94
Figure 4.6. Memory formation is protein-synthesis dependent.....	96
Figure 4.7. 3h incubation with puromycin, cycloheximide or MK-801 does not significantly alter unconditioned light and social environment preference	98
Figure 4.8. Exposure to social environment sustains exploratory behavior.....	100
Figure 5.1. Physical mapping of preliminary proteomic data	116

ABBREVIATIONS USED

- 4E-BP2:** eIF4E binding protein
- aaRS:** Aminoacyl-tRNA synthetase
- AHA:** Azidohomoalanine
- AMPA:** α -amino-3-hydroxy-5-methyl-4-isoxazolepropionic acid
- ANL:** Azidonorleucine
- ARC:** Activity-regulated cytoskeleton-associated protein
- ATF4:** Activation transcription factor 4
- BDNF:** Brain-derived neurotrophic factor
- BONCAT:** Bioorthogonal noncanonical amino acid tagging
- CaMKII:** Ca^{2+} /calmodulin-dependent protein kinase II
- cAMP:** Cyclic adenosine monophosphate
- CREB:** Cyclic-AMP-response-element-binding protein
- dpf:** Days post fertilization
- eIF2a:** Eukaryotic initiation factor 2a
- E-LTP:** Early LTP
- ERK:** Extracellular signal-regulated kinase
- FUNCAT:** Fluorescent noncanonical amino acid tagging
- GABA:** γ -Aminobutyric acid
- GFP:** Green fluorescent protein
- GCN-2:** General control norepressor 2
- HEK:** Human embryonic kidney
- hpf:** Hours post fertilization
- HPG:** Homopropargylglycine
- IEG:** Immediate early gene
- KO:** Knock-out
- L13G:** *E. coli* MetRS leucine 13 mutated to glycine
- LED:** Light-emitting diode
- L-LTP:** Late LTP
- LTP:** Long-term potentiation
- MAPK:** Mitogen-activated protein kinase
- MetRS:** Methionyl-tRNA synthetase

MK-801: Dizocilpine, non-competitive antagonist of the NMDA receptor
NGF: Nerve growth factor
NLL: *E. coli* MetRS mutation
NMDA: *N*-methyl-D-aspartate
OKR: Optokinetic response
OMR: Optomotor response
PBDTT: Phosphate-buffered solution containing DMSO, Triton X-100 and Tween-20
PBS: Phosphate-buffered solution
PLL: *E. coli* MetRS mutation
PKM ζ : Protein kinase M ζ
PSI: Protein synthesis inhibitor
PTZ: Pentylentetrazol
RT: Room temperature
SILAC: Stable isotope labeling with amino acids in cell culture
TCEP: *Tris*(2-carboxyethyl)phosphine
t-PA: Tissue plasminogen activator
UAS: Upstream activating sequence

Chapter I

INTRODUCTION

The role of protein synthesis in long-term memory formation

Changes in behavior, specifically memory formation, are thought to depend on synaptic plasticity in specific circuits of the nervous system. A central goal of neuroscience is to characterize these physical changes that underlie learning and memory. Learning, in the most general sense, is defined as the process by which new information about the environment is acquired. Memory formation is considered to be the process by which that knowledge is stored. Over the last hundred years, researchers have developed countless training paradigms to investigate these processes in a variety of different model organisms.

Generally, these paradigms can be classified into two main groups, those that induce non-associative learning and those that induce associative learning. Non-associative learning, such as habituation and sensitization, refers to a behavioral change that occurs in response to a single stimulus or to two stimuli not temporally related, while associative learning, such as entrained during place-conditioning, refers to the formation of an association either between two stimuli (classical conditioning) or between a behavior and a stimulus (operant conditioning).

Both non-associative and associative learning can have different time constants. While short-term memory is produced immediately after information is acquired and lasts minutes to hours, long-term memory is formed during a distinct second phase, lasting from hours to days or longer depending on the organism and the type of memory. Furthermore, short-term memory is thought to depend on post-translational modification at the synapse, such as residue-specific phosphorylation or proteolytic cleavage of key

proteins, which can alter enzymatic activity of target molecules and regulated trafficking of receptors. In contrast, long-term memory has been shown to require regulated changes in gene transcription and protein synthesis (reviewed in Abel and Lattal, 2001 and Goelet et al., 1986). The connection between long-term memory formation and protein synthesis has been extensively studied using both protein synthesis inhibitors (PSI) and genetic manipulation of key players of translational control.

Studies using protein synthesis inhibitors, such as the antibiotics puromycin, anisomycin and cycloheximide, in many different model organisms have shown that protein synthesis, during or shortly after learning, is an essential step in the formation of long-term memory (Davis and Squire, 1984). In a seminal experiment in 1964, Agranoff et al. showed that the PSI puromycin injected intracranially into the goldfish produced impairment of memory for a shock avoidance task and that this impairment was time- and PSI concentration-dependent (Agranoff and Klinger, 1964; Agranoff et al., 1966). Since then, protein synthesis has been shown to be necessary for long-term memory formation in a variety of learning paradigms, including appetitively and shock-motivated discrimination learning, passive and active avoidance learning, shuttle box learning, and long-term habituation (reviewed in Davis and Squire, 1984). These studies demonstrating the necessity of protein synthesis for long-term memory formation paved the way for the idea that the physical basis of memory lies in the learning-related growth or remodeling of synaptic connections in a protein synthesis-dependent manner.

In 1973, Bliss and Lømo found that a high frequency train of action potentials resulting from stimulation of the perforant path in the rabbit hippocampus lead to a long-term potentiation (LTP) of synaptic transmission in the dentate gyrus (Bliss and Lømo,

1973). This phenomenon, which can also be induced *in vitro* in cultured slices (Alger and Teyler, 1976; Lynch et al., 1977; Schwartzkroin and Wester, 1975), has been widely regarded as a potential cellular mechanism underlying information storage, both because of its occurrence in the hippocampus, a structure known to be involved in memory formation and because of its relative stability. Since then, the appeal of LTP has widened through accumulated evidence that LTP exhibits additional features that have been shown to reflect important characteristics of memory formation *in vivo*. For one, correlates of short-term and long-term memory have been identified in LTP, termed early (E-LTP) and late (L-LTP) LTP, respectively. Furthermore, L-LTP specifically has been shown to be both transcription- and translation-dependent using chemical stimulation with drugs such as PSI *in vitro* (Abraham and Williams, 2003).

Although extremely important in elucidating the connection between long-term memory formation and protein synthesis, PSI, which are thought to block ~90% of all cellular protein synthesis (Klann and Sweatt, 2008), are relatively blunt tools. The most frequently used PSI are antibiotics that interfere with the elongation step of translation. Puromycin causes premature chain termination as it can mimic the 3'-end of an aminoacylated tRNA, producing abnormal peptidyl-puromycin fragments (Flexner and Flexner, 1968; Nathans, 1964), while anisomycin binds to the 60S ribosomal subunit, blocking peptide bond formation (Pestka, 1971; Vasquez, 1979). Cycloheximide, another frequently used PSI, is specific to eukaryotic cells and also binds to the 60S ribosomal subunit, interfering with both initiation and the translocation step of elongation (Gale et al., 1981). Beyond being indiscriminant blockers of protein synthesis, most PSI have non-specific effects, such as activating the mitogen-activated protein kinase (MAPK)

superfamily pathways (Rudy et al., 2006), altering catecholamine function (Weiner and Rabadjija, 1968), impairing DNA and RNA synthesis (Gale et al., 1981), or causing toxic side effects such as seizures, lethargy and gustatory aversions when administered at high concentrations *in vivo* (Davis and Squire, 1984).

To investigate the role of protein synthesis in long-term memory formation while avoiding the use of PSI, researchers have recently started to genetically manipulate key players of translational control using knock-out (KO) mice models. Costa-Mattioli et al., for instance, examined plasticity in mice lacking general control norepressor 2 (GCN2), a protein kinase that inhibits translation initiation by phosphorylating eukaryotic initiation factor 2a (eIF2a). Phosphorylation of eIF2a stimulates translation of activating transcription factor 4 (ATF4), an antagonist of cyclic-AMP-response-element-binding protein (CREB). Thus, in the hippocampus of GCN2 KO mice expression of ATF4 is reduced and CREB activity is increased. In these animals, stimuli that normally lead to early LTP resulted in long-lasting LTP, whereas stimuli that normally lead to late LTP led to reduced LTP. Mirroring this phenotype, researchers observed an enhancement of learning in the Morris water maze following weak training, but a reduction in learning after intense training (Costa-Mattioli et al., 2005), indicating that tight translational control is necessary for normal memory formation. Furthermore, Banko et al. examined both LTP and spatial learning in mice lacking eIF4E binding protein 2 (4E-BP2), which normally inhibits translation by binding to eIF4E and observed the same plasticity phenotype as above. In these animals, disinhibition of protein translation results in impaired spatial learning and long-term contextual fear conditioning (Banko et al., 2005). In contrast, mice with conditional expression of a dominant-negative regulator of MAPK

in the forebrain exhibit inhibition of protein translation, which results in inhibition of LTP, as well as deficits in spatial learning and contextual fear conditioning (Kelleher et al., 2004). Although these elegant experiments provide further evidence that long-term memory formation is protein-synthesis dependent, they also have their disadvantages. As most of the gene deletions described above were not conditional, some or all of the deficits observed could be due to long-term loss of these molecules, changes in development that compensate for lack of these molecules or lack of these molecules in other cell types. Furthermore, it is possible that the deficits are due to other translation-independent functions of the genetically manipulated molecules.

Both *in vitro* studies of LTP and *in vivo* experiments investigating behavioral correlates of learning and memory have helped form our current understanding of the molecular mechanisms underlying memory formation. It is now known that once activated by coincident pre-synaptic release of glutamate and post-synaptic depolarization, *N*-methyl-D-aspartate (NMDA) receptors allow calcium entry into the cell, thereby triggering a range of intracellular signaling cascades (Collingridge et al., 1983; Cotman et al., 1989; reviewed in Sweatt, 2009). Among others, the influx of calcium stimulates calcium-binding protein Ca^{2+} /calmodulin and increases the production of cyclic adenosine monophosphate (cAMP) by adenylyl cyclases. cAMP, in turn, activates protein kinase A (PKA), which activates CREB, resulting in plasticity-related gene transcription and translation. CREB can also be activated via calcium signaling through the MAPK/extracellular signal-regulated kinase (ERK) pathway by a number of important kinases, including Ca^{2+} /calmodulin-dependent protein kinases II (CaMKII) and protein kinase C (PKC) (reviewed in Sweatt, 2009). CREB, in concert with other

activity-regulated transcription factors, then controls the expression of a variety of plasticity-related genes with CRE response elements in their promoters (Hagiwara et al., 1996). These include a number of immediate-early genes (IEG), such as C/EBP, zif/268, and krox 20, which in turn act as transcription factors regulating the expression of ‘effector’ genes (Sweatt, 2009). It is the protein products of these effector genes that are needed for growth or stabilization of synapses, the physical change thought to underlie memory formation. Effector proteins that show increased translation with memory formation include: neurotrophic factors such as brain-derived neurotrophic factor (BDNF) and neurotrophin-3; signaling molecules such as CaMKII and the atypical PKC protein kinase M ζ (PKM ζ) (Saktor, 2011); secreted proteases such as tissue plasminogen activator (t-PA); α -amino-3-hydroxy-5-methyl-4-isoxazolepropionic acid (AMPA) receptor subunits; the metabotropic receptor scaffolding protein homer; and activity-regulated cytoskeleton-associated protein (arc), a cytoskeleton-associated protein that may be involved in stabilizing structural changes at potentiated synapses (reviewed in Sweatt, 2009; Hernandez and Abel, 2008). In particular, the increased translation of secreted proteases is interesting, as degradation of proteins is not intuitively associated with synaptic growth or increased stability. But degradation of structural proteins may be integral to allow for the structural rearrangement that is synaptic plasticity (Mysore et al., 2008; Tai et al., 2008).

Most of the effector proteins that show activity-dependent changes in translation have so far been identified *in vitro* using targeted genetic manipulation of individual candidate proteins. Aakalu et al., for example, using GFP flanked by the 5’ and 3’ untranslated regions of CaMKII α , demonstrated that this reporter construct shows

increased local translation when neurons are stimulated with BDNF (Aakalu et al., 2001). More recently, Chen et al., using a photoconvertible fluorescent protein kaede to report new protein synthesis, have visualized CREB-dependent transcriptional activation of CaMKII and of period in the dorsal-anterior-lateral neurons of *Drosophila* after training that induces long-term memory formation (Chen et al., 2012). Using these techniques the researchers were both able to confirm that these proteins are translationally regulated with memory formation and identify the neural circuits in which these particular translational changes occur.

However, such studies rely on fluorescent protein reporter systems and a candidate-based approach, possibly perturbing endogenous localization of newly synthesized proteins and severely limited in their potential to identify unknown effector proteins and the circuits underlying memory formation. According to conservative estimates, vertebrate genomes may have about 30,000 genes and recent studies have shown that at least 50% are expressed in the brain (Pan et al., 2011). A large number of the protein products of these genes may play a role in signaling cascades and structural changes associated with memory and learning, which are unlikely to be identified using a candidate based approach. Furthermore, monitoring translation of one or maximally a few candidate proteins is unlikely to lead to a complete understanding of which neuronal circuits show changes in translation with memory formation. Instead, we hypothesize that by developing new techniques utilizing bioorthogonal chemistry to tag newly synthesized proteins specifically, we may circumvent these problems, enabling unbiased visualization and identification of proteins underlying memory formation.

Bioorthogonal chemistry

Recently, new techniques for labeling a variety of molecules based on the principle of bioorthogonal metabolic labeling have been developed (Best, 2009). Here, small functional groups that are commonly absent in the cellular environment, most prominently ketones and azides or alkynes, are introduced using the cells' own synthetic machinery. Using this approach, sugars (Laughlin and Bertozzi, 2009), lipids (Kho et al., 2004), virus particles (Bruckman et al., 2008), DNA and RNA (Weisbrod et al., 2008) have been labeled and subsequently visualized using fluorescent dyes or enriched and identified using affinity reagents. Bertozzi and coworkers, in particular, have demonstrated *in vivo* labeling of glycans in living organisms ranging from rodents (Prescher et al., 2004; Chang et al., 2010), to larval zebrafish (Laughlin et al., 2008; Baskin et al., 2010; Dehnert et al., 2011) and *C. elegans* (Laughlin and Bertozzi, 2009). In the case of larval zebrafish, embryos were treated with an unnatural azide-bearing sugar to metabolically label cell-surface glycans, which were subsequently reacted to fluorescent alkyne conjugates at different time points. This enabled spatiotemporal visualization of expression and trafficking of cell-surface glycans *in vivo* during development (Laughlin et al., 2008).

Using a similar method, proteins can be labeled with noncanonical amino acids bearing novel side chains. Noncanonical amino acids are amino acids that are not part of the canonical set of twenty used in translation by all living systems. Some of these noncanonical amino acids can act as surrogates for naturally occurring amino acids, be charged onto wild-type tRNAs by endogenous aminoacyl-tRNA synthetases (aaRS) and

therefore be metabolically incorporated into newly synthesized proteins. However, this is not a new area of research. In the 1950s, Cowie and Cohen demonstrated that selenomethionine serves as an effective surrogate of methionine (Cowie and Cohen, 1957). Since then a number of different amino acids, including methionine, leucine, phenylalanine, and tryptophan, have been replaced by noncanonical amino acid analogs bearing bromo-, iodo-, cyano- and ethynyl- substituents and thereby allowing for investigation of how these novel side chains effect structure and function of labeled proteins (reviewed in Link et al., 2003).

More recently, Tirrell and coworkers have established the use of the azide-bearing noncanonical amino acid azidohomoalanine (AHA) and the alkyne-bearing noncanonical amino acid homopropargylglycine (HPG) as surrogates for methionine in bacterial cells (Figure 1.1a) (Kiick et al., 2002; Link et al., 2004; Beatty et al., 2005). Azides and alkynes are stable under biological conditions, essentially absent from cellular environments and can be covalently linked via selective Cu(I)-catalyzed [3+2] azide-alkyne cycloaddition (Figure 1.1b) (Rostovtsev et al., 2002; Tornøe et al., 2002), making them ideal candidates to label proteins. Using this approach, Dieterich *et al.* developed the sister techniques bioorthogonal noncanonical amino acid tagging (BONCAT), and fluorescent noncanonical amino acid tagging (FUNCAT). During BONCAT, proteins labeled with noncanonical amino acids are tagged using affinity tags to enable affinity purification, while FUNCAT utilizes fluorescent tags to enable visualization, and thereby localization, of newly synthesized proteins in mammalian cells (Dieterich et al., 2006, 2007 and 2010).

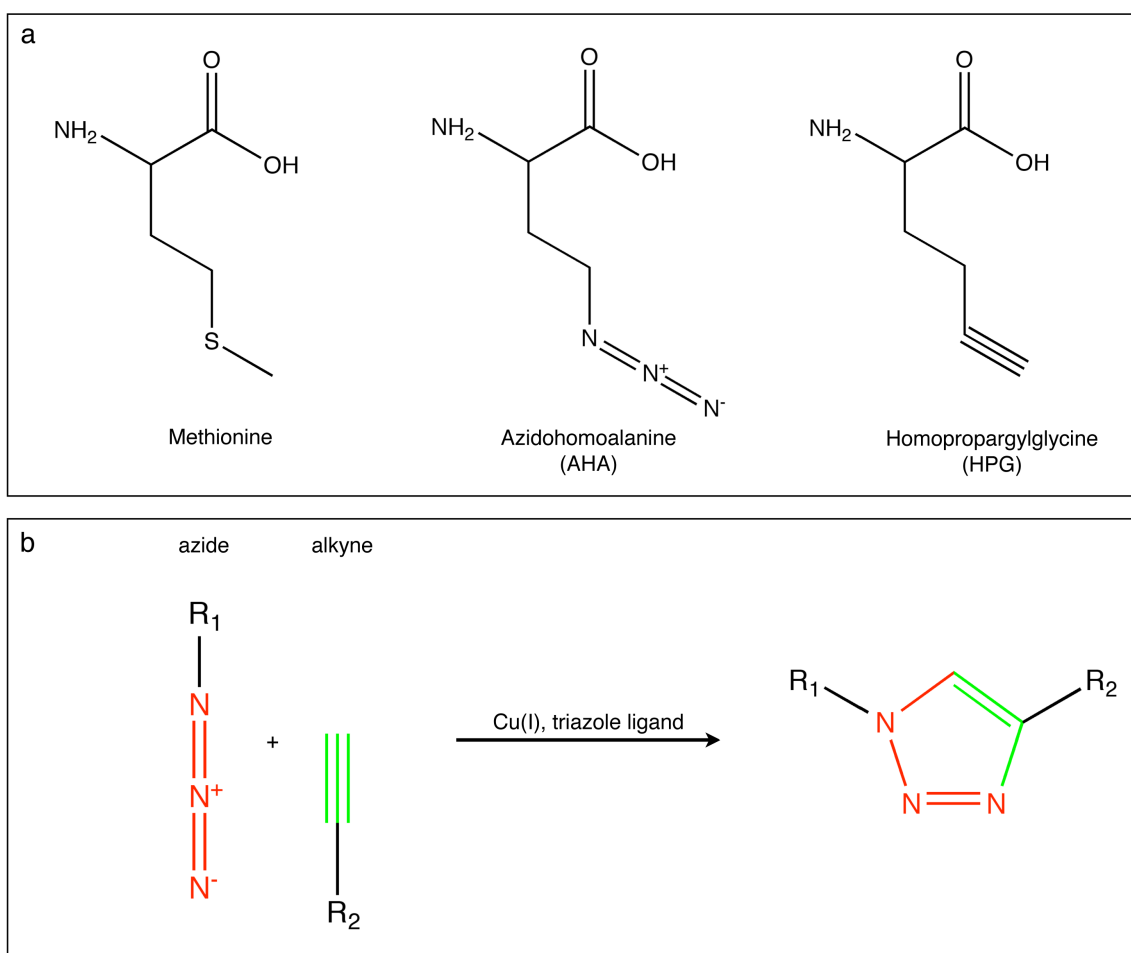


Figure 1.1. Chemical structures and ‘click chemistry’ reaction scheme

(a) Chemical structures of methionine, azidohomoalanine (AHA) and homopropargylglycine (HPG). (b) Scheme of Cu(I)-catalyzed of [3+2] azide-alkyne cycloaddition.

Affinity-tagged proteins can be quantified using immunoblot analysis or separated from the preexisting proteome by affinity purification and identified by tandem mass spectrometry. BONCAT has already been successfully applied to study the proteome of HEK293 cells during a two hour time window, allowing the identification of 195 newly synthesized proteins (Dieterich et al., 2006). Fluorescent tags can be used to visualize

newly synthesized proteins, including those proteins of interest whose identities may not be known. In this manner, FUNCAT has been used to investigate temporally defined protein populations in Rat-1 fibroblast (Beatty et al., 2006; Beatty and Tirrell, 2008) and local protein synthesis in dissociated hippocampal neurons and hippocampal slices (Dieterich et al., 2010). Furthermore, metabolic AHA incorporation has been used to identify regions of the *Drosophila* genome that show high levels of histone turnover (Deal et al., 2010), to show that *Chlamydia* co-opt the functions of the lysosomes of their host cells to acquire essential amino acids (Ouellette et al., 2011), as well as to demonstrate that treatment of primary sensory neurons with the cytokine interleukin-6 or the neurotrophin nerve growth factor (NGF) increases nascent protein synthesis in axons (Melemedjian et al., 2010). Recently, these techniques have also been used to show that the transmembrane receptor DCC may regulate protein synthesis in a localized manner within the cells, as DCC enrichment was found to mark areas of new protein synthesis at the tips of filopodia in commissural neurons (Tcherkezian et al., 2010).

AHA and HPG are able to penetrate cell membranes, bind to methionyl-tRNA synthetase (MetRS) and be charged onto met-tRNAs in wild-type cells. BONCAT and FUNCAT depend on this promiscuous nature of MetRS that enables the charging of these structurally similar methionine analogs and thereby their incorporation into newly synthesized proteins. AARS specificity is the most critical proofreading mechanism to ensure accurate translation of proteins from their respective mRNAs, as the ribosome lacks proofreading capabilities.

AARS catalyze the aminoacylation of their cognate tRNAs by activation of the amino acid by ATP, followed by transfer onto the 3' end of the tRNA molecule. The

recognition of the cognate amino acid by the aaRS is a multistep process. First, amino acids and ATP physically bind to aaRS to induce a conformational change in the aaRS that leads to the formation of the aminoacyl-adenylate complex. Next, misactivated noncognate aminoacyl-adenylate complexes are eliminated, followed by transfer of the aminoacyl group to the tRNA and pretransfer proofreading. Finally some aaRS have sieve-type post-transfer proofreading capabilities to eliminate mischarged tRNAs. Each of these steps leads to increased specificity for the cognate amino acid, while discriminating against the noncognate amino acid.

MetRS is a member of the class I aaRS. Crystal structures are available of *E. coli* MetRS both with and without bound methionine (Mechulam et al., 1999 [PDB:1QQT]; Serre et al., 2001 [PDB:1F4L]). From these structures, it has been determined that MetRS undergoes a significant conformational change upon binding its substrate, but apparently lacks a sieve-type proofreading mechanism. This structural change is thought to be associated with the main proofreading step in the selective recognition of methionine (Datta et al., 2004). Twelve amino acids are found within 4Å of bound methionine and are therefore predicted to be part of the catalytic binding pocket (Figure 1.2). These residues include L13, Y260 and H301. Both the NH₂ moiety and the sulfur atom of the side chain of methionine form hydrogen bonds with the L13 carbonyl oxygen atom and the L13 backbone amide, respectively. The sulfur atom of the side chain of methionine forms another hydrogen bond with Y260, while the backbone of methionine makes electrostatic interactions with H301 (Fourmy et al., 1991; Ghosh et al., 1991). Most of the residues that are in close contact with the methionine are strictly conserved among MetRS of different bacterial organisms. This is particularly the case for L13,

Y260, D52, W253, Y15, A256 and H301 (Serre et al., 2001). Although, MetRS has been observed to be slightly promiscuous and has been seen to incorporate a variety of different noncanonical amino acid analogs, such as AHA (Kiick et al., 2001), the significant conformational change of the catalytic pocket after binding of methionine increases the specificity of MetRS for methionine. This severely limits the chemical functionalities that can be introduced into newly synthesized proteins.

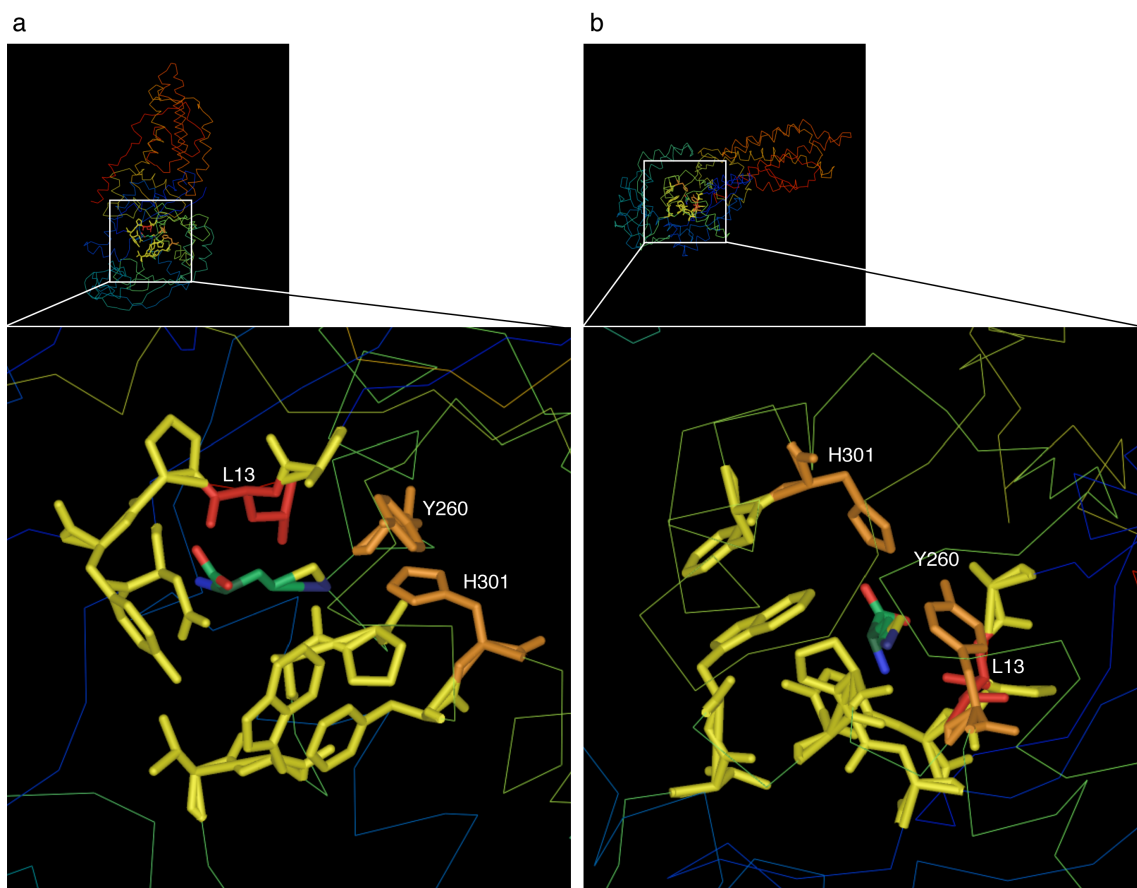


Figure 1.2. The twelve amino acid residues of MetRS found within 4Å of bound methionine are predicted to be part of the catalytic binding pocket.

(a) and (b) show two different orientations of MetRS (top) and its catalytic binding pocket (bottom). L13 is highlighted in red, Y260 and H301 are shown in orange and A12, P14, Y15, D52, V252, W253, A256, P257 and F300 are shown in yellow. The structure was first published by Serre et al., 2001; PDB:1F4L.

BONCAT and FUNCAT may be ideal techniques to visualize and identify effector proteins synthesized during memory formation. As opposed to genetically encoded fluorescent proteins, azides and alkynes are small, so labeling with AHA or HPG is likely to only cause modest, perhaps even insignificant, perturbations of protein folding and localization (Dieterich et al., 2006) and therefore function of the labeled proteins *in vivo*. Furthermore, introduction of a chemical handle allows for affinity purification of newly synthesized proteins specifically. As the nervous system proteome is extremely complex, reducing the complexity of the sample may facilitate the identification of proteins of low abundance. However, so far, these techniques have only been applied *in vitro*. Given the role of protein synthesis in learning and memory, described earlier, developing BONCAT and FUNCAT for use in an intact organism in which simple forms of learning may be investigated, such as the larval zebrafish, is the essential next step.

The larval zebrafish as a model organism

The zebrafish is a tropical sweet-water cyprinid found mainly on the Indian subcontinent, its range extending from Pakistan in the west to Myanmar in the east and Nepal in the north (Engeszer et al., 2007). Adults live in shallow vegetated areas in rivers and small streams and are thought to feed mainly on insects and zooplankton, while they themselves are hunted by a variety of fishes including the snakehead (*Channa*) (Spence et al., 2008). During the monsoon season, adults move to shallow flooded ponds, often

connected with rice cultivation, to spawn. Adult zebrafish are about 4cm long, become sexually mature after about 3 months and females lay clutches of several hundred eggs in a single spawning. They have been reported to survive temperature ranges from 6°C to 38°C (Spence et al., 2008) in the wild, and are usually found in environments with a pH range of pH 7.9-8.2 (Engeszer et al., 2007).

Due to their high fecundity, rapid development, relatively fast generation time, external fertilization and environmental robustness, the zebrafish has emerged as an important model organism for developmental genetics and biomedical research. In the laboratory, a large number of zebrafish can be housed in a small area as a result of their social nature. A number of companies sell customizable aquatic habitats that can self-regulate temperature, pH, conductivity and water quality, greatly reducing maintenance time. In captivity, females can spawn up to twice a week, laying large, optically transparent embryos. Eggs are fertilized externally and adult zebrafish provide no parental care, enabling researchers to collect single cell embryos for genetic manipulation and developmental study. Embryos develop rapidly; the first neurons can be identified approximately 24 hours post-fertilization (hpf) (Kimmel et al., 1995). After 3 days post-fertilization (dpf) larvae hatch; by 5dpf larvae are estimated to have 100,000 neurons and by 7dpf larvae, now approximately 5mm long, are capable of a diverse set of simple behaviors. Interestingly, in zebrafish, all gonads originally develop as ovaries, which in males start maturing around 6-7 weeks post-fertilization and reach maturity after approximately three months (Devlin and Nagahama, 2002; Maak and Segner, 2003). Although the genetic mechanism of sex determination is unknown, evidence suggests a role for food availability and water temperature (Lawrence et al., 2007). Furthermore,

larval zebrafish can absorb a variety of small chemical compounds directly from their surrounding environment, making them amenable to chemical screens (Zhong and Lin, 2011) and possibly noncanonical amino acid labeling techniques.

Over the last 15 years a number of genetic tools have been developed, mainly to study larval zebrafish development, but also extremely useful in investigating neuronal circuit morphology and function. The discovery and development of the Tol2 transposable element, originally described in medaka fish, which has a very high rate of genomic integration in the germline, immensely facilitates the construction of stable transgenics (Kawakami, 2005; Suster et al., 2009). DNA fragments of up to 10kb can be flanked with Tol2 sequences and co-injected with transposase mRNA into single-cell embryos to enable germline integration rates up to 50-70% (Suster et al., 2009). Using this system, a large number of gene- and enhancer-trap constructs have been generated to study the expression, function and localization of a number of genes.

More recently, Tol2 was used to create transgenic zebrafish for targeted gene expression in specific tissues and cells using the binary Gal4-UAS system (Figure 1.2.). Gal4 is a yeast transcriptional activator which can bind to its cognate upstream activating sequence (UAS) to activate transcription of target genes. The Gal4-UAS system can be used as a two-component gene expression system in a number of different model animals, including the zebrafish (Sheer and Campos-Ortega, 1999; Köster and Fraser, 2001). Two transgenic lines are created: one expressing the Gal4 sequence under the control of a cell-type-specific promoter (termed driver line), the other expressing a gene of interest, such as GFP, under the control of the UAS promoter (termed the responder line). Crossing driver lines with responder lines allows for expression of a variety of genes of interest

(determined by the responder line) in a variety of specific cells or tissues (determined by the driver line).

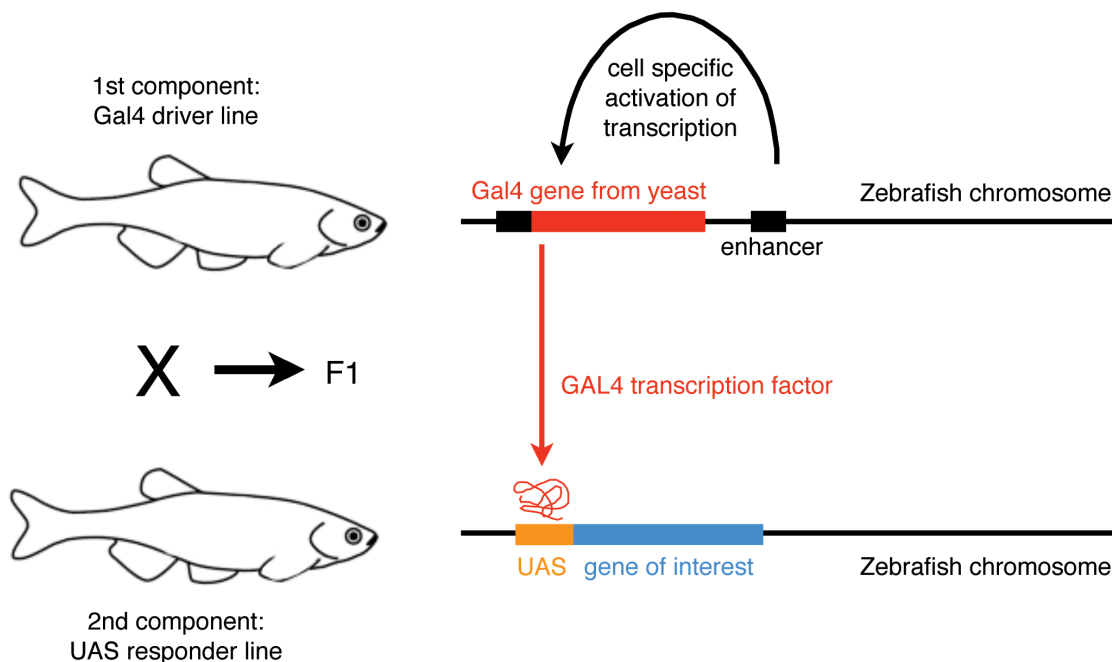


Figure 1.3. The binary Gal4-UAS gene expression system

Crossing Gal4 driver lines with UAS responder lines allows for expression of a variety of genes of interest (determined by the UAS responder line) in a variety of specific cells or tissues (determined by the Gal4 driver line). [Adult zebrafish schematic adapted from Smith and Croll, 2011.]

Recently, large enhancer-trapping screens have led to the creation of hundreds of nervous system-specific Gal4 driver lines with different, sometimes cell-type-specific expression patterns (Davison et al., 2007; Scott et al., 2007; Asakawa et al., 2008). Furthermore, a variety of different responder lines now allow for the visualization of expression using fluorescent proteins (Scott et al., 2007; Asakawa et al., 2008), targeted cell ablation using NTR system or KillerRed (Davidson et al., 2007; Del Bene et al., 2010), light-gated control of neuronal activity using engineered ion channels (Szobota et

al., 2007; Janovjak et al., 2010) and inhibition of neurotransmitter release by tetanus toxin light chain (Asakawa et al., 2008), making this binary system extremely useful for studying nervous system development and function (reviewed in Asakawa and Kawakami, 2009). Furthermore, pigment mutants lacking melanophores, such as the *nacre* line, have been identified in mutant screens, enabling direct imaging of the larval zebrafish nervous system in intact animals (Lister et al., 1999).

Despite some obvious differences in size and complexity of certain structures of the zebrafish brain, the overall organization of the major brain components is comparable to that of the mammalian brain (Tropepe and Sive, 2003). Furthermore, as in other vertebrates, zebrafish possess all of the classical senses (vision, olfaction, taste, tactile, balance and hearing) and their sensory pathways share an overall homology with mammals. However, in mammals the telencephalon undergoes evagination during development, while in teleost fish such as the zebrafish, the telencephalon is everted. As a result, the hippocampus, which in mammals is structurally derived from the medial part of the dorsal telencephalon, is thought to be structurally homologous to the dorsal lateral telencephalon in zebrafish. In contrast, the amygdala, which is a lateral structure in mammals, is thought to be structurally homologous to the dorsal medial telencephalon in zebrafish (Broglia et al., 2005).

Despite differences in location, a number of lesion studies in the closely related goldfish have demonstrated that lesions of the dorsal lateral telencephalon result in deficits in tasks that, in mammals, rely on the hippocampus, such as spatial learning and trace classical conditioning, but do not affect hippocampus-independent delay conditioning and heart-rate conditioning. In contrast, lesions of the dorsal medial

telencephalon disrupt amygdala-dependent emotional, heart-rate conditioning and avoidance conditioning, but spare spatial memory and temporal stimulus processing (Vargas et al., 2006; Saito and Watanabe, 2006; Salas et al., 1996; Overmier and Papini, 1986; Portavella et al., 2004a; Portabella et al., 2004b; Portavella et al., 2002; reviewed in Broglio et al., 2005). Gross similarity in brain structure and identification of homologous areas involved in memory storage indicate that this simple vertebrate, the zebrafish, is more comparable to humans than invertebrate models such as *Drosophila* and *C. elegans* and therefore a preferable model organism to investigate neuronal circuits underlying behavior.

Not only are zebrafish easily maintained, genetically tractable, simple vertebrates, they also have an extensive behavioral repertoire. Adults show a range of complex and well-described social behaviors including courtship (Darrow and Harris, 2004), shoaling, aggression and dominance (Larson et al., 2006), escape and avoidance (reviewed in Colwill and Creton, 2011) and exploratory behaviors (reviewed in Spence et al., 2008). Some simple behaviors develop early and can be observed during the first week of development. The spontaneous locomotor repertoire of the larval zebrafish includes routine turns and slow scoots, while they produce a well-characterized C-bend escape response to escape from threatening stimuli (Budick and O'Malley, 2000). Even before hatching from the chorion, larvae begin to show startle responses when exposed to abrupt stimuli. By 4dpf larvae will induce rapid escape responses to tactile stimuli (Granato et al., 1996; McLean and Fetcho, 2009), water flow (Froehlicher et al., 2009; Kohashi and Oda, 2008) and visual stimuli (Emran et al., 2008); by 5-6dpf larvae will respond to acoustic stimuli (Burgess and Granato, 2007). Between 4-5dpf larvae will begin to

follow moving objects with their eyes, a behavior that is referred to as the optokinetic response (OKR) and by 5dpf larvae are actively hunting for food (Neuhauss, 2003). Furthermore, larvae have been shown to swim in the same direction as a pattern of moving stripes, a behavior that is called the optomotor response (OMR) (Fleisch and Neuhauss, 2006) and display diurnal rhythms in activity (Prober et al., 2006).

Memory and learning capabilities of the zebrafish have been extensively explored in the adult. In the last decade, a number of conditioning paradigms have been developed, including avoidance-conditioning (Ng et al., 2012; Blank et al., 2009; Xu et al., 2006; Pradel et al., 2000; Pradel et al., 1999), place-conditioning (Mathur et al., 2011), plus maze learning (Sison and Gerlai, 2010) and shuttle box conditioning (Williams et al., 2002). These paradigms use food and social rewards (Al-Imari and Gerlai, 2007), as well as mild electroshock and exposure to alarm signal as unconditioned stimuli and visual, olfactory (Braubach et al., 2009) and acoustic stimuli as conditioned stimuli. However, very few conditioning paradigms exist for the larval zebrafish to date.

The first study investigating the learning capabilities of larval zebrafish showed that larvae can learn to habituate to an acoustic stimulus (Best et al., 2008). In this non-associative conditioning paradigm, 7dpf larvae individually placed in 96-well plates and repeatedly exposed to an acoustic stimulus exhibited an iterative reduction in startle response, which spontaneously recovered and showed dishabituation when exposed to a visual stimulus. This work was extended upon by the Wolman and colleagues, who showed that spaced training blocks of repetitive visual stimuli elicit protein synthesis-dependent long-term habituation in larval zebrafish, lasting up to 24h (Wolman et al., 2011). Finally, previous studies from our laboratory demonstrated that 6-8dpf larval

zebrafish can be associatively conditioned (Aizenberg and Schuman, 2011). Trained using an hour-long classical conditioning paradigm, larvae rapidly developed an enhanced motor response to a visual stimulus when it was paired with a tactile stimulus. Memory retention, in this very labor-intensive paradigm, is unfortunately not long term and decays to baseline within 1hr of acquisition. To enable visualization and identification of proteins newly synthesized with memory formation using bioorthogonal protein labeling techniques in the larval zebrafish, a high throughput, protein synthesis-dependent conditioning paradigm needs to be established.

To conclude, the larval zebrafish is an excellent model organism, as it is a genetically tractable, simple vertebrate which is transparent and therefore ideal for imaging. Furthermore, adult zebrafish, as well as larval zebrafish, have a well-defined behavioral repertoire (Colwill and Creton, 2012), and the range of experimental paradigms to test this has recently been expanded to include associative conditioning (Aizenberg and Schuman, 2011). Larval zebrafish can absorb small chemical compounds directly from their surrounding environment, all of which makes them not only amenable to chemical screens and an emerging human disease model, but also an excellent system in which to study the applicability of bioorthogonal metabolic labeling of newly synthesized proteins underlying memory formation *in vivo*.

Memory formation, thought to depend on physical changes at specific synapses, has been conclusively shown to be protein synthesis-dependent. However, a majority of proteins regulated with memory formation to bring about these changes in signaling cascades and

synaptic structure have most likely not yet been identified. Furthermore, although it is well established that the mammalian hippocampus is necessary for memory formation, precisely which neuronal circuits and how many neurons are involved has not been investigated using an unbiased approach. In this study we show that the bioorthogonal metabolic labeling techniques BONCAT and FUNCAT can be applied *in vivo* to visualize and affinity purify newly synthesized proteins of the larval zebrafish. We explore the possibility of genetically restricting metabolic labeling via selective expression of a mutant MetRS and demonstrate that larval zebrafish can undergo protein synthesis-dependent place-conditioning. Thus, we have developed the tools necessary to monitor changes in protein synthesis in the larval zebrafish nervous system and therefore possibly identify neuronal circuits involved in long-term memory formation. Furthermore, the techniques described here could be paired to facilitate the identification of effector proteins that are necessary for the physical changes underlying memory formation.

Chapter II

NONCANONICAL AMINO ACID LABELING *IN VIVO* TO VISUALIZE AND
AFFINITY PURIFY NEWLY SYNTHESIZED PROTEINS IN LARVAL ZEBRAFISH

Introduction

Long-term memory formation requires new protein synthesis. Understanding what physical changes within the nervous system underlie learning and memory, specifically what neuronal circuits are involved and what proteins are newly synthesized during memory formation, are major goals in modern neuroscience. However, the identification of newly synthesized proteins has been sparse and limited to individually identified candidate proteins. Advances in mass spectrometry-based approaches now permit the characterization and quantification of proteins, especially when paired with approaches such as stable isotope labeling with amino acids in cell culture (SILAC) (Ong et al., 2002), which allow for comparative quantification between proteomes of differentially stimulated cell populations. However, the proteome of the nervous system is complex and without a chemical handle to enable affinity purification of the newly synthesized proteins specifically, proteins of low abundance will likely be missed.

In addition, the identification of cells or neural circuits that show increased protein synthesis in response to memory formation would allow us to understand the components of memory circuits that undergo long-term modifications after learning. Genetically encoded fluorescent tags, such as GFP, have revolutionized cell biology by permitting visualization of fusion proteins of interest *in vivo* (Tsien, 1998). However, the size of GFP and the requirement for genetic manipulation of the target protein may interfere with its endogenous function, while at the same time only permitting investigation of a small number of candidates at once.

Recently, new techniques for labeling a variety of molecules based on the principle of bioorthogonal metabolic labeling have been developed (Best, 2009). Here, small functional groups that are commonly absent from the cellular environment, most prominently ketones and azides or alkynes, are introduced using the cells' own synthetic machinery. BONCAT (Dieterich et al., 2006; Dieterich et al., 2007) and FUNCAT (Dieterich et al., 2010), two such techniques, have been used to tag and identify or visualize newly synthesized proteins, respectively. BONCAT and FUNCAT utilize noncanonical methionine derivatives, such as the azide-bearing AHA, to bioorthogonally label newly synthesized proteins. AHA can cross cell membranes and be charged onto methionine tRNAs by the endogenous MetRS. During protein synthesis, AHA is introduced in place of methionine, resulting in the introduction of azide groups into the newly synthesized proteins. These azide groups can be used to tag proteins with either an alkyne affinity tag (BONCAT) or an alkyne fluorescent tag (FUNCAT) via selective Cu(I)-catalyzed or strain-promoted [3+2] azide-alkyne cycloaddition (Rostovtsev et al., 2002; Tornøe et al., 2002; Agard et al., 2004). Affinity-tagged proteins can be quantified using immunoblot analysis or separated from the pre-existing proteome by affinity purification and identified by tandem mass spectrometry. Fluorescent tags can be used to visualize newly synthesized proteins, including those proteins of interest whose identities may not be known. Alternatively, the alkyne moiety may also be introduced into newly synthesized proteins by replacing methionine with the noncanonical amino acid homopropargylglycine (HPG) and subsequently labeled using azide-bearing affinity or fluorescent tags. Azides and alkynes are small, so labeling with AHA or HPG is likely to only cause modest, perhaps even insignificant, perturbations of protein folding,

localization (Dieterich et al., 2006) and therefore function of the labeled protein *in vivo*. Furthermore, azides and alkynes are stable under biological conditions and essentially absent from vertebrate cells, which makes the azide-alkyne ligation ('click chemistry') very selective.

BONCAT and FUNCAT techniques have already successfully been applied to study changes in protein synthesis in a variety of different *in vitro* systems in order to investigate a diverse set of biological questions, as described in the introduction. However, given the role of protein synthesis in learning and memory, developing BONCAT and FUNCAT for use in an intact organism in which simple forms of learning may be investigated is the essential next step.

In this chapter we describe the application of these techniques *in vivo*, in the 7-day-old larval zebrafish. We show that AHA is metabolically incorporated into newly synthesized proteins, in a time- and concentration-dependent manner, but has no apparent toxic effects and does not influence simple behaviors. This enables fluorescent labeling of newly synthesized proteins in whole-mount larval zebrafish. Furthermore, we find that stimulation with the GABA antagonist, pentylenetetrazole (PTZ), causes an increase in protein synthesis throughout the proteome, which can also be visualized in intact larvae.

Application of BONCAT and FUNCAT techniques to larval zebrafish

The BONCAT and FUNCAT protocols were adapted to larval zebrafish (Figure 2.1a). All larvae, unless otherwise noted, were analyzed at 7dpf. We incubated larvae in E3

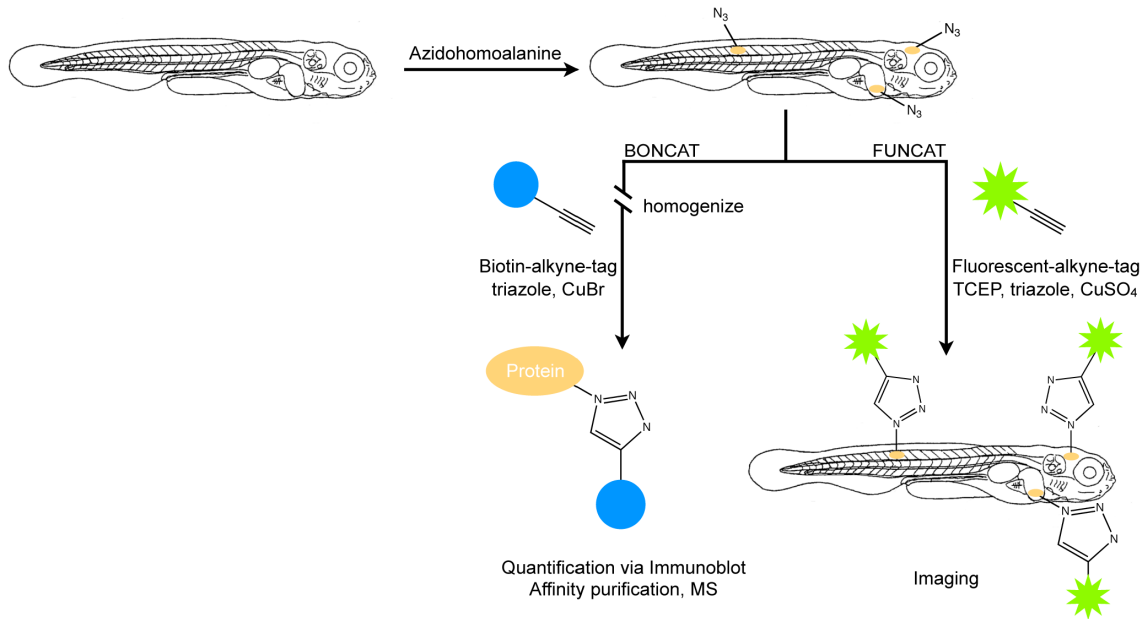


Figure 2.1. Labeling of newly synthesized proteins for quantification, affinity purification (BONCAT) and visualization (FUNCAT) in larval zebrafish

Scheme depicting metabolic labeling of newly synthesized proteins in 7-day-old larval zebrafish using AHA incorporation and Cu(I)-catalyzed [3+2] azide-alkyne cycloaddition. TCEP, *tris*(2-carboxyethyl)phosphine.

embryo medium supplemented with the methionine surrogate AHA (Figure 2.1b) for a period of 0-72h immediately prior to harvesting, with the aim of incorporating the azide group into newly synthesized proteins throughout the zebrafish proteome. To quantify successful incorporation of AHA into protein, larvae were washed, anesthetized, homogenized and the resulting lysate was reacted with biotin-alkyne in the presence of CuBr and the triazole ligand (see Methods). This allowed for detection and quantification of newly synthesized biotin-labeled proteins using immunoblot analysis or for affinity purification of the newly synthesized proteins (BONCAT). To visualize newly synthesized proteins following AHA exposure, larvae were washed, anesthetized,

fixed and permeabilized. Whole mounted larval zebrafish were reacted with AlexaFluor-488-alkyne in the presence of CuSO_4 , the reducing agent *tris*(2-carboxyethyl)phosphine (TCEP) and the triazole ligand, before being imaged using a confocal microscope (FUNCAT). This allowed for visualization of new protein synthesis in the intact larval zebrafish.

Incubation with AHA is not toxic to larval zebrafish and does not alter simple behaviors

Previously, Dieterich et al. showed that metabolic labeling of mammalian cell culture with AHA does not alter global protein synthesis rates or promote ubiquitin-mediated degradation, indicating that AHA incorporation does not cause severe protein misfolding or degradation (Dieterich et al., 2006). To ensure that incubation and incorporation of AHA into newly synthesized proteins is not toxic to the living animal, larvae were exposed to E3 embryo medium supplemented with 0 to 20mM AHA, or 10mM methionine, for 6 to 72h. Larvae were scored as healthy if after incubation they were still responsive to light touch. No significant toxic effects were observed when larvae were incubated with 1-10mM AHA, even after 72h incubations (Figure 2.2a). Only incubations with extremely high (20mM) concentrations of AHA were toxic, beginning around 24h after onset of incubation. This indicates that incubation with low-to-moderate concentrations of AHA, even over extended periods of time, is not toxic to the living animal. In the remainder of the studies reported here concentrations $\leq 4\text{mM}$ AHA were used.

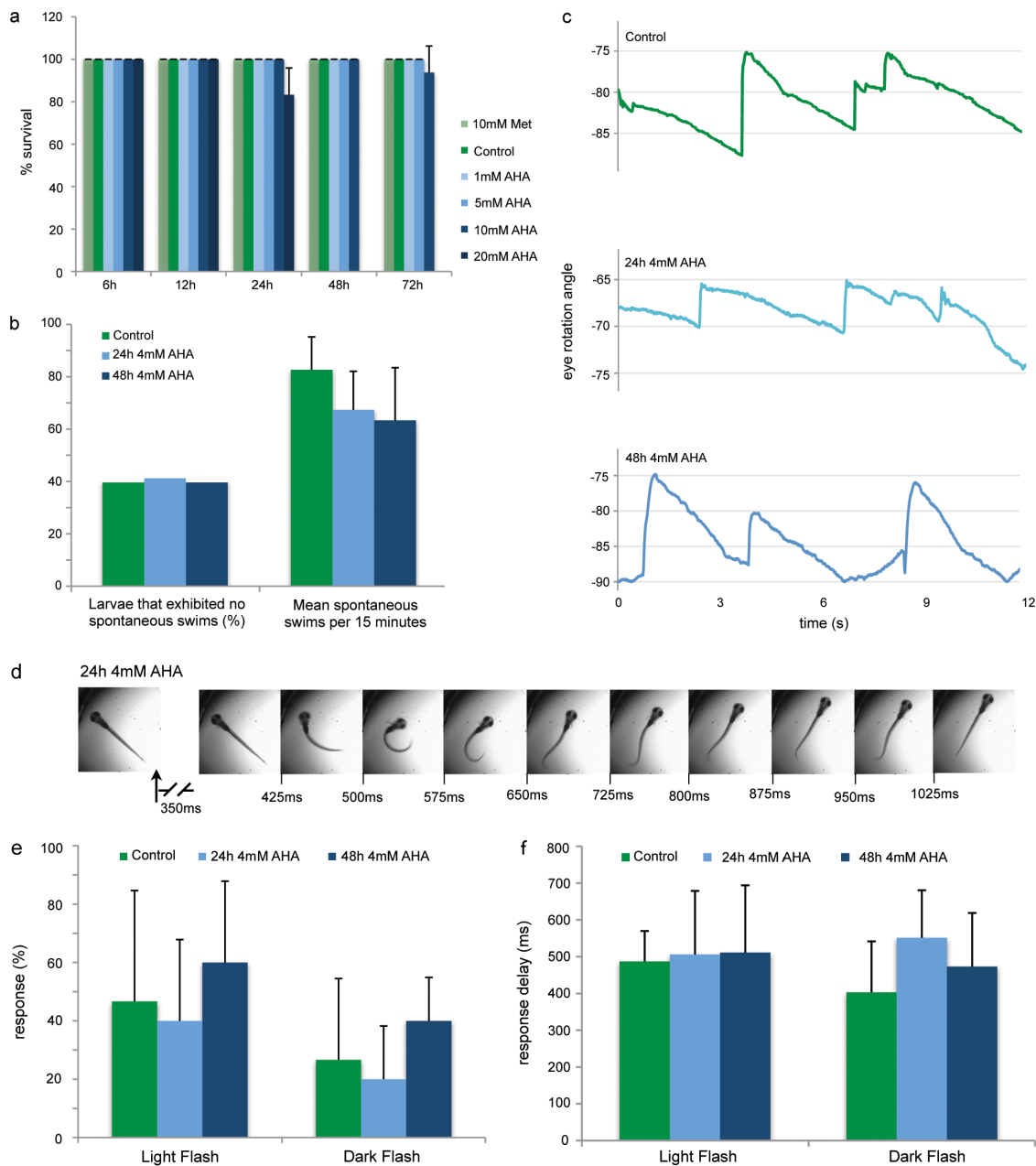


Figure 2.2. At low concentrations, AHA exposure is not toxic and does not significantly alter simple behaviors.

(a) Survival rate of 7-day-old larval zebrafish when incubated with AHA (0 to 20mM, 6 to 72h) or methionine (10mM, 6 to 72h), $n=20$. (b) Quantification of spontaneous swimming behavior of larval zebrafish after AHA incubation (4mM, 0 to 48h). Percentage of larvae that show no spontaneous swimming behavior per 15 minute interval. Mean swimming bursts per 15 minute interval, $n = 10-12$. Differences are not

statistically significant. (c) Traces depicting the angle of eye rotation during a typical optokinetic response after AHA incubation (4mM, 0h to 48h). (d) Sample startle response upon light flash after AHA incubation (4mM, 24h). (e) Mean response percentage to light or dark flash after AHA incubation (4mM, 0 to 48h), n=5 larvae, flashed three times each. Error bars represent standard deviation of response percentage. Differences are not statistically significant. (f) Mean delay in response to light or dark flash after AHA incubation (4mM, 0 to 48h), n=5 larvae, flashed three times each. Error bars represent standard deviation of response time. Differences are not statistically significant.

Next, we explored whether incorporation of AHA causes changes in simple behaviors. We conducted a series of behavioral tests after incubation in E3 medium supplemented with 4mM AHA, for 0-48h. First we investigated spontaneous swimming behavior. 7-day-old larval zebrafish were incubated in 4mM AHA for 0-48h prior to observation, and then placed individually into a 1-cm-by-7.5 cm swimming chamber (Figure 2.3) and their spontaneous swimming bouts were recorded for a period of 15 min. Sample traces of spontaneous swimming behavior are depicted in Figure 2.3. There was no significant difference in the number of individual spontaneous swimming bouts initiated between 48h AHA-incubated, 24h AHA-incubated and control larvae, although there was a small, not significant decrease in the 48h and 24h AHA groups as compared to the control group (Figure 2.2b). There was also no difference in the number of AHA incubated and control larvae that failed to exhibit spontaneous swimming bouts during the 15 minute trial period (Figure 2.2b).

To study whether AHA incubation causes deficits in visual tracking, 7-day-old larvae were tested for the optokinetic response (Huang and Neuhauss, 2008) after incubation in 4mM AHA for 24-48h. Larvae were immobilized in 0.4% low-melting-point agarose in a circular array of LEDs, which delivered a spot of white light that moved in a horizontal plane around the immobilized larvae. Similar to control larvae,

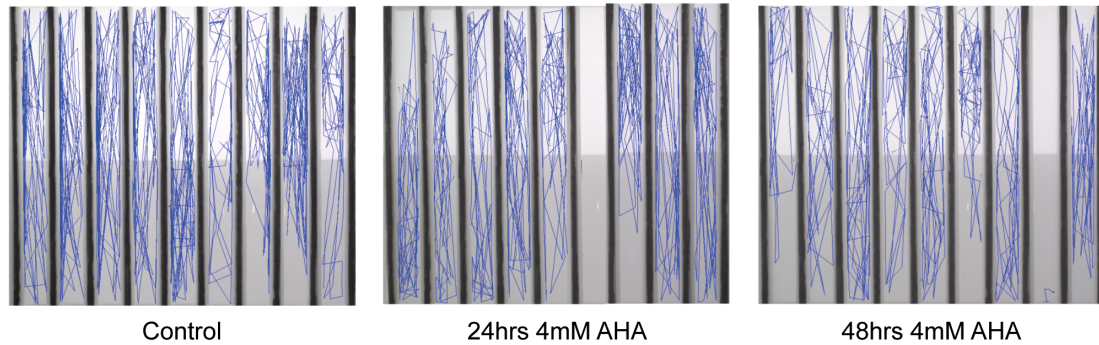


Figure 2.3. Tracks of spontaneous swimming behavior of 7-day-old larval zebrafish with AHA incubation (4mM, 0 to 48h), indicating that spontaneous swimming behavior is not altered by prolonged AHA incubation. 15min interval; frame captured every 10s.

AHA-incubated larvae were able to track the light stimulus, producing smooth tracking eye movements and rapid saccades (Figure 2.2c), indicating that neither visual acuity nor neural circuits underlying visual tracking behavior seem to be affected by prolonged incubation with 4mM AHA. To further test whether AHA incubation altered visual acuity and simple reflexive behaviors, we tested the animal's startle response to light flash and dark flash. Larvae were placed in a circular array of LEDs, which delivered either a light flash or a dark flash while the response of the larva was monitored. Figure 2.2d shows a representative startle response to a light flash in an animal following a 24h incubation with 4mM AHA. The larva is clearly exhibiting a stereotypical C-bend escape response (Kimmel et al., 1974) indicating that AHA has no effect on the motor function associated with escape behavior. Furthermore, incubation with 4mM AHA for 24-48h did not alter the percentage of larval zebrafish that responded to either light or dark flash (Figure 2.2e) nor did it affect the delay in response to either light or dark flash (Figure 2.2f). Therefore, we conclude that AHA incorporation is not toxic and has no effects on

simple behaviors at low concentrations (4mM), even over prolonged incubation periods, making it suitable for labeling newly synthesized proteins *in vivo*.

AHA is metabolically incorporated in larval zebrafish

To determine whether AHA is metabolically incorporated into newly synthesized proteins, we tagged lysates prepared from larval zebrafish incubated for 0-72h with 4mM AHA with biotin-alkyne in the presence of the Cu(I) catalyst. Subsequent dot blot analysis with a biotin antibody revealed successful incorporation of AHA into proteins in an incubation-time dependent manner. A sample dot blot is shown in Figure 2.4a, along with quantification of several experiments. After only a 6h incubation period with E3 embryo medium supplemented with 4mM AHA, statistically significant ($p < 0.005$) AHA incorporation could be detected. After 24h, 48h and 72h incubations, approximately 140ng (± 8 ng), 375ng (± 34 ng) and 699ng (± 72 ng) of biotinylated protein were detected per homogenized larva, respectively. The total soluble protein per larva under the experimental conditions we used was 6.38 μ g (± 0.53 μ g). From this we can estimate that 24h, 48h or 72h incubation with 4mM AHA leads to labeling and tagging of approximately 2.2%, 5.9% and 10.9%, respectively, of the total soluble protein per larval zebrafish. However, as different proteins may show different levels of AHA incorporation, and therefore different biotin signal strength, the analysis given here should be regarded as semi-quantitative.

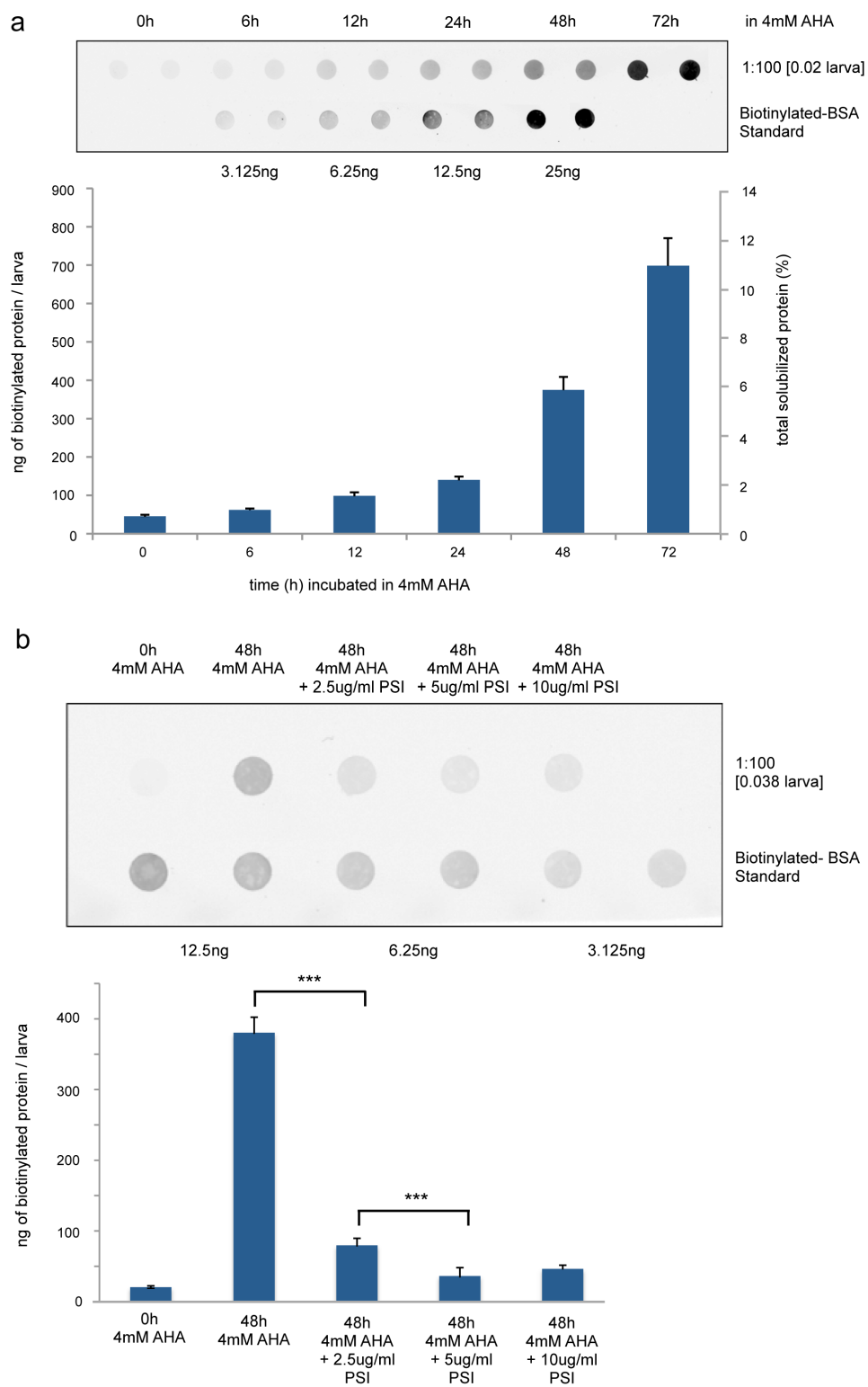


Figure 2.4. AHA is metabolically incorporated into larval zebrafish proteins *in vivo*.

Labeling is both incubation time- and protein synthesis-dependent. Sample immunoblot and quantification of immunoblots of lysates from AHA-treated 7-day-old larval zebrafish reacted with biotin-alkyne (10 μ M) for 12h, probed with antibody against biotin. (a) Larval zebrafish were incubated with 4mM AHA for 0 to 72h, n=4 (b) Larval zebrafish were incubated with AHA (0 or 4mM) or 4mM AHA in the presence of puromycin (2.5 μ g/ml to 10 μ g/ml) for 48 h, n=3. ***p<0.001.

To verify the specificity of AHA incorporation into newly synthesized proteins, we incubated larval zebrafish in E3 embryo medium supplemented with AHA along with low concentrations of the protein synthesis inhibitor puromycin. These very low concentrations of PSI did not have a toxic effect on larval zebrafish (data not shown). Although abundant biotin signal was detected in lysates of larval zebrafish incubated with AHA only, no signal was detected when larval zebrafish were incubated without AHA, and a significantly lower signal was detected when larval zebrafish were incubated in AHA in the presence of puromycin (Figure 2.4b). Furthermore, when the concentration of PSI in the incubation medium was increased from 2.5 μ g/ml to 5 μ g/ml, a significant decrease in AHA-labeled and biotinylated proteins was observed. However, no further decrease was observed when the PSI concentration was further increased to 10 μ g/ml.

The above results confirm that BONCAT labels newly synthesized proteins with high specificity in the larval zebrafish. In addition, we observed that AHA incorporation in larval zebrafish scales non-linearly with incubation time (Figure 2.4a) and we assume that an incorporation plateau would be reached after even longer incubation periods. Also, labeling was AHA concentration-dependent (Figure 2.5). While no signal was detected when 4-day-old larval zebrafish were incubated with 0mM AHA, increasing the concentration of AHA in the incubation medium from 1mM to 4mM resulted in a detectable signal increase. Furthermore, AHA was incorporated not only into a few

select proteins, but into a large variety of newly synthesized proteins throughout the proteome over time, as is shown by the abundance of protein bands on the western blot of affinity purified biotinylated proteins from whole larval zebrafish lysates reacted with the biotin-alkyne and probed against biotin (Figure 2.6a). Biotin signal detected in the samples not incubated with AHA are likely a result of endogenous biotinylation.

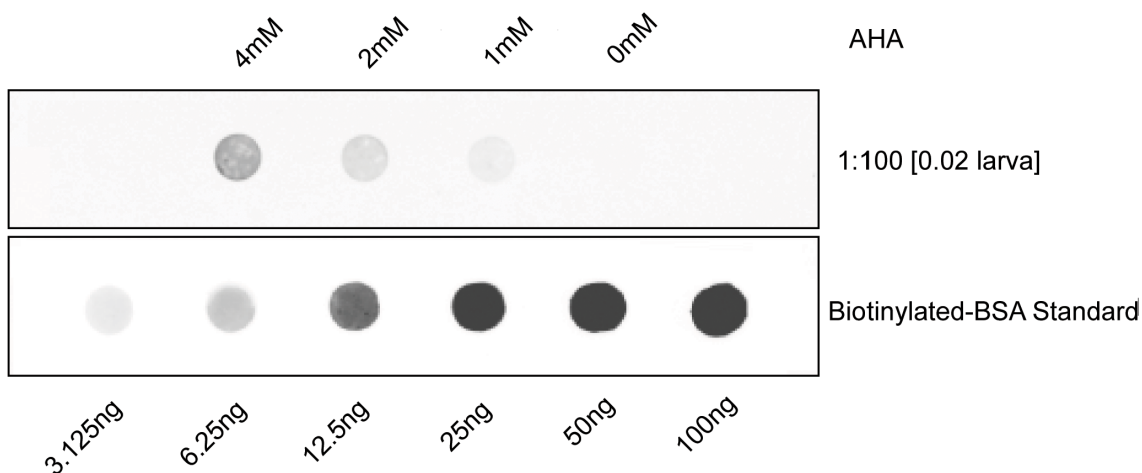


Figure 2.5. Metabolic labeling is AHA concentration-dependent.

Immunoblot of lysates from 4-day-old larval zebrafish reacted with biotin-alkyne ($10\mu\text{M}$) for 12h, probed with an antibody against biotin. Larval zebrafish were incubated with 0 to 4mM AHA for 48h.

To examine whether AHA is also incorporated into newly synthesized proteins in deeper structures such as the nervous system, we incubated 4-day-old transgenic HuC::GFP larval zebrafish with 4mM AHA for 48h. HuC encodes an RNA-binding protein that serves as an excellent early marker for differentiating neurons and the HuC::GFP line is a stable zebrafish transgenic line in which GFP is expressed

specifically in neurons (Park *et al.*, 2000). With the exception of a few cells in the olfactory pit and the lateral line, the majority of these neurons are not surface structures. As before, whole zebrafish lysates were labeled with the biotin-alkyne, affinity purified, and then analyzed using western blot probed against GFP. Only in the sample that was incubated in 4mM AHA for 48h were we able to affinity purify AHA-labeled, biotin-tagged GFP, indicating that AHA is not only incorporated into newly synthesized proteins in surface structures of the larval zebrafish, but also in the nervous system, the sole area of GFP expression in the HuC::GFP transgenic line (Figure 2.6b).

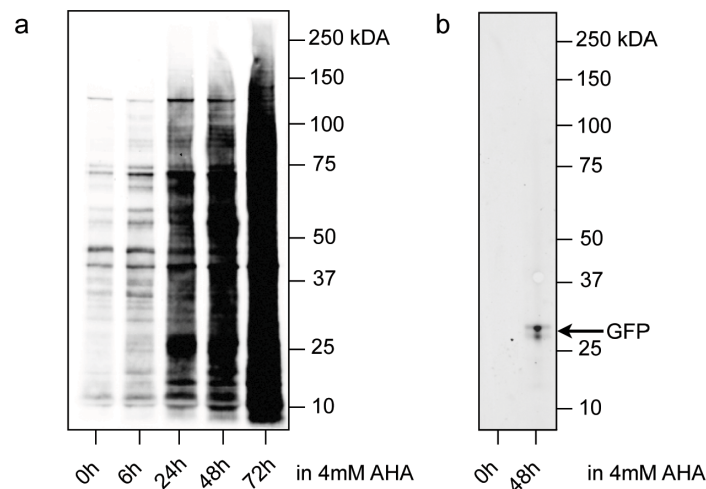


Figure 2.6. AHA incorporation occurs throughout the proteome.

(a-b) Western blot analysis of biotin affinity-purified lysates of larval zebrafish incubated with 4mM AHA for 0 to 72h. (a) Probed with an antibody against biotin. (b) HuC::GFP larval zebrafish lysates probed with an antibody against GFP.

Newly synthesized proteins can be visualized in whole-mount larval zebrafish

We next optimized the labeling and reaction conditions to maximize specific visualization of newly synthesized proteins (FUNCAT) in the intact larval zebrafish. For this purpose we used the mutant zebrafish line *nacre*, which lacks melanophores throughout development (Lister et al., 1999) and thus is relatively transparent and ideal for imaging. Larval zebrafish were, as before, incubated in E3 medium supplemented with 4mM AHA for 0-72h. Larvae were anesthetized, fixed, and permeabilized before whole mount samples were reacted with 5 μ M AlexaFluor-488-alkyne, in the presence of CuSO₄, TCEP and the triazole ligand at room temperature overnight. After several washes in PBDTT buffer, samples were immobilized in 0.4% agarose and imaged using a confocal microscope.

Incubation of larval zebrafish with 4mM AHA followed by reaction with Alexa-488-alkyne resulted in an incubation time-dependent fluorescent labeling of newly synthesized proteins throughout the larval zebrafish (Figure 2.7a). Low fluorescent signals, especially in the muscles of the tail, could be detected after as little as 12h incubation with AHA. Other structures, including the brain, spinal cord, liver, intestines and heart could be readily visualized after 24h incubation with AHA. Specifically, sensory organs such as the neuromasts of the lateral line (indicated by arrow heads in Figure 2.7a, 72h incubation dorsal view panel) and the olfactory pit (Figure 2.7c) seem to be areas of especially high levels of fluorescence. Furthermore, deeper structures such as the optic tectum, cerebellum (Figure 2.7b), and the spinal cord (Figure 2.7d) are not only readily labeled and tagged using the AlexaFluor-488 alkyne, but show differences in

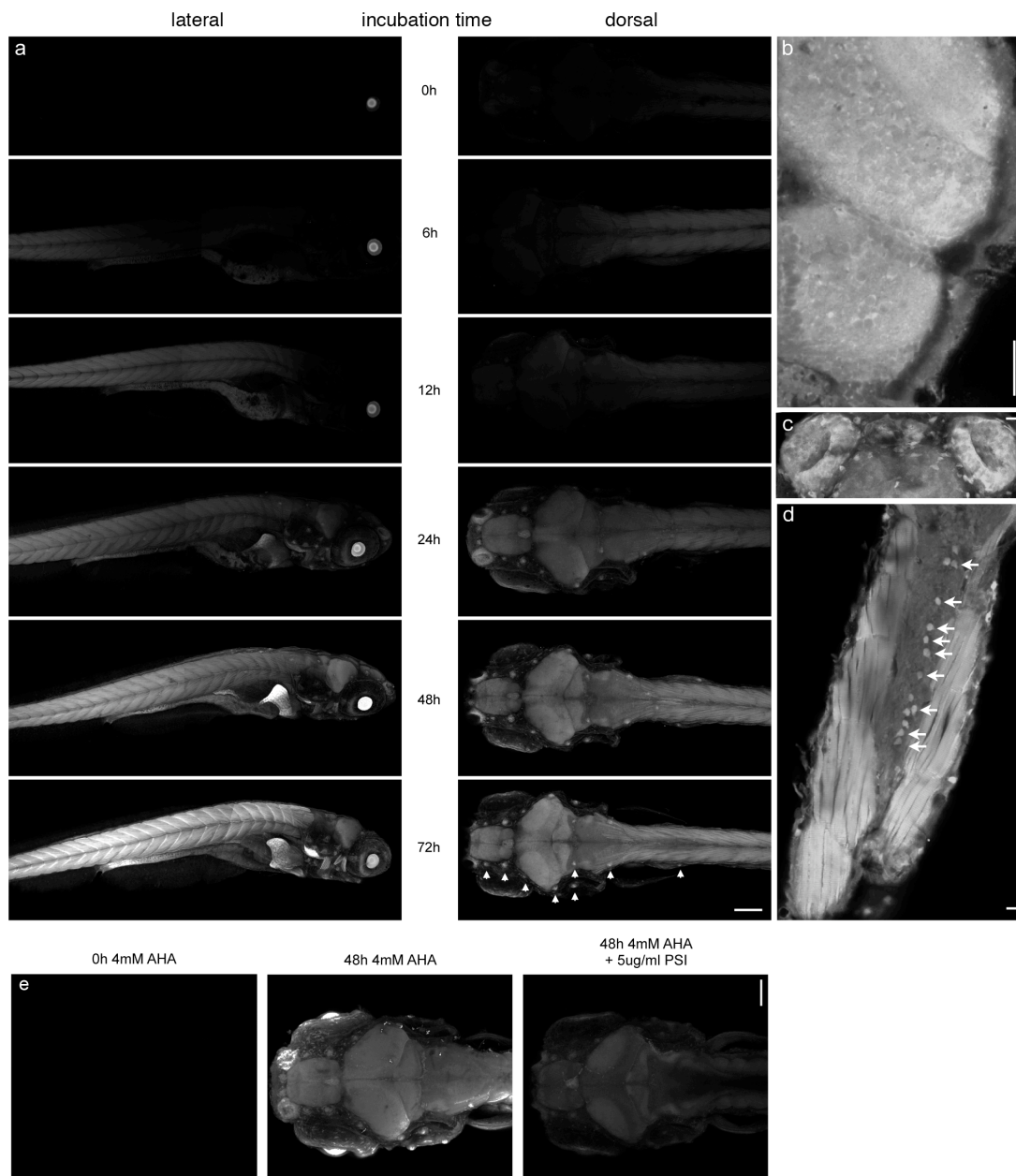


Figure 2.7. Newly synthesized proteins can be visualized in whole-mount larval zebrafish after *in vivo* labeling.

Labeling is both incubation time- and protein synthesis-dependent. (a) 7dpf larval zebrafish were metabolically labeled with 4mM AHA for 0 to 72h prior to fixation and reacted with 5 μ M AlexaFluor-488-alkyne tag for 12h. Left panel, lateral view; right panel, dorsal view. Arrowheads indicate neuromasts of the lateral line. (b-d) 7-day-old larval zebrafish labeled with 4mM AHA for 48h imaged at higher magnification. Dorsal views of (b) optic tectum and cerebellum, (c) olfactory pits, (d) dorsal cross-section of tail, showing tail muscles and spinal cord. Arrows indicate potential DRG neurons. Scale

bar in (a), 150 μ m; in (b-e), 20 μ m. (e) Larval zebrafish were metabolically labeled with 4mM AHA for 0h, 48h or 48h in the presence of 5 μ g/ml puromycin. Dorsal view, scale bar is 100 μ m, n=5.

fluorescence intensity on the cellular level. In the case of the spinal cord, we believe this population of brightly labeled cells corresponds to dorsal root ganglion (DRG) neurons (An et al., 2002) (Figure 2.7d, as indicated by arrows). To verify that the fluorescent signal observed in the above experiments represents incorporation of AHA into newly synthesized proteins, larval zebrafish were incubated in E3 medium containing 4mM AHA in the presence of 5 μ g/ml puromycin (Figure 2.7e). In agreement with previously described results from lysates, abundant fluorescent signal was detected in whole mounts of larval zebrafish incubated with AHA only, while no signal was detected when larval zebrafish were incubated without AHA, and only background signal was detected when larval zebrafish were incubated in AHA in the presence of puromycin. These results suggest that FUNCAT may be used to visualize regions of protein synthesis, specific cells or groups of cells that are metabolically active, during the AHA incubation window in intact larval zebrafish.

The identification of these metabolically active cells or groups of cells may be facilitated by FUNCAT/antibody co-labeling. Antibody staining in whole-mount larval zebrafish has previously been described (Nüsslein-Volhard and Dahm, 2002) and can be used to visualize cell morphology, as well as characterize specific subpopulations of cells based on the expression of marker proteins. However, it was unclear whether the FUNCAT signal would be stable enough to withstand the further sample processing required for concurrent antibody staining. To investigate this, we probed the whole-mount larval zebrafish with an antibody specific to parvalbumin, a calcium-binding

albumin localized in fast-contracting muscles and GABAergic neurons, such as the Purkinje cells of the cerebellum (Schwaller et al., 2002) after the FUNCAT reaction. Larval zebrafish were incubated in E3 medium supplemented with 4mM AHA for 0h or 72h. Following the previously described FUNCAT procedure, samples were probed with parvalbumin primary antibody overnight, washed with PBDTT and incubated with AlexaFluor-488 secondary antibody overnight. After several washes in PBDTT buffer, samples were immobilized in 0.4% agarose and imaged using a confocal microscope, as before.

Visualization of highly metabolically active cells via FUNCAT can be combined with antibody staining to identify these cells in whole-mount larval zebrafish. When paired with antibody staining, larval zebrafish incubated without AHA (Figure 2.8a) showed no FUNCAT signal, while larval zebrafish incubated with 4mM AHA for 72h showed strong FUNCAT signal (Figure 2.8b). Fluorescent signal from parvalbumin antibody staining, however, remained constant, indicating that metabolic labeling with AHA does not interfere with antibody specificity or development and differentiation of specific cell types. Co-labeling with FUNCAT and parvalbumin antibody allows for identification for Purkinje cells of the cerebellum (Figure 2.8c) and GABAergic neurons in the telencephalon (Figure 2.8d), fast-spiking muscle cells in the pectorial fin (Figure 2.8e) as well as GABAergic interneurons in the hindbrain (Figure 2.8f) and spinal cord (Figure 2.8g), while at the same time enabling visualization of relative amounts of new proteins synthesis in these cells. Areas of new protein synthesis can be visualized either with AlexaFluor-488-alkyne concurrently with antibody staining using AlexaFluor-594 secondary (Figure 2.8a-e) or vice versa (Figures 2.8f-g), where newly synthesized

proteins are labeled with AlexaFluor-488-alkyne while parvalbumin presence is detected using AlexaFluor-488 secondary. These results demonstrate that FUNCAT can be combined with antibody labeling in whole-mount larval zebrafish to help identify metabolically active cells.

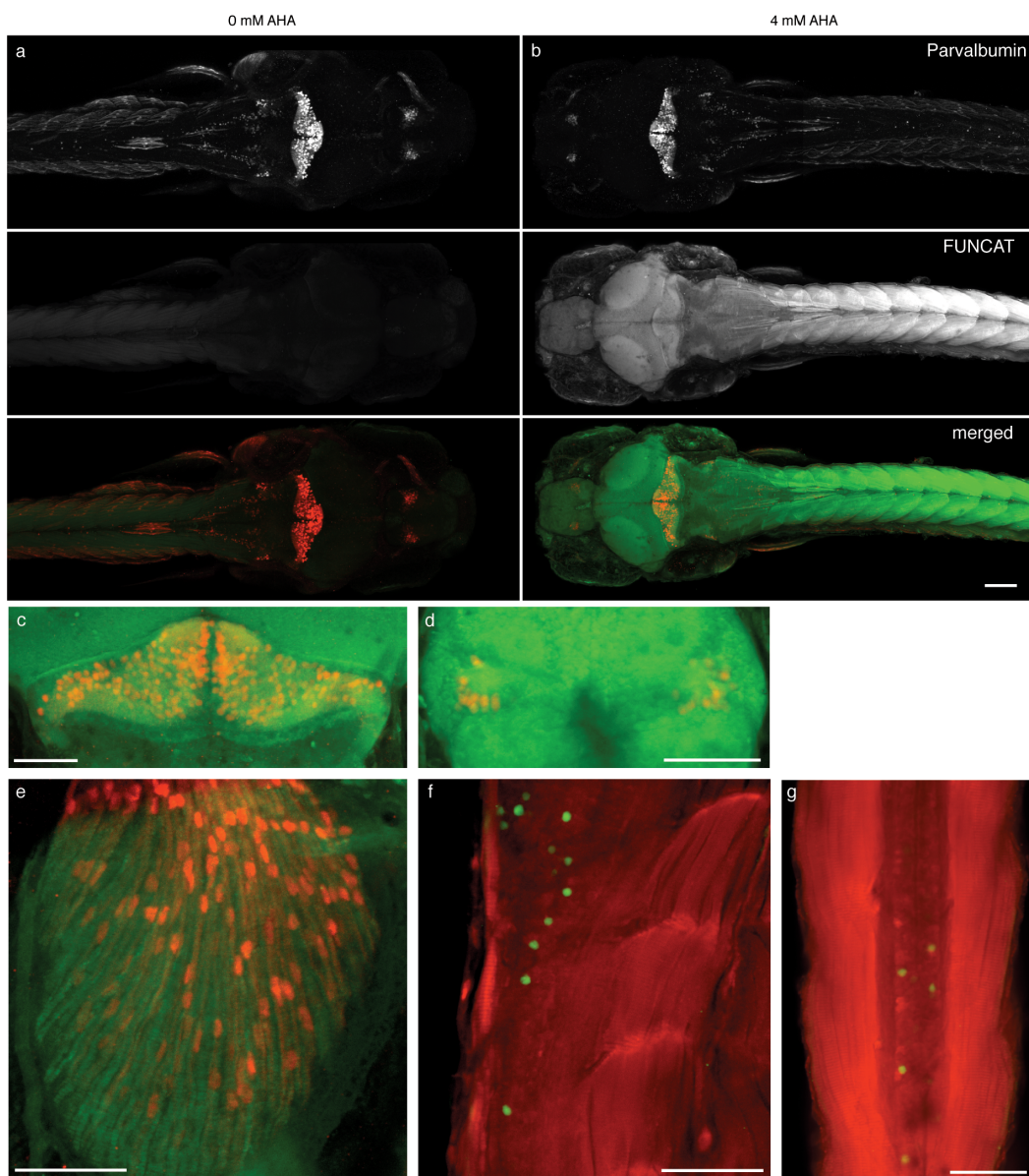


Figure 2.8. FUNCAT can be combined with antibody staining to identify specific cell populations in the whole-mount larval zebrafish.

Larval zebrafish were metabolically labeled with 0mM (a) or 4mM AHA (b) for 72h prior to fixation, reacted with 5 μ M AlexaFluor-488-alkyne for 12h and then probed with primary antibody against parvalbumin and AlexaFluor-594 secondary antibody. (c-e) 7-day-old larval zebrafish labeled with 4mM AHA for 72h (green signal; AlexaFluor-488-alkyne), probed against parvalbumin (red signal; AlexaFluor-594 secondary), imaged at higher magnification. Dorsal view of Purkinje cells of the cerebellum (c); dorsal view of GABAergic neurons in telencephalon (d); lateral view of pectoral fin (e). (f-g) 7-day-old larval zebrafish labeled with 4mM AHA for 72h (AlexaFluor-594-alkyne tag), probed against parvalbumin (AlexaFluor-488 secondary), imaged at higher magnification. Lateral view of hindbrain and caudal spinal cord (f); dorsal view of dorsal cross-section of tail, showing tail muscles and spinal cord, as well as GABAergic interneurons. Scale bar in (a-b) is 100 μ m; in (c-f), 10 μ m.

FUNCAT and BONCAT can be used to detect changes in protein synthesis with chemical stimulation in larval zebrafish

To further investigate whether BONCAT and FUNCAT can be used to identify changes in protein synthesis *in vivo*, larval zebrafish were exposed to PTZ, a GABAergic receptor antagonist that induces epileptic-like neuronal discharges and seizure-like behaviors in rodents and zebrafish (Baraban et al., 2005; Baraban et al., 2007; Naumann et al., 2010). It has been shown that exposure to PTZ induces expression of immediate early genes in larval zebrafish (Baraban et al., 2005), and leads to changes in postsynaptic GABA receptor expression (Brooks-Kayal et al., 1998) and hilar neurogenesis (Parent et al., 1997) in rodents.

Larval zebrafish were exposed to 15mM PTZ for two two-hour periods, 24h and 6h before anesthesia while, being incubated in 4mM AHA for 30h. The amount of biotinylated protein per larva was detected using dot blot analysis, as previously described. We observed a significant increase in the amount of biotinylated protein in larval zebrafish exposed to PTZ during AHA incubation, as compared to larvae that were

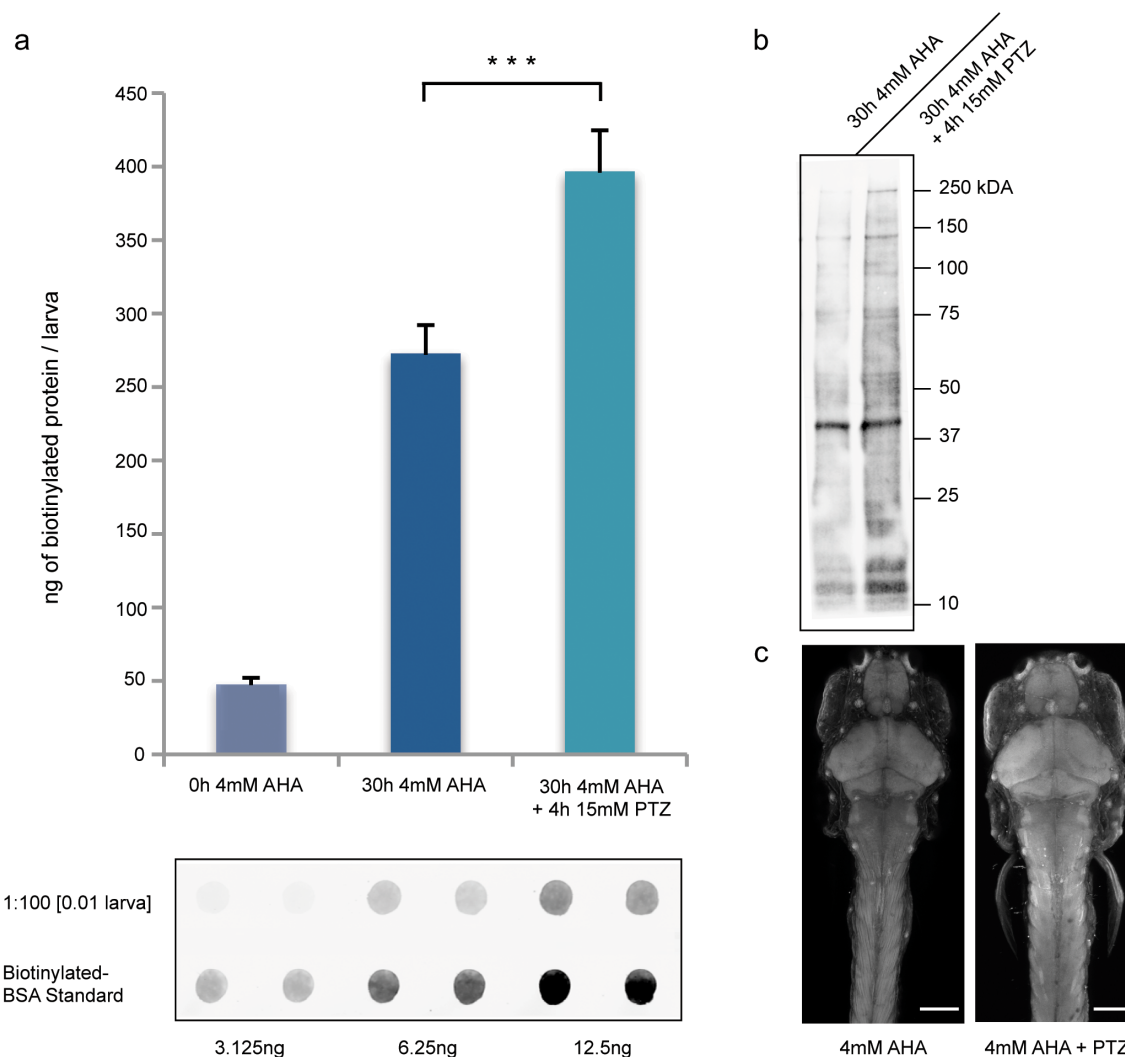


Figure 2.9. The GABA antagonist PTZ induces increased protein synthesis in larval zebrafish.

(a) Sample immunoblot and quantification of immunoblots of lysates from 7-day-old larval zebrafish reacted with biotin-alkyne tag (10 μ M) for 12h, probed with antibody against biotin. Zebrafish were incubated with 4mM AHA (0h or 30h) or with 4mM AHA for 30h as well as 15mM PTZ for two periods of 2h, at 20h and 6h before harvesting, n=3. ***p<0.001. (b) Western blot of biotin affinity-purified lysates of zebrafish incubated with 4mM AHA for 30h with or without 4h 15mM PTZ exposure. (c) Imaging of 7-day-old larval zebrafish after 48h 4mM AHA incubation with or without 4h 15mM PTZ exposure, reacted with AlexaFluor-488-alkyne (5 μ M, 12h); dorsal view. Scale bar is 150 μ m; n=6.

not exposed to PTZ (Figure 2.9a), indicating that PTZ induces an increase in protein synthesis. This increase in biotinylated protein signal is not specific to one or a few protein bands, but seems to be the result of a general increase of protein synthesis throughout the proteome, as detected by western blot analysis of affinity-purified samples (Figure 2.9b). Furthermore, using the FUNCAT technique, we were able to visualize an increase in fluorescent signal in the brain and tail muscles in larval zebrafish that had been incubated in 4mM AHA for 48h and exposed to 15mM PTZ for two two-hour periods (Figure 2.9c). These results indicate that chemical stimulation with the GABAergic receptor antagonist PTZ induces an increase in protein synthesis, which can be quantified and localized using the BONCAT and FUNCAT techniques in larval zebrafish.

Discussion

In this chapter we have shown that the BONCAT and FUNCAT techniques, which introduce bioorthogonal chemical groups into newly synthesized proteins using the endogenous cellular translation machinery, can be applied to the live, 7-day-old larval zebrafish. This enables the enrichment and quantification of newly synthesized proteins when using an affinity tag such as the biotin-alkyne, and the visualization of protein synthesis when using fluorescent-alkyne tags such as the AlexaFluor-488-alkyne. Furthermore, we have shown that chemical stimulation with the proconvulsant PTZ increases protein synthesis, which can be detected using the methods developed in this study.

BONCAT and FUNCAT techniques enable labeling of newly synthesized proteins only when methionine is substituted by noncanonical amino acids during translation. However, AHA competes with endogenous methionine for charging onto methionyl-tRNA by the somewhat promiscuous MetRS. Previous work by the Tirrell group has shown that the charging rate of AHA relative to that of methionine onto methionyl-tRNA in bacterial cells is 1/390, as indicated by the specificity constant k_{cat}/K_m (Kiick et al., 2002), suggesting that not all newly synthesized proteins may incorporate AHA in the presence of endogenous methionine. Furthermore, only proteins that contain at least one methionine residue can be labeled. This, however, is not an important factor in zebrafish, as 97.97% of zebrafish proteins contain at least one non-terminal methionine. Only two of 27,014 currently annotated zebrafish proteins contain no methionine at all (NCBI *Danio rerio* protein database, 5.17.2011).

Recently, the larval zebrafish has become a model organism for small molecule screens, permitting identification of small neuroactive molecules, which alter motor activity (Kokel et al., 2010) or circadian rhythm (Rihel et al., 2010). In the future, the FUNCAT and BONCAT techniques can be paired with different chemical stimuli that cause behavioral changes in order to investigate underlying adjustments of the proteome in distinct regions of the nervous system. Even complex tasks known to be protein synthesis-dependent, such as long-term memory formation, may now be tackled with these techniques to elucidate which neurons and neuronal circuits are affected or involved.

Methods

Reagents

All chemical reagents were of analytical grade, obtained from Sigma unless otherwise noted, and used without further purification. We prepared AHA as described previously (Link et al., 2007). The AlexaFluor-488 alkyne was purchased from Invitrogen (catalog number A10267), while the biotin-alkyne tag was purchased from Jena Biosciences (catalog number TA105).

Zebrafish stocks and husbandry

Adult fish strains AB, HuC::GFP and *nacre* were kept at 28°C on a 14h light/10h dark cycle. Embryos were obtained from natural spawnings and were maintained in E3 embryo medium (5mM NaCl, 0.17mM KCl, 0.33mM CaCl₂, 0.33mM MgSO₄) (Nüsslein-Volhard and Dahm, 2002).

Toxicity and behavioral tests

To test AHA toxicity, larvae were placed five at a time in a 24-well Falcon culture dish well. Each well contained approximately 2ml of embryo medium. Medium was replaced with embryo medium supplemented with 0-20mM AHA or 10mM methionine at the appropriate time point. Larvae were checked for response to light touch at 7 dpf.

For other behavioral tests larvae were incubated in 10ml of embryo medium or embryo medium supplemented with 4mM AHA for 24-48h in a 6-cm petri dish. To monitor spontaneous swimming bouts, larvae were placed individually in a 1cm-by-7.5cm behavioral chamber and spontaneous swimming was recorded using a webcam for 15min. Subsequently, swimming bouts were scored. The optokinetic response was measured by immobilizing 7dpf larval zebrafish in a drop of 0.4% low-melting-point agarose (Promega) in embryo medium. Immobilized larvae were placed in a circular array of LEDs, which delivered a spot of white light that moved in a horizontal plane around the immobilized larvae. The optokinetic response was recorded using a high-speed camera (Redlake MotionScope M3) and eye movements were analyzed using Matlab. The startle response was measured by placing larval zebrafish in a 5cm petri dish in a circular array of LEDs. LEDs delivered 50ms light or dark flashes, while a high-speed camera mounted above the arena recorded responses. Response onset was scored.

Copper-catalyzed [3+2] azide-alkyne cycloaddition chemistry and detection of tagged proteins using biotin-alkyne (BONCAT)

Zebrafish larvae were incubated in embryo medium supplemented with AHA, after which larvae were washed three times in 25ml embryo medium. Larvae were moved into a 1ml Eppendorf tube in ~1ml of embryo medium and anesthetized on ice for one hour. Remaining medium was removed and anesthetized fish were washed once with 1ml of ice-cold PBS + protease inhibitor (PI; Roche, complete ULTRA Tablets, Mini,

EDTA-free Protease Inhibitor cocktail tablets). PBS+PI was removed and replaced with 100 μ L of fresh PBS+PI. Zebrafish larvae were homogenized using a Kontes Pellet Pestle Motor. 1% SDS and 1 μ L of Benzonase (\geq 500U) were added and the lysate vortexed and heated at 95°C for 10min. Lysate was allowed to cool to room temperature, before 400 μ L of PBS+PI and 0.2% triton X-100 were added. Then, lysates were centrifuged at 15,000g at 4°C for 10min. Supernatant was transferred to a new 1ml Eppendorf tube. For BONCAT, samples were reacted with 10 μ M biotin-alkyne in the presence of 200 μ M triazole ligand (*tris*[(1-benzyl-1H-1,2,3-triazol-4-yl)methyl]amine, 97%) and 5mg/ml CuBr suspension and incubated at 4°C with agitation overnight. Samples were then centrifuged at 4°C for 5min at 5,000g to pellet CuBr. Supernatant was moved into a new 1ml Eppendorf tube. To remove excess, unligated biotin-alkyne, samples were applied to a PD MiniTrap G-25 size exclusion column (GE Healthcare). Samples were then analyzed using 'dot blots' and affinity purified as described in Dieterich et al. (2007). For western blot analysis of affinity purified samples, 25 μ L of washed NeutrAvidin beads (Thermo Scientific) previously incubated with sample were heated at 95°C for 5min in 50 μ L of LDS sample buffer (Invitrogen) containing reducing agent (Invitrogen). Proteins were separated on precast NuPAGE 4-12% Bis-Tris gels (Invitrogen) and transferred to PVDF membranes and blocked in PBST (PBS+0.1% Tween-20) containing 5% milk. For detection, membranes were probed with goat anti-biotin (Biomol) and mouse anti-goat LI-COR-IR 800 secondary antibody and analyzed using the Odyssey Infrared Imaging System (LI-COR).

Copper-catalyzed [3+2] azide-alkyne cycloaddition chemistry and detection of tagged proteins using fluorescent-alkyne (FUNCAT)

To image AHA-labeled proteins, larval zebrafish were incubated in embryo medium supplemented with AHA, washed and anesthetized as described above. Remaining embryo medium was removed and replaced with ~1ml of fixation solution (4% PFA, 88mM sucrose in PBS). Larvae were fixed at room temperature for 3h, dehydrated in 100% methanol and stored at -20°C overnight. Larvae were rehydrated through successive 5min washes with 75% methanol in PBST, 50% methanol in PBST, 25% methanol in PBST and finally PBST. This was followed by two washes in PBDTT (PBST + 1% DMSO and 0.5% Triton X-100) and an hour permeabilization in Protease K (10µg/ml in PBST). After permeabilization, larvae were briefly washed with PBST and then immediately post-fixed for 20min. Larvae were washed twice for 5 minutes with PBST and three times for 5min with PBDTT, before blocking (5% BSA, 10% goat serum in PBDTT) for at least 3h at 4°C. Larvae were washed three times in PBST (pH 7.8), before being conjugated to the probe by addition of 200µM triazole ligand, 5µM AlexaFluor-488-alkyne, 200µM CuSO₄ and 400µM TCEP at room temperature overnight with gentle agitation. Samples were washed four times for 30min in PBDTT+0.5mM EDTA, and twice for 1h in PBDTT, before being rinsed in PBST and immobilized on Matek dishes using 0.4% low-melting-point agarose.

For subsequent antibody staining, samples were washed four times for 30min in PBDTT+0.5mM EDTA after ligation to fluorescent-alkyne. Samples were then incubated in primary antibody (mouse monoclonal parvalbumin, concentration of 1:500;

Shimizu lab) in a 1:5 dilution of blocking solution overnight at 4°C. Samples were washed four times for 30min in PBDTT before incubation with secondary antibody overnight at 4°C. Finally, samples were washed four times for 30min, and twice for 1h in PBDTT, before being washed in PBST and immobilized on Matek dishes using 0.4% low-melting-point agarose. Images were obtained using a Zeiss LSM780 laser scanning confocal microscope with 10X or 20X air lens. AlexaFluor-488 was excited with the 488nm line of an argon ion laser and the emitted light was detected between 510 and 550 nm. We performed all post-acquisition processing and analysis with ImageJ (NIH). Significance was tested for using the two-tailed T-test and error bars represent standard deviation.

Chapter III

LABELING NEWLY SYNTHESIZED PROTEINS IN GENETICALLY SPECIFIED
LARVAL ZEBRAFISH CELL POPULATIONS MEDIATED BY SELECTIVE
EXPRESSION OF A MUTANT MetRS

Introduction

MetRS catalyzes the charging of methionine onto methionyl-tRNAs through a two-step mechanism involving activation of methionine by ATP, followed by transfer onto the 3' end of methionyl-tRNA. The binding specificity and the catalytic efficiency of aaRS, such as MetRS, are key features of the translation process. Despite the specificity of MetRS for methionine, BONCAT and FUNCAT have exploited the somewhat promiscuous nature of this enzyme that enables the charging of the structurally similar methionine analog AHA to methionyl-tRNA and thereby the incorporation of AHA into newly synthesized proteins in wild-type cells. Although the number of noncanonical amino acids, such as AHA, which are conclusively translationally active *in vivo* is growing, it is generally still limited to only those analogs that are structurally and functionally similar to the cognate amino acids they are replacing.

The introduction of specific mutations into the protein sequences of aaRS' eases these limitations. In particular, the Tirrell group showed that altering the specificity of *E. coli* MetRS enables metabolic incorporation of otherwise inert noncanonical amino acids, such as the long-chain azide-bearing Azidonorleucine (ANL), in a bacterial system. ANL cannot bind to wild-type MetRS and therefore cannot be incorporated into newly synthesized proteins in wild-type cells. MetRS is the ideal candidate for such an approach due to the wealth of structural data available and the fact that MetRS lacks the 'sieve-type' editing activity found in related aaRS, so that only mutations of the well-characterized synthetic binding pocket region of MetRS need to be considered. Using a rapid, flow-cytometry-based screening protocol, the investigators first examined a non-

saturated library of mutant MetRS for their ability to enable incorporation of ANL into proteins (Link et al., 2006). Four highly conserved residues, L13, P257, Y260 and H301, thought to be essential to binding specificity, were mutated to all other possible amino acids and the L13G mutation was identified as sufficient to enable incorporation of ANL into newly synthesized proteins in *E. coli*. In 2009, Tanrikulu et al. followed up on this study by describing a screen of a saturated library of mutant MetRS, focusing exclusively on mutations of L13, Y260 and H301 (Tanrikulu et al., 2009). Here, two new *E. coli* MetRS mutants with higher charging rates and greater specificity for ANL in the presence of methionine than the previously described L13G mutant were introduced: NLL in which L13, Y260 and H301 are replaced by asparagine (N), leucine (L) and leucine (L), respectively, and PLL in which L13, Y260 and H301 are replaced with proline (P), leucine (L) and leucine (L), respectively.

The ability of cells expressing these mutant MetRS constructs to incorporate ANL, a noncanonical amino acid that is excluded by the endogenous protein synthesis machinery, opens the door to cell-specific metabolic labeling of proteins. Building on the previously described work, Ngo et al. showed that *E. coli* cells bearing the NLL mutant MetRS are able to utilize ANL as a surrogate for methionine in protein synthesis, while wild-type cells are inert to ANL and proteins made in these cells are not labeled. In co-culture experiments, labeling of newly synthesized proteins with affinity reagents or fluorescent dyes is restricted to cells expressing the mutant MetRS, therefore enabling cell-specific enrichment, identification and visualization, even in mixtures of different cell types. This approach, when applied to complex bacterial communities, may allow for the selective investigation of proteomes of specific species in their native

environmental niche, which might be occupied by hundreds of other microorganisms and be otherwise inaccessible to specific metabolic labeling.

When applied to multicellular organisms, cell-type-specific metabolic labeling will facilitate the visualization of protein synthesis in specific cell types by preventing labeling in other cell types. This will improve detection of protein synthesis differences between cells within the labeled group, within different cellular compartments of the labeled cell, as well as between the same cells after different types of stimulation, either chemical or behavioral. Also, removal of background labeling will improve the visualization of the morphology of the labeled cells, thereby permitting the identification of cells of high metabolic activity. Furthermore, genetic restriction of metabolic labeling will reduce the complexity of the newly synthesized proteome during the labeling window, thereby possibly permitting the identification of proteins of low abundance that might otherwise have been missed.

In this chapter, we demonstrate that genetically restricted expression of a zebrafish mutant MetRS in the larval zebrafish enabled cell-specific metabolic labeling of proteins *in vivo*. MetRS binding pocket residues are highly conserved between *E. coli* and zebrafish and when the L13G mutation was introduced into the zebrafish MetRS protein sequence, COS7 cells transiently expressing this mutant MetRS incorporated ANL into newly synthesized proteins specifically. Furthermore, cell-specific transient and stable expression of the L13G-MetRS permitted restricted metabolic labeling and therefore visualization of newly synthesized proteins in the larval zebrafish. In contrast, neither NLL nor PLL mutations of the zebrafish MetRS protein sequence resulted in incorporation of ANL either *in vitro* or *in vivo*.

Cell-specific metabolic labeling of a multicellular organism, the larval zebrafish

The azide-bearing noncanonical amino acid AHA is structurally similar to methionine, allowing it to act as a surrogate for methionine and to bind to the catalytic domain of wild-type zebrafish MetRS. This allows for charging of AHA onto methionyl-tRNA and incorporation of AHA in place of methionine into newly synthesized proteins both *in vitro* (Dieterich et al., 2006; Dieterich et al., 2007; Dieterich et al., 2010) and *in vivo* (Hinz et al., 2012). As described previously, metabolic labeling with AHA occurs throughout all tissues of the larval zebrafish, but cell-type-specific labeling has obvious advantages. ANL, a long-chain azide bearing noncanonical amino acid could alternatively be used for the click chemistry ligation of labeled, newly synthesized proteins to alkyne-affinity and alkyne-fluorescent tags. However, ANL has been shown to be metabolically inert in wild-type cells, as it is too bulky to fit into the binding pocket of endogenous MetRS and can therefore not be charged onto methionyl-tRNA in wild-type cells. Hence, wild-type larval zebrafish incubated with ANL show no fluorescent signal after click reaction with fluorescent-alkyne.

However, screens of *E. coli* mutant MetRS libraries have identified specific mutations that impart bacterial cells with the ability to metabolically incorporate ANL. Specifically, the residues L13, Y260 and H301 were shown to play an important role in the substrate specificity of MetRS. As schematically depicted in Figure 3.1, we propose that introduction of the L13G mutation into the zebrafish MetRS protein sequence will enable metabolic labeling with ANL. By constructing a stable transgenic zebrafish expressing this zebrafish mutant MetRS in specific cell populations, such as the

telencephalon, we aim to restrict metabolic labeling *in vivo*. Subsequent incubation of the transgenic fish with ANL should enable us to observe labeling and downstream identification of newly synthesized proteins in these specific cell populations, as opposed to the whole organism.

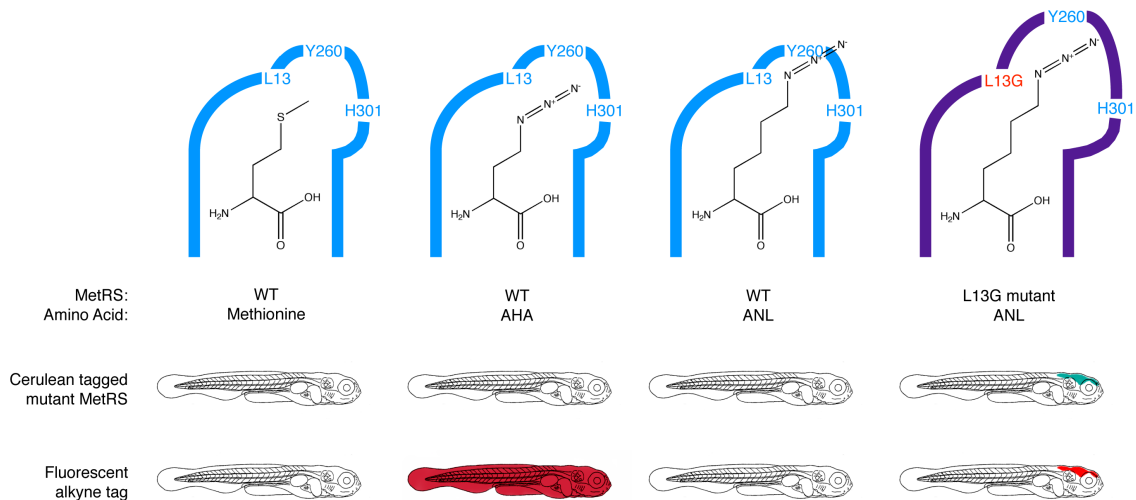


Figure 3.1. Genetically restricted metabolic labeling

Scheme of binding pocket of wild-type (WT) and mutant (L13G) MetRS, highlighting residues important for binding specificity, which interact with methionine, AHA or Azidonorleucine (ANL). Cartoons of larvae indicate hypothetical scenarios in which either the WT MetRS or the L13G mutant is expressed. Cerulean signal indicates hypothetical expression of mutant MetRS in the telencephalon. Red signal indicates hypothetical FUNCAT signal. Restricted expression of L13G MetRS in larval zebrafish enables cell-specific metabolic labeling with ANL.

The residues involved in forming the catalytic domain and hence in determining the substrate specificity of MetRS, are highly conserved between different species ranging from *E. coli* to humans, as evidenced by the sequence alignment of *E. coli*, zebrafish, mouse and human MetRS protein sequences (Figure 3.2). Residues highlighted in Figure 3.2 have been determined to be less than 4Å away from the bound

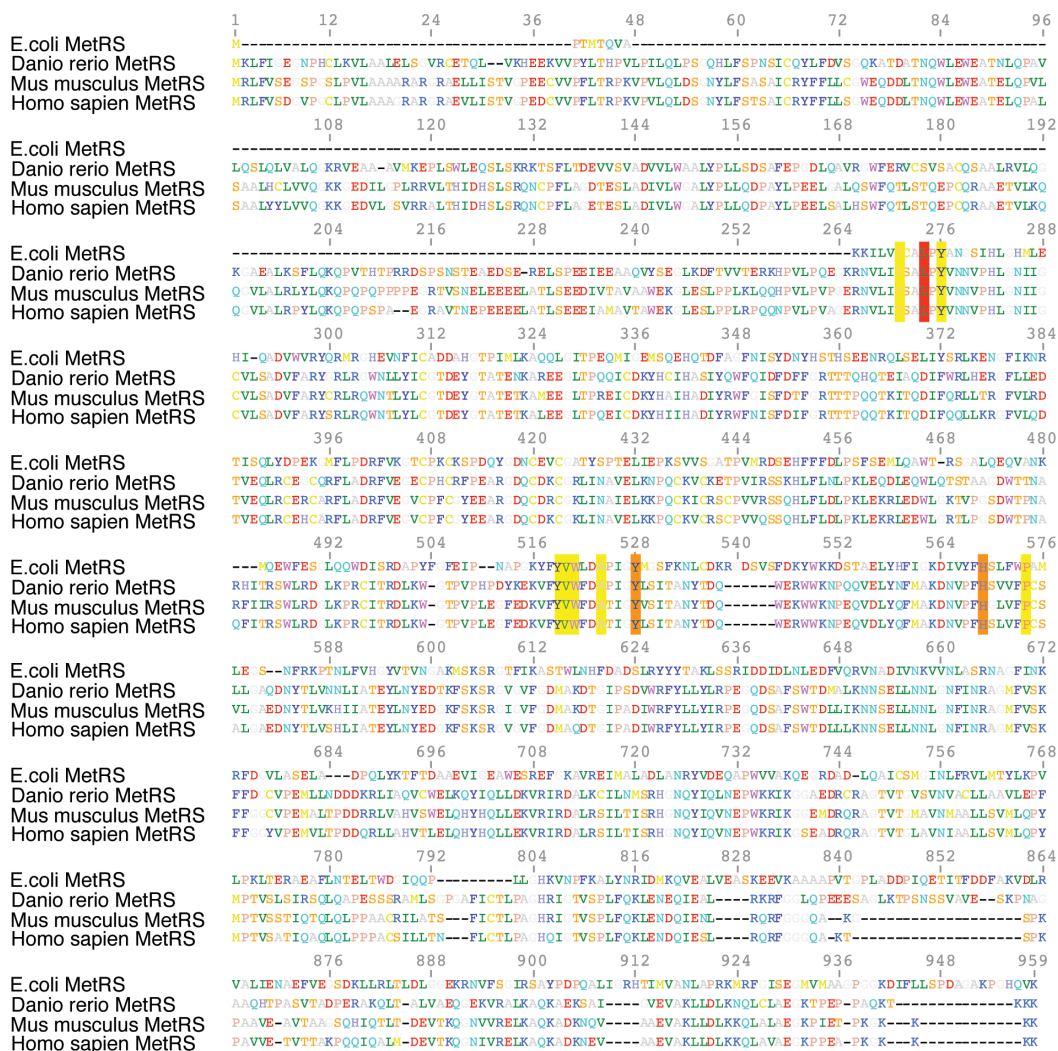


Figure 3.2. MetRS protein sequence alignment of *E. coli*, *Danio rerio*, *Mus musculus* and *Homo sapiens*

Residues highlighted are involved in binding pocket formation and highly conserved between species. L13 is highlighted in red.

methionine using structural analysis of the 3-dimensional model of methionine-charged MetRS (Serre et al., 2001), and therefore are likely to play an important role in determining the substrate specificity of the enzyme. These residues are all highly conserved between species and include the residues L13 (highlighted in red), Y260 and

H301 (highlighted in orange) that were mutated in the *E. coli* MetRS to enable ANL charging onto methionyl-tRNA. Due to this conservation between the mutated residues of the *E. coli* and the zebrafish MetRS protein sequence, we hypothesized that introducing the same mutations into the zebrafish MetRS protein sequence would permit ANL charging onto methionyl-tRNA in cells expressing this mutant zebrafish MetRS.

Zebrafish L13G-MetRS mutant enables metabolic labeling with ANL in vitro.

To investigate whether the zebrafish L13G-MetRS mutant enables ANL incorporation *in vitro*, we cloned the zebrafish MetRS cDNA sequence into the Clontech pEGFP-C2 vector to create a CMV-promoter-driven, MetRS N-terminal EGFP fusion construct (L13G MetRS-C2-EGFP; see Appendix A for vector map and sequence). The L13G mutation was introduced into the zebrafish MetRS sequence of this construct using site-directed mutagenesis and the construct was transiently transfected into COS7 cells. Transfected COS7 cells were incubated with 4mM AHA for 4h in the presence or absence of the protein synthesis inhibitor anisomycin. These samples served as positive controls to ensure that transfection with the L13G MetRS-C2-EGFP construct does not interfere with metabolic labeling. Alternatively, transfected cells were incubated with 4mM ANL for 4h in the presence or absence of anisomycin. Additionally, untransfected cells were incubated with 4mM ANL for 4h. This sample served as a negative control. Lysates of all samples were reacted to 10 μ M biotin-alkyne overnight and analyzed using western blots probed against biotin. Equal volumes of samples were loaded onto a second

gel, which was stained with Coomassie Brilliant Blue. Biotinylated-protein signal was normalized to Coomassie signal to evaluate relative incorporation of ANL and AHA into newly synthesized proteins.

Only COS7 cells expressing L13G MetRS-C2-EGFP incubated in AHA or ANL in the absence of protein synthesis inhibitors showed labeling after reaction to the biotin-alkyne (Figure 3.3). Co-incubation with anisomycin abolished the biotin signal, indicating that specifically newly synthesized proteins were detected. COS7 cells not expressing the L13G MetRS-C2-EGFP but incubated with ANL in the absence of anisomycin also showed no biotin signal. This demonstrates that metabolic ANL incorporation and subsequent detection of newly synthesized proteins using the biotin-alkyne is specific to cells expressing the L13G MetRS-C2-EGFP (Figure 3.3a). Normalized biotin signals from transfected cells incubated with either AHA or ANL were very similar (Figure 3.3b). However, due to limitations of transfection rates, only approximately 70-80% of COS7 cells expressed the L13G MetRS-C2-EGFP construct, as determined by visual inspection of EGFP expressing cultured cells before harvesting. This suggests that the charging rate of ANL by the zebrafish L13G-MetRS mutant onto methionyl-tRNAs may be slightly higher than the charging rate of AHA by wild-type MetRS, possibly making metabolic labeling with ANL in cells expressing the mutant MetRS more efficient. The results described in this section confirm that the L13G mutation discovered in *E. coli*, when introduced into the zebrafish MetRS protein sequence and expressed *in vitro*, imparts to cells the ability to metabolically incorporate the larger noncanonical amino acid ANL.

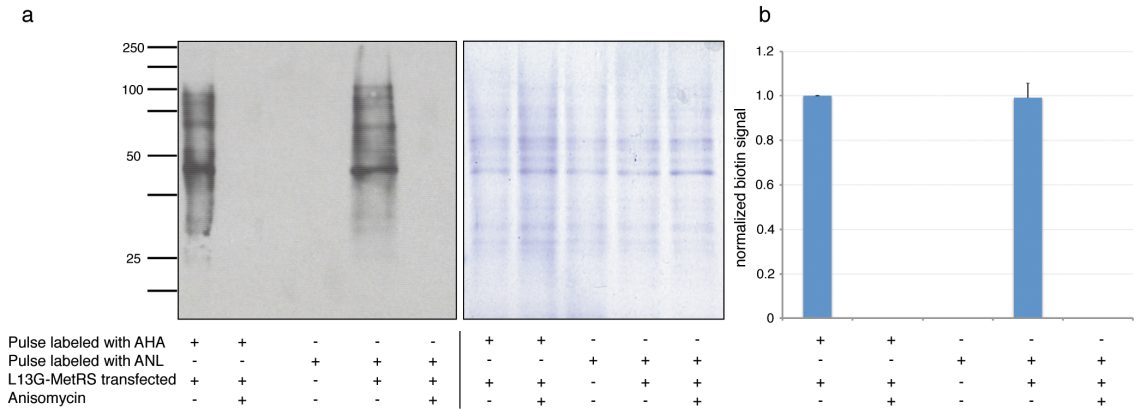


Figure 3.3. Cell-selective labeling with ANL *in vitro*

(a) COS7 cells were transfected with the zebrafish L13G MetRS-GFP fusion construct, metabolically labeled with 4mM AHA, 4mM ANL or no noncanonical amino acid in the presence or absence of anisomycin (40 μ M). Cells were homogenized and reacted to the biotin-alkyne (10 μ M) for 12h. Coomassie detection of total protein from pulse-labeled cells (right) and western blot probed against biotin (left). (b) Relative quantification of biotin signal.

Zebrafish L13G-MetRS mutant enables metabolic labeling with ANL in vivo

To investigate whether the zebrafish L13G-MetRS mutant enables ANL incorporation *in vivo*, we created the Upstream Activator Sequence (UAS)::L13G-MetRS responder construct illustrated in Figure 3.4a (for vector map and sequence see Appendix A). Here the 4x non-repetitive (nr) UAS sequence designed by the Halpern lab (Akitake et al., 2011) drives expression of the fluorescent protein cerulean and zebrafish mutant L13G-MetRS. The 4x nr UAS sequence has been shown to be far less susceptible to methylation than the previously standard 14x UAS sequence and thereby decreases the likelihood of variegation of expression in subsequent generations. The viral 2A peptide

sequence (Szymczak et al., 2004; Provost et al., 2007) causes ribosomal skipping and therefore hinders peptide bond formation between the penultimate glycine residue and the terminal proline residue within the 2A sequence (Donnelly et al., 2001). The inclusion of this sequence enables translation of equimolar amounts of the fluorescent protein and the L13G-MetRS. As a result, the cerulean contains a short 2A peptide C-terminal fusion (17 AA), whereas the L13G-MetRS only contains a single proline residue at its N-terminus, unlikely to interfere with protein folding. The short 6X His tag was included as a C-terminal fusion to the L13G-MetRS to enable antibody detection and quantification of the mutant MetRS protein levels, while the Tol2 transposable element sequences originally discovered in Medaka fish (Kawakami, 2005), when co-injected with transposase mRNA, facilitate integration into the genome.

First, we investigated whether transient mosaic expression of the UAS::L13G-MetRS construct would enable metabolic labeling with ANL and subsequent fluorescent labeling of newly synthesized proteins *in vivo*. The UAS::L13G-MetRS construct was injected into single-cell embryos of a pan-neuronally expressing Gal4 driver line (s1101t) and embryos were sorted for cerulean fluorescence at 30hpf. Cerulean-positive embryos were incubated in E3 embryo medium without noncanonical amino acid, or supplemented with either 4mM AHA or 4mM ANL for 48h, beginning 5dpf. Cerulean-negative embryos were incubated in E3 embryo medium supplemented with 4mM ANL for 48h, again beginning 5dpf. Larvae were anesthetized, fixed, and permeabilized, before whole-mount samples were reacted with 5 μ M AlexaFluor-488-alkyne, in the presence of CuSO₄, TCEP and the triazole ligand, at room temperature overnight. After several

washes in PBDDTT buffer, samples were immobilized in 0.4% agarose and imaged using a confocal microscope.

Only the larvae transiently expressing the UAS::L13G-MetRS construct, as indicated by cerulean fluorescence, and incubated in 4mM ANL showed cell-type-specific metabolic labeling (Figure 3.4). Larvae expressing the L13G-MetRS, incubated without noncanonical amino acid, showed no fluorescent signal after reaction to AlexaFluor-594 (signal seen in Figure 3.4b represents laser line reflection off of the lens), while those incubated in 4mM AHA showed non-cell-specific metabolic labeling throughout all tissues. Larval zebrafish incubated in 4mM ANL but not expressing the L13G-MetRS, as evident by lack of cerulean expression at 30hpf, did not show metabolic labeling (Figure 3.4e). Higher magnification images of a dorsal view of the telencephalon and nasal cavity of cerulean-positive larvae incubated with either AHA (Figure 3.4f) or ANL (Figure 3.4g) clearly showed that incubation with AHA leads to diffuse labeling, while incubation with ANL leads to cell-specific labeling. In Figure 3.4g, cell-type-specific metabolic labeling allows for differences in fluorescent signal between individual labeled cells to be easily observed and in some cases for neurites to be identified.

Next, metabolic labeling with ANL or AHA in L13G-MetRS transiently transfected zebrafish larvae was examined using the biotin-alkyne tag. As before, the UAS::L13G-MetRS construct was injected into single-cell embryos of the pan-neuronally expressing Gal4 driver line and embryos were sorted for cerulean fluorescence at 30hpf. Cerulean-positive embryos were incubated in E3 embryo medium without noncanonical amino acid, or supplemented with either 4mM AHA or 4mM ANL for 48h, beginning 5dpf. Cerulean-negative embryos were incubated in E3 embryo medium supplemented

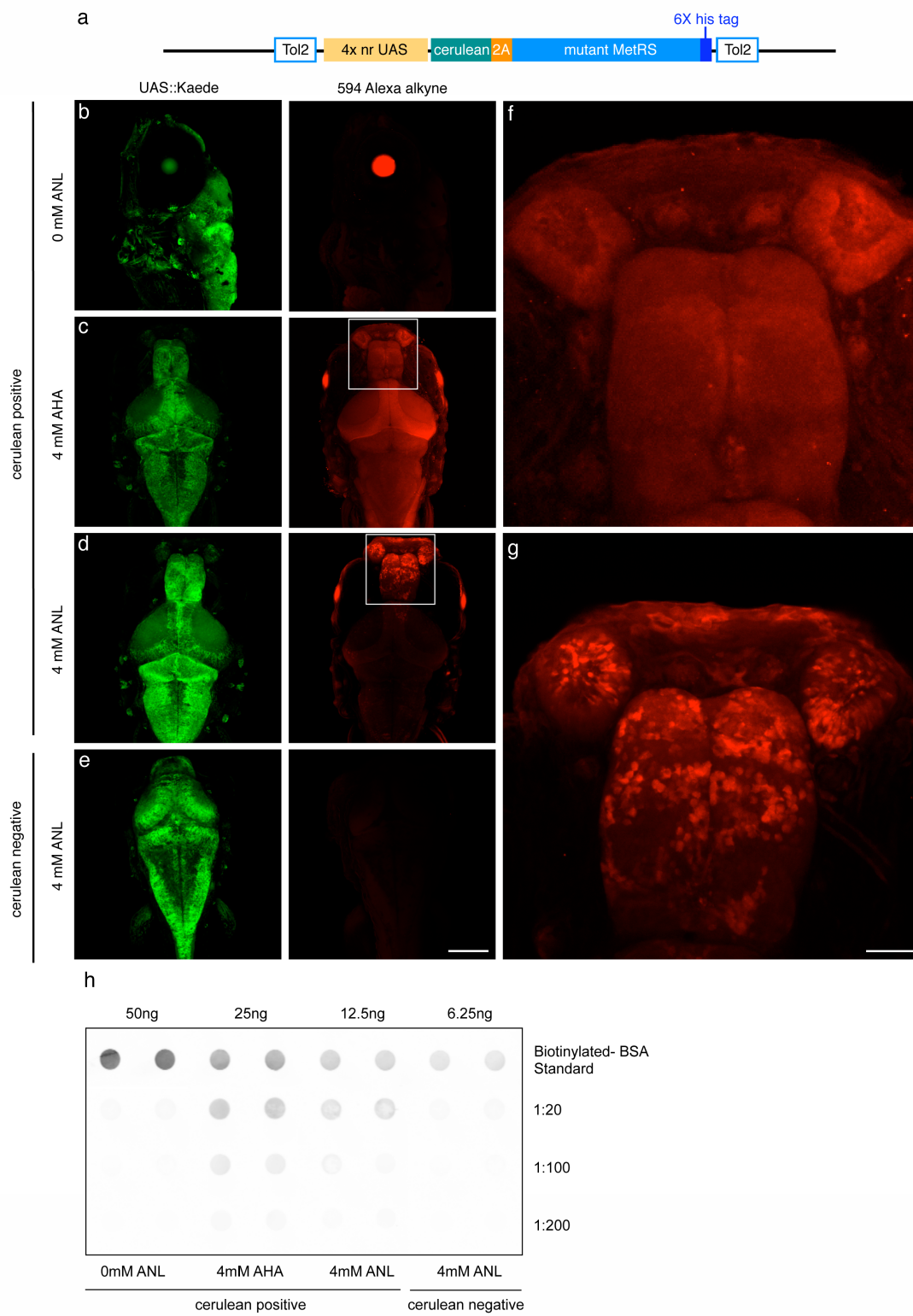


Figure 3.4. Cell-selective labeling with ANL in transiently L13G-MetRS-expressing larval zebrafish

(a) Scheme of zebrafish UAS::L13G-MetRS construct. (b-g) Single-cell embryos from pan-neuronally expressing Gal4 driver line were injected with zebrafish L13G-MetRS construct, sorted for cerulean expression after 30h and metabolically labeled with 4mM AHA, 4mM ANL or no noncanonical amino acid for 48h, 5dpf. 7dpf, larvae were fixed and reacted with 5 μ M AlexaFluor-488-alkyne tag for 12h (right panels). Transgenic line also expressed UAS::kaede, which is used as a marker for orientation (left panels). (f-g) Higher magnification of telencephalon and nasal cavity of (c) and (d), respectively. Scale bar in (b-e), 200 μ m; in (f-g), 50 μ m. (h) Single cell embryos from pan-neuronally expressing Gal4 driver line were injected with zebrafish L13G-MetRS construct, sorted for cerulean expression after 30h and metabolically labeled with 4mM AHA, 4mM ANL or no noncanonical amino acid for 48h. Sample immunoblot of three dilutions of lysates reacted with biotin-alkyne tag (10 μ M) for 12h, probed with antibody against biotin, as well as biotinylated-BSA-standards (50-6.25ng).

with 4mM ANL for 48h, again beginning 5dpf. Larvae were then anesthetized and homogenized and the lysate was reacted with biotin-alkyne in the presence of CuBr and the triazole ligand. Three different dilutions of sample reactions were spotted on a dot blot, which was then probed against biotin.

Similar to previous results using the AlexaFluor-594-alkyne, lysates from larvae expressing L13G-MetRS incubated with ANL or AHA showed metabolic labeling (Figure 3.4h). Lysates from larvae not incubated with a noncanonical amino acid, or incubated with ANL but not expressing L13G-MetRS, did not contain detectable amounts of biotinylated proteins. Interestingly, the amount of biotinylated protein in lysates from larvae expressing L13G-MetRS and incubated in ANL is only slightly less than that from lysates of larvae incubated in AHA. All cells can charge and incorporate AHA, whereas only cells expressing L13G-MetRS can charge and incorporate ANL into newly synthesized proteins. Expression of the L13G-MetRS in these larvae is very mosaic within the Gal4-expressing nervous system. These results are in line with previous observations that the charging rate of ANL by zebrafish L13G-MetRS onto methionyl-tRNAs may be slightly higher than the charging rate of AHA by wild-type MetRS.

Stable transgenic UAS::L13G-MetRS animals were created by injecting the UAS::L13G-MetRS construct previously described as well as Tol2 transposase mRNA into single-cell *nacre* embryos. Larvae were raised to adult stage and crossed with the s1101t Gal4 pan-neuronal driver line. F1 embryos resulting from these crosses were inspected for cerulean fluorescence to identify UAS::L13G-MetRS founder fish. Select F1 embryos were tested for ability to metabolically incorporate ANL using the AlexaFluor-594-alkyne. Embryos identified as cerulean positive at 30hpf, when incubated in 4mM ANL for 48h, showed cell-specific metabolic labeling in regions of the telencephalon, while embryos sorted as cerulean negative under the same conditions showed no fluorescent signal (Figure 3.5).

So far only one founder fish has been identified and the L13G-MetRS expression in F1 embryos from this founder was not pan-neuronal and therefore, did not seem to fully recapitulate Gal4 expression. Furthermore, expression of the L13G-MetRS construct seemed to be variegated between larvae of the same spawning, as shown in Figure 3.5b. However, many of the potential founder fish have not yet been screened, and we expect that future screening will identify additional, more stably expressing founder fish.

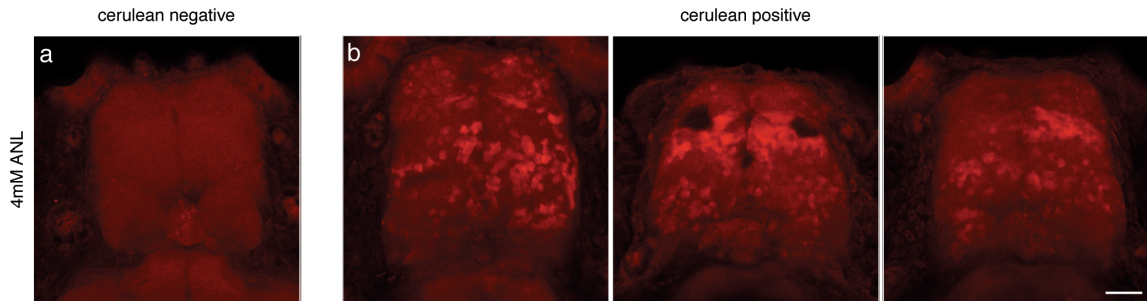


Figure 3.5. Cell-selective labeling with ANL in F1 transgenic larval zebrafish expressing L13G-MetRS

5dpf larval zebrafish siblings from crosses between UAS::L13G-MetRS founders and pan-neuronal Gal4 driver lines, were sorted as cerulean negative (a) and cerulean positive (b). Larvae were metabolically labeled with 4mM ANL for 48h prior to fixation and reacted with 5 μ M AlexaFluor-488-alkyne tag for 12h. Shown are dorsal views of the telencephalon and nasal cavity. In cerulean-positive samples, strong FUNCAT labeling can be observed in ~50-100 cells of the anterior dorsal telencephalon and slight FUNCAT labeling can be observed in some cells of the dorsal olfactory bulbs. FUNCAT labeling of different samples is not stereotyped within the telencephalon and olfactory bulbs, but uniformly restricted to these two brain regions. Scale bar is 40 μ m.

Parallel efforts in collaboration with Dr. Le Trinh are underway to create a stable transgenic zebrafish expressing zebrafish mutant MetRS in the telencephalon, utilizing the newly developed ‘FlipTrap’ system (Trinh et al., 2011). The ‘FlipTrap’ is a multifunctional gene trap that, once inserted into the genome, allows for FLP recombinase-mediated excision and replacement of the FlipTrap cassette for any other exogenous DNA containing the same FRT sites (Figure 3.6a). This allows for targeted genetic manipulation of the FlipTrap locus. 170 FlipTrap zebrafish lines with diverse tissue-specific expression patterns have been generated, including line ct500a, which traps nucleolar protein 4 and shows telencephalon-specific expression. In goldfish lesion studies, the telencephalon has been shown to be involved in memory formation and is

thought to be homologous to the mammalian hippocampus and amygdala (Broglia et al., 2005). This makes it an ideal structure to which to localize metabolic labeling in order to investigate new protein synthesis in the context of memory formation.

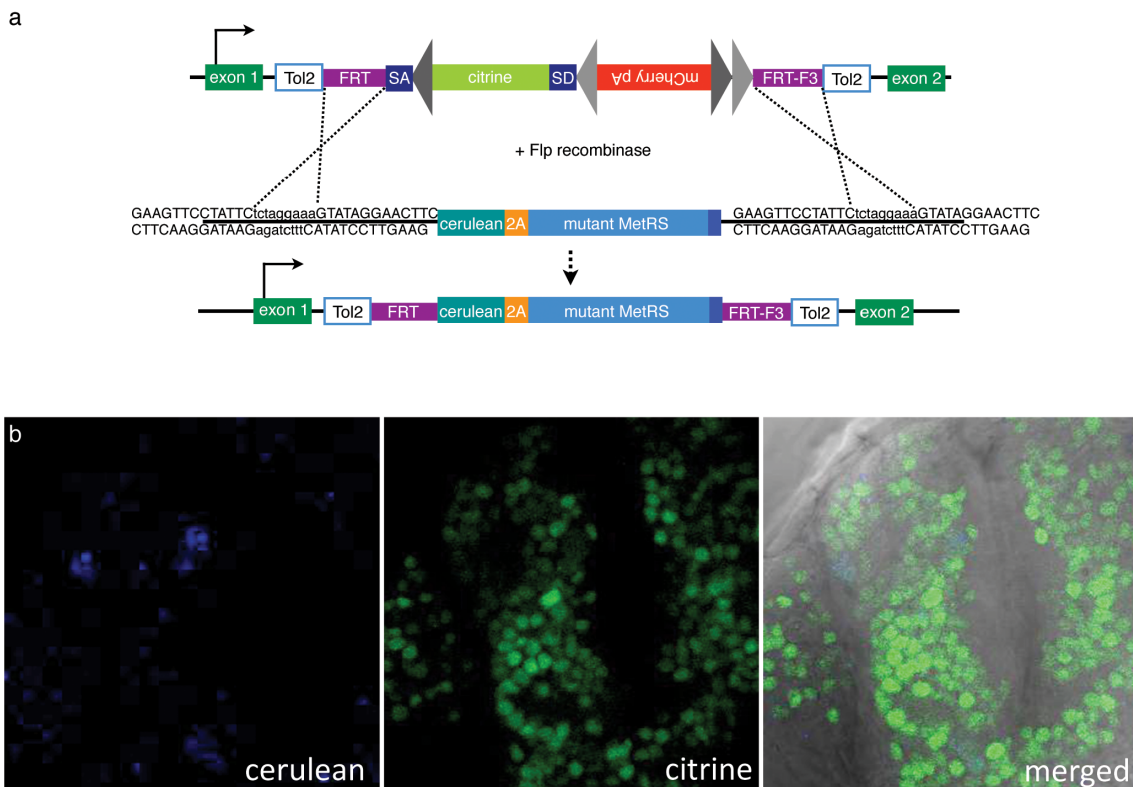


Figure 3.6. Restricted mutant MetRS expression in the telencephalon of larval zebrafish via FlipTrap gene trapping

(a) Scheme of mutant MetRS-FlipTrap insertion construct and replacement of FlipTrap cassette in the genome by Flp recombinase. (b) Fluorescent images showing replacement of FlipTrap cassette, driving citrine expression, by mutant MetRS-FlipTrap insertion construct, driving cerulean expression, in the telencephalon of founder larvae.

The MetRS-FlipTrap exchange vector (Figure 3.6a, second line; Appendix A for vector map and full sequence), containing the cerulean-2A-mutant MetRS-6XHis cassette

previously described (Figure 3.4a) flanked by FRT sites, was created and injected with Flp recombinase into single-cell embryos of the ct500a FlipTrap line. This should permit excision and replacement of the citrine-containing FlipTrap cassette with the cerulean-containing MetRS-FlipTrap exchange cassette, to enable expression of exon 1-cerulean fusion proteins, as well as equimolar amounts of mutant MetRS. When the injected embryos were imaged, cerulean expression with a background of citrine expression could be detected in the telencephalon (Figure 3.6b), indicating that the FlipTrap cassette was successfully replaced by the MetRS-FlipTrap exchange cassette in some cells. These F0 founder fish are currently being raised and F1 embryos will be screened and tested for the ability to incorporate ANL. As the FlipTrap system allows for targeted locus, single-copy integration of the mutant MetRS sequence, we hope that variegated expression will be prevented.

NLL and PLL mutations of the zebrafish MetRS sequence enable ANL incorporation neither in vitro nor in vivo

The NLL and PLL *E. coli* MetRS mutations were identified by Tanrikulu and colleagues (Tanrikulu et al., 2009). *In vitro*, the mutations were found to have both higher ANL charging rates (410 ± 80 $k_{\text{cat}}/k_{\text{m}}$ and 650 ± 150 $k_{\text{cat}}/k_{\text{m}}$, respectively) and greater selectivity¹ for ANL in the presence of methionine (1.2 and 3.2, respectively) than the L13G *E. coli* MetRS mutant previously described by Link *et al.* (which Tanrikulu et al. report as

¹ Selectivity is defined as the ratio of $k_{\text{cat}}/k_{\text{m}}$ for ANL to that for methionine.

having a charging rate of 170 ± 40 k_{cat}/k_m and a selectivity of 0.03). As the L13, the T260 and the H301 residue are all conserved between *E. coli* and zebrafish, we introduced not only the L13G mutation into the zebrafish MetRS protein sequence, but also made zebrafish NLL MetRS and zebrafish PLL MetRS constructs, in order to test both in COS7 cells and in larval zebrafish.

In contrast to results from studies using *E. coli*, we found that neither the zebrafish NLL MetRS mutant nor the zebrafish PLL MetRS mutant, when expressed in COS7 cells enabled metabolic labeling with ANL (Figure 3.7a and 3.7b). When COS7 cells were incubated with 4mM AHA or transfected with the zebrafish L13G MetRS mutant and incubated in 4mM ANL before lysis and reaction to biotin-alkyne, strong metabolic labeling was detected throughout the proteome, as previously described. However, when COS7 cells were not transfected or transfected with zebrafish NLL or PLL MetRS mutants and incubated in 4mM ANL before lysis and reaction to biotin-alkyne, no metabolic labeling was observed.

Furthermore, transient expression of the zebrafish NLL MetRS mutant, via injection of the construct into single-cell, pan-neuronally expressing Gal4 embryos, followed by incubation in 4mM ANL for 48h at 5dpf, did not result in cell-specific fluorescent labeling (Figure 3.7e), as previously described when using the L13G MetRS (Figure 3.4d). Only when larvae were incubated with AHA (Figure 3.7d) could FUNCAT signal be detected. These results together indicate that, although the residues involved are conserved between *E. coli* and zebrafish, expression of the zebrafish NLL and PLL MetRS mutations do not enable metabolic labeling with ANL.

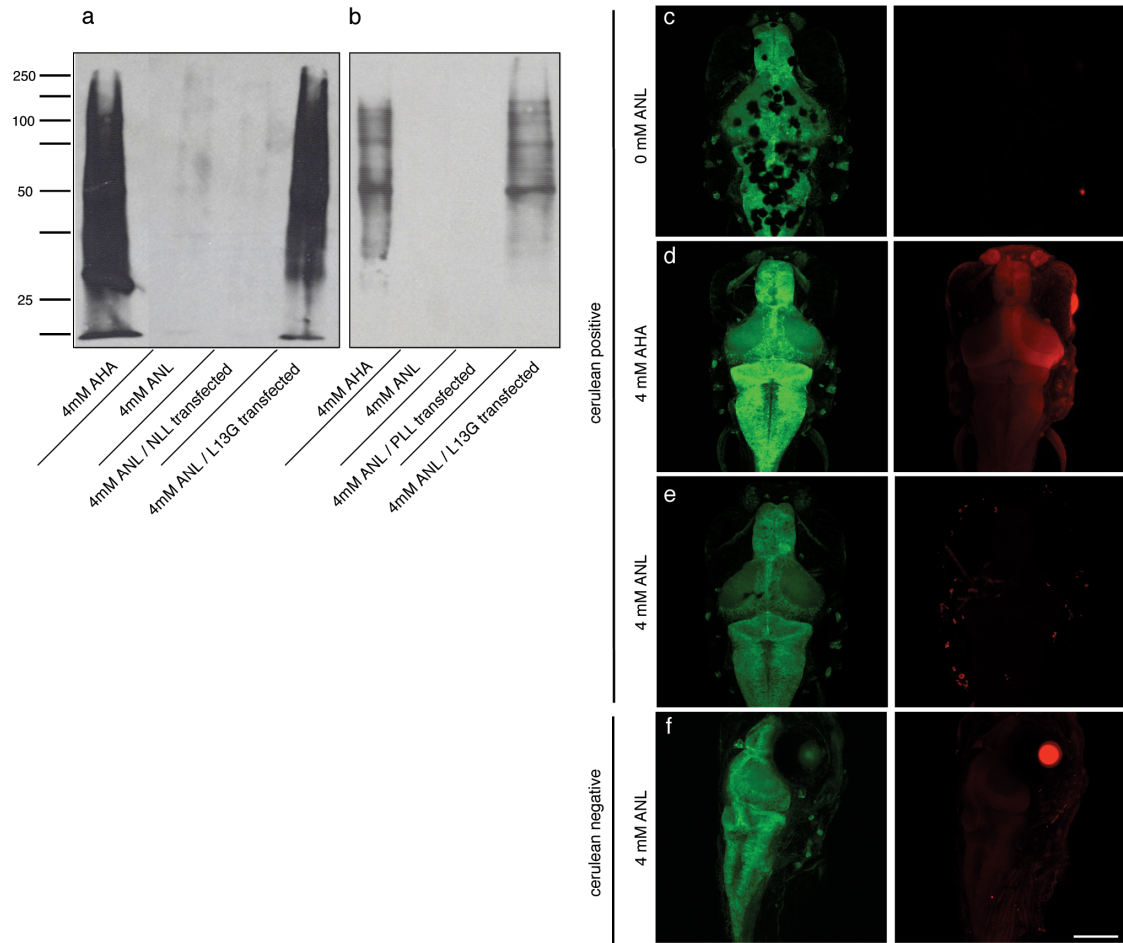


Figure 3.7. NLL and PLL mutations of zebrafish MetRS do not enable metabolic labeling with ANL *in vitro* or *in vivo*.

(a-b) COS7 cells were transfected with zebrafish NLL (a) or PLL (b) MetRS-GFP fusion construct, or L13G MetRS-GFP fusion construct (positive control). Untransfected cells were metabolically labeled with 4mM AHA or 4mM ANL; transfected cells were metabolically labeled with 4mM ANL. Cells were homogenized, reacted to the biotin-alkyne (10 μ M) for 12h and analyzed using western blots probed against biotin. (c-f) Single-cell embryos from a pan-neuronally expressing Gal4 driver line were injected with zebrafish NLL-MetRS construct, sorted for cerulean expression after 30h and metabolically labeled with 4mM AHA, 4mM ANL or no noncanonical amino acid for 48h, 5dpf. At 7dpf, larvae were fixed and reacted with 5 μ M AlexaFluor-488-alkyne tag for 12h (right panels). FUNCAT labeling (red) was not observed in (c), (e) or (f) [red signal in (e) is minor background and signal in (f) is caused by reflection of the laser line from the lens of the eye]. Only when larvae were incubated with AHA (d) could FUNCAT signal be detected. The transgenic line was also expressed UAS::kaede (green), which is used as a marker for orientation (left panels).

Discussion

In this chapter we have shown that expression of the zebrafish L13G-MetRS mutant endows cells with the ability to incorporate the larger, usually metabolically inert, noncanonical amino acid ANL into newly synthesized proteins. The MetRS sequence, especially those residues involved in forming the catalytic binding pocket, is highly conserved between *E. coli* and zebrafish. Introduction of the L13G mutation, first described in *E. coli*, into the zebrafish MetRS sequence enables labeling with ANL both in COS7 cells and in larval zebrafish. This labeling is specific to the cells expressing the L13G-MetRS, thereby enabling genetically restricted metabolic labeling in a multicellular organism. Currently, efforts to create a stable transgenic zebrafish using either the UAS-Gal4 binary expression system or via targeted replacement using FlipTrap recombination are underway and will soon allow us to target metabolic labeling specifically to structures of the nervous system involved in memory formation.

Interestingly, the NLL and PLL MetRS mutations, which were described in *E. coli* as having higher ANL charging rates and higher specificity for ANL in the presence of methionine than the L13G MetRS mutation, do not show the same behavior when introduced into the zebrafish MetRS protein sequence. Although the residues of the MetRS binding pocket are highly conserved between species, the *E. coli* MetRS sequence lacks ~250 residues at its N-terminal end when compared to vertebrate MetRS sequences such as zebrafish and mouse. Structural rearrangements in the conformation of the MetRS binding pocket caused by such protein sequence differences, may lead to the L13 residue playing a more important role in substrate specificity in vertebrates than in

bacteria. In the mouse MetRS, the L13G mutation also enables incorporation of ANL *in vitro* and *in vivo*, while the NLL and PLL mutations do not (data not shown). This similarity between the vertebrate species further supports the idea that sequence differences between the vertebrate MetRS and the *E. coli* MetRS may influence the ANL charging efficiencies of the different MetRS mutations.

In the future, cell-type-specific metabolic labeling in stable transgenic zebrafish will enable identification of more subtle differences in protein synthesis in response to either chemical or behavioral stimuli. This may enable the visualization of cells or neuronal circuits involved in memory formation, as well as facilitate the identification of proteins of low abundance expressed during memory formation in specific cell populations.

Methods

Reagents

All chemical reagents were of analytical grade, obtained from Sigma unless otherwise noted, and used without further purification. We prepared ANL as described previously (Link et al., 2007), using Boc-Lys as a starting reagent. The AlexaFluor-488 alkyne and AlexaFluor-594 alkyne were purchased from Invitrogen (catalog number A10267 and A10275, respectively), while the biotin-alkyne tag was purchased from Jena Biosciences (catalog number TA105). All primers were purchased from IDT (Integrated DNA Technologies) or eurofins mwg/operon.

Zebrafish stocks and husbandry

Adult fish strains AB, *nacre* and Gal4 s1101t driver line were kept at 28°C on a 14h light/10h dark cycle. Embryos were obtained from natural spawnings and were maintained in E3 embryo medium (5mM NaCl, 0.17mM KCl, 0.33mM CaCl₂, 0.33mM MgSO₄) (Nüsslein-Volhard and Dahm, 2002). The Gal4 s1101t driver line was a kind gift from Dr. Arrestedes Arrenberg.

Construction of MetRS-EGFP vectors

Clone-containing zebrafish MetRS cDNA sequence (identification number: Zebrafish 2639182, pME18S-FL3) was purchased from ATCC, transformed, amplified and sequenced using the following primers:

Primer	Sequence 5'-3'
MARS247F	CAG CTT GTG AAA CAC GAG GA
MARS789F	CAG AGA CAG TCC CAG CAA CA
MARS1237F	CAC CAG ACA GAA ATC GCT CA
MARS2172F	GCT GCT GAA TGA CGA CGA TA
MARS2268F	GCT GAA GTG CAT CCT CAA CA
MARS994R	GCG GCA CAT TGT TGA CAT AC
MARS2397R	ATT CAC TGA CAC ACC CGT CA

pME18S-FL3 zebrafish MetRS sequence was cloned into Clontech pEGFP-C1 vector (GenBank Accession #: U55763, Catalog #:6084-1) and the NLL mutations (CTC → GAC at position 807-809 after ATG; TAC → CUC at position 1566-1568 after ATG; CAC → CUC at position 1671-1673 after ATG) were introduced by Genscript. This construct was named NLL MetRS-C1-EGFP. Concurrently, the MetRS sequence was amplified from pME18S-FL3 using primers 144*Xho*I and *Eco*RIR and cloned into Clontech pEGFP-C2 (GenBank Accession #:U57606, Catalog #:6083-1) using *Eco*RI and *Xho*I sites. This construct was named MetRS-C2-EGFP. NLL MetRS sequence was amplified from NLL MetRS-C1-EGFP and cloned into Clontech pEGFP-C2, again using *Eco*RI and *Xho*I sites. This construct was named NLL MetRS-C2-EGFP. A Stratagene QuikChange Site-Directed Mutagenesis Kit, in combination with primers L13GQCF and L13GQCR, was used to insert L13G mutation (CTC → GGC at position 807-809 after ATG) into MetRS-C2-EGFP vector. This construct was named L13G MetRS-C2-EGFP. The same method was employed in combination with primers ZFNtoPF and ZFNtoPR to insert PLL mutation (GAC → CCC at position 807-809 after ATG) into NLL MetRS-C2-EGFP vector. This construct was named PLL MetRS-C2-EGFP. Vector map and sequence are included in Appendix A.

Primer	Sequence 5'-3'
144 <i>Xho</i> I	CCG CTC GAG CGG CAT AAT CGC G
<i>Eco</i> RIR	GCC GGA ATT CCG TCC ATC CTC AT
L13GQCF	GAT CAC CAG CGC TGG CCC GTA TGT CAA C
L13GQCR	GTT GAC ATA CGG GCC AGC GCT GGT GAT C
ZFNtoPF	GTT GAT CAC CAG CGC TCC CCC GTA TGT CAA CAA TGT G
ZFNtoPR	CAC ATT GTT GAC ATA CGG GGG AGC GCT GGT GAT CAA C

Construction of MetRS-FlipTrap exchange vectors

Mutated MetRS sequence were amplified from MetRS-C2-EGFP vectors using MRS-*NcoI*-F and MRS-His-*EcoRI*-R primers and cloned into FlipTrap vector (Trinh et al., 2011; NCBI accession no. JN564735) using *NcoI* and *EcoRI* sites. Vectors were amplified and sequenced using sequencing primers previously described. Vector map and sequence are included in Appendix A.

Primer	Sequence 5'-3'
MRS- <i>NcoI</i> -F	ATC CCG GGC CCC CAT GGA TGA AGC TGT TTA TCG GTG AGG GAA
MRS-His- <i>EcoRI</i> -R	TGG ATA TTG AAT TCC TAA TGA TGA TGA TGA TGA TGA GAC CCC CC

Construction of UAS::MetRS vectors

Genscript amplified the Cerulean-2A-MetRS-6XHis tag sequence from L13G-MetRS-FlipTrap exchange vectors and cloned it into pBT2-4Xnr UAS-GFP (Akitake et al., 2011). Vectors were named UAS::L13G-MetRS and UAS::NLL-MetRS, amplified and sequenced using previously described sequencing primers. Vector map and sequence are included in Appendix A.

Splice site removal from MetRS-FlipTrap exchange vectors and UAS::MetRS vectors

Stratagene QuikChange Site-Directed Mutagenesis Kit and QuikChange Multi Site-Directed Mutagenesis Kit were used to remove nine high-scoring splice donor sites from L13G MetRS-FlipTrap exchange vector, NLL MetRS-FlipTrap exchange vector, UAS::L13G-MetRS vector and UAS::NLL-MetRS vector (see table below). Splice sites were identified using the Splice Site Prediction by Neural Network tool provided by the Berkeley Drosophila Genome Project (http://www.fruitfly.org/seq_tools/splice.html).

Splice Site	Sequence	Score
1	CGGCGACGTAACGG	0.41
2	TTTATCGGTGAGGGA	0.87
3	CTGCAGGGTAAAGGA	0.72
4	TCGCCAGGTATGGC	0.99
5	GTGTAAGGTGTGTAA	0.98
6	GTGACGGGTGTGTCA	0.56
7	CCCACAGTGAGTCT	0.83
8	CGGCACGGTCAGTCC	0.97
9	GAACAAGGTGAAAAA	0.73

The Multi Site-Directed Mutagenesis Kit was used in combination with primers ss1-ss4 and ss6-ss9 to remove all splice sites except site 5 from UAS::MetRS vectors. Simultaneously, an ATG-start site was inserted into cerulean in these vectors using primer startsite. The Site-Directed Mutagenesis Kit, in combination with primers ss_5singleT3F and ss_5singleT3R, was used to remove splice site 5.

The Multi Site-Directed Mutagenesis Kit was used in combination with primers

ss1-ss4, ss_5singleT3F, ss6, ss8 and ss9 to remove all splice sites except site 7 from MetRS-FlipTrap exchange vectors. The Site-Directed Mutagenesis Kit, in combination with primers ss7 and ss_7R, was used to remove splice site 5.

Primer	Sequence 5'-3'
startsite	CGCGTGGATCCATGGTCAGCAAGGGCGAGG
Ss1	CTGGACGGCGACGTGAACGGCCACAAG
Ss2	GCTGTTTATCGGCGAGGGAAACCCGC
Ss3	GTCCTGCAGGGCAAAGGAGCCGAAGC
Ss4	GTGTTGCGCCAGATATGGGCGTCTGCG
Ss6	GACTGTGACGGGCGTGTTCAGTGAATG
Ss7	CATGCCACACGTCAGTCTCAGCATCC
Ss8	CATCGGCACGGTGAGTCCTCTGTTCC
Ss9	GTGGCAGAACAAGGCGAAAAAGTTCGAGC
Ss_5singleT3F	GAATCCTCAGTGTAAGTGTGTAAGGAGACGCC
Ss_5singleT3R	GGCGTCTCCTTACACACTTTACACTGAGGATTC
Ss_7R	GGATGCTGAGACTGACTGTGGGCATG

Transfecting COS7 cells with MetRS-EGFP vectors

1.5ml of 80-90% confluent COS7 cells were plated in a T25 cell flask in 5ml of prewarmed DMEM++ (Gibco) and incubated overnight at 37°C. To transfect, 5.875µg plasmid DNA was diluted in prewarmed OptiMEM+GlutaMax (Gibco) to bring it to a final volume of 300µl. 11.75µl lipofectamin-2000 (Invitrogen) was diluted in 282µl of prewarmed OptiMEM+GlutaMax. Both the plasmid DNA mixture and lipofectamin

mixture were incubated for 5min at room temperature. Then the lipofectamin mixture was added to the plasmid DNA mixture, vortexed and incubated at room temperature for 20min. COS7 cells were washed with 5ml of prewarmed OptiMEM (Gibco). 2.35ml of prewarmed OptiMEM was added to the plasmid DNA/lipofectamin mixture, vortexed and added to COS7 cells. Cells were incubated at 37°C for 24h.

Metabolic labeling of transfected COS7 cells

COS7 cells were washed with 5ml prewarmed HBS (20mM HEPES (Gibco), 238mM NaCl, 4mM CaCl₂, 4mM MgCl₂, 10mM KCl, 60mM Glucose), then incubated in HBS supplemented with either 4mM ANL or 4mM AHA in the presence or absence of 40μM anisomycin for 4h at 37°C. Cells were washed with 5ml of ice-cold PBS-MC (1XPBS, 1mM MgCl₂, 0.1mM CaCl₂) on ice, before cells were scraped from flask in 500μl PBS (pH 7.6) + Protease Inhibitor (PI; Roche, complete ULTRA Tablets, Mini, EDTA-free Protease Inhibitor cocktail tablets) twice. Cell solution was collected in an 1.5ml Eppendorf tube and centrifuged. Supernatant was removed, 25μl of PBS+PI was added and the cells were homogenized using a Kontes Pellet Pestle Motor. 1% SDS and 0.1μL of Benzonase (≥500U) were added and the lysate was vortexed and heated at 95°C for 5min. Lysate was cooled to room temperature before 220μl of PBS+PI and 0.1% triton X-100 were added. Then lysates were centrifuged at 15,000g at 4°C for 10min. Supernatant was transferred to a new 1.5ml Eppendorf tube. For BONCAT, samples were reacted with 10μM biotin-alkyne and processed as previously described in Chapter II.

Microinjection to transiently express UAS::MetRS construct in vivo

To transiently express UAS::MetRS constructs in larval zebrafish, ~2nl DNA injection solution (Suster et al., 2007) was injected into one-cell-stage embryos of the Gal4 s1101t driver line. The injected embryos were screened for cerulean fluorescence at 30hpf and metabolically labeled as described in Chapter 2.

Microinjection to create stable UAS::MetRS responder line

To create stable UAS::MetRS responder lines, ~2nl DNA injection solution (Suster et al., 2007) was injected into one-cellstage *nacre* embryos. The injected embryos were raised and crossed to Gal4 s1101t lines. Resulting F1 embryos were screened and metabolically labeled as previously described.

Chapter IV

PROTEIN SYNTHESIS-DEPENDENT PLACE-CONDITIONING IN LARVAL
ZEBRAFISH

Introduction

Long-term memory formation has been shown to be protein synthesis-dependent in a number of different model organisms including teleost fish (Agranoff and Klinger, 1964; reviewed in Davis and Squire, 1984). In the previous chapters, we have described the development of metabolic labeling techniques that allow for the visualization of newly synthesized proteins in genetically restricted cell populations of the larval zebrafish nervous system. One main goal of these studies was to develop techniques that could be paired with a protein synthesis-dependent learning paradigm to visualize circuits involved in memory formation, as well as to identify proteins newly synthesized during memory formation in these circuits.

Although the larval zebrafish has become a prominent model organism for studying neural circuitry underlying behavior in recent years (e.g. Wyart et al., 2009; Del Bene et al., 2010; Fetcho and McLean, 2010; reviewed in Fetcho and Lui, 1998), there is still a dearth of robust, protein synthesis-dependent learning paradigms. While a number of associative conditioning paradigms have recently been developed for adult zebrafish, including one-trial avoidance learning (Blank et al., 2009), olfactory conditioning (Braubach et al., 2009), shuttle box active appetitive conditioning (Pather and Gerlai, 2009), place-conditioning (Eddins et al., 2009; Mathur et al., 2011), appetitive choice discrimination (Bilotta et al., 2005), active avoidance conditioning (Pradel et al., 1999; Pradel et al., 2000; Xu et al., 2007), an alternation memory task (Williams et al., 2002), and a plus-maze non-spatial and spatial associative learning task (Sison and Gerlai, 2010), currently only non-associative paradigms (Best et al., 2006; Wolman et al., 2011;

Roberts et al., 2011) or restrained associative paradigms (Aizenberg and Schuman, 2011) exist for larval zebrafish. Memory retention in all of these larval zebrafish paradigms is short-lived, suggesting that these paradigms entrain forms of protein synthesis-independent short-term memory. Furthermore, the restrained associative paradigms are often very labor intensive and therefore not easily paired with high-throughput screening or proteomics approaches. Only very recently, have Wolman et al. shown that spaced training blocks of repetitive visual stimuli elicit protein synthesis-dependent long-term habituation in larval zebrafish lasting up to 24h, that is disrupted by cycloheximide incubation during training (Wolman et al., 2011).

In this chapter, we describe a simple unrestrained associative place-conditioning paradigm. Using a custom built conditioning chamber, we show that visual access to a group of conspecifics has rewarding properties for 6-8-day-old larval zebrafish, as previously described for adult zebrafish (Al-Imari and Gerlai, 2007; Gomez-Laplaza and Gerlai, 2009; Sison and Gerlai, 2011). We then use this social reward as an unconditioned stimulus and pair it with a distinct visual environment over a three hour training period. Following training, larvae retained a preference for the visually demarcated area of the chamber previously paired with the social reward for up to 36h, indicating that this novel reinforcer can support long-term associative learning in zebrafish larvae. Furthermore, incubation with the protein synthesis inhibitors puromycin or cycloheximide, as well as the non-competitive NMDAR-antagonist, MK-801, during the three hour training period impaired memory retention. This demonstrates that the associative place-conditioning paradigm described here is protein synthesis- and partially

NMDAR-dependent. In future experiments, this learning paradigm will be paired with cell-specific metabolic labeling to visualize circuits underlying memory formation.

Associative place-conditioning paradigm for 6-8dpf larval zebrafish

This place-conditioning paradigm pairs a social reward, visual access to a group of conspecifics, with a distinct environment indicated by light intensity. We designed two different behavioral chambers (Figure 4.1a) custom built from plastic and Plexiglas elements. The testing chamber consisted of 14 channels (to house individual larvae) separated by opaque barriers, while in the training chamber, only one half of each of the barriers was opaque and the remainder was transparent. This created two distinct environments: one, an individual environment in which the larvae could not see their neighbors, the other a social environment in which the larvae had visual access to their conspecifics in neighboring channels. Both the testing and the training chamber were approximately the size of a 96-well plate, had a transparent bottom and slightly slanted dividing barriers, which allowed for visual monitoring of larvae position from a fixed camera mounted above. The testing and training chambers were placed in a custom-built, white plastic, enclosed behavioral chamber (Figure 4.1b) which isolated the chambers from any outside visual or acoustic stimuli or cues. The behavioral chamber had a semi-transparent bottom, onto which different light environments were projected using a computer-controlled beamer, and a fixed opening at the top, into which a camera was fixed to monitor larvae position.

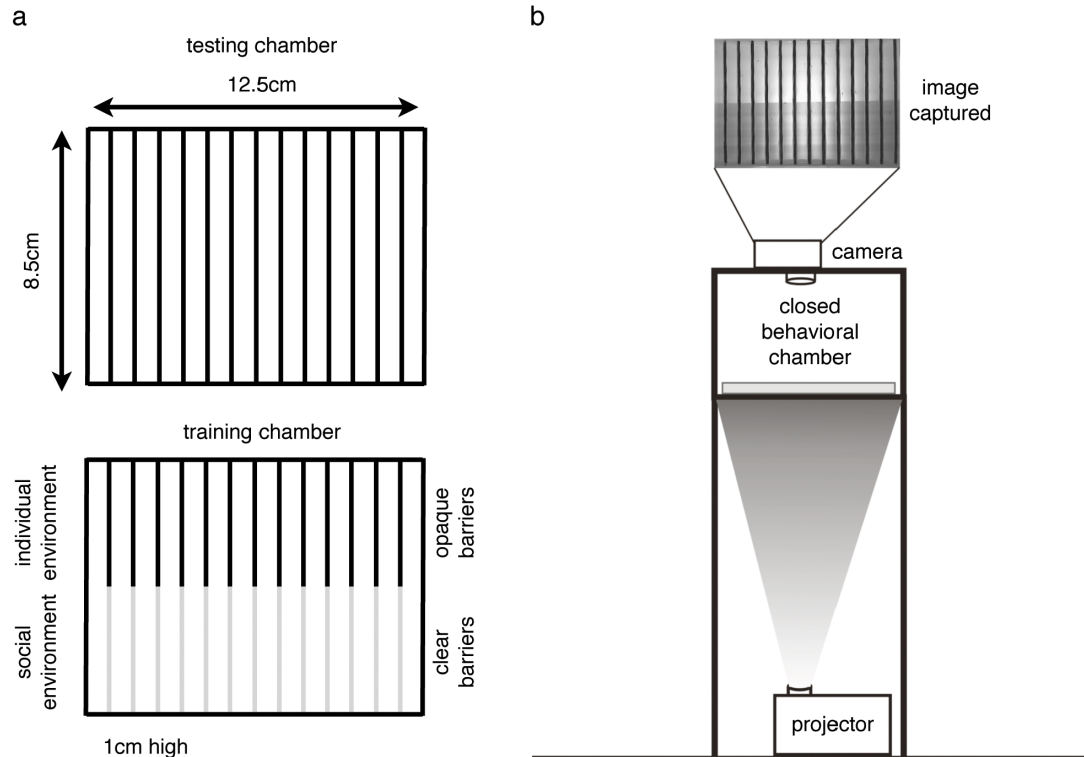


Figure 4.1. Place-conditioning apparatus and experimental set up

(a) Testing and training chambers are the size of 96-well plates. Testing chamber consists of 14 individual channels separated by opaque barriers. Training chamber consists of 14 individual channels, separated on one side of the chamber by opaque barriers, creating an individual environment and on the other side by clear barriers, creating a social environment in which larvae can see their conspecifics in neighboring channels. (b) Testing or training chambers were placed in a closed behavioral chamber, which allowed for projection of different light environments from below and monitoring of larva position from above.

First, we determined the light and social preference of unconditioned larval zebrafish. To test for light preference, 6-8 dpf wild-type larvae were individually placed in the channels of the testing chamber, which was then illuminated with two different light intensities creating equally sized dark and light environments (Figure 4.2a, scheme). Larvae position was captured every 10 seconds for a 15 minute period (90 frames in

total) and scored. If the larva was in the light environment during a given frame it was scored as +1, while if it was in the dark environment it was scored as -1. If the larva could not be detected, it did not receive a score. Scores for all 90 frames were added individually for each larva and normalized to one hundred to determine light preference with age (Figure 4.2a). Positive scores indicate a preference for the light environment, negative scores indicate a preference for the dark environment and a score of zero indicates no preference. Social preference was evaluated in a similar manner. Here larvae were placed individually in the training chamber (with an opportunity to view conspecifics) in either completely dark or completely light environments for a 15 minute period (Figure 4.2b, scheme). Larvae that were detected in the social environment (transparent barrier) were scored as +1, while larvae detected in the individual environment (opaque barrier) were scored as -1. Scores for all frames were added and normalized to determine social preference with age in both a light and a dark environment (Figure 4.2b). Positive scores indicate a preference for the social environment, while negative scores indicate a preference for the individual environment.

6-8dpf larvae showed a moderate preference for light under the conditions tested here, which increased slightly, though not significantly (6dpf vs. 8dpf, $p=0.091$), with age (Figure 4.2a). In contrast, 6-8dpf larvae showed a strong preference for the social environment where they had visual access to their conspecifics, both in light and dark conditions (Figure 4.2b). Despite a trend for slightly higher scores in the light environment that likely resulted from better visibility of conspecifics in neighboring chambers, this social preference remained stable with age and was not significantly affected by illumination conditions. Placing an individual larva in the training chamber

when the neighboring chambers were unoccupied did not cause preference for the social (transparent) environment (data not shown). This indicates that visual access to conspecifics, not some other aspect of the social environment such as light intensity or transparency, acted as the reward. These results demonstrate that 6-8dpf larval zebrafish show moderate light environment preference and strong social environment preference, which remains stable during the ages investigated. Thus, unconditioned preferences may be exploited to “place condition” 6-8dpf larvae.

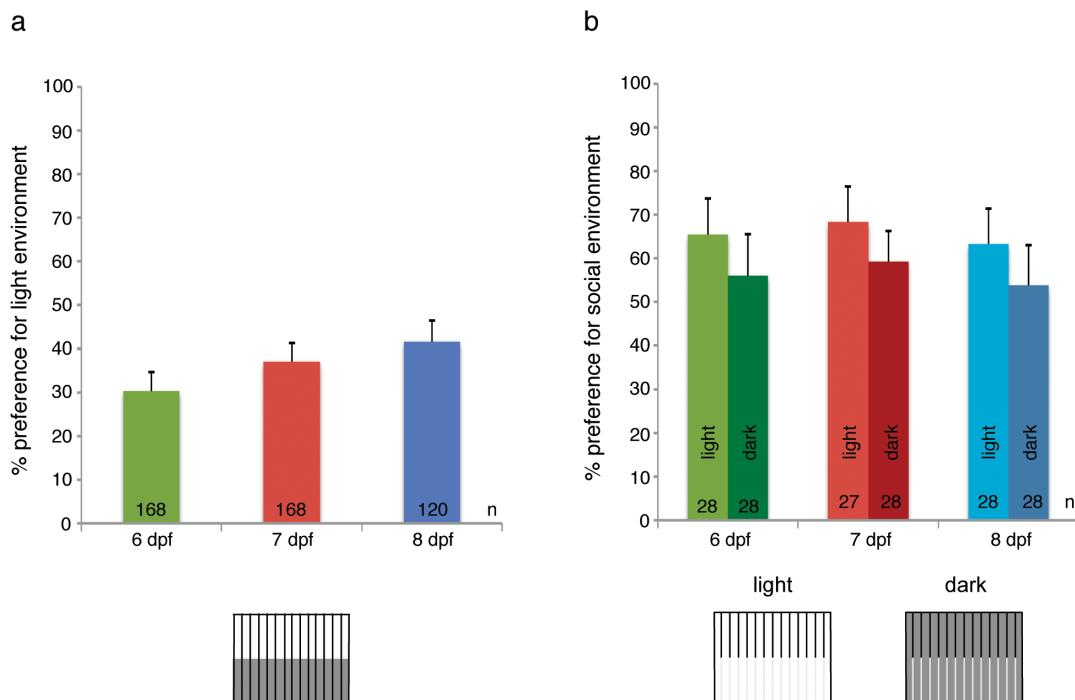


Figure 4.2. 6-8dpf larval zebrafish show unconditioned preference for light and social environment.

(a) Mean light preference during 15 minute period of 6-8dpf larval zebrafish. Differences are not statistically significant. (b) Mean social preference during 15 minute period of 6-8dpf larval zebrafish, in both light and dark conditions. Differences are not statistically significant. Error bars in (a) and (b) denote SEM.

The place-conditioning paradigm that we establish here consisted of three distinct phases (Figure 4.3a). During test 1, the naive light environment preference of individual larval zebrafish was determined over two 15 minute periods. Between the two periods of test 1, the orientation of the testing chamber within the behavioral chamber remained constant, but the light/dark environment orientation was rotated by 180° to ensure that the monitored larval position truly reflected light environment preference and not testing chamber side preference. During training, the social environment was paired with the dark environment for a three-hour period. Every 45 minutes during the training phase, the orientation of the training chamber in the behavioral chamber was rotated by 180° along with the illumination to prevent association between the social environment and visual cues that may have been present in the behavioral chamber. After training the larvae were individually placed overnight in a 12-well plate, which in turn was placed in an incubator with a 10h dark 14h light cycle. Approximately 14h after training, the (conditioned) light environment preference of each larval zebrafish was determined (test 2) as previously described for test 1. Control larvae were exposed to exactly the same procedure, except that this group was placed in the testing chamber, which did not possess a social environment, during training.

During the two 15 minute periods of test 1, larval zebrafish generally spent most of their time in the light environment, regardless of orientation with respect to the testing chamber (Figure 4.3b, test 1). This supported our previous observation that 6-8dpf larval zebrafish have a moderate preference for the light environment (Figure 4.2a). However, after training, during the first part of test 2, this preference was abolished. In some cases, individual larvae now preferred the dark environment to the light environment, while in

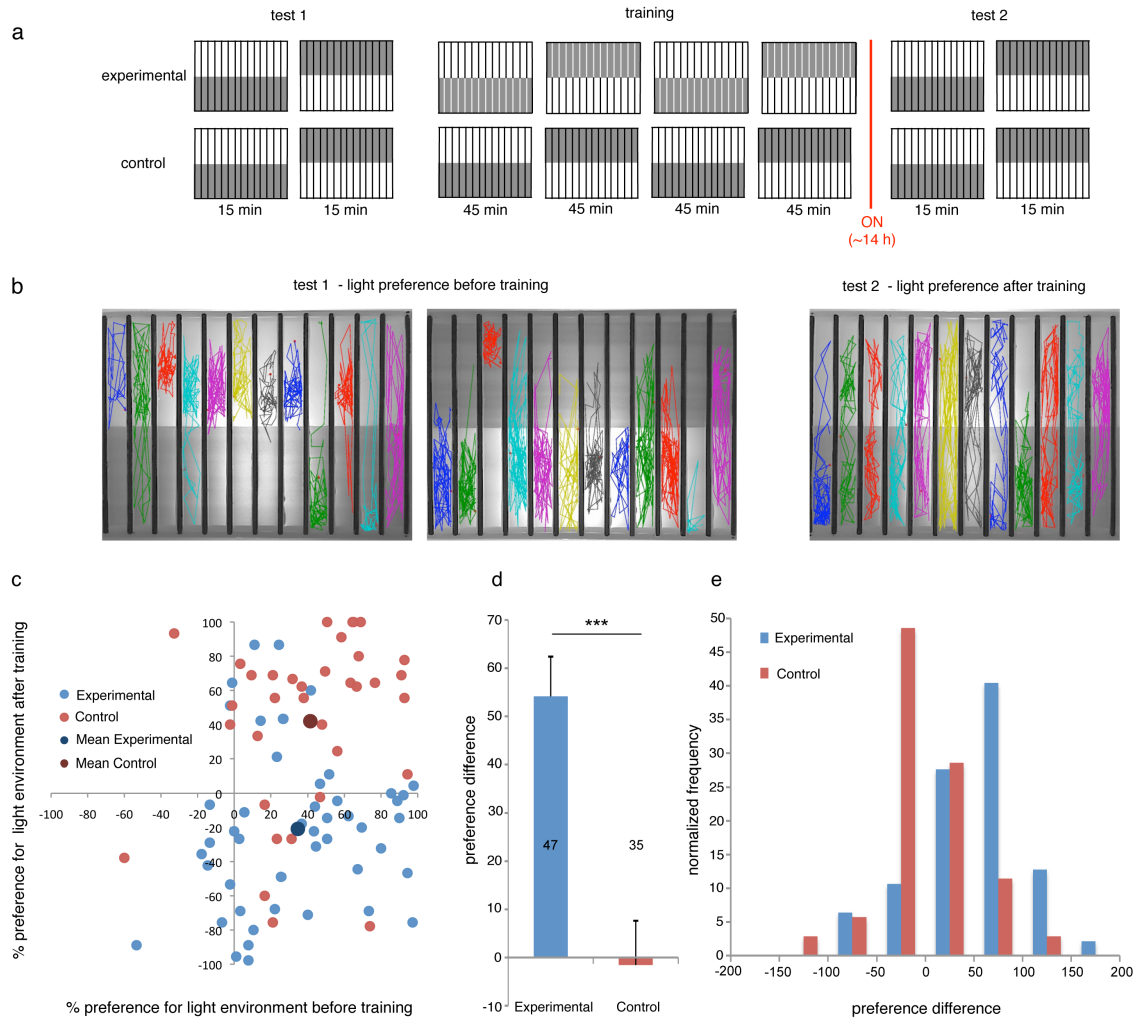


Figure 4.3. Associative place-conditioning paradigm for 6-8dpf larval zebrafish

(a) Scheme depicting associative place-conditioning paradigm. Unconditioned light preference was determined during test 1, followed by a 3h training period during which dark and social environment were paired, but orientation of the training chamber in the behavioral enclosure was rotated by 180° every 45 minutes. Light preference after conditioning was determined during test 2, 14h after training. Control fish were exposed to the same pattern of light and dark environments in the testing chamber, which contained no social environment. (b) Sample position traces during test 1 and first part of test 2, 14h after training. Frames captured every 10s. (c) Light preference before (x-axis) and after (y-axis) training of experimental (blue) and control (red) larvae. Larger markers denote mean light preference. (d) Light preference difference of experimental (blue) and control (red) groups, determined by subtracting light preference after training from light preference before training. Error bars denote SEM, *** $p < 0.001$. (e) Preference difference distribution of experimental (blue) and control (red) groups.

most cases we observed a preference shift from light environment towards dark environment (Figure 4.3b, test 2). This change in preference is quantified in Figure 4.3c, where the preference for light environment before training (test 1) of both experimental (blue) and control (red) larvae is plotted on the x-axis, while preference for light environment after training (test 2, first 15 minute period) is plotted on the y-axis. While control larvae clustered in the upper right quadrant of the scatter plot, indicating that their preference for light environment remained constant, experimental larvae clustered in the lower right quadrant. This confirmed that while experimental larvae, like controls, preferred the light environment before training, their preference had changed after training. Here experimental larvae shifted their preference toward the dark environment, which during training was paired with the social reward, the environment in which larvae had visual access to their conspecifics.

By subtracting the light environment preference score calculated for the first 15 minute period of test 2 from the light environment preference score calculated for test 1, we quantified this preference difference after training for both experimental and control groups (Figure 4.3d). While the control group showed no light environment preference difference, the experimental group showed a very large preference difference. Differences in light environment preference difference between experimental and control were statistically significant ($p=2.4 \cdot 10^{-5}$). This indicates that the larvae exposed to dark environment paired with the social reward were able to learn the association between the two stimuli. The distribution of this preference difference centered on zero for the control group, while it was significantly shifted in the direction of dark environment preference for the experimental group. However, the shape and width of the preference

distribution curve was the same for control and experimental groups. We therefore conclude that larval zebrafish can learn to associate the dark environment with the social environment, which caused individuals to change their light environment preference after a training period during which these two were paired.

Memory extinction occurs rapidly, whereas memory retention lasts up to 36h

Memory extinction is defined as a process in which a conditioned response diminishes over time when the association between unconditioned and conditioned stimuli are no longer present. Extinction occurred rapidly in the place-conditioning paradigm described here. Test 2, the light environment preference after conditioning, consisted of two 15-minute periods between which the illumination orientation with respect to the testing chamber was rotated by 180°, while the orientation of the testing chamber remained constant within the behavioral chamber. This means that larvae positioned in the dark environment at the end of the first period of test 2 were automatically in the light environment at the beginning of the second period of test 2 (Figure 4.4a).

While experimental larvae shifted their preference toward the dark environment during the first part of test 2, as compared to test 1 before training, these larvae spent the majority of the second part of test 2 in the light environment (Figure 4.4b). In contrast, control larvae preferred the light environment during both parts of test 2. The difference of light environment preference difference within test 2 between control and experimental groups was statistically significant ($p=3.13 \cdot 10^{-7}$) (Figure 4.4c). The shift

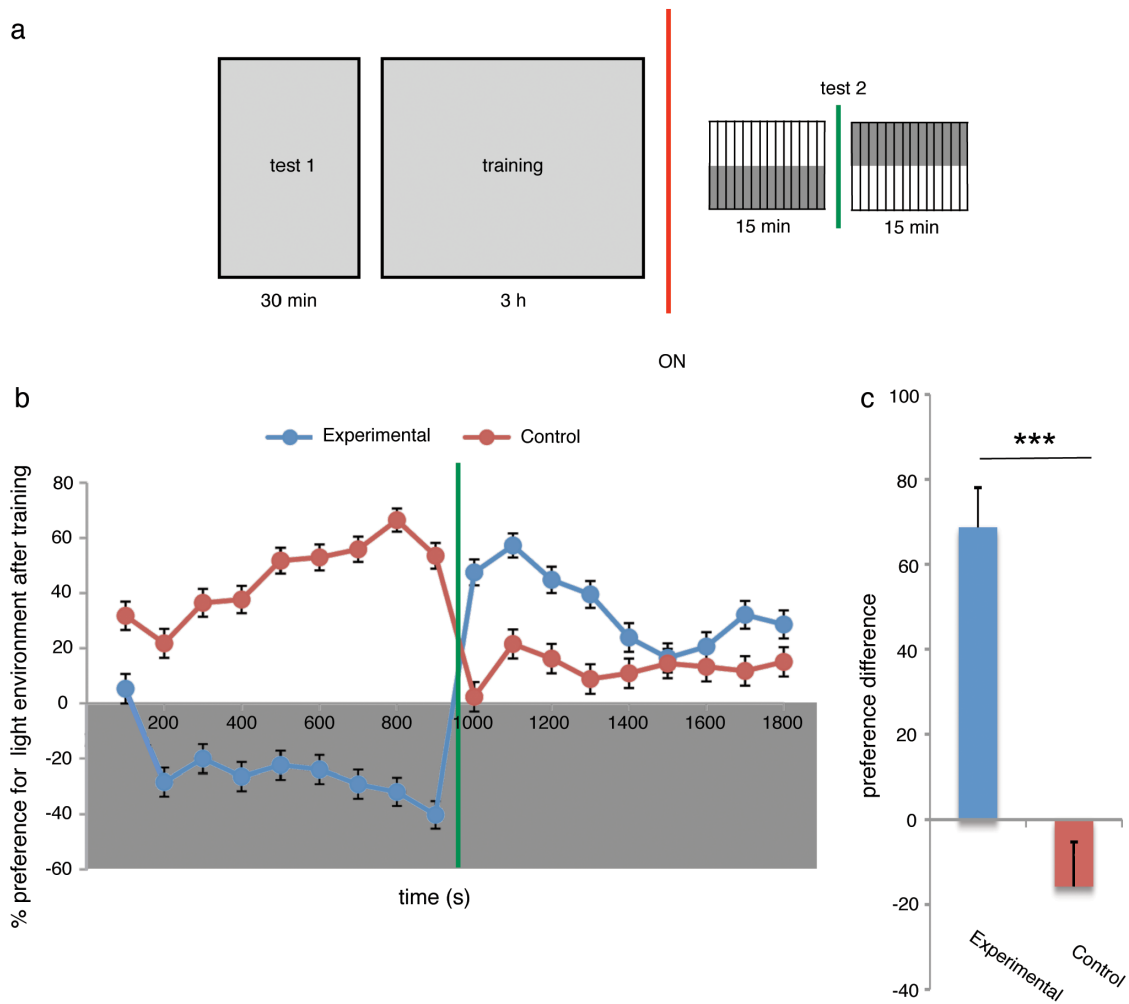


Figure 4.4. Rapid extinction of the conditioned association

(a) Scheme depicting test 2, during which larvae were exposed to dark environment, not paired with social environment. Green vertical line denotes time when the position of light and dark environment was switched. (b) Mean light preference of experimental (blue) and control (red) during every 100s period during test 2 (30 minutes total). Green vertical line denotes time when the position of light and dark environment was switched. (c) Light preference difference of experimental (blue) and control (red) between the first and second 15-minute period of test 2. Error bars in (b) and (c) denote SEM; *** $p < 0.001$.

back to preference for the light environment after a 15 minute exposure to the dark environment that no longer predicts social reward, suggests that memory of the

association undergoes rapid extinction. Under conditions in which preference for dark environment was no longer reinforced, larvae quickly learned to uncouple the social reward from the dark environment stimulus.

To test how long memory retention of the learned association remains stable, we varied the length of the interval between training and test 2 from 14h-48h (Figure 4.5a). Memory retention, as measured by preference difference, was significantly different from untrained control group when the interval between training and test 2 is 14h, 24h and 36h (Figure 4.5b). Only when the interval between training and test 2 was increased to 48h was the light environment preference difference no longer significantly different from the control group. These results demonstrate that memory of the association between dark environment and social reward was stable for at least 36h in 6-8dpf larvae. Interestingly, the preference difference distributions of the 36h and 48h interval groups did not show a normal distribution like control, 14h and 24h interval groups (Figure 4.5c). Instead, the preference difference distribution of the 36h interval group revealed that the population had split into two groups, one with low negative preference difference (indicating a slight preference shift towards the light environment after training) and the other with a moderate positive preference difference (indicating a preference shift towards the dark environment after training). The emergence of two distinct populations was even more dramatic in the 48h interval group (Figure 4.5c). While on average the 48h interval group did not show a significant preference difference associated with learning, these results indicated that a subpopulation may still be able to retain the associative memory after intervals as great as 48h between training and test 2. These results indicated that,

while extinction of the learned association occurred rapidly, memory retention in this paradigm was remarkably stable.

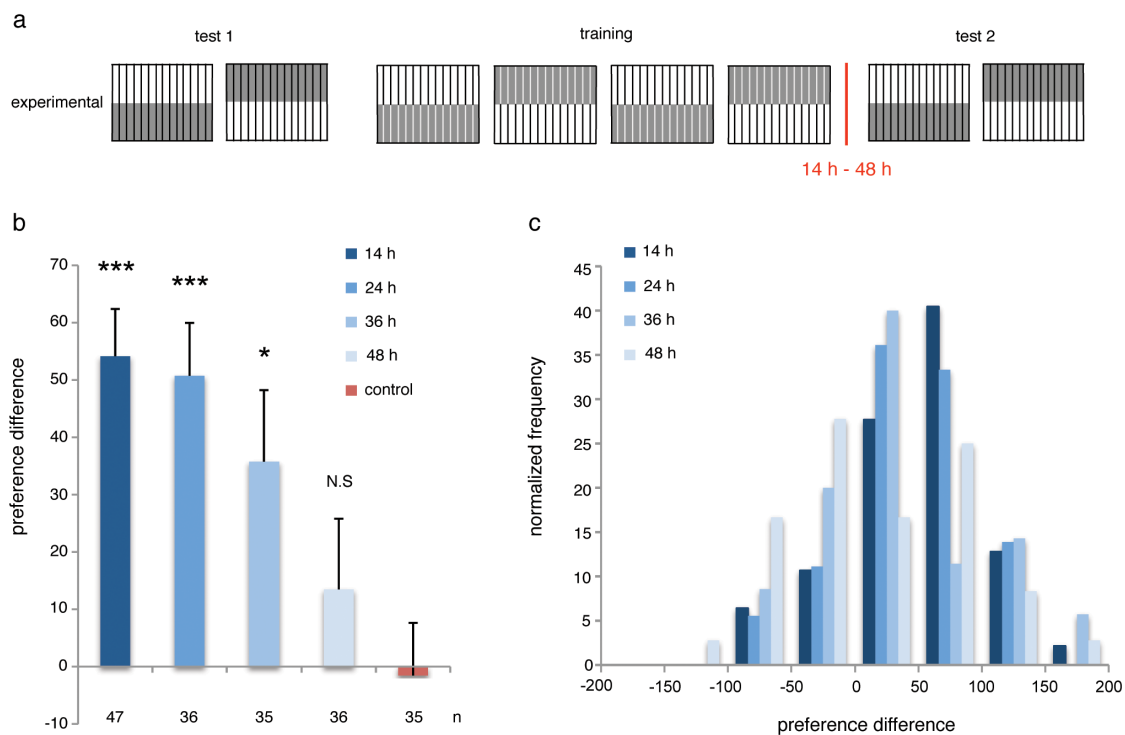


Figure 4.5. Memory of association persists for at least 36h.

(a) Scheme depicting place-conditioning paradigm. To test memory retention, time between training and test 2 was increased up to 48h. (b) Light preference difference of larvae tested 14h-48h (blue to light blue) after training and control (red) larvae, determined by subtracting light preference after training from light preference before training. Error bars denote SEM, *** $p < 0.001$, ** $p < 0.01$, * $p < 0.05$. (c) Preference difference distribution of larvae tested 14h-48h (blue to light blue) after training.

Memory formation is protein synthesis- and NMDAR-dependent

FUNCAT and BONCAT were adapted for larval zebrafish to permit investigation of protein synthesis in cells and neuronal circuits underlying memory formation. Therefore, any learning paradigm that is to be paired with these techniques must induce protein synthesis during memory formation. We tested whether the long-lasting memory described above requires new protein synthesis directly, by applying the protein synthesis inhibitors puromycin or cycloheximide during the three hour training period (Figure 4.6a).

Incubation with 5 μ g/ml puromycin exclusively during training completely abolished memory formation, while incubation with 10 μ M cycloheximide, a concentration previously used by others to impair long-term habituation in larval zebrafish (Wolman et al., 2011), had a less profound but still marked effect (Figure 4.6b). The distributions of preference differences are shown in Figure 4.6c. The preference difference distributions of both puromycin- and cycloheximide-incubated groups centered on zero and showed a normal distribution, reflecting normal variability of the light environment preference. Scatter plots of light environment preference before training plotted against light environment preference after training further illustrate that most larvae incubated in the protein synthesis inhibitors showed no change in light environment preference after training (Figure 4.6d and e). The difference in the impairment of memory retention caused by puromycin and cycloheximide may be concentration-dependent and memory retention may be completely abolished by incubations in higher concentrations of cycloheximide during training.

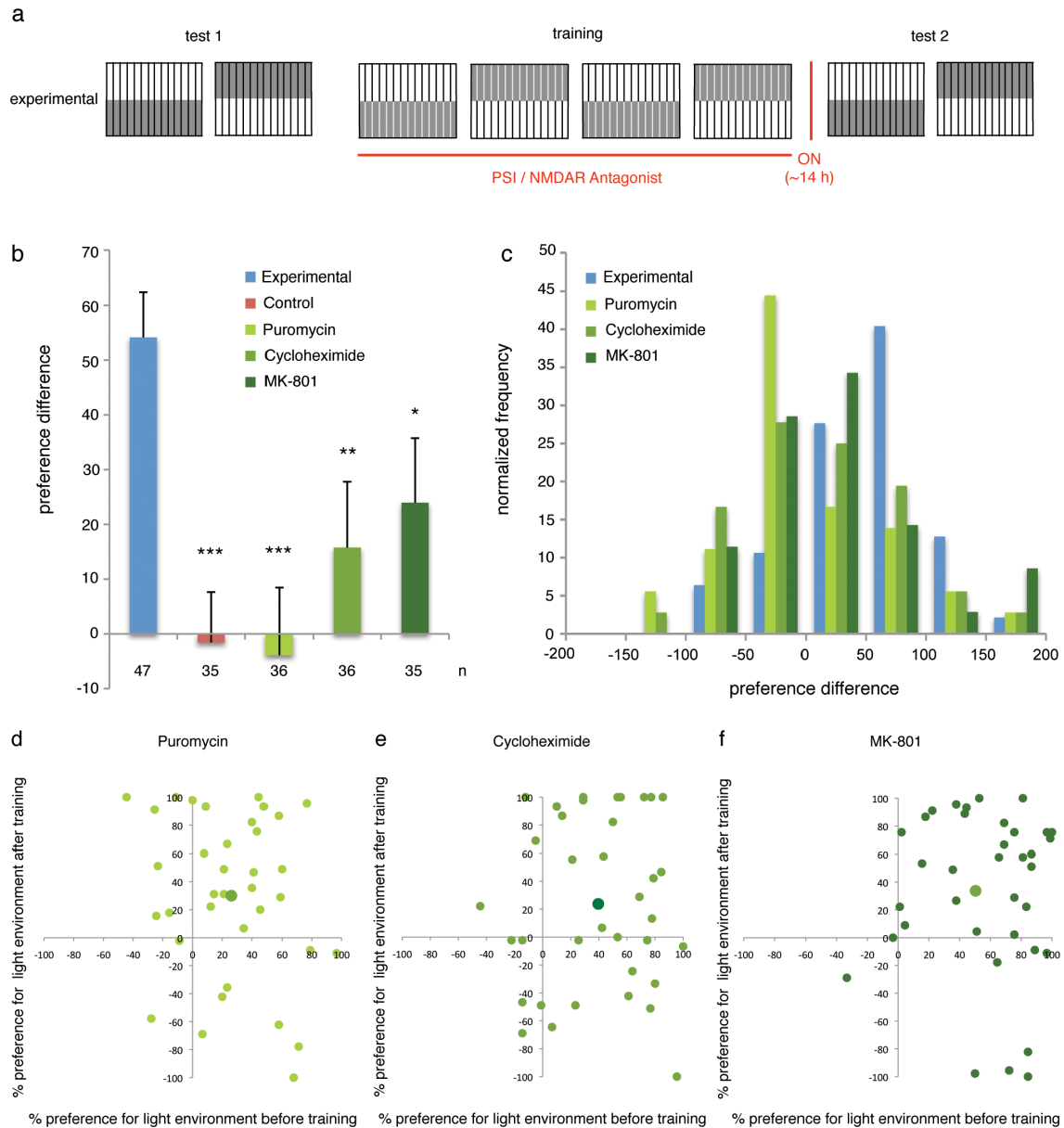


Figure 4.6. Memory formation is protein-synthesis dependent.

(a) Scheme depicting place-conditioning paradigm. To test whether memory formation is protein-synthesis dependent, larval zebrafish were incubated in puromycin (5 μ g/ml), cycloheximide (10 μ M) or MK-801 (100 μ M) during the 3h-training period. (b) Light preference differences of experimental (blue), control (red) and larvae exposed to puromycin (light green), cycloheximide (green) or MK-801 (dark green) tested 14h after training. Error bars denote SEM, *** p <0.001, ** p <0.01, * p <0.05. (c) Preference difference distributions of larvae incubated in puromycin (light green), cycloheximide (green) and MK-801 (dark green) during 3h training period. (d-f) Light preference before

(x-axis) and after (y-axis) training of puromycin-incubated (light green), cycloheximide-incubated (green) and MK-801-incubated (dark green) larvae. Larger markers denote mean light preference.

The NMDA receptor (NMDAR) has been shown to play a fundamental role in learning and memory and to underlie synaptic processes including LTP and LTD, especially in rodents. Two paralogs of each of the five mammalian NMDA receptor subunits (NR1 and NR2A through D) have been found in zebrafish. The nucleotide sequences of the subunit genes, especially NR1, are highly conserved between zebrafish and rodents (Cox et al., 2005). As observed in mammals, NR1 is widely expressed in the zebrafish brain, while NR2 subunits show more specific distribution patterns in distinct neuronal populations (Pan et al., 2010; Cox et al., 2005). Recently, Sison and Gerlai, as well as Blank and colleagues, showed that associative learning in adult zebrafish is NMDAR-dependent, using the selective non-competitive NMDAR antagonist, MK-801 (Wong et al., 1986; Sison and Gerlai, 2011; Blank et al., 2009).

Here we incubated larval zebrafish in 100 μ M MK-801 to investigate whether memory formation during the place-conditioning paradigm developed was NMDAR-dependent. Although not completely abolished, memory retention after incubation with MK-801 was significantly impaired, as compared to the experimental group, suggesting at least partial NMDAR dependence (Figure 4.6b). It is worth noting that most larvae exposed to MK-801 during training exhibited very little preference difference after conditioning, as illustrated by the fact that most clustered in the upper-right-hand quadrant of the light environment preference scatter plot (Figure 4.6f). However, four individuals (11.4%) showed significant changes in light environment preference towards

dark, indicating that they learned the trained association and that memory formation in these individuals may not be NMDAR-dependent.

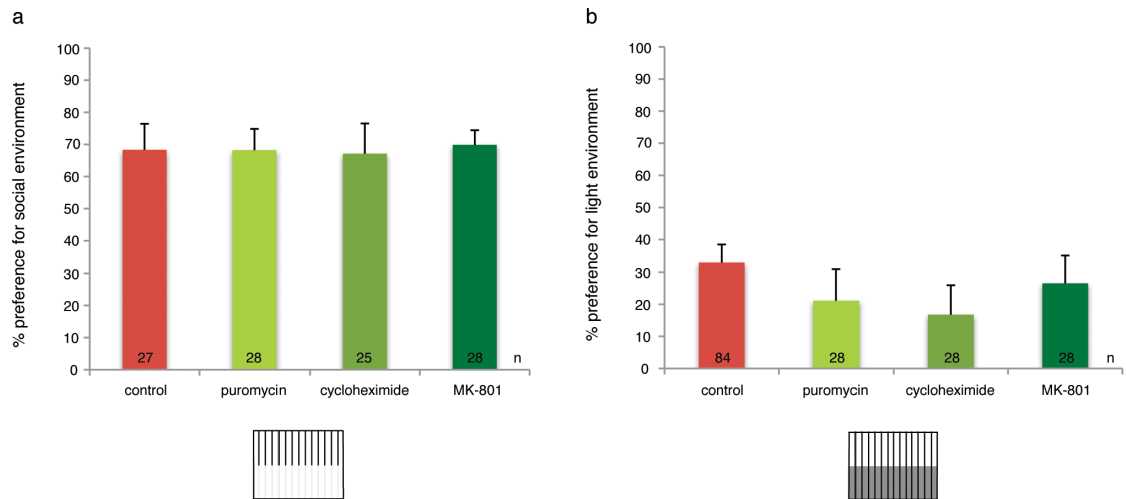


Figure 4.7. 3h incubation with puromycin, cycloheximide or MK-801 does not significantly alter unconditioned light and social environment preference.

Mean social (a) and light (b) preference during 15 minute period of 6-8dpf larval zebrafish after 3h incubation in puromycin (5 μ g/ml), cycloheximide (10 μ M) or MK-801 (100 μ M). Differences are not statistically significant. Error bars denote SEM.

Incubation with PSI and NMDAR-antagonists may affect behaviors other than learning and memory, which may indirectly impair performance in the place-conditioning paradigm. To examine whether the incubation conditions used influence simple behaviors, larval zebrafish were incubated in puromycin, cycloheximide or MK-801 for three hours, after which time the unconditioned social environment and light environment preferences were monitored as described previously. Both social and light environment preference did not change in the presence of PSI or the NMDAR antagonist (Figure 4.7).

Although, larvae incubated in cycloheximide showed a slight decrease in light environment preference, this decrease was not statistically significant. Together, these results demonstrate that formation of the association memory is protein synthesis-dependent and partially NMDAR-dependent, making the place-conditioning paradigm described here an ideal candidate for pairing with metabolic labeling techniques to identify cells and circuits involved in memory formation.

Exposure to social environment sustains exploratory behavior

Next, we investigated whether exposure to the training protocol or learning induced other quantifiable behavioral changes, such as changes in the level of exploratory behavior. Midline crossing, movement from the light environment to the dark environment or vice versa between subsequent frames during test 1 or test 2, can be used as a measure of exploratory behavior. During test 1, both control and experimental groups showed a mean midline crossing of around 13 crossings per 15 minute period. However after mock-training in the testing chamber (in which there were no conspecifics visible), control fish showed a drastic decrease in midline crossing to about 6 crossings per 15 minute period, while experimental larvae that were exposed to the social environment of the training chamber showed no such decrease (Figure 4.8c). The difference in midline crossing between test 1 and test 2 was significantly different between control and experimental groups. To test whether this sustained exploratory behavior of the experimental group was a result of associative learning or simply caused by exposure to

the social environment of the training chamber, we designed and tested a second ‘unpaired’ control.

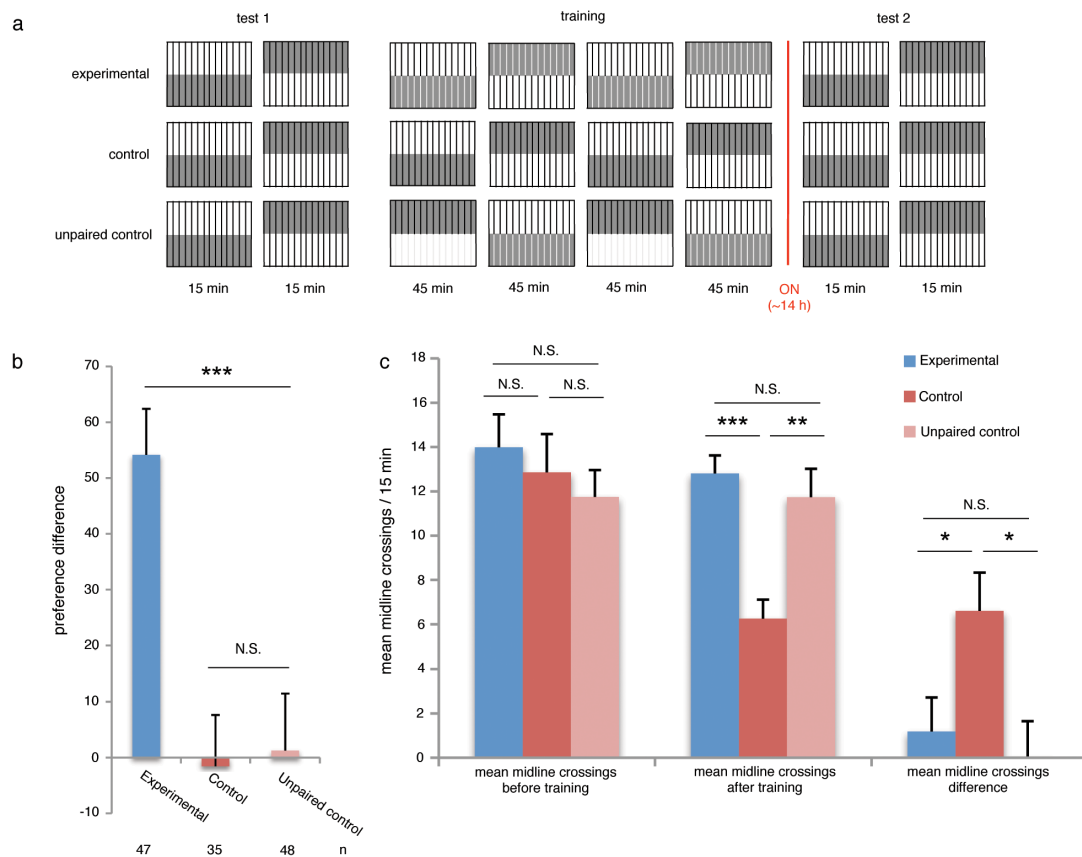


Figure 4.8. Exposure to social environment sustains exploratory behavior.

(a) Scheme depicting place-conditioning paradigm. Unpaired control larvae were exposed to unpaired social and dark environments during the training period. (b) Light preference difference of experimental (blue), control (red) and unpaired control (pink). Error bars denote SEM, *** $p < 0.001$. (c) Mean midline crossing during 15 minute period before training, after training and mean midline crossing difference. Midline crossing was scored as movement of larva from light to dark environment or vice versa between two subsequent frames (10 second interval). Error bars denote SEM, *** $p < 0.001$, ** $p < 0.01$, * $p < 0.05$.

Under unpaired control conditions, larvae were subjected to unpaired presentations of social environment and dark environment during the training period

(Figure 4.8a). While the dark environment orientation with respect to the behavioral chamber was rotated by 180° every 45 minutes, the orientation of the training chamber and hence the social environment with respect to the behavioral chamber was kept constant. This way dark and social environment were only paired during two of the four 45 minute training intervals. During the other two training intervals light and social environment were paired. As dark environment does not predict the social reward under these conditions, larvae should not learn to associate the two and therefore should not shift light environment preference toward the dark environment after training. However, as larvae were still exposed to the social environment, this allowed us to distinguish whether sustained exploratory behavior was linked with social reward exposure or learning.

The unpaired control group, like the control group, did not show a preference for light environment difference after training (Figure 4.8b) demonstrating that under the unpaired control conditions described above, larvae did not learn to associate dark environment and social reward. Furthermore, unpaired controls produced a similar number of midline crossing during test 1, before training, as both the control and experimental groups. However, unlike the control group, the unpaired control group showed a high number of midline crossings after training, during test 2. This difference in mean midline crossing between test 1 and test 2 was significantly different between unpaired control and control groups, while it was not significantly different between unpaired control and experimental groups. As the unpaired control groups were exposed to the social environment which allowed visual access of conspecifics, but did not learn to associate this social reward with the dark environment, we conclude that sustained

exploratory behavior, as measured by midline crossing, is a result of exposure to the social environment and not related to associative learning.

Discussion

In this chapter we have described a new associative place-conditioning paradigm for larval zebrafish. During a three hour training period experimental larvae learned to associate the social reward of visual access to a group of conspecifics with a dark environment. In contrast, control groups that were either not exposed to the social reward or to whom the social reward was presented in a manner unpaired with light environment, did not change their preference for light environment. Furthermore, we have demonstrated that this associative memory underwent rapid extinction but was remarkably stable, lasting for up to 36h. Incubating larvae in protein synthesis inhibitors or NMDAR antagonists during training, prevented and impaired memory formation, respectively, confirming that this associative learning is protein synthesis and partially NMDAR-dependent.

In establishing this paradigm, we have demonstrated both that 6-8dpf larvae are capable of associative learning and that the unconditioned stimulus of visual access to a group of conspecifics may act as a social reward. Previous attempts to associatively condition larval zebrafish relied on restriction of the larva by embedding it in agarose (Aizenberg and Schuman, 2011; Florian Engert personal communication), with the aim of combining these paradigms with calcium imaging of neural activity. However, using

this technique, larval zebrafish were only weakly trained and rapidly forgot the learned association or did not learn the association at all. One cause of weak training with agarose embedding may be that movement restriction of larval zebrafish significantly decreases overall neural activity, as was recently shown using bioluminescence to monitor neural activity (Naumann et al, 2010). In contrast, the associative place-conditioning paradigm described here does not require immobilization and may therefore enable associative conditioning of larval zebrafish.

Furthermore, we have shown that sight of conspecifics may act as social reward for larval zebrafish, supporting associative learning. The zebrafish is a social species known to aggregate, and visual access of conspecifics has previously been described to have rewarding properties in other species of fish (Gerlai and Hogan, 1992), as well as in adult zebrafish (Al-Imari and Gerlai, 2007; Gomez-Laplaza and Gerlai, 2010; Sison and Gerlai, 2011). One of the most commonly used conditioning paradigms in rodents is appetitive conditioning, in which a conditioned stimulus predicts timing or location of access to a food reward. However, precise delivery of small amounts of food in a localized manner as required in most learning tasks is technically more difficult in water. Food may dissolve and diffuse in the water and if left unconsumed may decrease water quality and interfere with conditioning. Thus, the demonstration that sight of conspecifics may be used as a practical way to reward zebrafish may enable development of other associative paradigms that, among other things, could be used to investigate sensory perception of larval zebrafish.

Interestingly, even though the studied larvae are virtually clones, as a result of generations of inbreeding, they still exhibit a great deal of variability. This variability

can be observed both in unconditioned light and social preference (Figure 4.3b), as well as in susceptibility of memory impairment to chemical stimulation with the NMDAR antagonist MK-801 (Figure 4.6f). Although most larvae tend to prefer the light and incubation with MK-801 impairs memory formation in most individuals, there are always outliers even in such a genetically homogenous group. In the future, it might be interesting to investigate regulation of gene methylation, expression and protein translation specifically in these outliers in order to identify genes and their proteins involved in mediating these divergent behaviors.

As this paradigm is simple and does not involve restraining of larvae or food reward, we believe it can easily be serialized for high-throughput behavioral screens, pharmacological screens or proteomic approaches. Furthermore, as the formation of the associative memory made here is protein synthesis-dependent, this paradigm may be ideally suited to be paired with FUNCAT and BONCAT techniques to visualize cells or neuronal circuits underlying memory formation, as well as to identify proteins differentially translated during memory formation.

Methods

Zebrafish stocks and husbandry

Wild-type adult fish strains were kept at 28°C on a 14h light/10h dark cycle. Embryos were obtained from natural spawnings and were maintained in E3 embryo

medium (5mM NaCl, 0.17mM KCl, 0.33mM CaCl₂, 0.33mM MgSO₄) (Nüsslein-Volhard and Dahm, 2002) at 28°C on a 14h light/10h dark cycle. Larvae were not fed before the training period.

Behavioral chambers

The testing and training chambers were custom constructed from white plastic and transparent Plexiglas. Both chambers were 12.5cm by 8.5cm and 1cm deep, divided into 14 individual channels by removable partitions, which were slanted at increasing angle from the middle outwards to prevent the creation of blind spots during video monitoring. The bottom of the training and testing chamber was made of transparent Plexiglas, while the sides were made of white plastic. The testing chamber was identical to the training chamber, except that it had completely opaque partitions made of single pieces of white plastic, while the training chamber had partitions that are half transparent Plexiglas and half opaque white plastic. The behavioral chamber was custom constructed from white plastic, transparent Plexiglas and a semitransparent soft plastic. It measured 23cm in total height, while the enclosed compartment was 11cm by 16cm by 13cm. The bottom was made of Plexiglas covered with a thin layer of semitransparent soft plastic. The rest of the behavioral chamber was constructed of white plastic. The front of the behavioral chamber had a sliding door and the top had a hole to allow visual access. Sketches of behavioral chambers can be found in Appendix B.

Behavioral Assay, video recording and behavioral analysis

The testing chamber was filled with approximately 30ml of E3 embryo medium and 6-8dpf larval zebrafish that showed high exploratory behavior (swam across petri dish instead of remaining at the walls, swam near the surface indicating that swim bladders were fully inflated and avoided capture) were placed individually into the 12 center channels. The testing chamber was placed in the behavioral chamber. To monitor light environment preference, the projector (Optoma Pico Pocket DLP Projector, model no. PK301) was controlled using Matlab (testFish.m, Appendix C) to illuminate the behavioral chamber, creating two different but equally sized light environments. The dark environment was created by setting the projector to emit red, green, blue (RGB) values of 120, while the light environment was created by the projector emitting RGB values of 230. The testing chamber was oriented such that the light and dark environments met at the midline of the testing chamber. Larval zebrafish position was captured using a Phillips webcam (SPC 2050NC) every 10 seconds for a period of 15 minutes (testFish.m, Appendix C).

During test 1, in which we quantified unconditioned light environment preference, larval zebrafish position in the testing chamber was monitored for two 15-minute periods. In between these two periods the orientation of the light environments projected onto the behavioral chamber was rotated by 180°, but the orientation of the testing chamber within the behavioral chamber remained constant. For the experimental condition, the training chamber was filled with E3 embryo medium. Larvae previously in the testing chamber were moved into the training chamber in the same order. The training chamber was

placed into the behavioral chamber. The same light environments as previously described were projected onto the behavioral chamber and the training chamber was oriented such that the social environment was placed over the dark environment. The orientation of light environment and the training chamber were rotated by 180° every 45 minutes. Training consisted of four 45-minute periods, for a total of 3h. Larval position was not monitored during training and light environment was controlled using Matlab (trainFish.m, Appendix C). Control group larvae were gently suctioned out of the testing chamber after test 1, immediately returned to the same channel in the testing chamber and exposed to the same training light environment conditions as the experimental group.

After training, larvae were individually placed in a 12 well plate containing 1.5ml E3 embryo medium per well. The plate was marked to keep track of each individual larva and was incubated at 28°C on a 14h light, 10h dark cycle for approximately 14h. Next, larvae were returned to the testing chamber in the same order as before to quantify light environment preference after conditioning. As previously described for test 1, test 2 consisted of two 15-minute periods during which the light environments were projected onto the bottom of the behavioral chamber while the position of the larvae was monitored from above. The orientation of the light environment with regard to the testing chamber was switched between the two periods, while the orientation of the testing chamber in the behavioral chamber remained constant.

Each frame of larvae position taken during test 1 and test 2 was saved automatically and scored manually. Larvae detected in the light environment were scored as +1, while larvae detected in the dark environment were scored at -1. If larvae position could not be identified, a score of 0 was recorded for that frame. Scores for all 90 frames

(taken every 10 seconds for 15 minutes) were added and normalized to 100 to give final light environment preference scores. Preference difference scores, as a measure of memory retention, were calculated by subtracting light environment preference scores for the first period of test 2 from the mean light environment preference score of test 1. Significance was calculated using the unpaired two-tailed t-test and all error bars represent standard error of the mean.

Memory retention was investigated by prolonging the isolation periods between training and test 2. As described before, larvae were placed individually in 12 well plates at 28°C on a 14h light, 10h dark cycle for 24h-48h. Unconditioned and conditioned light environment preference, as well as training, remained the same.

Pharmacology

Larvae were incubated in each compound exclusively during the 3h training period. 1000X stock solutions were made by dissolving MK-801 (M107; Sigma-Aldrich), puromycin (P8833; Sigma-Aldrich) and cycloheximide (PS1002; Sigma-Aldrich) in 100% DMSO (D2650; Sigma-Aldrich) and stored at -20°C. Stock solutions were dissolved in E3 embryo medium to final concentration. This was used to fill the training chamber, into which larvae were placed, while making sure to transfer as little excess embryo medium from the testing chamber as possible. After training, larvae were removed from the training chamber and washed twice in 1.5ml E3 embryo medium before being placed in a 12 well plate as described above.

Chapter V

DISCUSSION AND FUTURE DIRECTIONS

Discussion

Long-term memory formation has been shown to be protein synthesis-dependent. Using both chemical manipulations of total protein synthesis via temporally and structurally targeted application of PSI and genetic manipulation of key proteins involved in translational control, researchers over the last half century have shown conclusively that new protein synthesis is required to implement the physical changes underlying memory formation (reviewed in Sweatt, 2009). Although many proteins involved in the signaling cascades, structural changes and synaptic strengthening that result in long-term memory formation have been identified, hundreds more could play important roles that have yet to be discovered. Currently available techniques to identify proteins synthesized in response to certain stimulations, such as SILAC, do not permit selective affinity purifications of newly synthesized proteins. This means that sample complexity cannot be reduced before identification using tandem mass spectrometry, possibly preventing identification of proteins of low abundance. It is precisely these proteins of low abundance that might be some of the most interesting signaling molecules involved in memory formation.

Furthermore, the role of the hippocampus, which is thought to be homologous to the dorsal lateral telencephalon in teleosts, in memory formation has been well demonstrated using both surgical and chemical lesions *in vivo*. However, which specific cells participate in long-term coding of a discrete memory and how many show changes in protein synthesis is not known. Using genetically encoded fluorescent proteins, such as GFP, the translation and localization of specific candidate proteins can be visualized.

Unfortunately, these techniques rely on overexpression of the target gene, which along with the size of the fluorescent protein tag may alter protein function and localization. Furthermore, these techniques will always depend on *a priori* candidate selection and may therefore severely hinder, if not altogether prevent, the unbiased identifications of effector proteins underlying long-term memory formation.

Here, we have described the development of novel tools for the visualization of cells underlying protein synthesis-dependent memory formation in intact animals, as well as the purification and identification of effector proteins that are regulated in this process. First, we have demonstrated that the bioorthogonal metabolic labeling techniques BONCAT and FUNCAT, originally developed *in vitro*, can be applied to the larval zebrafish to quantify, purify and visualize newly synthesized proteins *in vivo*. We show that incubation with the noncanonical amino acid AHA does not affect simple behaviors but leads to incorporation and labeling of newly synthesized proteins specifically in a time- and concentration-dependent manner. These newly synthesized proteins can be tagged in a click chemistry reaction with either a biotin-alkyne to permit quantification using immunoblots and affinity purification (BONCAT) or a fluorescent-alkyne to enable visualization (FUNCAT) in whole-mount larval zebrafish. These approaches are not candidate based and, due to the small size of the azide moiety, introduction of AHA is unlikely to interfere with endogenous function and localization of tagged proteins. Using these techniques as adapted to the larval zebrafish, we have demonstrated that chemical stimulation with the proconvulsant GABA antagonist PTZ increases protein synthesis.

Next, we genetically restricted these metabolic labeling techniques to specific cell populations via selective expression of a mutant aminoacyl-tRNA synthetase (MetRS) in

larval zebrafish. Previous work by Tirrell and coworkers has provided evidence that introduction of specific residue mutations of the *E. coli* MetRS catalytic cleft allows the mutant enzyme to charge the larger noncanonical amino acid ANL. The MetRS catalytic binding pocket residues are highly conserved between *E. coli* and *Danio rerio* and we have demonstrated here that introduction of the mutations characterized in *E. coli* enables zebrafish MetRS to charge ANL both *in vitro* and *in vivo*. Only COS7 cells that were expressing the zebrafish L13G-MetRS in the absence of a PSI incorporated ANL. Both transient and stable expression of the L13G-MetRS in the larval zebrafish nervous system allowed for cell-specific visualization of newly synthesized proteins. Restriction of metabolic labeling techniques *in vivo* opens new avenues to study the proteome of specific neuronal populations by biochemical and imaging assays.

Finally, we developed a protein synthesis-dependent place-conditioning paradigm for 6-8dpf larval zebrafish. By pairing a social reward, visual access to a group of conspecifics, with a specific light environment, we were able to train larvae to prefer the light environment associated with the reward. Learned light preference underwent rapid extinction under conditions in which the association was not reinforced, but remained stable for up to 36h after training. Exposure to the PSI puromycin and cycloheximide during the 3h training period completely abolished and severely inhibited memory formation, respectively. Furthermore, incubation with the NMDAR-antagonist MK-801 also impaired memory formation. This protein synthesis-dependent place-conditioning paradigm is achieved in freely moving animals and does not rely on food reward, which is difficult to administer and remove in an aquatic environment, and could easily be serialized for high-throughput screening.

Future directions

Chemical screening

Adult zebrafish lay clutches of hundreds of eggs; the larvae are small, transparent and easily absorb chemicals present in their environment. These characteristics, among others, have recently made the larval zebrafish a prominent model organism for small molecule chemical screening. Large libraries can quickly be screened for both developmental and behavioral phenotypes and have been successfully used to identify chemicals that influence the photomotor response (Kokel et al., 2010; Kokel and Peterson, 2011), sleep and arousal (Rihel et al., 2010; Rihel, Prober and Schier, 2010) and short-term habituation (Wolman et al., 2011).

Both the metabolic labeling techniques and the place-conditioning paradigm developed in this study could be combined with high-throughput chemical screening. As we demonstrated, stimulating larval zebrafish with chemical compounds such as the GABA antagonist PTZ can alter protein synthesis, which can be detected using BONCAT and FUNCAT techniques. In the future, pairing chemical screening with AHA incubation could be used to identify compounds that alter protein synthesis, as well as elucidate in which specific organs or cell types of the larval zebrafish these effects are most prominent. Furthermore, incubation with PSI cycloheximide and puromycin, as well as the NMDAR-antagonist MK-801, impaired memory formation of the place-conditioning paradigm described here, showing that learning is protein-synthesis and partially NMDAR-dependent. Small molecule screening could be paired with the high-

throughput associative conditioning paradigm developed in this study to identify chemicals that disrupt or enhance memory formation.

Proteomics

The BONCAT technique enables affinity purification specifically of those proteins that were newly synthesized during the noncanonical amino acid incubation window from total protein samples. Affinity purification thereby allows for the identification of specific proteins in the pool of newly synthesized proteins using western blotting, but has a main advantage in that it reduces sample complexity in order to permit identification of less abundant proteins using tandem mass spectrometry. Using BONCAT in HEK293 cells, Dieterich and colleagues were able to identify 195 proteins that were newly synthesized during the 2h AHA incubation period (Dieterich et al., 2006). Establishing affinity purification and tandem mass spectrometry protocols that allow for the identification of newly synthesized proteins from whole larval zebrafish, as well as from specifically labeled cell populations using genetically restricted BONCAT techniques, is an immediate future goal.

In preliminary experiments using a 72h AHA incubation, we were able to affinity purify and identify over 540 proteins from 7dpf larval zebrafish (Appendix D). Briefly, 4dpf larval zebrafish were incubated in E3 embryo medium supplemented with 4mM AHA for 72h before being anesthetized on ice, homogenized and reacted to the biotin-alkyne tag as described in Chapter II. Labeled proteins were affinity purified using NeutrAvidin beads followed by on-bead digestion with trypsin and submitted to a liquid-

chromatography-coupled tandem mass spectrometric analysis for protein identification (Dionex nanoRSLC and ThermoScientific Orbitrap Elite). This resulted in the detection of both soluble and membrane proteins associated with a variety of different cellular functions and subcellular localizations (Figure 5.1), indicating that AHA incorporation is generally unbiased in larval zebrafish. In the future, we will aim to replicate these findings, as well as optimize the protocols to enable identification of newly synthesized proteins from specific cell populations.

Live labeling

Currently, BONCAT and FUNCAT techniques depend on covalent linking of alkyne and azide groups via a selective Cu(I)-catalyzed [3+2] azide-alkyne cycloaddition. As the copper catalyst necessary for this reaction is toxic, live labeling of protein synthesis using ‘click chemistry’ is not possible. Recently, the Bertozzi group described a strain-promoted [3+2] cycloaddition between cyclooctynes and azides that proceeds under physiological conditions without the need for a catalyst and is not toxic *in vivo* (Agard, Prescher and Bertozzi, 2004; Baskin et al., 2007; Dieterich et al., 2010). Unfortunately, these fluorescent difluorinated cyclooctyne (DIFO) tags are not cell membrane permeable and therefore not suitable for live imaging of cytoplasmic proteins *in vivo*.

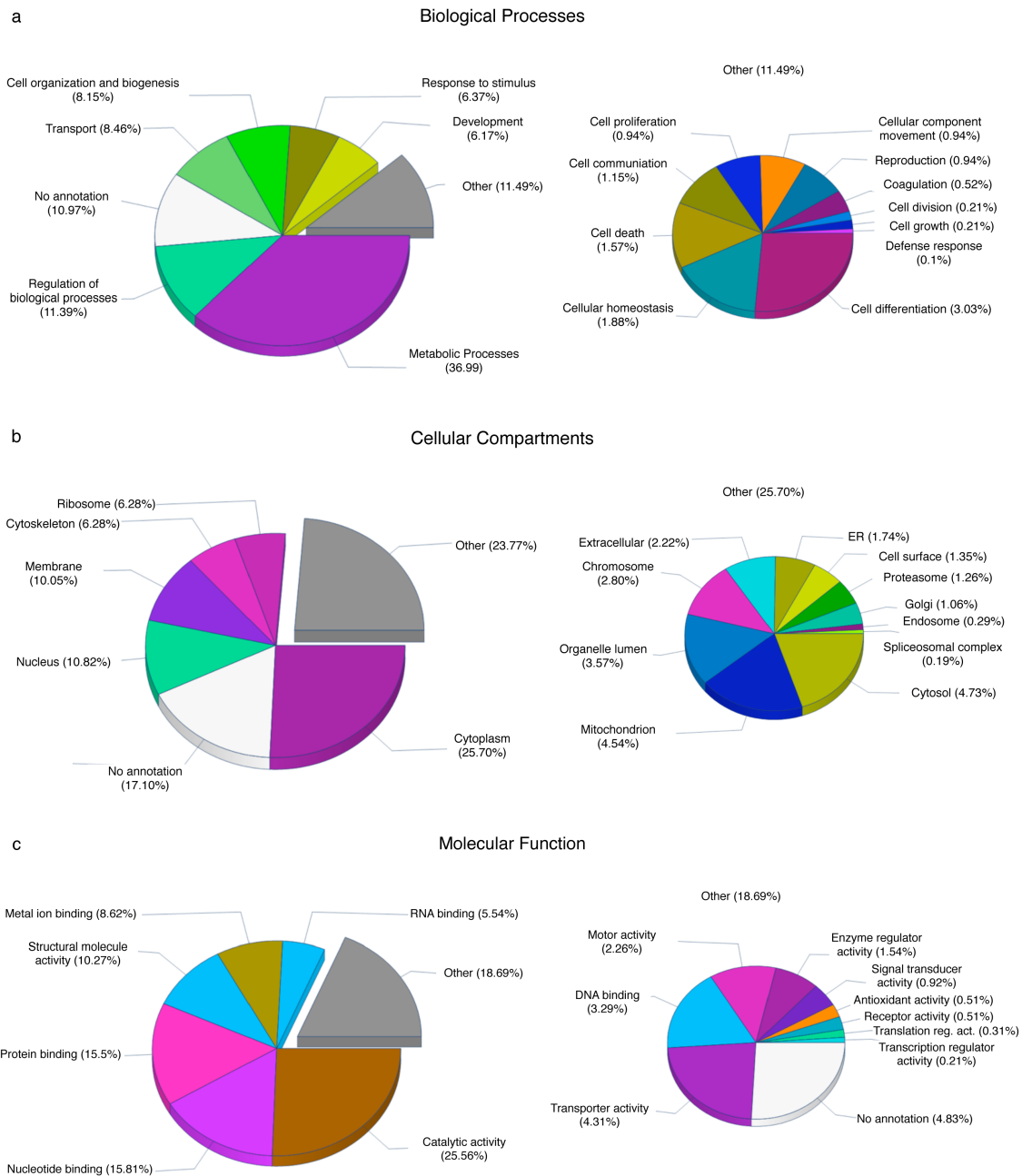


Figure 5.1. Physical mapping of preliminary proteomic data

Gene ontology categorization of newly synthesized proteins identified by tandem MS after 72h AHA incubation and affinity purification into (a) biological process, (b) cellular compartment and (c) molecular function.

However, progress towards live labeling of cytoplasmic proteins is being made. Beatty and coworkers are currently developing a set of cyclooctyne tags coupled to small, cell membrane-permeable fluorophores such as coumarin and BODIPY and have shown first results that these tags may enable cytoplasmic protein labeling in live mammalian cell lines (Beatty et al., 2010, Beatty et al., 2011). Development of such cell membrane-permeable tags will permit live imaging of newly synthesized proteins in cells and possibly whole organisms, thereby opening new avenues for investigating dynamic metabolic responses in complex systems to both chemical and possibly even behavioral stimuli.

Visualizing memory formation

The ultimate aim of this study was to develop tools that would enable the visualization of neuronal circuits involved in memory formation, as well as the characterization of these newly synthesized proteins. Although long-term memory formation has been proven to depend on protein synthesis, there is still an ongoing debate as to whether this means that memory formation will induce *increases* in protein synthesis in specific neurons or at specific synapses involved, or whether memory formation simply causes *altered* protein synthesis. Studies using ³⁵S-methionine labeling after serotonin stimulation of Aplysia sensory neurons have shown that this chemical stimulation initiates a pronounced change in total protein synthesis rate (Barzilai et al., 1989). Furthermore, genetic manipulations that cause disruption of translation inhibition, resulting in an increased protein synthesis rate, concurrently caused increased L-LTP formation (Kelleher et al., 2004). Both of

these studies provide evidence that increased protein synthesis is necessary for long-term memory formation.

However, Klann and Sweatt propose an alternative model by which a transient memory triggers limited translation initiation and synthesis of new proteins, but is subsequently stabilized and perpetuated by a positive feedback mechanism requiring only ongoing constitutive protein synthesis (Klann and Sweatt, 2008). In this refinement of the “synaptic tagging and capture” model, only a very small number of proteins would need to show increased synthesis rates to initiate memory formation, while the functional changes associated with memory formation may be instantiated by localized recruitment of constitutively synthesized proteins. FUNCAT can be used to visualize global changes in the rate of protein synthesis during specific time windows, but cannot be used to visualize altered levels of protein synthesis of specific proteins. Therefore, pairing FUNCAT techniques with the larval zebrafish place-conditioning paradigm developed in this study may enable us to distinguish between these two hypotheses and determine whether memory formation relies on increased or altered rates of protein synthesis. If indeed increased protein synthesis is visualized during memory formation, the location of this increase in fluorescence will identify cells and circuits involved in memory formation.

Furthermore, identifying the proteins that are translated during long-term memory formation may be possible by pairing the place-conditioning paradigm with BONCAT to label, affinity purify and then analyze the newly synthesized proteins using tandem mass spectrometry. By comparing the proteomes of larvae that showed learning of the association and those that were exposed only to the control conditions or those that did

not show changed light preference when exposed to the training protocol, we may be able to identify specific effector proteins that show altered translation with memory formation. These most likely will include proteins involved in signaling cascades regulating LTP, such as CaMKII and PKM ζ , as well as proteins involved in structural change and synaptic strengthening, such as cadherins and AMPA receptors. Hopefully, such experiments will confirm known effector proteins and will identify as-yet-unknown proteins underlying memory formation.

Two further points should be considered. For one, depending on the time window of AHA incubation, different populations of proteins will likely be tagged as a result of specific synthesis and degradation rates. During prolonged incubation periods proteins of short half-life may be both synthesized and degraded, thereby preventing their affinity purification and identification. Arc, for example, has been shown to be synthesized and degraded within 30 minutes of memory induction. Incubation periods of 12h may therefore not be able to capture low abundant proteins with short life-spans, even though these may be of most interest in elucidating the signaling cascades underlying memory formation. Whether AHA diffusion rates into deep tissue, such as the nervous system, will be fast enough to allow for precise capture of different waves of translation will have to be determined experimentally. Secondly, mass spectrometry analysis may enable the identification of post-translational modifications of effector proteins, such as phosphorylation of signaling molecules and glycosylation of membrane proteins, thereby providing us with an even more complete picture of molecular changes occurring during long-term memory formation.

In conclusion, the tools developed in this study may be used to investigate a number of different scientific questions, including what small molecules effect memory formation and regulate protein synthesis rates in zebrafish. New developments, such as the generation of small fluorescent tags may enable live intracellular labeling while proteins are being synthesized, and the optimization of affinity purification and mass spectrometry analysis, will permit us to identify these newly synthesized larval zebrafish proteins. Finally, these techniques will be paired in order to investigate changes in translation with memory formation, potentially enabling identification of neuronal circuits and specific proteins involved in long-term memory formation.

WORK CITED

- Aakalu G, Smith WB, Nguyen N, Jiang C, Schuman EM. (2001) Dynamic visualization of local protein synthesis in hippocampal neurons. *Neuron*. **30**:489–502.
- Abel T, Lattal KM. (2001) Molecular mechanisms of memory acquisition, consolidation and retrieval. *Curr Opin Neurobiol*. **11**:180–187.
- Abraham WC, Williams JM. (2003) Properties and mechanisms of LTP maintenance. *Neuroscientist*. **9**:463–474.
- Agard NJ, Prescher JA, Bertozzi CR. (2004) A strain-promoted [3 + 2] azide-alkyne cycloaddition for covalent modification of biomolecules in living systems. *J Am Chem Soc*. **126**:15046–15047.
- Agranoff BW, Davis RE, Brink JJ. (1966) Chemical Studies on Memory Fixation in Goldfish. *Brain Research*. **1**:303–309.
- Agranoff BW, Klinger PD. (1964) Puromycin Effect on Memory Fixation in the Goldfish. *Science*. **146**:952–953.
- Aizenberg M, Schuman EM. (2011) Cerebellar-dependent learning in larval zebrafish. *J Neurosci*. **24**:8708–8712.
- Alger BE, Teyler TJ. (1976) Long-term and short-term plasticity in the CA1, CA3, and dentate regions of the rat hippocampal slice. *Brain Res*. **110**:463–480.
- Al-Imari L, Gerlai R. (2008) Sight of conspecifics as reward in associative learning in zebrafish (*Danio rerio*). *Behav Brain Res*. **189**:216–219.
- An M, Luo R, Henion PD. (2002) Differentiation and maturation of zebrafish dorsal root and sympathetic ganglion neurons. *J Comp Neurol*. **446**:267–275.
- Asakawa K, Kawakami K. (2009) The Tol2-mediated Gal4-UAS method for gene and enhancer trapping in zebrafish. *Methods*. **49**:275–281.
- Asakawa K, Suster ML, Mizusawa K, Nagayoshi S, Kotani T, Urasaki A, Kishimoto Y, Hibi M, Kawakami K. (2008) Genetic dissection of neural circuits by Tol2 transposon-mediated Gal4 gene and enhancer trapping in zebrafish. *Proc Natl Acad Sci U S A*. **105**:1255–1260.
- Akitake CM, Macurak M, Halpern ME, Goll MG. (2011) Transgenerational analysis of transcriptional silencing in zebrafish. *Dev Biol*. **352**:191–201.

Banko JL, Poulin F, Hou L, DeMaria CT, Sonenberg N, Klann E. (2005) The translation repressor 4E-BP2 is critical for eIF4F complex formation, synaptic plasticity, and memory in the hippocampus. *J Neurosci.* **25**:9581–9590.

Baraban SC, Dinday MT, Castro PA, Chege S, Guyenet S, Taylor MR. (2007) A large-scale mutagenesis screen to identify seizure-resistant zebrafish. *Epilepsia.* **6**:1151–1157.

Baraban SC, Taylor MR, Castro PA, Baier H. (2005) Pentylentetrazole induced changes in zebrafish behavior, neural activity and c-fos expression. *Neuroscience.* **3**:759–768.

Barzilai A, Kennedy TE, Sweatt JD, Kandel ER. (1989) 5-HT modulates protein synthesis and the expression of specific proteins during long-term facilitation in Aplysia sensory neurons. *Neuron.* **2**:1577–1586.

Baskin JM, Dehnert KW, Laughlin ST, Amacher SL, Bertozzi CR. (2010) Visualizing enveloping layer glycans during zebrafish early embryogenesis. *Proc Natl Acad Sci U S A.* **23**:10360–10365.

Baskin JM, Prescher JA, Laughlin ST, Agard NJ, Chang PV, Miller IA, Lo A, Codelli JA, Bertozzi CR. (2007) Copper-free click chemistry for dynamic in vivo imaging. *Proc Natl Acad Sci U S A.* **104**:16793–16797.

Beatty KE, Fisk JD, Smart BP, Lu YY, Szychowski J, Hangauer MJ, Baskin JM, Bertozzi CR, Tirrell DA. (2010) Live-cell imaging of cellular proteins by a strain-promoted azide-alkyne cycloaddition. *ChemBiochem.* **11**:2092–2095.

Beatty KE, Liu JC, Xie F, Dieterich DC, Schuman EM, Wang Q, Tirrell DA. (2006) Fluorescence visualization of newly synthesized proteins in mammalian cells. *Angew Chem Int Ed Engl.* **45**:7364–7367.

Beatty KE, Szychowski J, Fisk JD, Tirrell DA. (2011) A BODIPY-cyclooctyne for protein imaging in live cells. *ChemBiochem.* **12**:2137–2139.

Beatty KE, Tirrell DA. (2008) Two-color labeling of temporally defined protein populations in mammalian cells. *Bioorg Med Chem Lett.* **18**:5995–5999.

Beatty KE, Xie F, Wang Q, Tirrell DA. (2005) Selective dye-labeling of newly synthesized proteins in bacterial cells. *J Am Chem Soc.* **127**:14150–14151.

Best, MD. (2009) Click chemistry and bioorthogonal reactions: unprecedented selectivity in the labeling of biological molecules. *Biochemistry.* **28**:6571–6584.

Best JD, Berghmans S, Hunt JJ, Clarke SC, Fleming A, Goldsmith P, Roach AG. (2008) Non-associative learning in larval zebrafish. *Neuropsychopharmacology.* **33**:1206–1215.

- Bilotta J, Risner ML, Davis EC, Haggbloom SJ. (2005) Assessing appetitive choice discrimination learning in zebrafish. *Zebrafish*. **2**:259–268.
- Blank M, Guerim LD, Cordeiro RF, Vianna MR. (2009) A one-trial inhibitory avoidance task to zebrafish: rapid acquisition of an NMDA-dependent long-term memory. *Neurobiol Learn Mem*. **92**:529–534.
- Bliss TV, Lomo T. (1973) Long-lasting potentiation of synaptic transmission in the dentate area of the anaesthetized rabbit following stimulation of the perforant path. *J Physiol*. **232**:331–356.
- Braubach OR, Wood HD, Gadbois S, Fine A, Croll RP. (2009) Olfactory conditioning in the zebrafish (*Danio rerio*). *Behav Brain Res*. **198**:190–198.
- Broglio C, Gómez A, Durán E, Ocaña FM, Jiménez-Moya F, Rodríguez F, Salas C. (2005) Hallmarks of a common forebrain vertebrate plan: specialized pallial areas for spatial, temporal and emotional memory in actinopterygian fish. *Brain Res Bull*. **66**:277–281.
- Brooks-Kayal AR, Shumate MD, Jin H, Rikhter TY, Coulter DA. (1998) Selective changes in single cell GABA(A) receptor subunit expression and function in temporal lobe epilepsy. *Nat Med*. **10**:1166–1172.
- Bruckman, MA, Kaur, G, Lee, L.A, Xie, F, Sepulvecla, J, Breitenkamp, R, Zhang, X, Joralemon, M, Russel, TP, Emrick, T, Wang, Q. (2008) Surface modification of tobacco mosaic virus with “Click” chemistry. *ChemBioChem*. **9**:519–523.
- Budick SA, O'Malley DM. (2000) Locomotor repertoire of the larval zebrafish: swimming, turning and prey capture. *J Exp Biol*. **203**:2565–2579.
- Burgess HA, Granato M. (2007) Sensorimotor gating in larval zebrafish. *J Neurosci*. **27**:4984–94.
- Chang PV, Prescher JA, Sletten EM, Baskin JM, Miller IA, Agard NJ, Lo A, Bertozzi CR. (2010) Copper-free click chemistry in living animals. *Proc Natl Acad Sci U S A*. **5**:1821–1826.
- Chen CC, Wu JK, Lin HW, Pai TP, Fu TF, Wu CL, Tully T, Chiang AS. (2012) Visualizing long-term memory formation in two neurons of the *Drosophila* brain. *Science*. **335**:678–685.
- Clarke JD, Hayes BP, Hunt SP, Roberts A. (1984) Sensory physiology, anatomy and immunohistochemistry of Rohon-Beard neurones in embryos of *Xenopus laevis*. *J Physiol*. **348**:511–525.

- Collingridge GL, Kehl SJ, McLennan H. (1983) Excitatory amino acids in synaptic transmission in the Schaffer collateral-commissural pathway of the rat hippocampus. *J Physiol.* **334**:33–46.
- Colwill RM, Creton R. (2011) Imaging escape and avoidance behavior in zebrafish larvae. *Rev Neurosci.* **22**:63–73.
- Costa-Mattioli M, Gobert D, Harding H, Herdy B, Azzi M, Bruno M, Bidinosti M, Ben Mamou C, Marcinkiewicz E, Yoshida M, Imataka H, Cuello AC, Seidah N, Sossin W, Lacaille JC, Ron D, Nader K, Sonenberg N. (2005) Translational control of hippocampal synaptic plasticity and memory by the eIF2alpha kinase GCN2. *Nature.* **436**:1166–1173.
- Cotman CW, Lynch GS. (1989) The neurobiology of learning and memory. *Cognition.* **33**:201–241.
- Cowie DB, Cohen GN. (1957) Biosynthesis by *Escherichia coli* of active altered proteins containing selenium instead of sulfur. *Biochim Biophys Acta.* **26**:252–261.
- Cox JA, Kucenas S, Voigt MM. (2005) Molecular characterization and embryonic expression of the family of N-methyl-D-aspartate receptor subunit genes in the zebrafish. *Dev Dyn.* **234**:756–766.
- Darrow KO, Harris WA. (2004) Characterization and development of courtship in zebrafish, *Danio rerio*. *Zebrafish.* **1**:40–45.
- Datta D, Vaidehi N, Zhang D, Goddard WA 3rd. (2004) Selectivity and specificity of substrate binding in methionyl-tRNA synthetase. *Protein Sci.* **13**:2693–2705.
- Davison JM, Akitake CM, Goll MG, Rhee JM, Gosse N, Baier H, Halpern ME, Leach SD, Parsons MJ. (2007) Transactivation from Gal4-VP16 transgenic insertions for tissue-specific cell labeling and ablation in zebrafish. *Dev Biol.* **304**:811–824.
- Davis HP, Squire LR (1984) Protein Synthesis and Memory: A Review. *Psychol Bull.* **96**:518–559.
- Deal RB, Henikoff JG, Henikoff S. (2010) Genome-wide kinetics of nucleosome turnover determined by metabolic labeling of histones. *Science.* **5982**:1161–1164.
- Dehnert KW, Beahm BJ, Huynh TT, Baskin JM, Laughlin ST, Wang W, Wu P, Amacher SL, Bertozzi CR. (2011) Metabolic labeling of fucosylated glycans in developing zebrafish. *ACS Chem Biol.* **6**:547–552.
- Del Bene F, Wyart C, Robles E, Tran A, Looger L, Scott EK, Isacoff EY, Baier H. (2010) Filtering of visual information in the tectum by an identified neural circuit. *Science.* **330**:669–673.

- Devlin RH, Nagahama, Y. (2002). Sex determination and sex differentiation in fish: an overview of genetic, physiological, and environmental influences. *Aquaculture*. **208**:191–364.
- Dieterich DC, Hodas JJ, Gouzer G, Shadrin IY, Ngo JT, Triller A, Tirrell DA, Schuman EM. (2010) In situ visualization and dynamics of newly synthesized proteins in rat hippocampal neurons. *Nat Neurosci*. **7**:897–905.
- Dieterich DC, Lee JJ, Link AJ, Graumann J, Tirrell DA, Schuman EM. (2007) Labeling, detection and identification of newly synthesized proteomes with bioorthogonal non-canonical amino-acid tagging. *Nat Protoc*. **2**:532–540.
- Dieterich DC, Link AJ, Graumann J, Tirrell DA, Schuman EM. (2006) Selective identification of newly synthesized proteins in mammalian cells using bioorthogonal noncanonical amino acid tagging (BONCAT). *Proc Natl Acad Sci U S A*. **103**:9482–9487.
- Donnelly ML, Hughes LE, Luke G, Mendoza H, ten Dam E, Gani D, Ryan MD. (2001) The 'cleavage' activities of foot-and-mouth disease virus 2A site-directed mutants and naturally occurring '2A-like' sequences. *J Gen Virol*. **82**:1027–1041.
- Eddins D, Petro A, Williams P, Cerutti DT, Levin ED. (2009) Nicotine effects on learning in zebrafish: the role of dopaminergic systems. *Psychopharmacology (Berl)*. **202**:103–109.
- Emran F, Rihel J, Dowling JE. (2008) A behavioral assay to measure responsiveness of zebrafish to changes in light intensities. *J Vis Exp*. (20).
- Engeszer RE, Patterson LB, Rao AA, Parichy DM. (2007) Zebrafish in the wild: a review of natural history and new notes from the field. *Zebrafish*. **4**:21–40.
- Fetcho JR, Liu KS. (1998) Zebrafish as a model system for studying neuronal circuits and behavior. *Ann N Y Acad Sci*. **860**:333–345
- Fetcho JR, McLean DL. (2010) Some principles of organization of spinal neurons underlying locomotion in zebrafish and their implications. *Ann N Y Acad Sci*. **1198**:94–104.
- Fleisch VC, Neuhauss SC. (2006) Visual behavior in zebrafish. *Zebrafish*. **3**:191–201.
- Flexner LB, Flexner JB. (1968) Intracerebral saline: effect on memory of trained mice treated with puromycin. *Science*. **159**:330–331.
- Fourmy D, Mechulam Y, Brunie S, Blanquet S, Fayat G. (1991) Identification of residues involved in the binding of methionine by *Escherichia coli* methionyl-tRNA synthetase. *FEBS Lett*. **292**:259–263.

- Froehlicher M, Liedtke A, Groh KJ, Neuhaus SC, Segner H, Eggen RI. (2009) Zebrafish (*Danio rerio*) neuromast: promising biological endpoint linking developmental and toxicological studies. *Aquat Toxicol.* **95**:307–319.
- Ghosh G, Pelka H, Schulman LH, Brunie S. (1991) Activation of methionine by *Escherichia coli* methionyl-tRNA synthetase. *Biochemistry.* **30**:9569–9575.
- Goelet P, Castellucci VF, Schacher S, Kandel ER. (1986) The long and the short of long-term memory—a molecular framework. *Nature.* **322**:419–422.
- Gómez-Laplaza LM, Gerlai R. (2010) Latent learning in zebrafish (*Danio rerio*). *Behav Brain Res.* **208**:509–515.
- Granato M, van Eeden FJ, Schach U, Trowe T, Brand M, Furutani-Seiki M, Haffter P, Hammerschmidt M, Heisenberg CP, Jiang YJ, Kane DA, Kelsh RN, Mullins MC, Odenthal J, Nüsslein-Volhard C. (1996) Genes controlling and mediating locomotion behavior of the zebrafish embryo and larva. *Development.* **123**:399–413.
- Hagiwara M, Shimomura A, Yoshida K, Imaki J. (1996) Gene expression and CREB phosphorylation induced by cAMP and Ca²⁺ in neuronal cells. *Adv Pharmacol.* **36**:277–285.
- Hernandez PJ, Abel T. (2008) The role of protein synthesis in memory consolidation: progress amid decades of debate. *Neurobiol Learn Mem.* **89**:293–311.
- Hinz FI, Dieterich DC, Tirrell DA, Schuman EM. (2012) Non-canonical amino acid labeling in vivo to visualize and affinity purify newly synthesized proteins in larval zebrafish. *ACS Chem Neurosci.* **3**:40–49.
- Huang YY, Neuhaus SC. (2008) The optokinetic response in zebrafish and its applications. *Front Biosci.* **13**:1899–1916.
- Janovjak H, Szobota S, Wyart C, Trauner D, Isacoff EY. (2010) A light-gated, potassium-selective glutamate receptor for the optical inhibition of neuronal firing. *Nat Neurosci.* **13**:1027–1032.
- Kawakami K. (2005) Transposon tools and methods in zebrafish. *Dev Dyn.* **234**:244–254.
- Kelleher RJ 3rd, Govindarajan A, Jung HY, Kang H, Tonegawa S. (2004) Translational control by MAPK signaling in long-term synaptic plasticity and memory. *Cell.* **116**:467–479.
- Kho Y, Kim SC, Jiang C, Barma D, Kwon SW, Cheng J, Jaunbergs J, Weinbaum C, Tamanoi F, Falck J, Zhao Y. (2004) A tagging-via-substrate technology for detection and proteomics of farnesylated proteins. *Proc Natl Acad Sci U S A.* **34**:12479–12484.

- Kiick KL, Saxon E, Tirrell DA, Bertozzi CR. (2002) Incorporation of azides into recombinant proteins for chemoselective modification by the Staudinger ligation. *Proc Natl Acad Sci U S A.* **1**:19–24.
- Kimmel CB, Ballard WW, Kimmel SR, Ullmann B, Schilling TF. (1995) Stages of embryonic development of the zebrafish. *Dev Dyn.* **203**:253–310
- Kimmel CB, Patterson J, Kimmel RO. (1974) The development and behavioral characteristics of the startle response in the zebra fish. *Dev Psychobiol.* **1**:47–60.
- Klann E, Sweatt JD. (2008) Altered protein synthesis is a trigger for long-term memory formation. *Neurobiol Learn Mem.* **289**:247–259.
- Kohashi T, Oda Y. (2008) Initiation of Mauthner- or non-Mauthner-mediated fast escape evoked by different modes of sensory input. *J Neurosci.* **28**:10641–10653.
- Kokel D, Peterson RT. (2011) Using the zebrafish photomotor response for psychotropic drug screening. *Methods Cell Biol.* **105**:517–524.
- Kokel D, Bryan J, Laggner C, White R, Cheung CY, Mateus R, Healey D, Kim S, Werdich AA, Haggarty SJ, Macrae CA, Shoichet B, Peterson RT. (2010) Rapid behavior-based identification of neuroactive small molecules in the zebrafish. *Nat Chem Biol.* **3**:231–237.
- Köster RW, Fraser SE. (2001) Tracing transgene expression in living zebrafish embryos. *Dev Biol.* **233**:329–346.
- Larson ET, O'Malley DM, Melloni JR RH. (2006). Aggression and vasotocin are associated with dominant-subordinate relationships in zebrafish. *Behavioural Brain Research.* **167**, 94–102.
- Laughlin ST, Baskin JM, Amacher SL, Bertozzi CR. (2008) In vivo imaging of membrane-associated glycans in developing zebrafish. *Science.* **5876**:664–667
- Laughlin ST, Bertozzi CR. (2009) Imaging the glycome. *Proc Natl Acad Sci U S A.* **1**:12–7.
- Laughlin ST, Bertozzi CR. (2009) In vivo imaging of *Caenorhabditis elegans* glycans. *ACS Chem Biol.* **12**:1068–1072.
- Lawrence C, Ebersole JP, Kesseli RV. (2007) Rapid growth and outcrossing promote female development in zebrafish (*Danio rerio*). *Environmental Biology of Fishes.* DOI: 10.1007/s10641-007-9195-8.

- Link AJ, Mock ML, Tirrell DA. (2003) Non-canonical amino acids in protein engineering. *Curr Opin Biotechnol.* **14**:603–609.
- Link AJ, Vink MK, Tirrell DA. (2004) Presentation and detection of azide functionality in bacterial cell surface proteins. *J Am Chem Soc.* **126**:10598–10602.
- Link AJ, Vink MK, Agard NJ, Prescher JA, Bertozzi CR, Tirrell DA. (2006) Discovery of aminoacyl-tRNA synthetase activity through cell-surface display of noncanonical amino acids. *Proc Natl Acad Sci U S A.* **103**:10180–10185.
- Link JA, Vink MKS, Tirrell DA. (2007) Preparation of the functionalizable methionine surrogate azidohomoalanine via copper-catalyzed diazo transfer. *Nat Protoc.* **8**:1879–1883.
- Lister JA, Robertson CP, Lepage T, Johnson SL, Raible DW. (1999) *nacre* encodes a zebrafish microphthalmia-related protein that regulates neural-crest-derived pigment cell fate. *Development.* **17**:3757–3767.
- Lynch GS, Dunwiddie T, Gribkoff V. (1977) Heterosynaptic depression: a postsynaptic correlate of long-term potentiation. *Nature.* **266**:737–739.
- Maack G, Segner H. (2003) Morphological development of the gonads in zebrafish. *Journal of Fish Biology.* **62**, 895–906.
- Mathur P, Lau B, Guo S. (2011) Conditioned place preference behavior in zebrafish. *Nat Protoc.* **6**:338–345.
- McLean DL, Fetcho JR. (2009) Spinal interneurons differentiate sequentially from those driving the fastest swimming movements in larval zebrafish to those driving the slowest ones. *J Neurosci.* **29**:13566–13577.
- Mechulam Y, Schmitt E, Maveyraud L, Zelwer C, Nureki O, Yokoyama S, Konno M, Blanquet S. (1999) Crystal structure of *Escherichia coli* methionyl-tRNA synthetase highlights species-specific features. *J Mol Biol.* **294**:1287–1297.
- Melemedjian OK, Asiedu MN, Tillu DV, Peebles KA, Yan J, Ertz N, Dussor GO, Price TJ. (2010) IL-6- and NGF-induced rapid control of protein synthesis and nociceptive plasticity via convergent signaling to the eIF4F complex. *J Neurosci.* **45**:15113–15123.
- Mysore SP, Tai CY, Schuman EM. (2008) N-cadherin, spine dynamics, and synaptic function. *Front Neurosci.* **2**:168–175.
- Naumann EA, Kampff AR, Prober DA, Schier AF, Engert F. (2010) Monitoring neural activity with bioluminescence during natural behavior. *Nat Neurosci.* **4**:513–520.

- Nathans D. (1964) Puromycin inhibition of protein synthesis: incorporation of puromycin into peptide chains. *Proc Natl Acad Sci U S A*. **51**:585–592.
- Neuhauss SC. (2003) Behavioral genetic approaches to visual system development and function in zebrafish. *J Neurobiol*. **54**:148–160.
- Ng MC, Hsu CP, Wu YJ, Wu SY, Yang YL, Lu KT. (2012) Effect of MK-801-induced impairment of inhibitory avoidance learning in zebrafish via inactivation of extracellular signal-regulated kinase (ERK) in telencephalon. *Fish Physiol Biochem*. (Epub ahead of print.)
- Ngo JT, Champion JA, Mahdavi A, Tanrikulu IC, Beatty KE, Connor RE, Yoo TH, Dieterich DC, Schuman EM, Tirrell DA. (2009) Cell-selective metabolic labeling of proteins. *Nat Chem Biol*. **10**:715–717.
- Nüsslein-Volhard C, Dahm R. (2002) *Zebrafish. A Practical Approach*, 2nd Edition. Oxford University Press.
- Ong SE, Blagoev B, Kratchmarova I, Kristensen DB, Steen H, Pandey A, Mann M. (2002) Stable isotope labeling by amino acids in cell culture, SILAC, as a simple and accurate approach to expression proteomics. *Mol Cell Proteomics*. **5**:376–386.
- Ouellette SP, Dorsey FC, Moshiach S, Cleveland JL, Carabeo RA. (2011) Chlamydia species-dependent differences in the growth requirement for lysosomes. *PLoS One*. **3**:16783.
- Overmier JB, Papini MR. (1986) Factors modulating the effects of teleost telencephalon ablation on retention, relearning, and extinction of instrumental avoidance behavior. *Behav Neurosci*. **100**:190–199.
- Pan Y, Kaiguo M, Razak Z, Westwood JT, Gerlai R. (2011) Chronic alcohol exposure induced gene expression changes in the zebrafish brain. *Behav Brain Res*. **216**:66–76.
- Parent JM, Yu TW, Leibowitz RT, Geschwind DH, Sloviter RS, Lowenstein DH. (1997) Dentate granule cell neurogenesis is increased by seizures and contributes to aberrant network reorganization in the adult rat hippocampus. *J Neurosci*. **10**:3727–3738.
- Park HC, Kim CH, Bae YK, Yeo SY, Kim SH, Hong SK, Shin J, Yoo KW, Hibi M, Hirano T, Miki N, Chitnis AB, Huh TL. (2000) Analysis of upstream elements in the HuC promoter leads to the establishment of transgenic zebrafish with fluorescent neurons. *Dev Biol*. **2**:279–293.
- Pather S, Gerlai R. (2009) Shuttle box learning in zebrafish (*Danio rerio*). *Behav Brain Res*. **196**:323–327.
- Pestka S. (1971) Inhibitors of ribosome functions. *Annu Rev Microbiol*. **25**:487–562.

- Portavella M, Torres B, Salas C. (2004) Avoidance response in goldfish: emotional and temporal involvement of medial and lateral telencephalic pallium. *J Neurosci.* **24**:2335–2342.
- Portavella M, Torres B, Salas C, Papini MR. (2004) Lesions of the medial pallium, but not of the lateral pallium, disrupt spaced-trial avoidance learning in goldfish (*Carassius auratus*). *Neurosci Lett.* **362**:75–78.
- Pradel G, Schachner M, Schmidt R. (1999) Inhibition of memory consolidation by antibodies against cell adhesion molecules after active avoidance conditioning in zebrafish. *J Neurobiol.* **39**:197–206.
- Pradel G, Schmidt R, Schachner M. (2000) Involvement of L1.1 in memory consolidation after active avoidance conditioning in zebrafish. *J Neurobiol.* **43**:389–403.
- Prescher JA, Dube DH, Bertozzi CR. (2004) Chemical remodelling of cell surfaces in living animals. *Nature.* **7002**:873–877.
- Prober DA, Rihel J, Onah AA, Sung RJ, Schier AF. (2006) Hypocretin/orexin overexpression induces an insomnia-like phenotype in zebrafish. *J Neurosci.* **26**:13400–13410.
- Provost E, Rhee J, Leach SD. (2007) Viral 2A peptides allow expression of multiple proteins from a single ORF in transgenic zebrafish embryos. *Genesis.* **45**:625–629.
- Rihel J, Prober DA, Arvanites A, Lam K, Zimmerman S, Jang S, Haggarty SJ, Kokel D, Rubin LL, Peterson RT, Schier AF. (2010) Zebrafish behavioral profiling links drugs to biological targets and rest/wake regulation. *Science.* **5963**:348–351.
- Rihel J, Prober DA, Schier AF. (2010) Monitoring sleep and arousal in zebrafish. *Methods Cell Biol.* **100**:281–294.
- Roberts AC, Reichl J, Song MY, Dearing AD, Moridzadeh N, Lu ED, Pearce K, Eskin J, Glanzman DL. (2011) Habituation of the C-start response in larval zebrafish exhibits several distinct phases and sensitivity to NMDA receptor blockade. *PLoS One.* **6**:e29132.
- Rostovtsev VV, Green LG, Fokin VV, Sharpless KB. (2002) A stepwise Huisgen cycloaddition process: copper(I)-catalyzed regioselective "ligation" of azides and terminal alkynes. *Angew Chem.* **14**:2596–2599.
- Rudy JW, Biedenkapp JC, Moineau J, Bolding K. (2006) Anisomycin and the reconsolidation hypothesis. *Learn Mem.* **13**:1–3.
- Sacktor TC. (2011) How does PKM ζ maintain long-term memory? *Nat Rev Neurosci.* **12**:9–15.

- Saito K, Watanabe S. (2006) Deficits in acquisition of spatial learning after dorsomedial telencephalon lesions in goldfish. *Behav Brain Res.* **172**:187–194.
- Salas C, Rodríguez F, Vargas JP, Durán E, Torres B. (1996) Spatial learning and memory deficits after telencephalic ablation in goldfish trained in place and turn maze procedures. *Behav Neurosci.* **110**:965–980.
- Scheer N, Campos-Ortega JA. (1999) Use of the Gal4-UAS technique for targeted gene expression in the zebrafish. *Mech Dev.* **80**:153–158.
- Schwaller B, Meyer M, Schiffmann S. (2002) 'New' functions for 'old' proteins: the role of the calcium-binding proteins calbindin D-28k, calretinin and parvalbumin, in cerebellar physiology. Studies with knockout mice. *Cerebellum.* **1**:241–258.
- Schwartzkroin PA, Wester K. (1975) Long-lasting facilitation of a synaptic potential following tetanization in the in vitro hippocampal slice. *Brain Res.* **89**:107–119.
- Scott EK, Mason L, Arrenberg AB, Ziv L, Gosse NJ, Xiao T, Chi NC, Asakawa K, Kawakami K, Baier H. (2007) Targeting neural circuitry in zebrafish using GAL4 enhancer trapping. *Nat Methods.* **4**:323–326.
- Serre L, Verdon G, Choinowski T, Hervouet N, Risler JL, Zelwer C. (2001) How methionyl-tRNA synthetase creates its amino acid recognition pocket upon L-methionine binding. *J Mol Biol.* **306**:863–876.
- Sison M, Gerlai R. (2010) Associative learning in zebrafish (*Danio rerio*) in the plus maze. *Behav Brain Res.* **207**:99–104.
- Smith FM, Croll RP. (2011) Autonomic control of the swimbladder. *Auton Neurosci.* **165**:140–148.
- Spence R, Gerlach G, Lawrence C, Smith C. (2008) The behaviour and ecology of the zebrafish, *Danio rerio*. *Biol Rev Camb Philos Soc.* **83**:13–34.
- Suster ML, Kikuta H, Urasaki A, Asakawa K, Kawakami K. (2009) Transgenesis in zebrafish with the tol2 transposon system. *Methods Mol Biol.* **561**:41–63.
- Sweatt DJ. (2009) *Mechanisms of Memory*, 2nd Edition. Academic Press.
- Szobota S, Gorostiza P, Del Bene F, Wyart C, Fortin DL, Kolstad KD, Tulyathan O, Volgraf M, Numano R, Aaron HL, Scott EK, Kramer RH, Flannery J, Baier H, Trauner D, Isacoff EY. (2007) Remote control of neuronal activity with a light-gated glutamate receptor. *Neuron.* **54**:535–545.

Szymczak AL, Workman CJ, Wang Y, Vignali KM, Dilioglou S, Vanin EF, Vignali DA. (2004) Correction of multi-gene deficiency in vivo using a single 'self-cleaving' 2A peptide-based retroviral vector. *Nat Biotechnol.* **22**:589–594.

Tai CY, Kim SA, Schuman EM. (2008) Cadherins and synaptic plasticity. *Curr Opin Cell Biol.* **20**:567–575.

Tanrikulu IC, Schmitt E, Mechulam Y, Goddard WA 3rd, Tirrell DA. (2009) Discovery of *Escherichia coli* methionyl-tRNA synthetase mutants for efficient labeling of proteins with azidonorleucine in vivo. *Proc Natl Acad Sci U S A.* **106**:15285–15290

Tcherkezian J, Brittis PA, Thomas F, Roux PP, Flanagan JG. (2010) Transmembrane receptor DCC associates with protein synthesis machinery and regulates translation. *Cell.* **4**:632–644.

Tierney KB. (2011) Behavioural assessments of neurotoxic effects and neurodegeneration in zebrafish. *Biochim Biophys Acta.* **3**:381–389.

Tornøe CW, Christensen C, Meldal M. (2002) Peptidotriazoles on solid phase: [1,2,3]-triazoles by regiospecific copper(i)-catalyzed 1,3-dipolar cycloadditions of terminal alkynes to azides. *J Org Chem.* **9**:3057–3064.

Trinh le A, Hochgreb T, Graham M, Wu D, Ruf-Zamojski F, Jayasena CS, Saxena A, Hawk R, Gonzalez-Serricchio A, Dixson A, Chow E, Gonzales C, Leung HY, Solomon I, Bronner-Fraser M, Megason SG, Fraser SE. (2011) A versatile gene trap to visualize and interrogate the function of the vertebrate proteome. *Genes Dev.* **25**:2306–2320.

Tropepe V, Sive HL. (2003) Can zebrafish be used as a model to study the neurodevelopmental causes of autism? *Genes Brain Behav.* **2**:268–281.

Tsien RY. (1998) The green fluorescent protein. *Annu Rev Biochem.* **67**:509–544.

Vargas JP, Bingman VP, Portavella M, López JC. (2006) Telencephalon and geometric space in goldfish. *Eur J Neurosci.* **24**:2870–2878.

Weiner N, Rabadjija M. (1968) The regulation of norepinephrine synthesis. Effect of puromycin on the accelerated synthesis of norepinephrine associated with nerve stimulation. *J Pharmacol Exp Ther.* **164**:103–114.

Weisbrod SH and Marx A. (2008) Novel strategies for the site-specific covalent labeling of nucleic acids. *Chem. Commun.* 5675–5658.

Williams FE, White D, Messer WS. (2002) A simple spatial alternation task for assessing memory function in zebrafish. *Behav Processes.* **58**:125–132.

Wolman MA, Jain RA, Liss L, Granato M. (2011) Chemical modulation of memory formation in larval zebrafish. *Proc Natl Acad Sci U S A.* **108**:15468–15473.

Wong EH, Kemp JA, Priestley T, Knight AR, Woodruff GN, Iversen LL. (1986) The anticonvulsant MK-801 is a potent N-methyl-D-aspartate antagonist. *Proc Natl Acad Sci U S A.* **83**:7104–7108.

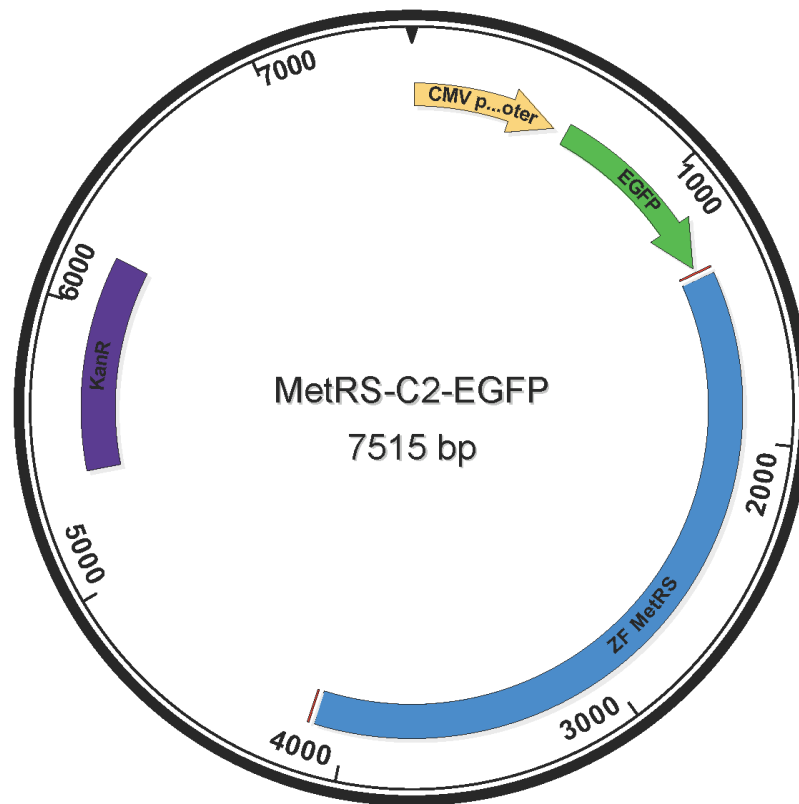
Wyart C, Del Bene F, Warp E, Scott EK, Trauner D, Baier H, Isacoff EY. (2009) Optogenetic dissection of a behavioural module in the vertebrate spinal cord. *Nature.* **461**:407–410.

Xu X, Scott-Scheiern T, Kempker L, Simons K. (2007) Active avoidance conditioning in zebrafish (*Danio rerio*). *Neurobiol Learn Mem.* **87**:72–77.

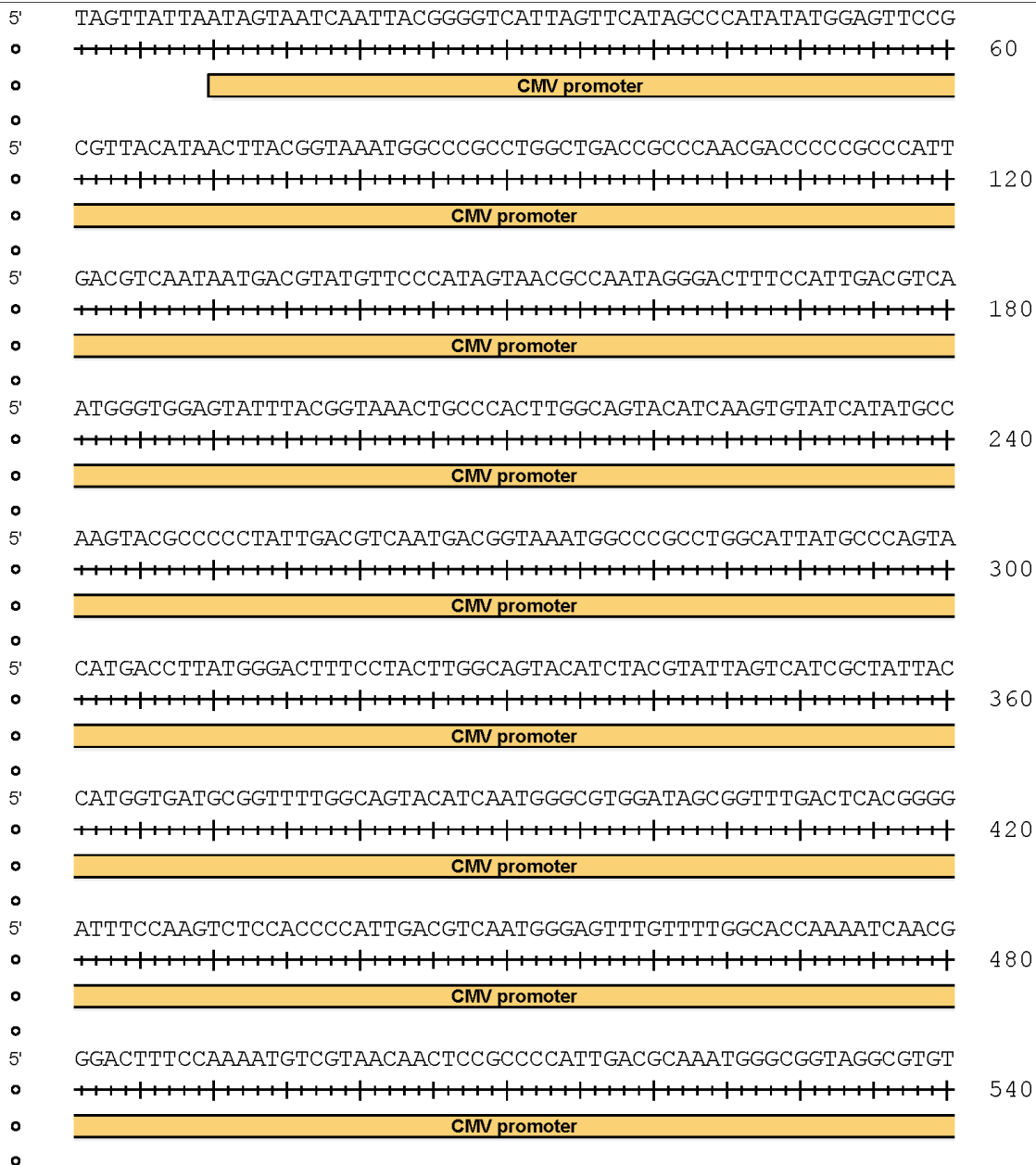
Zhong H, Lin S. (2011) Chemical screening with zebrafish embryos. *Methods Mol Biol.* **716**:193–205.

APPENDIX A

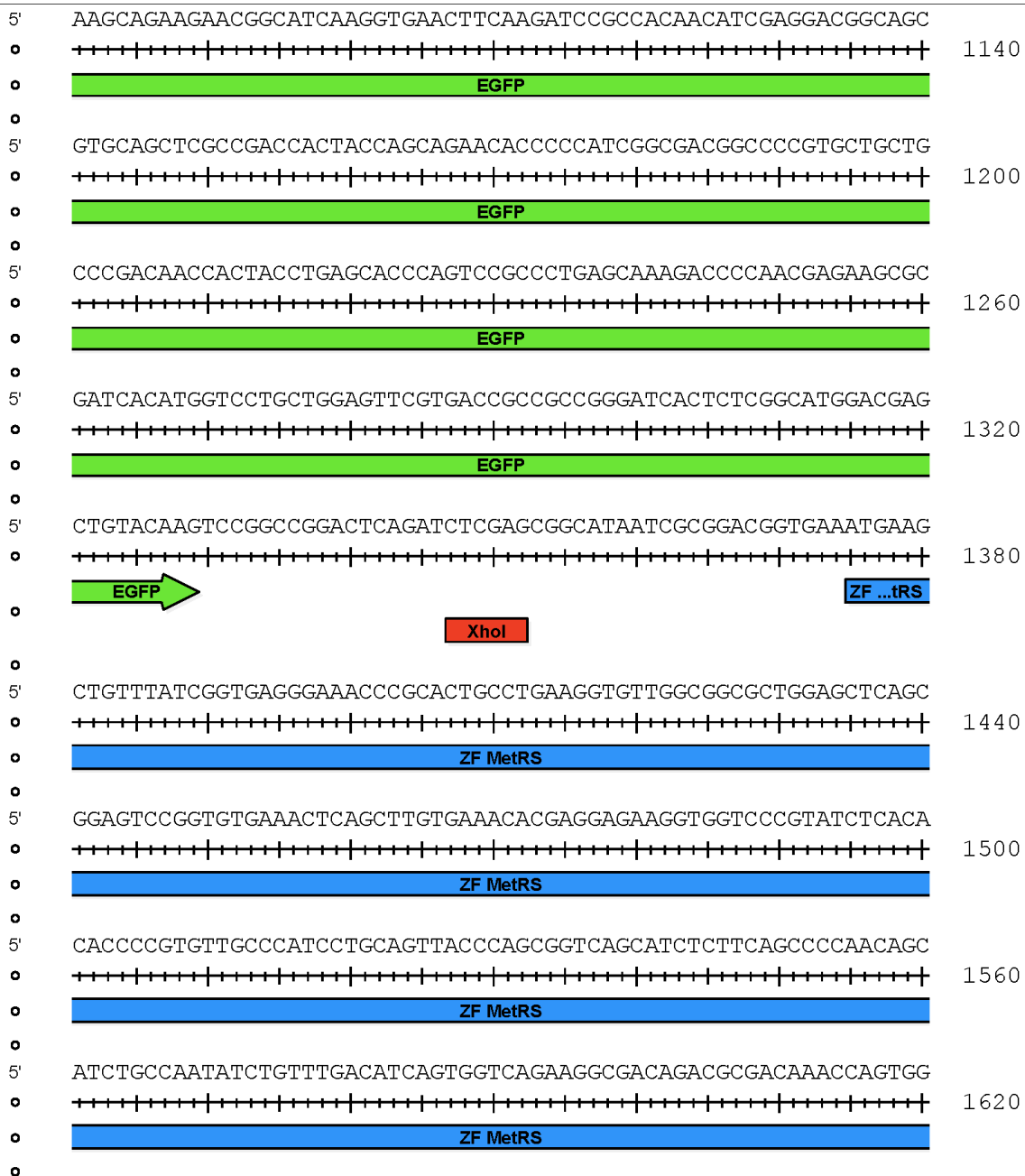
Vector maps



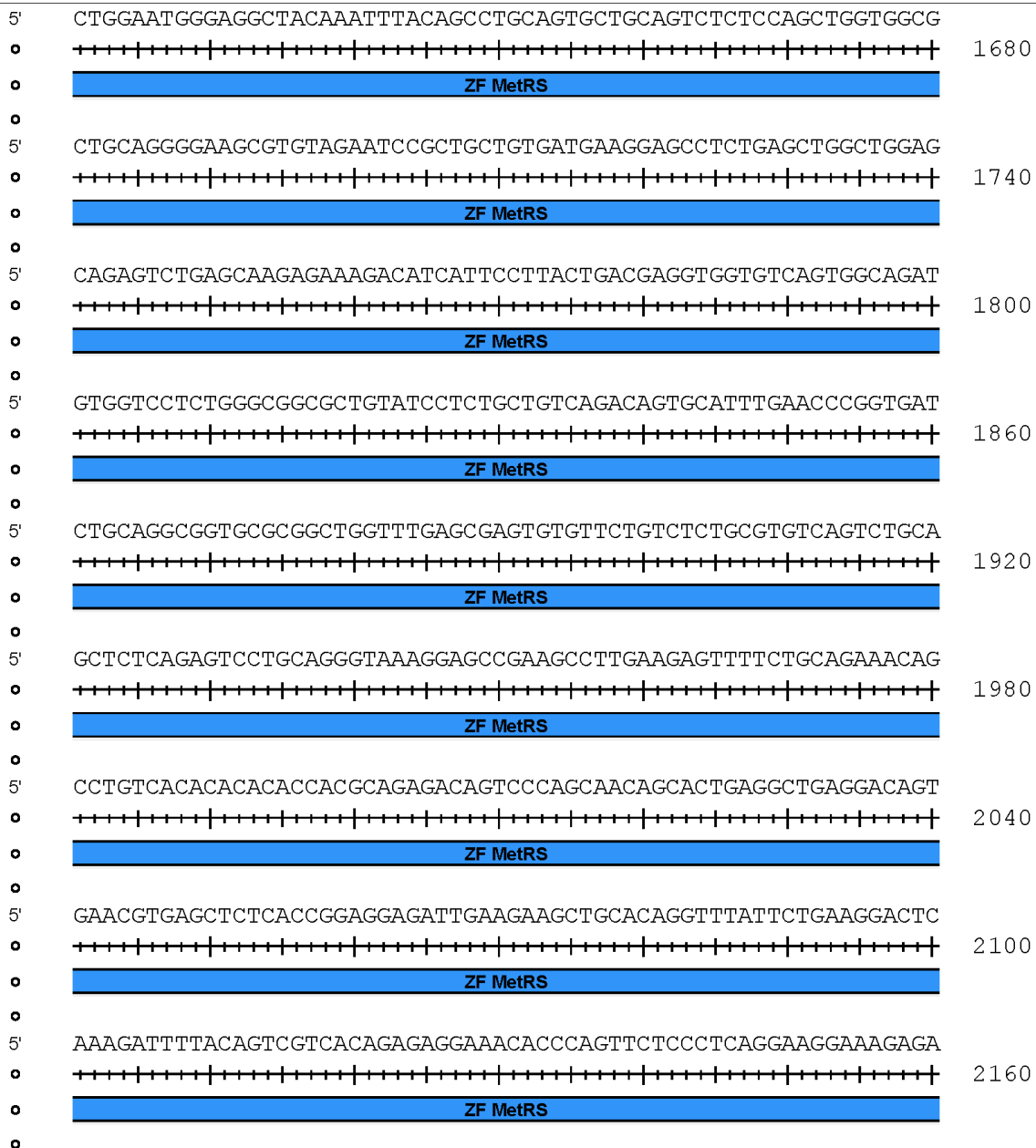
MetRS-C2-EGFP



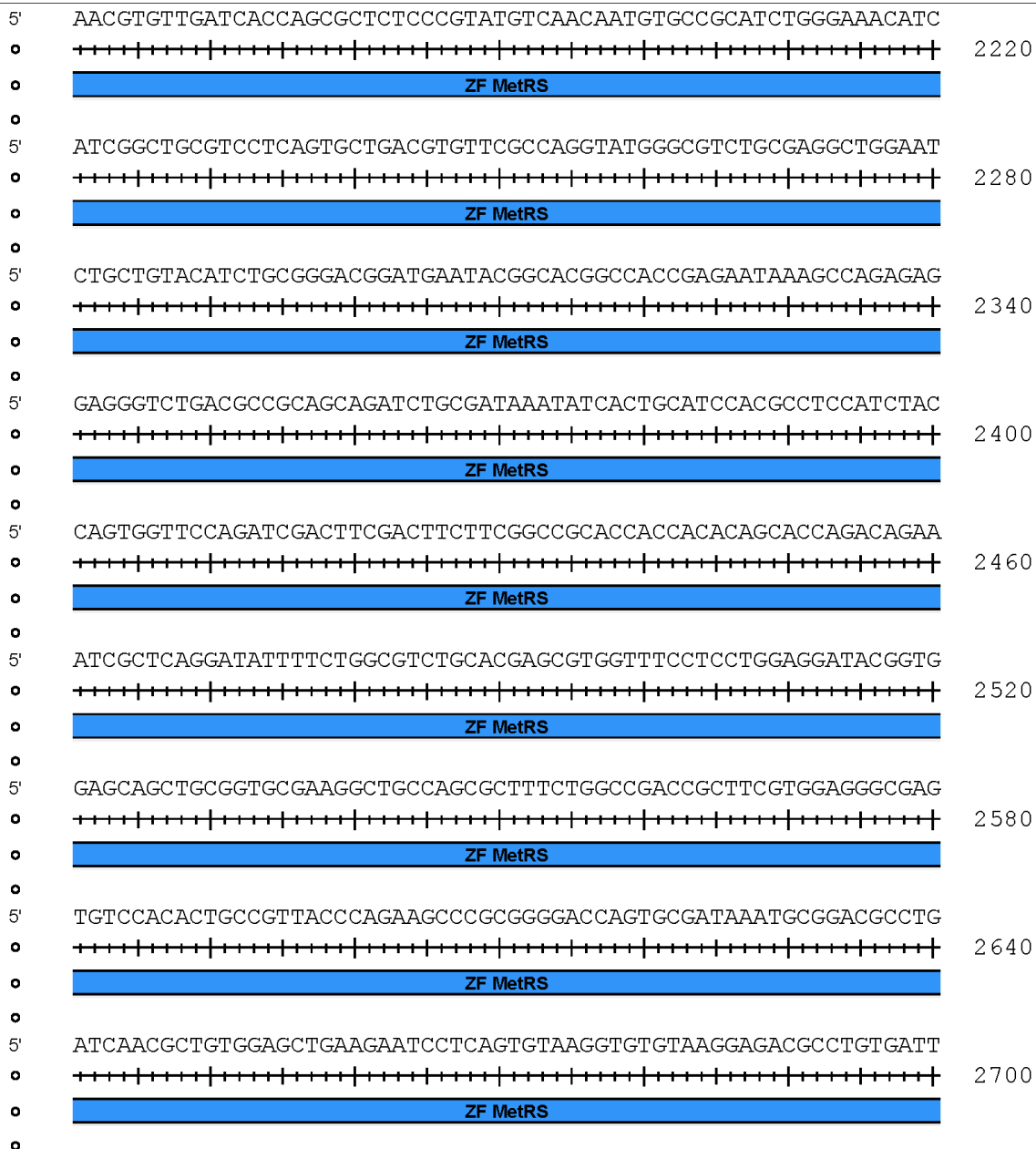
MetRS-C2-EGFP



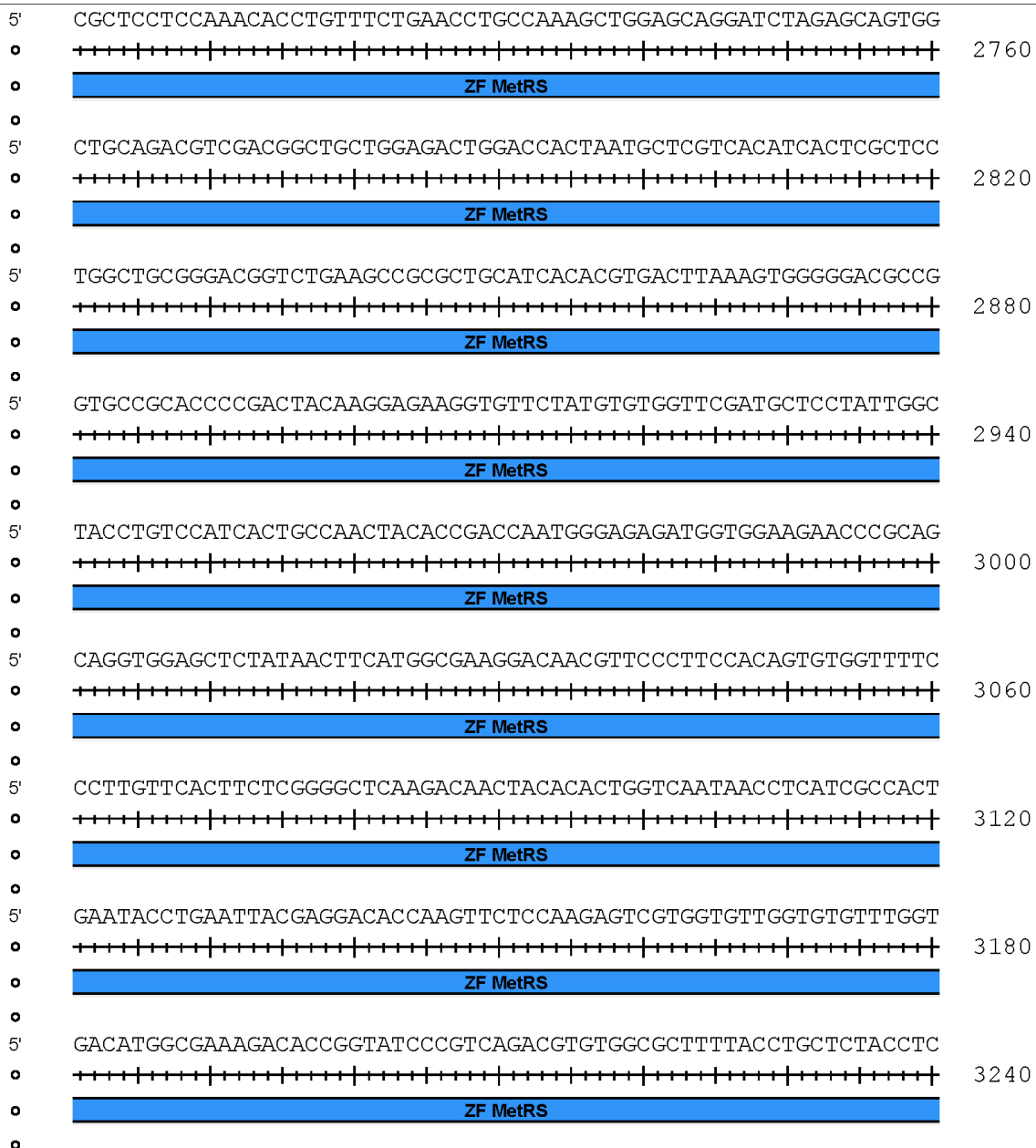
MetRS-C2-EGFP



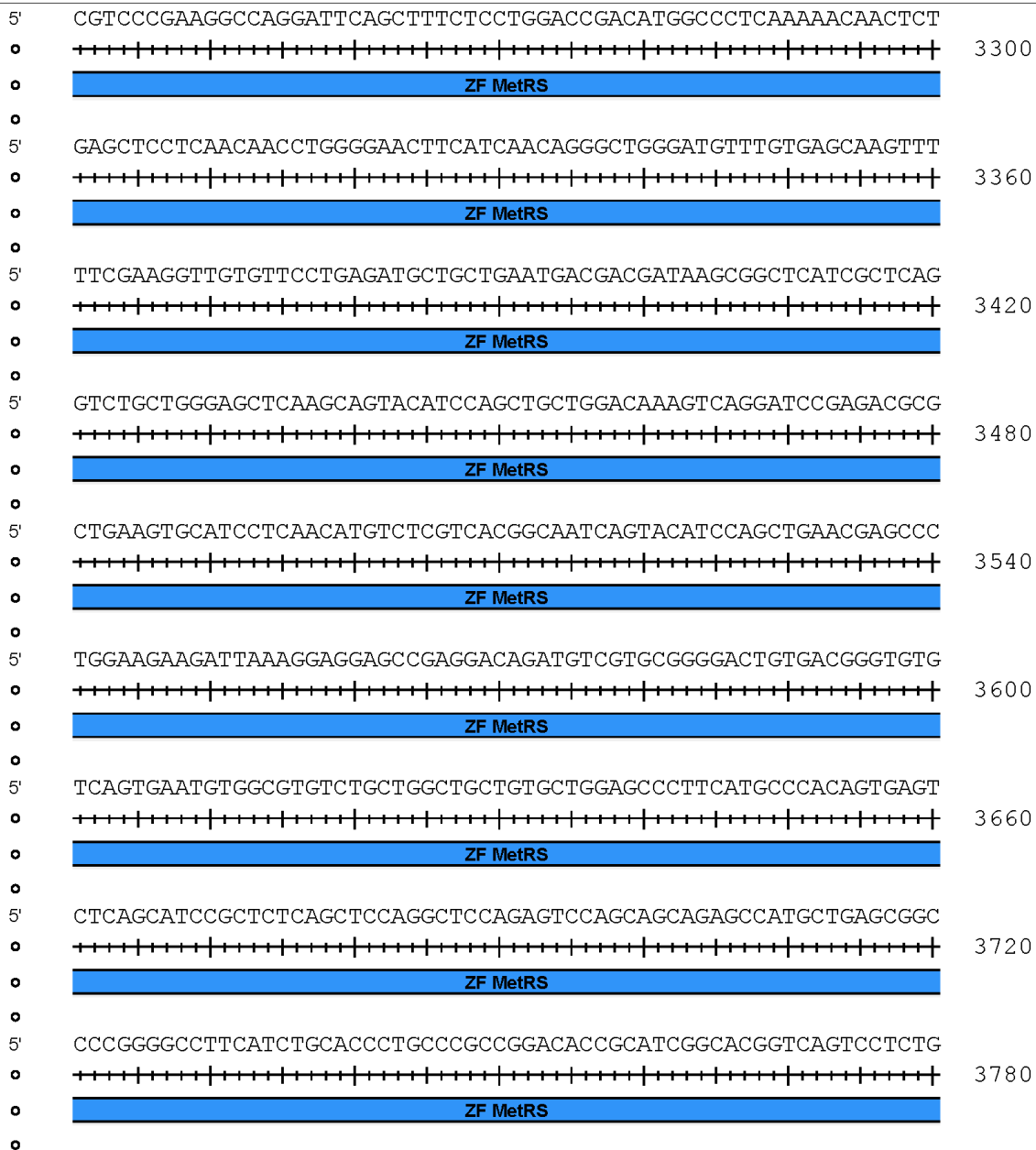
MetRS-C2-EGFP



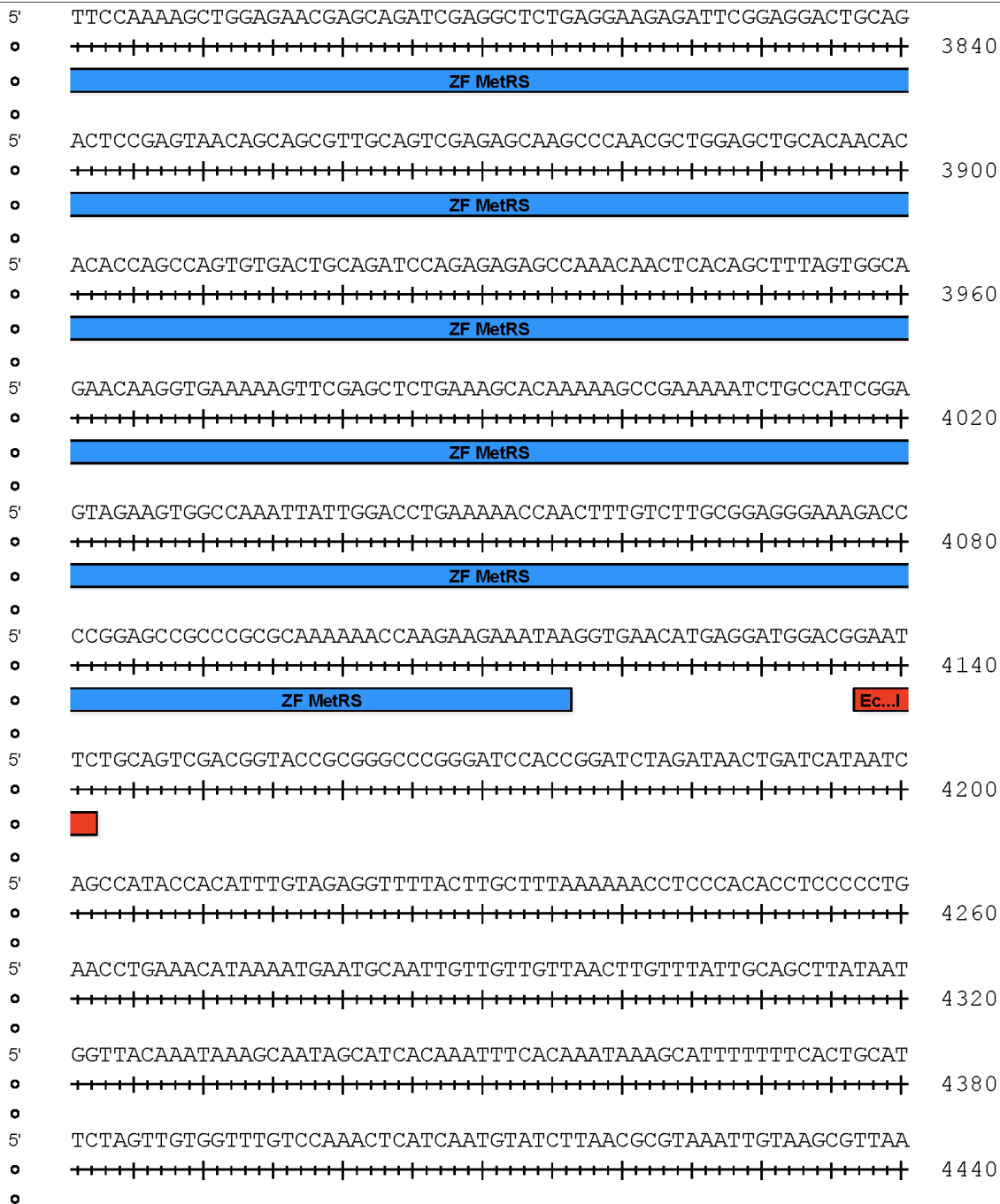
MetRS-C2-EGFP



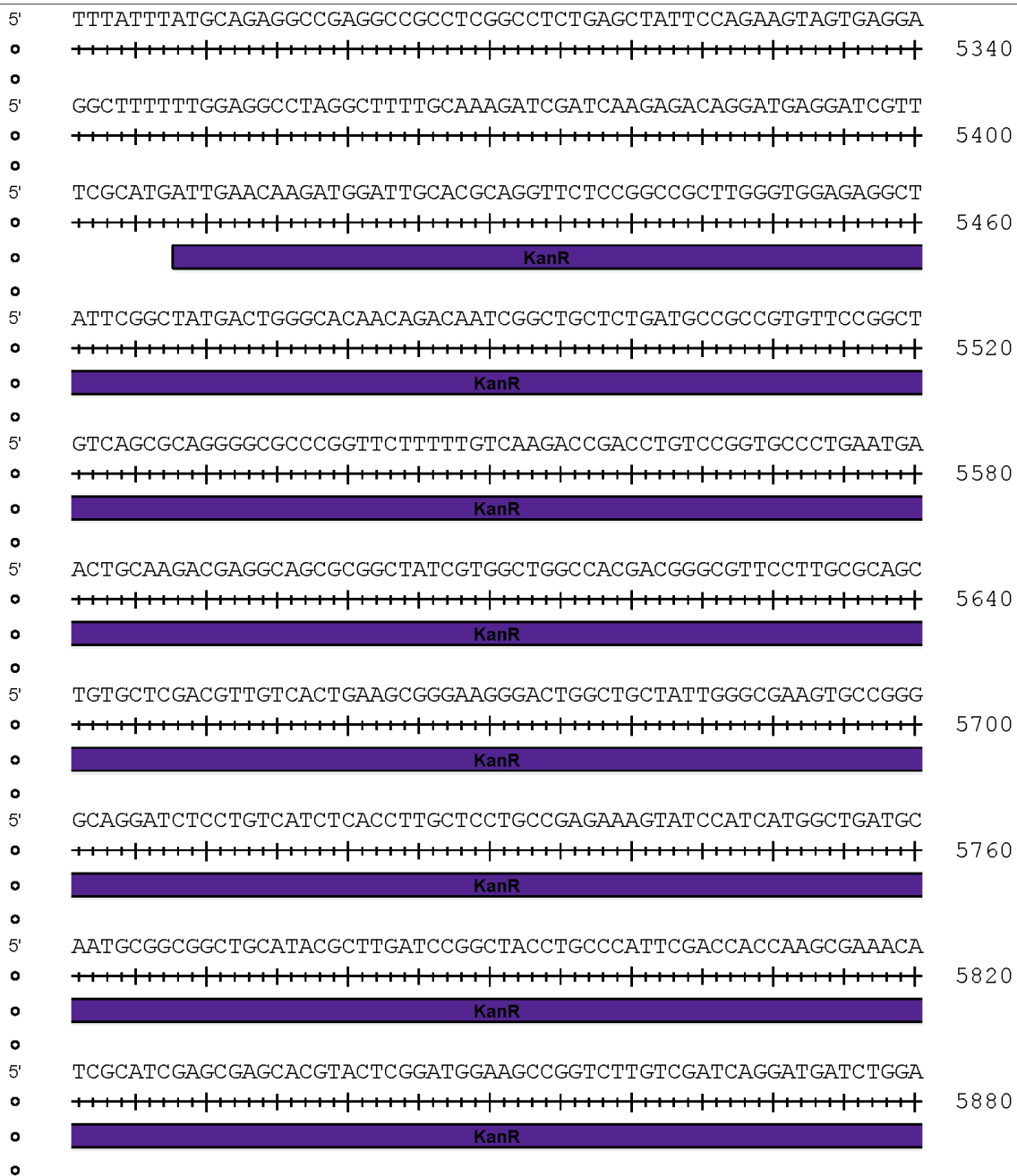
MetRS-C2-EGFP



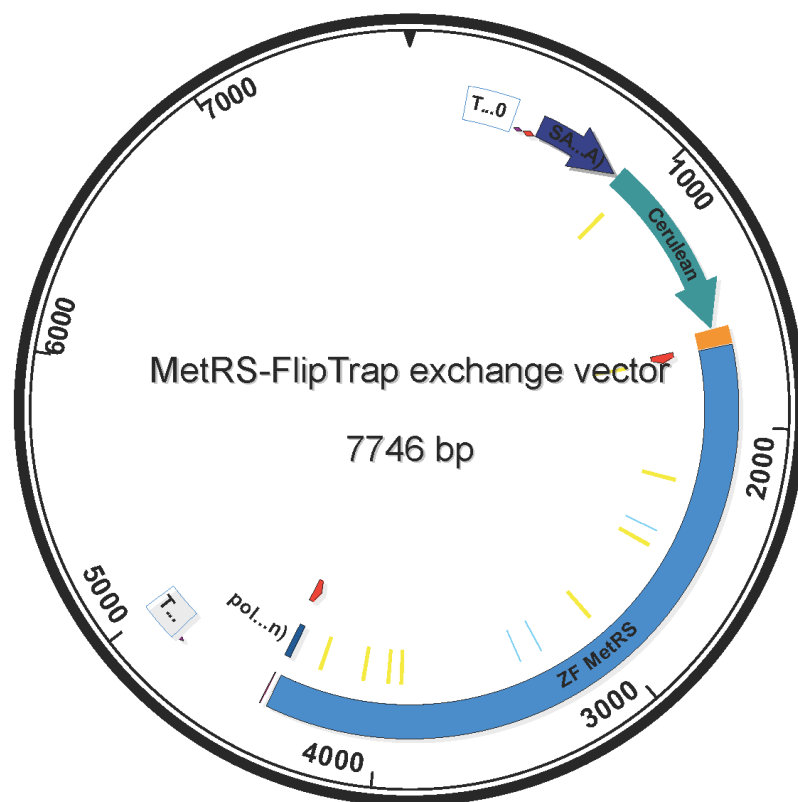
MetRS-C2-EGFP



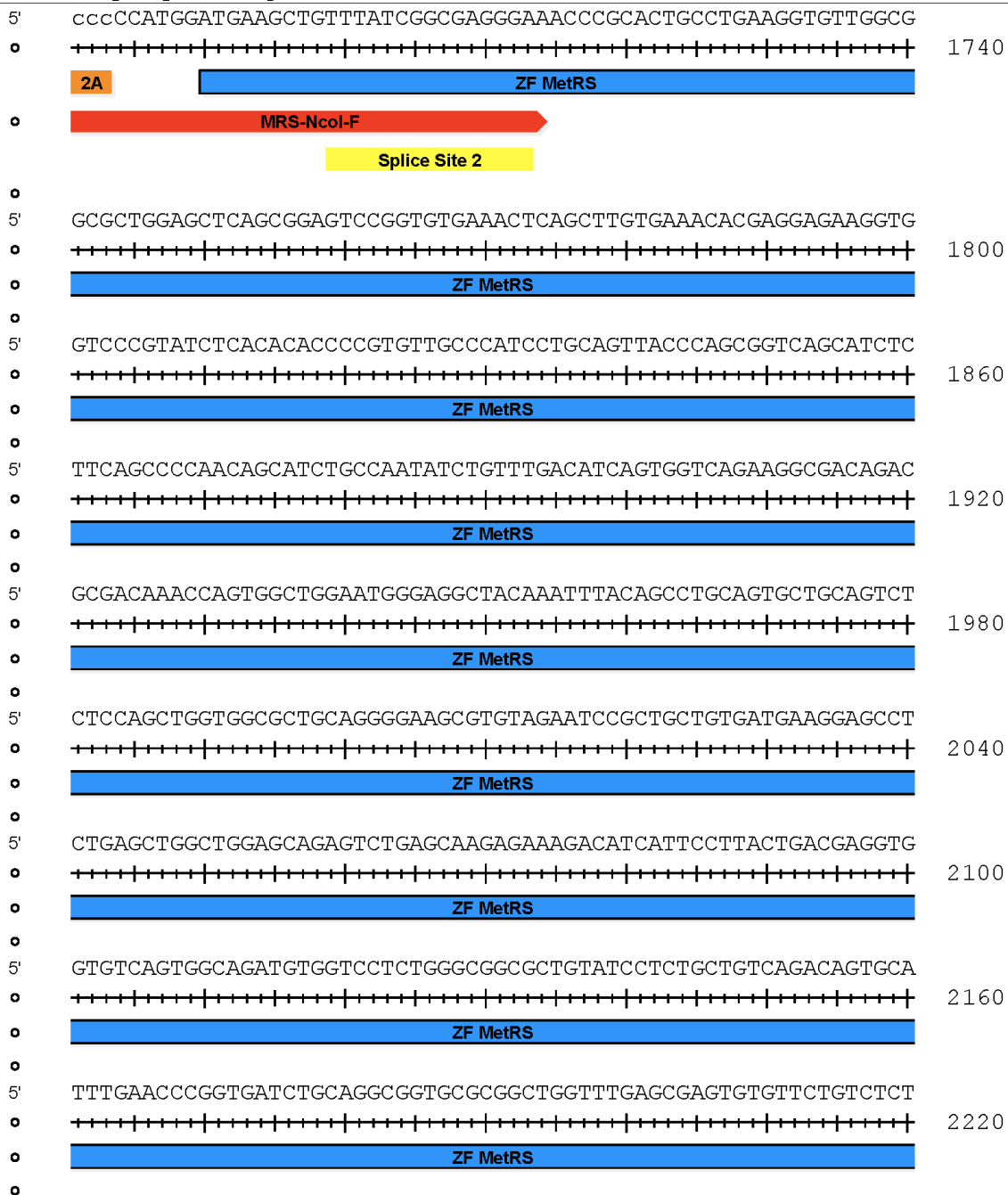
MetRS-C2-EGFP



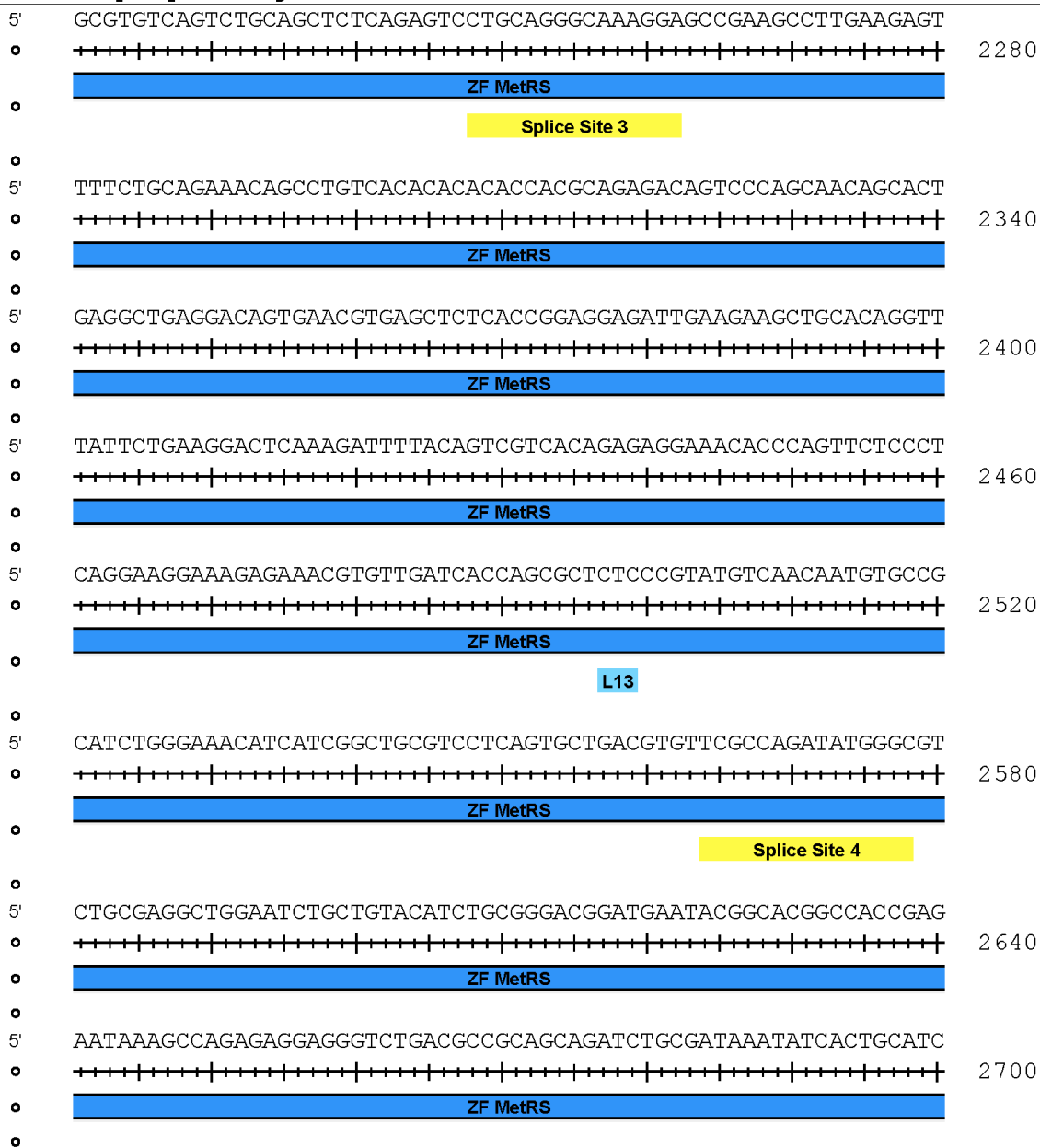
MetRS-FlipTrap exchange vector



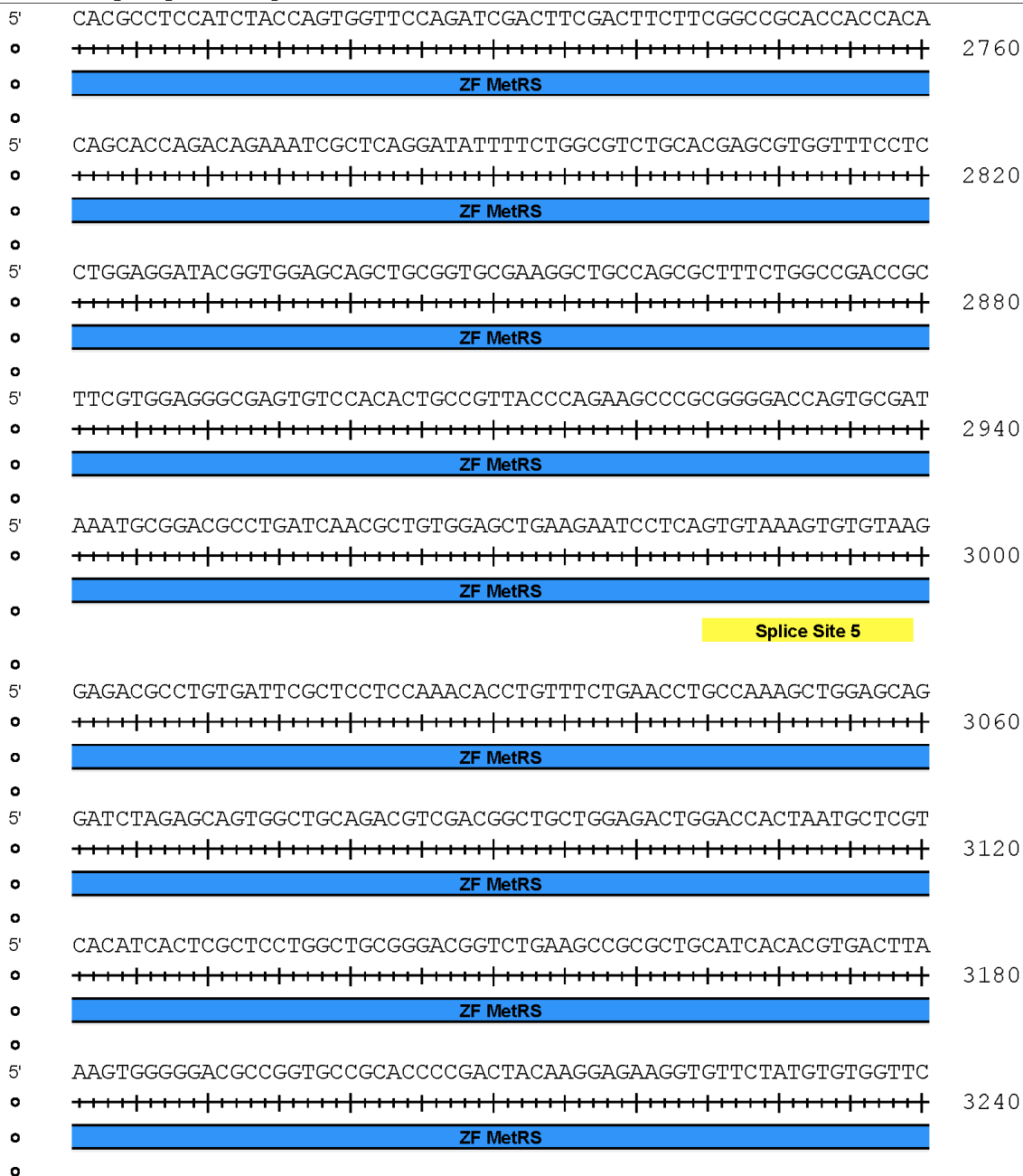
MetRS-FlipTrap exchange vector



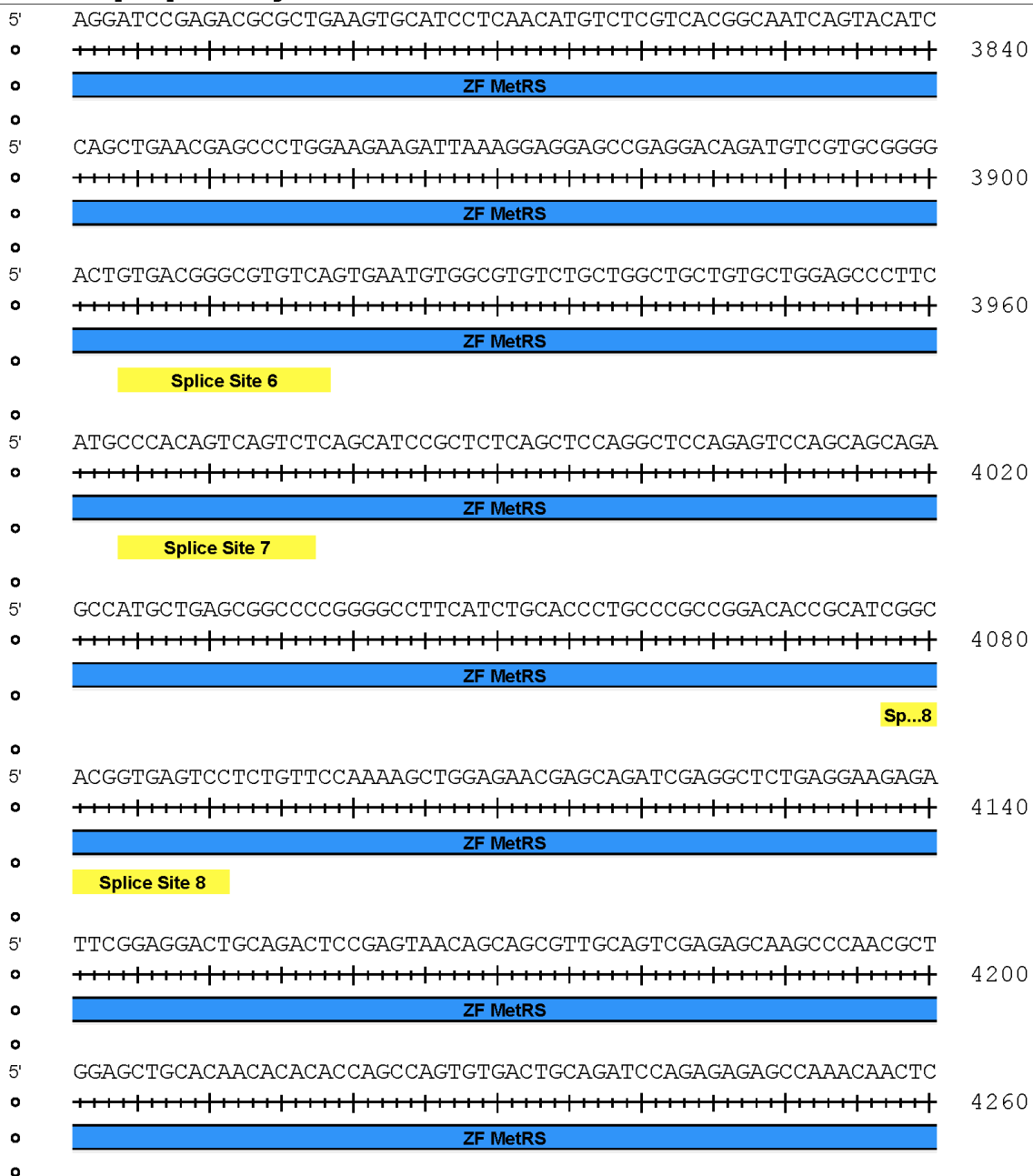
MetRS-FlipTrap exchange vector



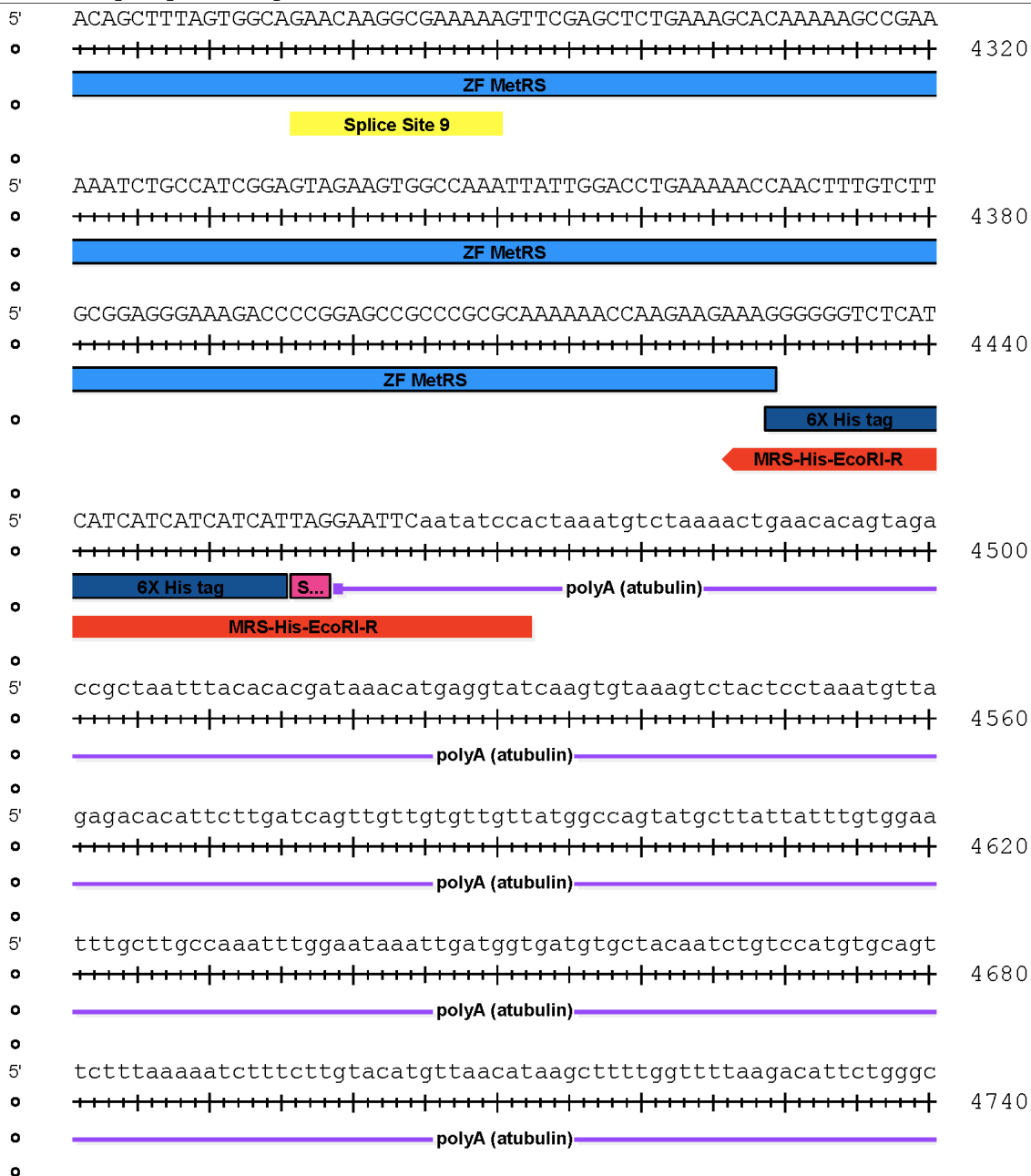
MetRS-FlipTrap exchange vector



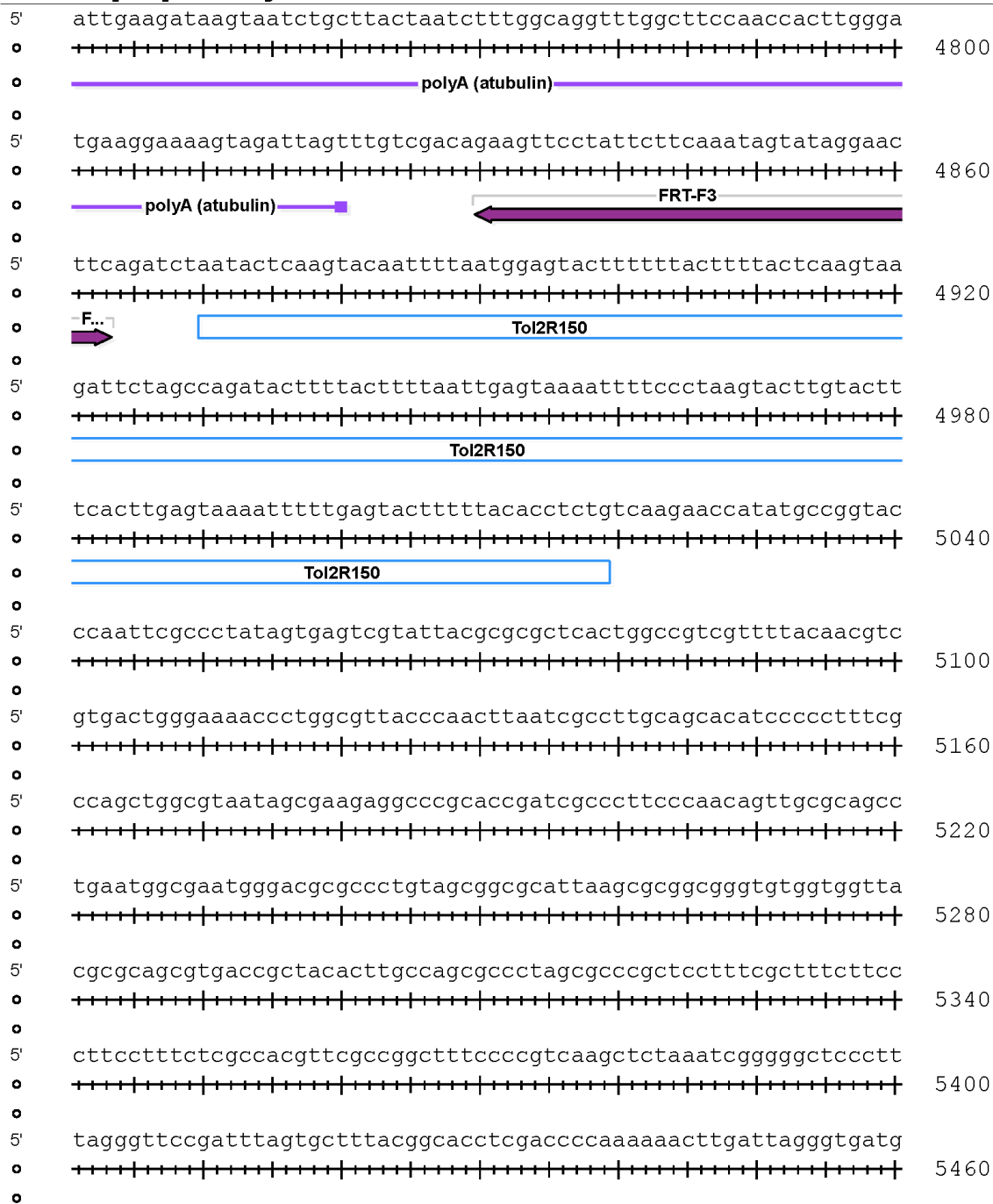
MetRS-FlipTrap exchange vector



MetRS-FlipTrap exchange vector



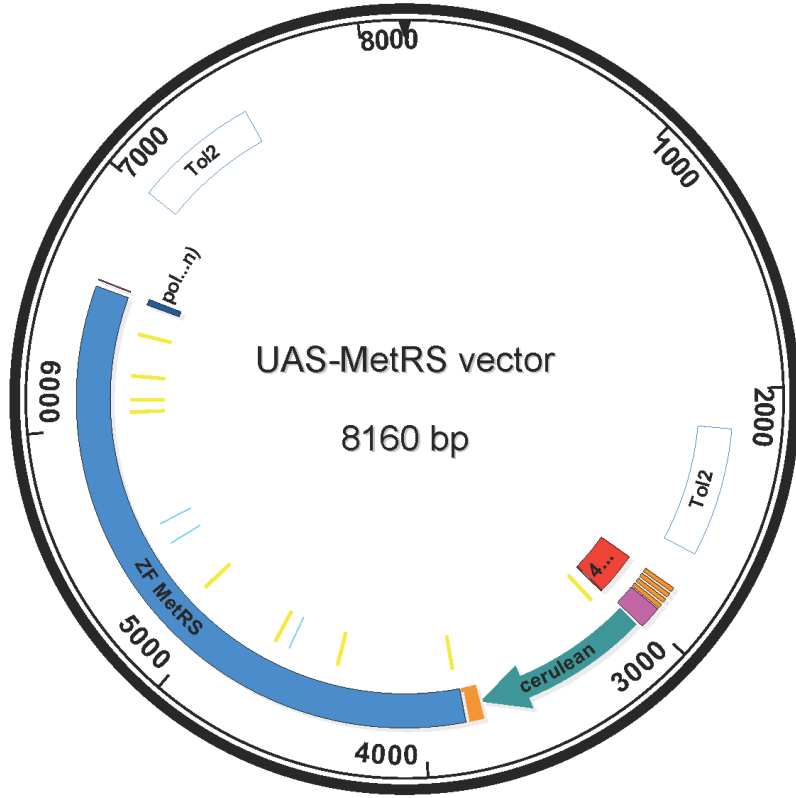
MetRS-FlipTrap exchange vector



MetRS-FlipTrap exchange vector

5'	gttaccggataaggcgcagcggtcgggctgaacggggggttcgtgcacacagcccagctt	
o	+++++	7200
o		
5'	ggagcgaacgacctacaccgaactgagatacctacagcgtgagctatgagaaagcggcac	
o	+++++	7260
o		
5'	gcttcccgaagggagaaaggcggacaggtatccggtgaagcggcagggtcggaacaggaga	
o	+++++	7320
o		
5'	gcgcacgaggagcttccaggggaaacgcctggtatctttatagtcctgtcgggtttcg	
o	+++++	7380
o		
5'	ccaccttgacttgagcgtcgatTTTTgtgatgctcgtcagggggcggagcctatggaa	
o	+++++	7440
o		
5'	aaacgccagcaacgcggcctTTTTacggttcttggccttttgccttttgccttttgcacat	
o	+++++	7500
o		
5'	gttctttcctgcgttatcccctgattctgtggataaccgtattaccgcctttgagtgagc	
o	+++++	7560
o		
5'	tgataccgctcgccgcagccgaacgaccgagcgcagcagtcagtgagcgaggaagcggga	
o	+++++	7620
o		
5'	agagcgcccaatacgcgaaaccgcctctccccgcgcggttgccgattcattaatgcagctg	
o	+++++	7680
o		
5'	gcacgacaggtttcccactggaaagcgggcagtgagcgcgcaacgcaattaatgtgagtta	
o	+++++	7740
o		
5'	gctcac	
o	+++++	7746
o		

UAS-MetRS vector



UAS-MetRS vector

5' TCTAAATACATTCAAATATGTATCCGCTCATGAGACAATAACCCTGATAAATGCTTCAAT
 ○ +-----+-----+-----+-----+-----+-----+-----+-----+-----+-----+ 60

5' AATATTGAAAAAGGAAGAGTATGAGTATTCAACATTTCCGTGTCGCCCTTATTCCCTTTT
 ○ +-----+-----+-----+-----+-----+-----+-----+-----+-----+-----+ 120

5' TTGCGGCATTTTGCCTTCCTGTTTTGCTCACCCAGAAACGCTGGTGAAAGTAAAAGATG
 ○ +-----+-----+-----+-----+-----+-----+-----+-----+-----+-----+ 180

5' CTGAAGATCAGTTGGGTGCACGAGTGGGTACATCGAACTGGATCTCAACAGCGGTAAGA
 ○ +-----+-----+-----+-----+-----+-----+-----+-----+-----+-----+ 240

5' TCCTTGAGAGTTTTCGCCCCGAAGAACGTTTTCCAATGATGAGCACTTTTAAAGTTCTGC
 ○ +-----+-----+-----+-----+-----+-----+-----+-----+-----+-----+ 300

5' TATGTGGCGCGGTATTATCCCGTATTGACGCCGGGCAAGAGCAACTCGGTGCGCCGCATAC
 ○ +-----+-----+-----+-----+-----+-----+-----+-----+-----+-----+ 360

5' ACTATTCTCAGAATGACTTGGTTGAGTACTCACCAGTCACAGAAAAGCATCTTACGGATG
 ○ +-----+-----+-----+-----+-----+-----+-----+-----+-----+-----+ 420

5' GCATGACAGTAAGAGAATTATGCAGTGCTGCCATAACCATGAGTGATAAACTGCGGCCA
 ○ +-----+-----+-----+-----+-----+-----+-----+-----+-----+-----+ 480

5' ACTTACTTCTGACAACGATCGGAGGACCGAAGGAGCTAACCGCTTTTTTGCACAACATGG
 ○ +-----+-----+-----+-----+-----+-----+-----+-----+-----+-----+ 540

5' GGGATCATGTAACTCGCCCTTGATCGTTGGGAACCGGAGCTGAATGAAGCCATACCAAACG
 ○ +-----+-----+-----+-----+-----+-----+-----+-----+-----+-----+ 600

5' ACGAGCGTGACACCACGATGCCTGTAGCAATGGCAACAACGTTGCGCAAACCTATTAAC TG
 ○ +-----+-----+-----+-----+-----+-----+-----+-----+-----+-----+ 660

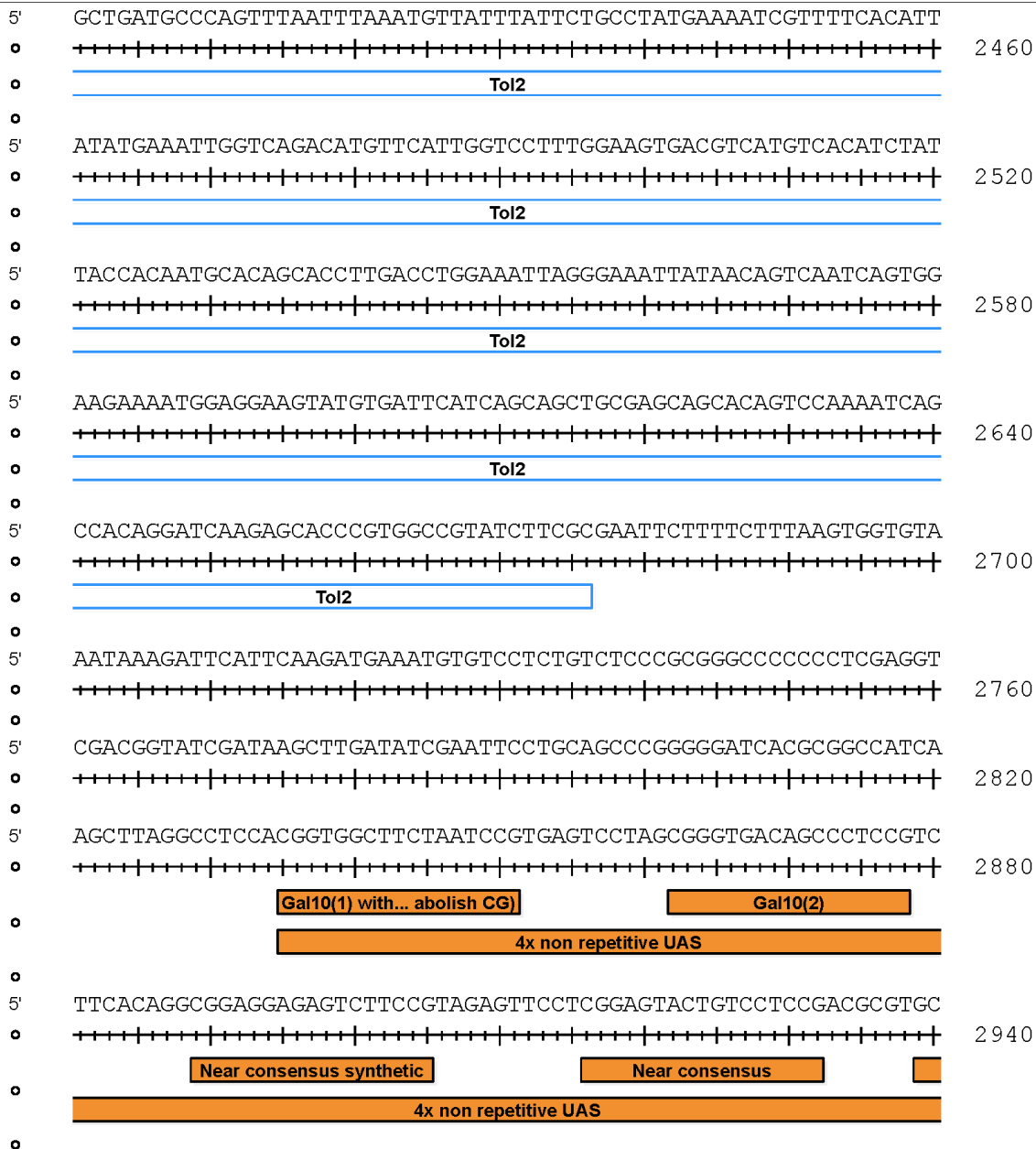
5' GCGAACTACTTACTCTAGCTTCCCGGCAACAATTAATAGACTGGATGGAGGCGGATAAAG
 ○ +-----+-----+-----+-----+-----+-----+-----+-----+-----+-----+ 720

5' TTGCAGGACCACTTCTGCGCTCGGCCCTTCCGGCTGGCTGGTTTATTGCTGATAAATCTG
 ○ +-----+-----+-----+-----+-----+-----+-----+-----+-----+-----+ 780

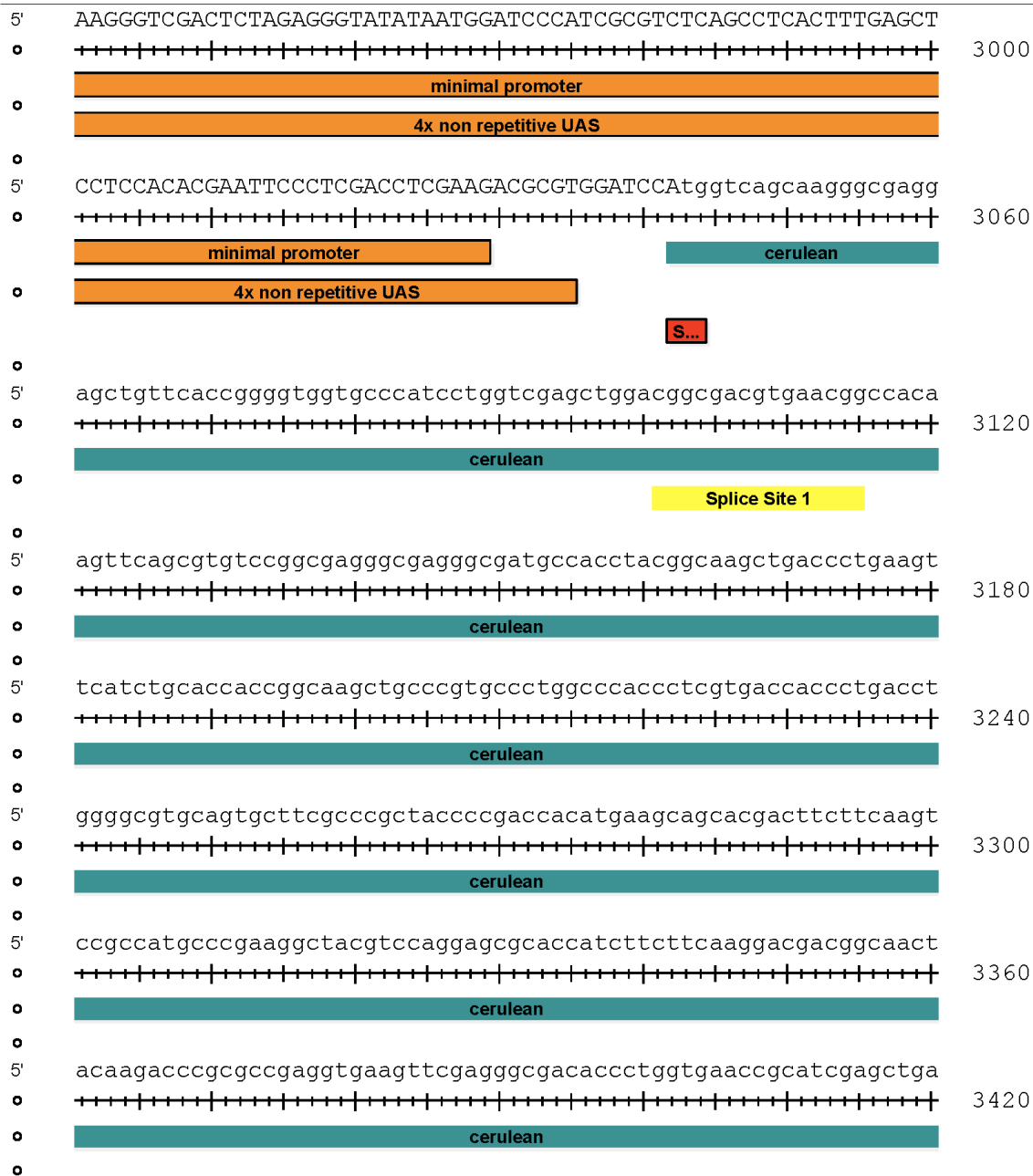
5' GAGCCGGTGAGCGTGGGTCGCGGTATCATTGCAGCACTGGGGCCAGATGGTAAGCCCT
 ○ +-----+-----+-----+-----+-----+-----+-----+-----+-----+-----+ 840

○

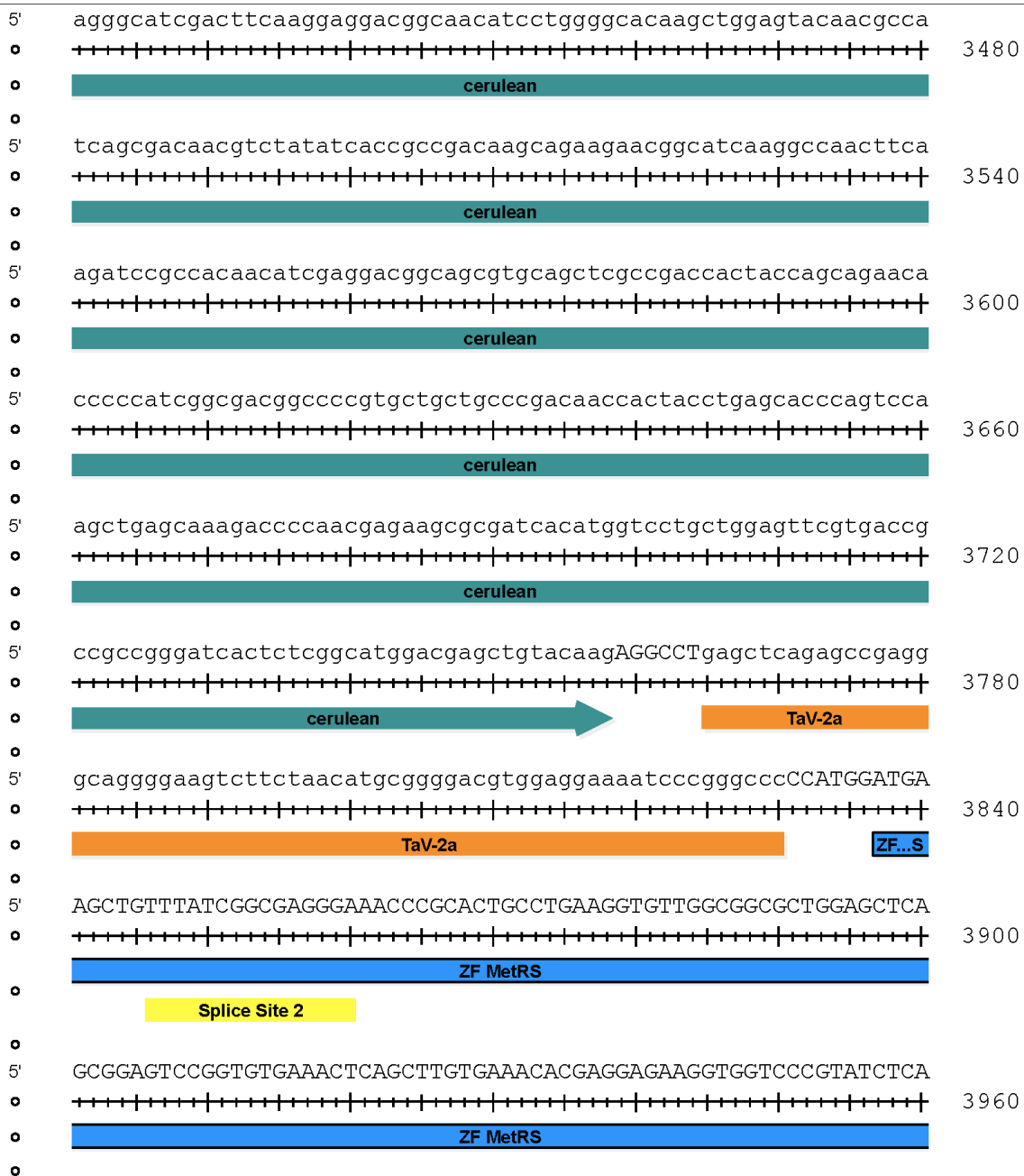
UAS-MetRS vector



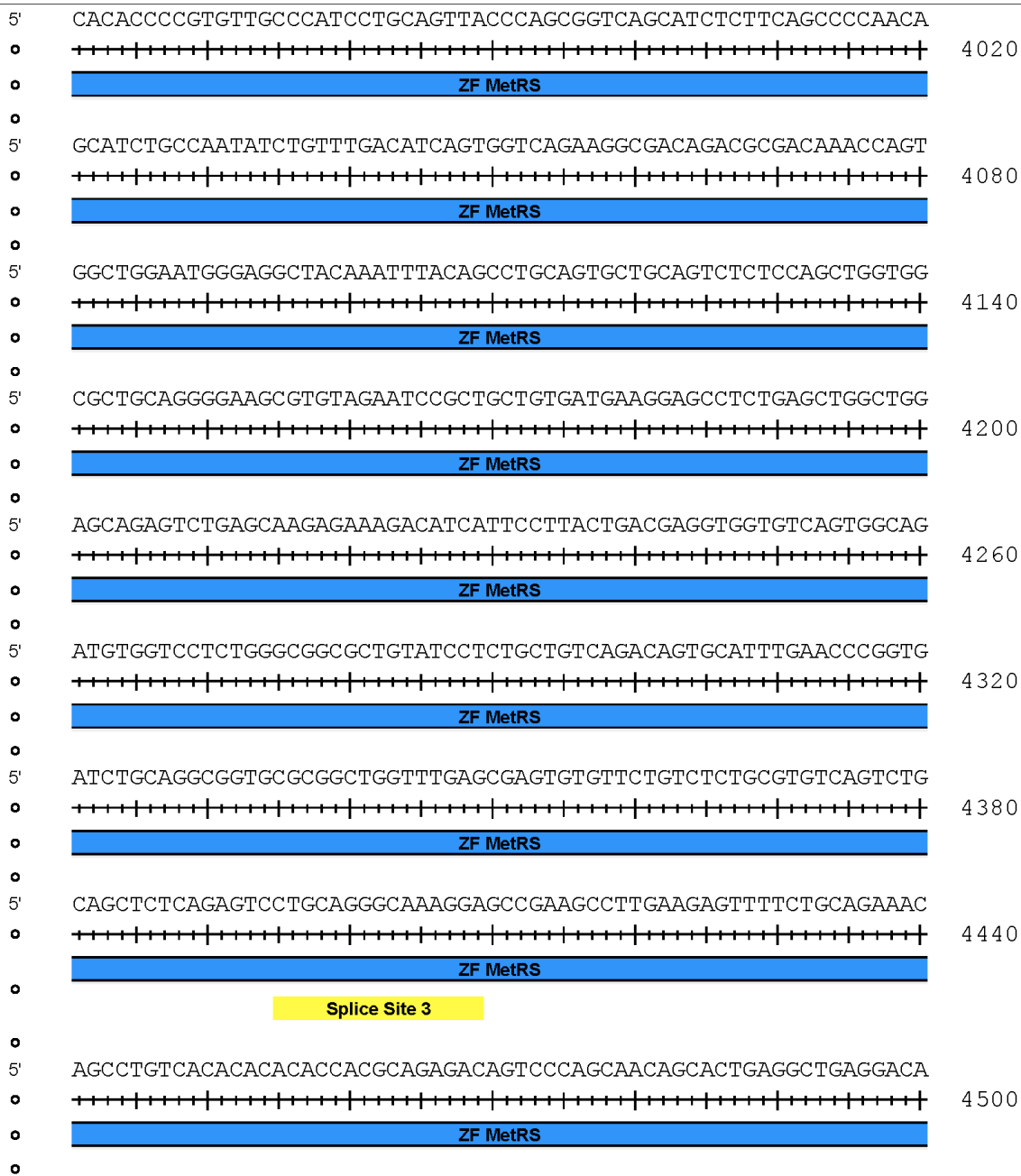
UAS-MetRS vector



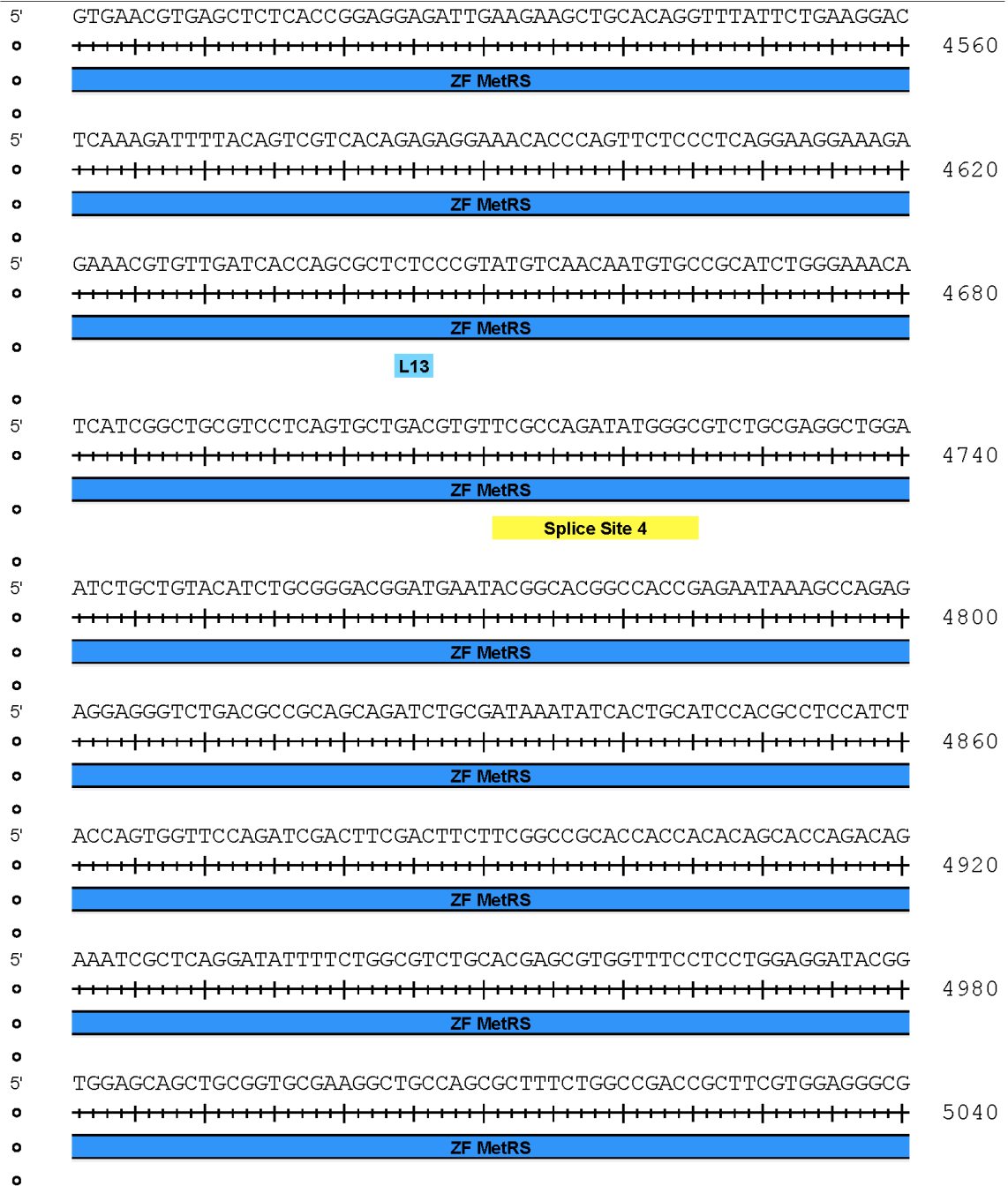
UAS-MetRS vector



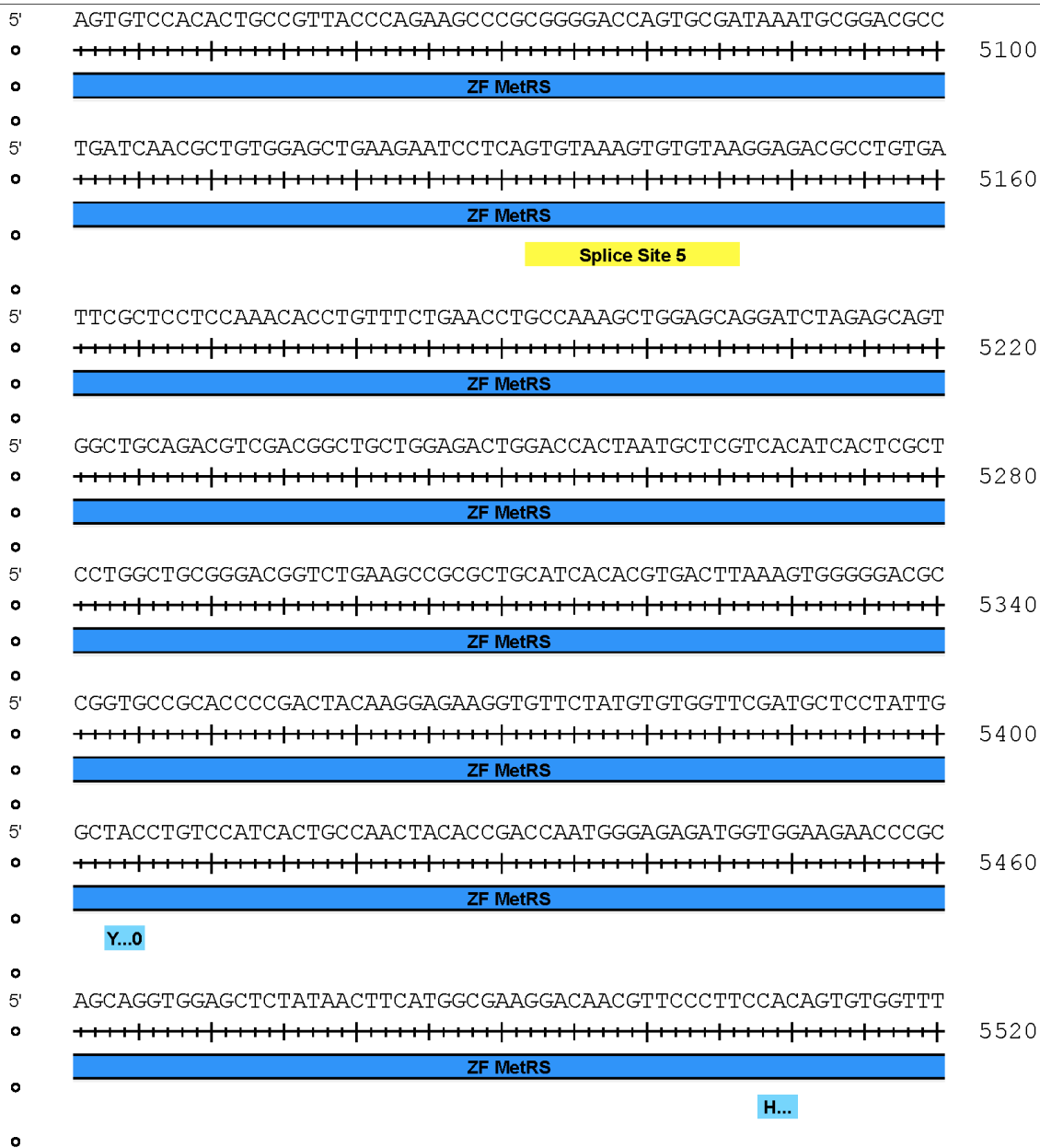
UAS-MetRS vector



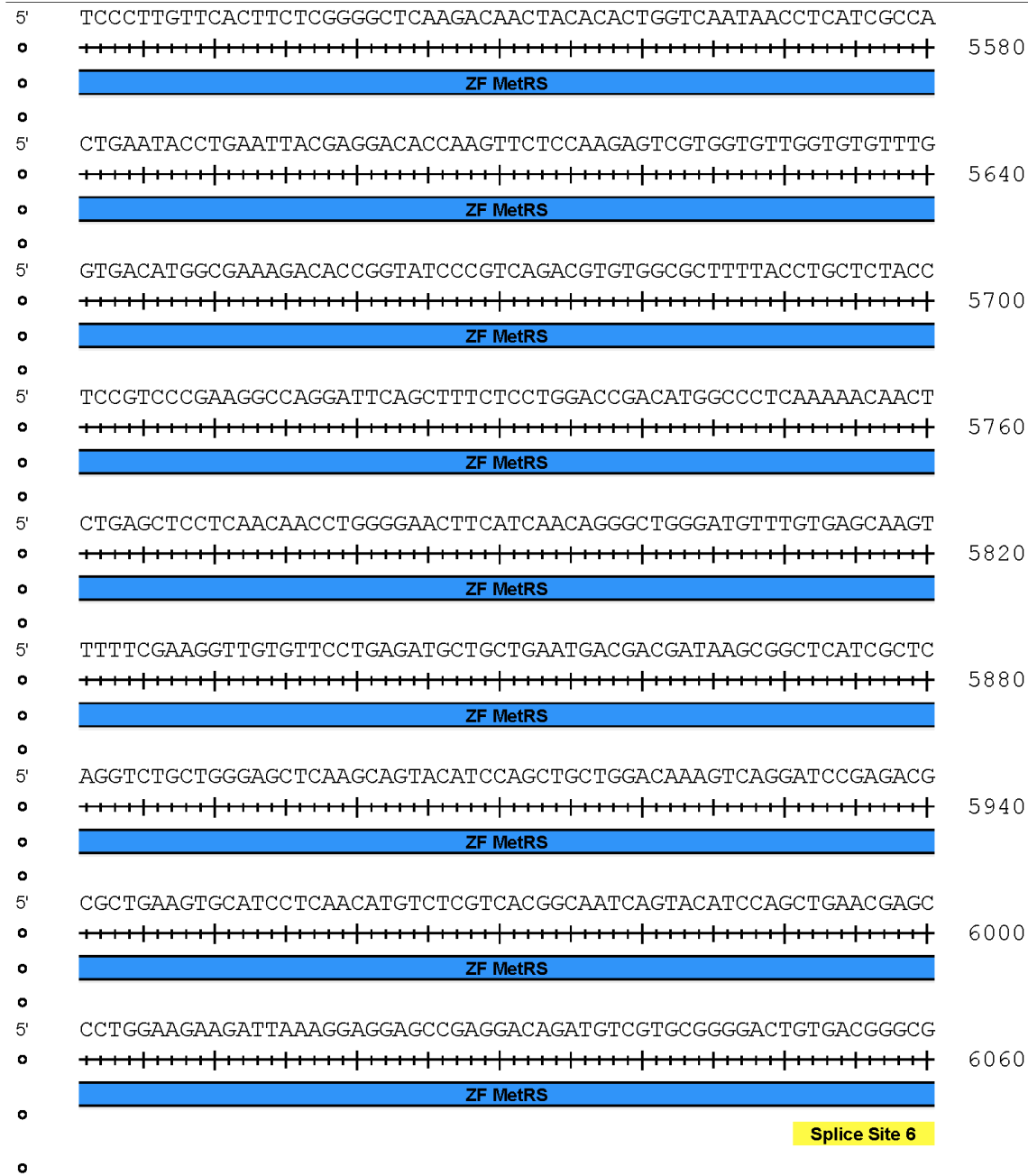
UAS-MetRS vector



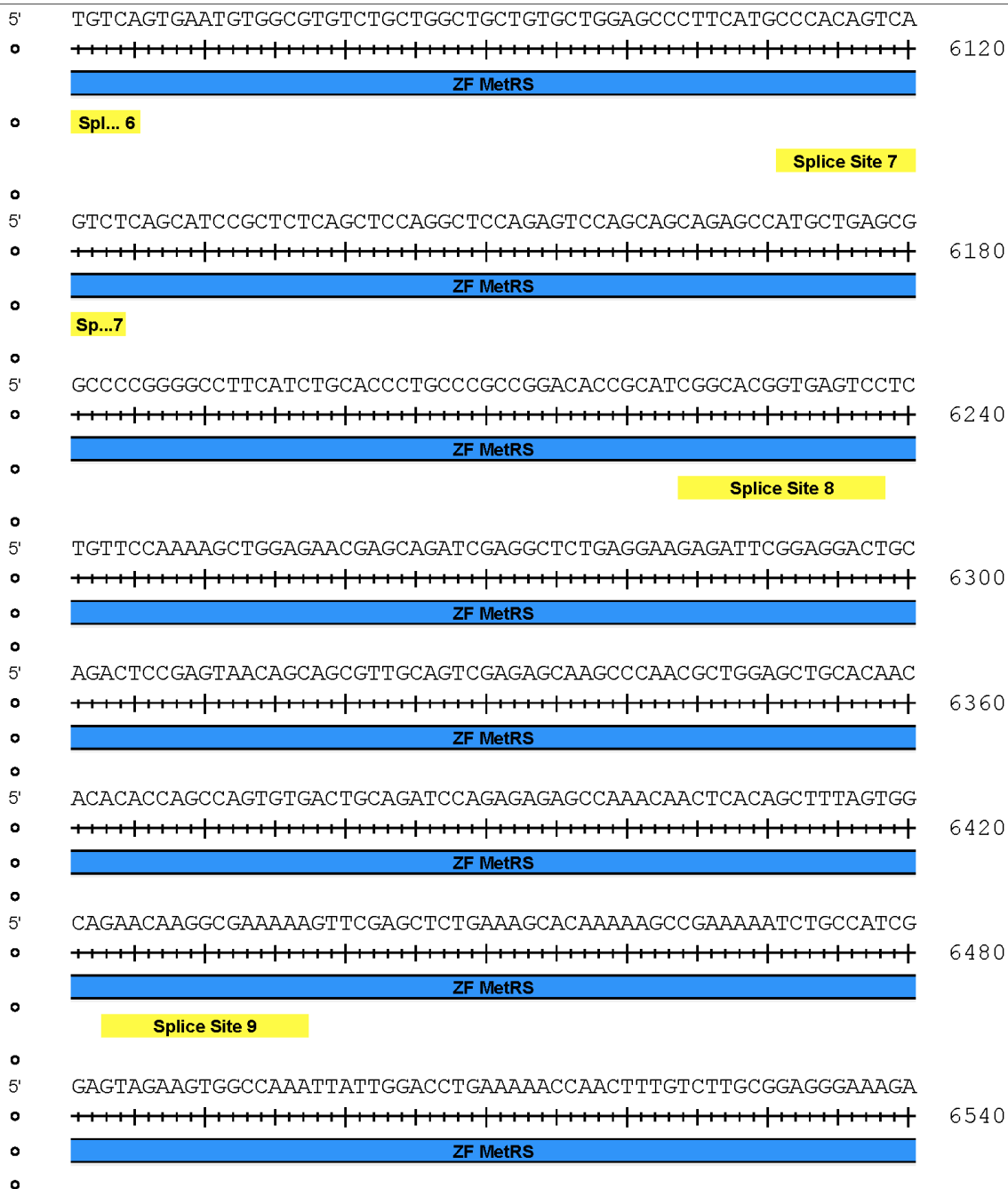
UAS-MetRS vector



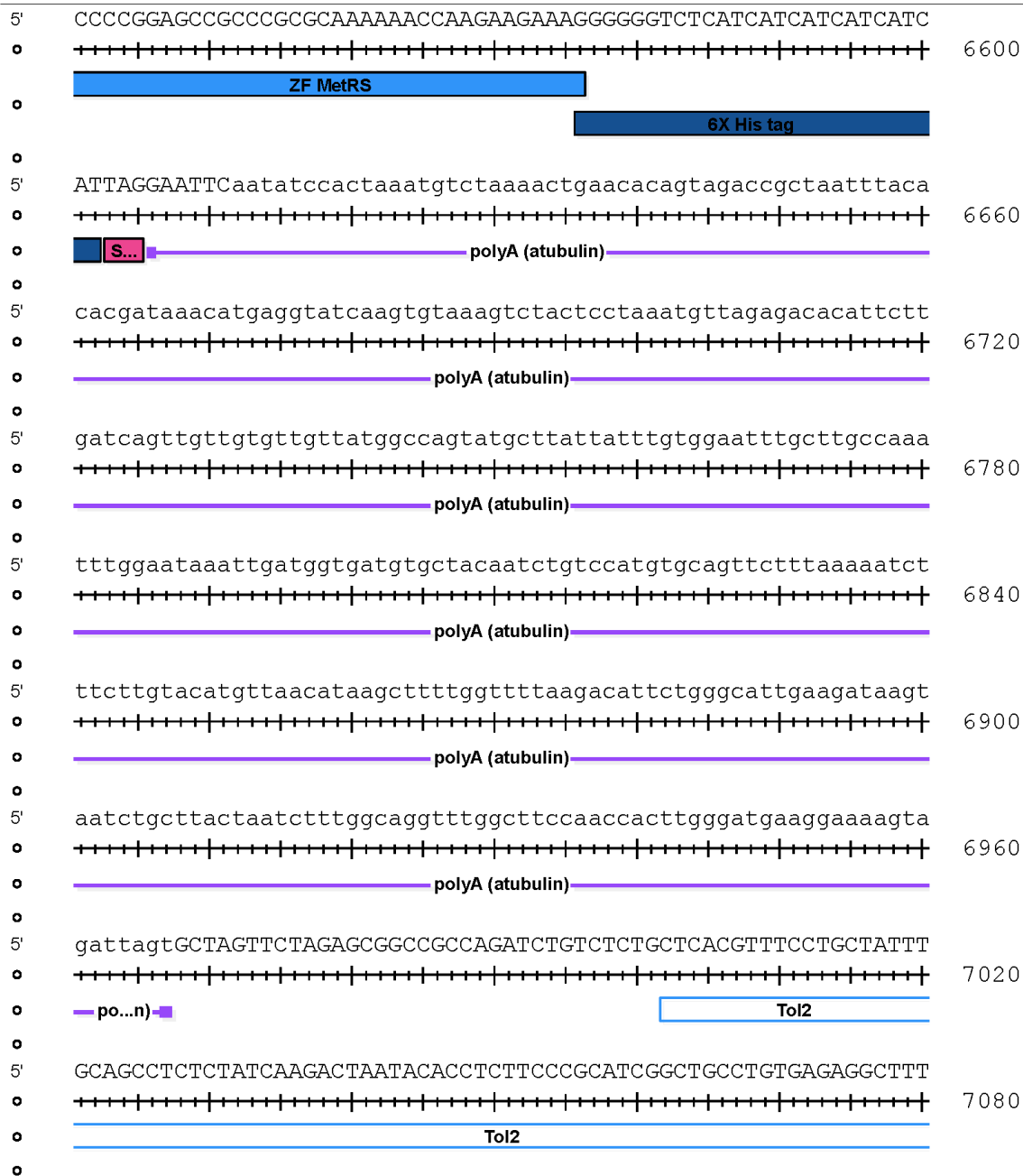
UAS-MetRS vector



UAS-MetRS vector

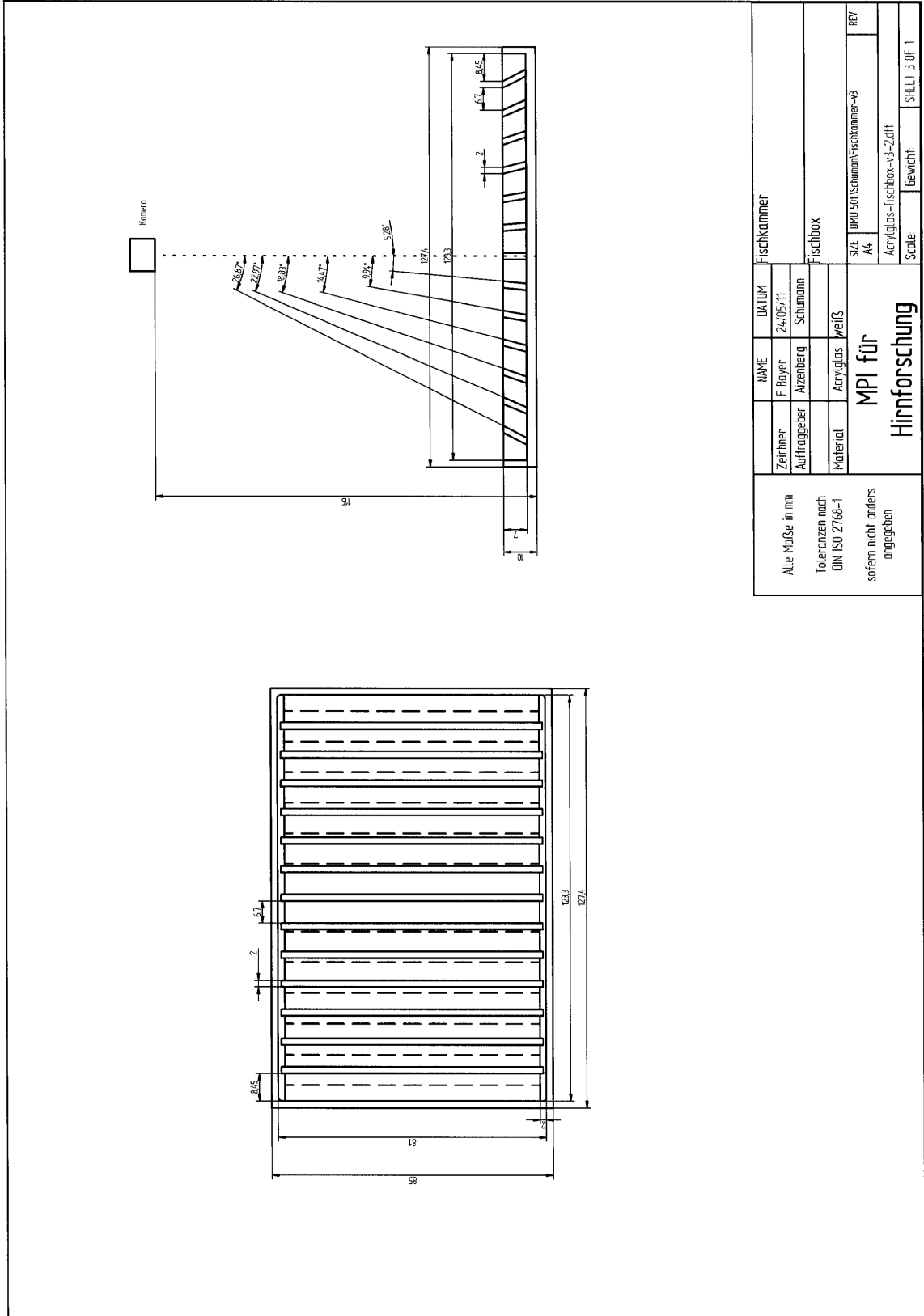


UAS-MetRS vector

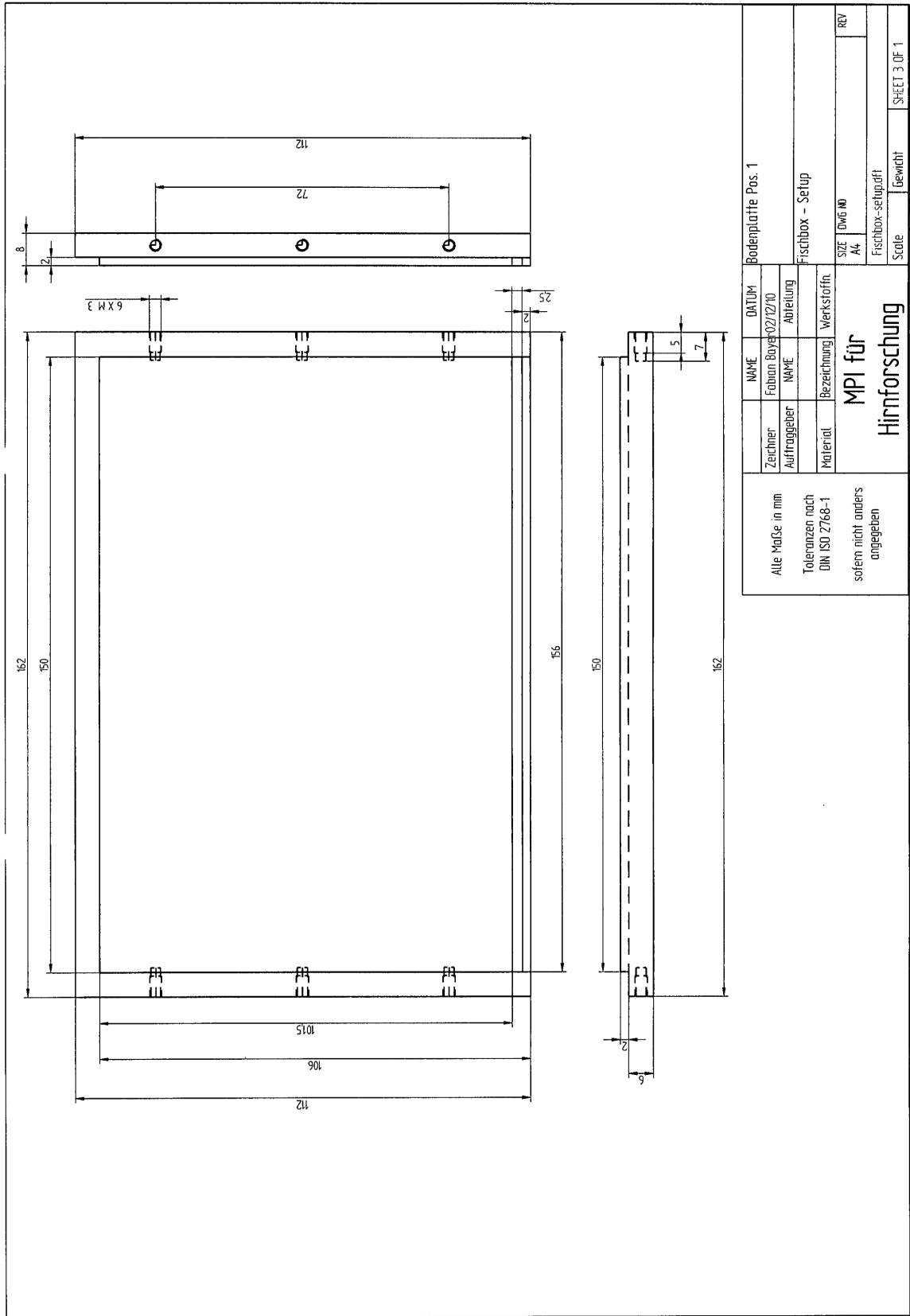


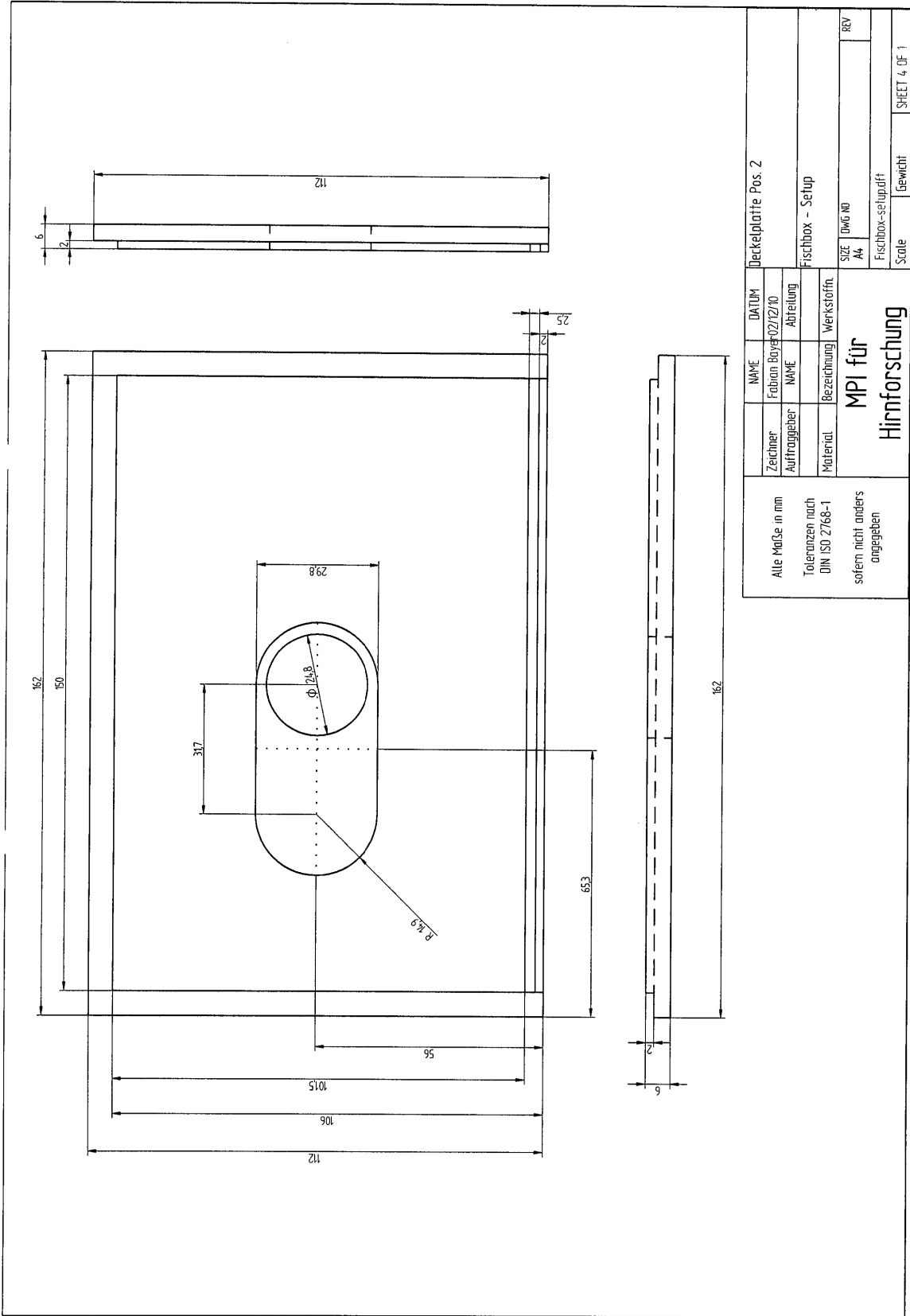
APPENDIX B

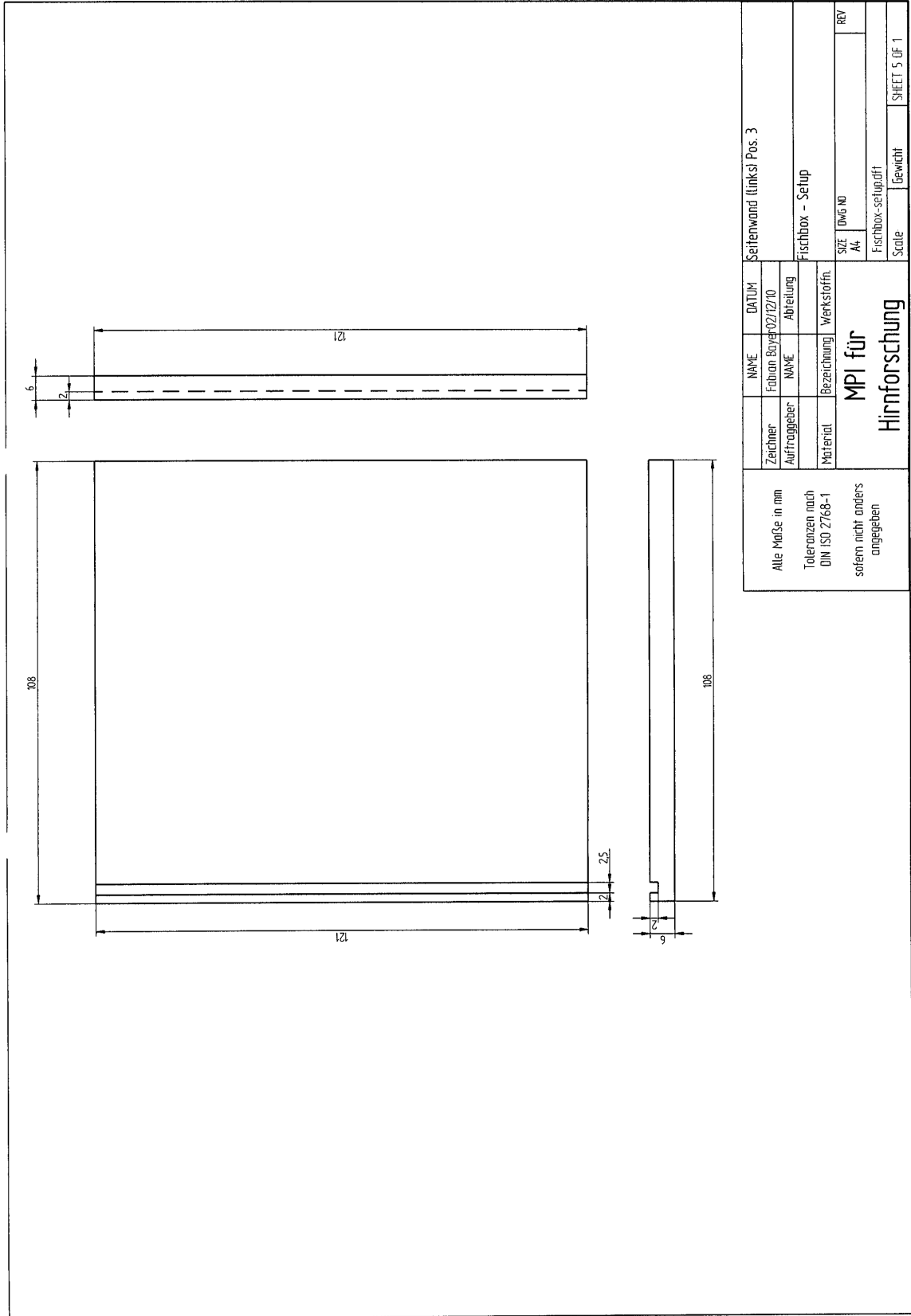
Drawings of behavioral chambers



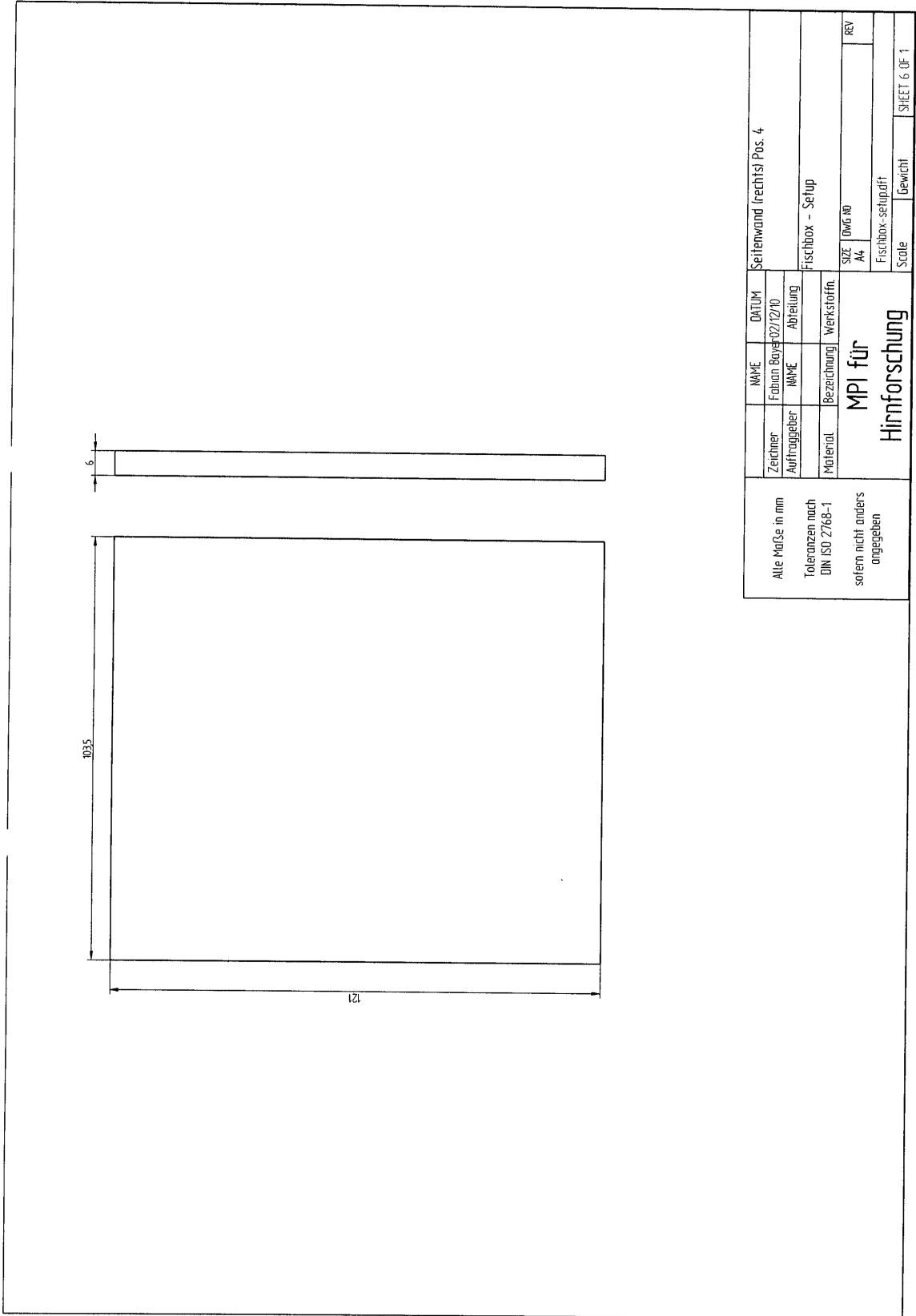
Alle Maße in mm Toleranzen nach DIN ISO 2768-1 sofern nicht anders angegeben	NAME	DTUM	Fischkammer
	Zeichner Auftraggeber	24/05/11 Schumann	Fischbox
	MATERIAL	Acrylglas weiß	
MPI für Hirnforschung			
	SIZE	DIN 5015 SchumannFischkammer-v3	REV
	Scale	Acrylglas-fischbox-v3-2.dft	
		Gewicht:	SHEET 3 OF 1



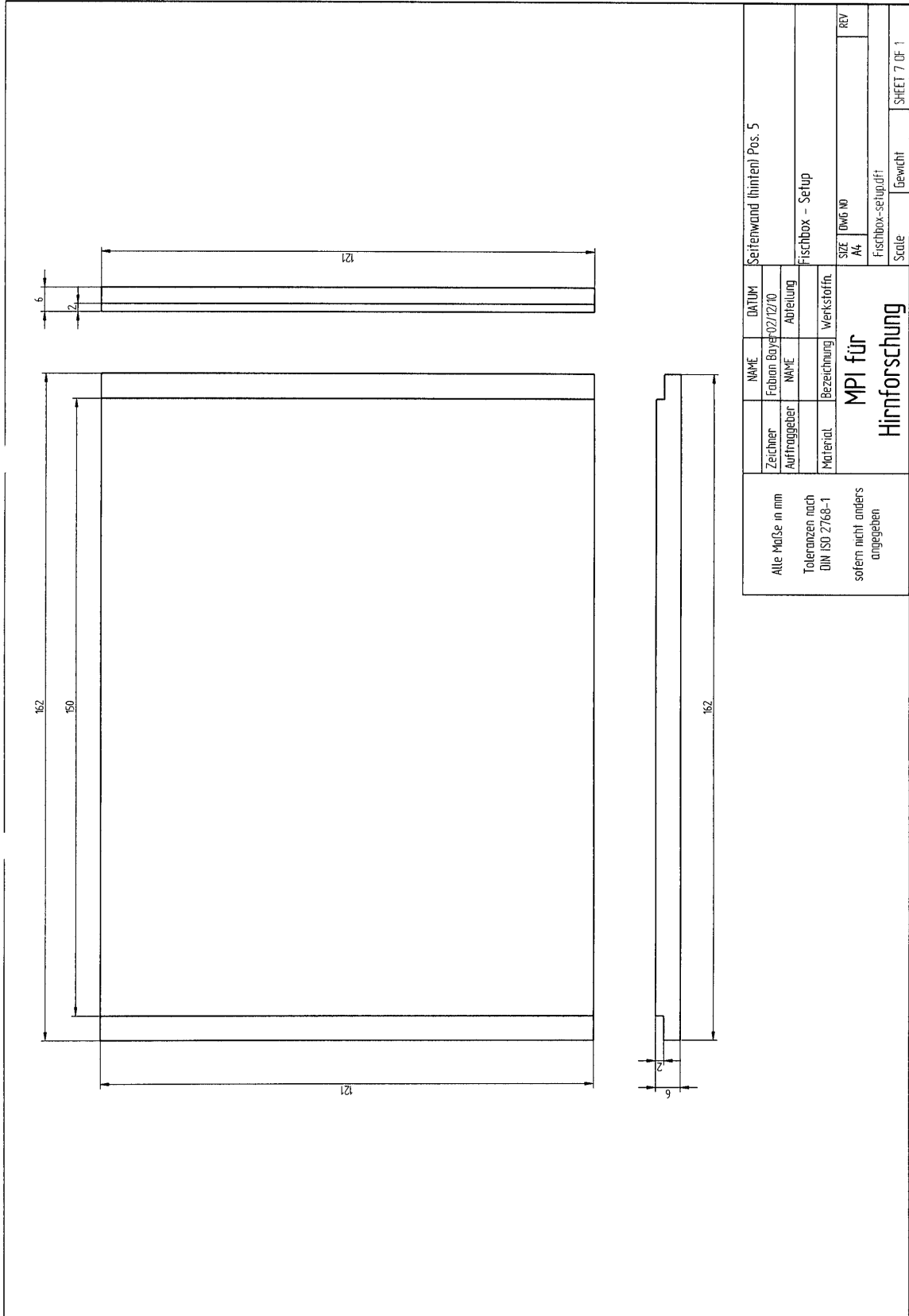


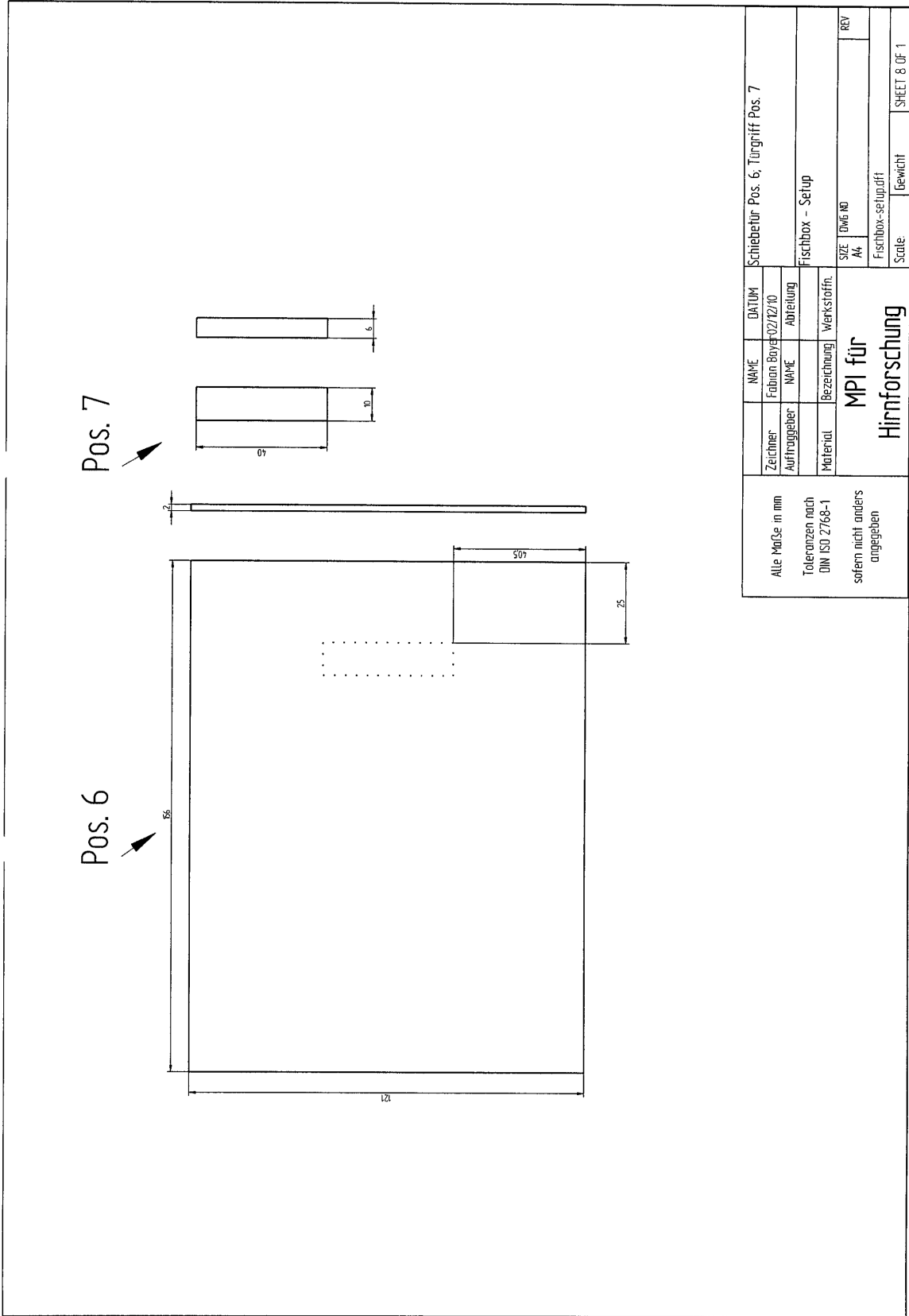


Alle Maße in mm Toleranzen nach DIN ISO 2768-1 sofern nicht anders angegeben		NAME Foluan Bayer02/12/10	DATE Abteilung	Seitenwand (links) Pos. 3	
		Auftraggeber		Fischbox - Setup	
		Material	Bezeichnung	Werkstoffnr.	
		MPI für Hirnforschung		SIZE	REV
				AW	
		Fischbox-setup.dxf		Scale	Gewicht
				SHEET 5 OF 1	

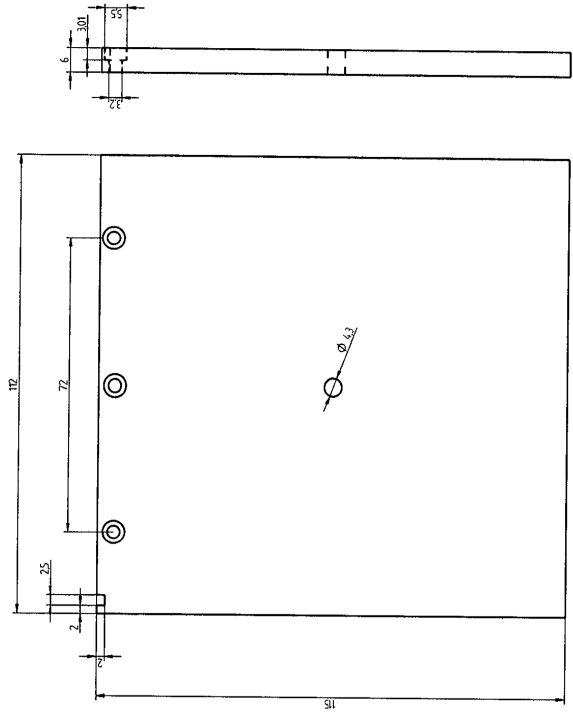


Zeichner Fabian Bayer 02/12/10		NAME Fabian Bayer	DATUM 02/12/10	Seitenwand (rechts) Pos. 4	
Auftraggeber		NAME	Abteilung	Fischbox - Setup	
Material		Bezeichnung	Werkstoff	SIZE DWG NO A4	REV
MPI für Hirnforschung			Fischbox-schlupf		
Alle Maße in mm Toleranzen nach DIN ISO 2768-1 sofern nicht anders angegeben			Scale	Gewicht	SHEET 6 OF 1

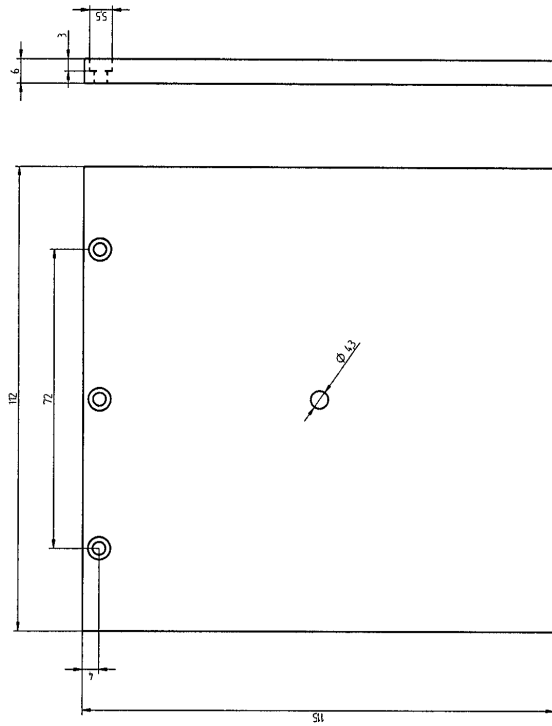




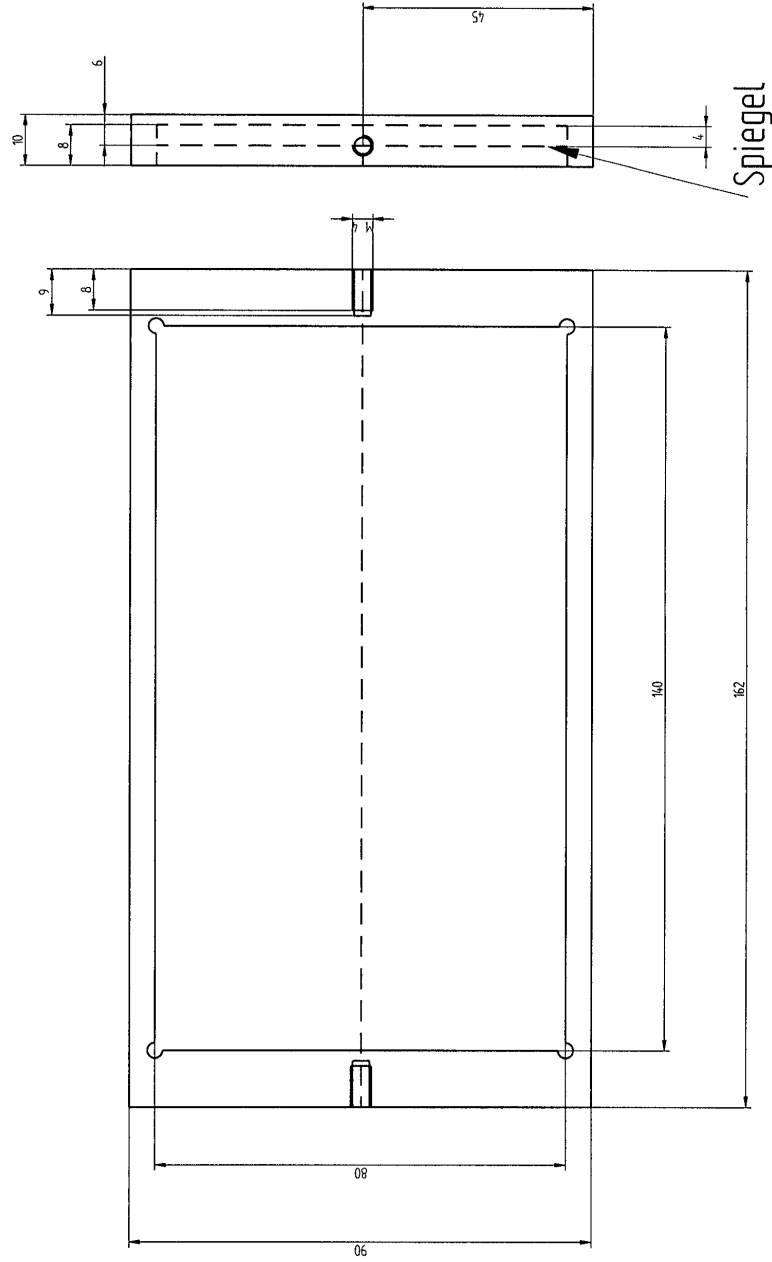
Alle Maße in mm Toleranzen nach DIN ISO 2768-1 sofern nicht anders angegeben		Zeichner: Auftraggeber	NAME: Fabian Boyd	DATUM: 02/02/10	Schiebetür Pos. 6, Türgriff Pos. 7	
Material	Bezeichnung	Abteilung	Werkstoffnr.	Fischbox - Setup		
MPI für Hirnforschung				SIZE	DWG NO	REV
				A4		
Scale:				Fischbox-setup.dxf		
				Gewicht		SHEET 8 OF 1



Alle Maße in mm Toleranzen nach DIN ISO 2768-1 sofern nicht anders angegeben		Zeichner Auftraggeber	NAME Fahno Boyer 02/12/10	DATEUM Abfertigung	Fußplatte (rechts) Pos. 8	
		Material	Bezeichnung	Werkstoffnr.	Fischbox - Setup	
		MPI für Hirnforschung			SIZE	DWG NO
					A4	RCV
		Scale			Fischbox-setup.dft	
		Gewicht			SHEET 9 OF 1	



Alle Maße in mm Toleranzen nach DIN ISO 2768-1 sofern nicht anders angegeben		Zeichner Auftraggeber	NAME Fabian Boys/02/12/10	DATUM Abteilung	Fußplatte links! Pos. 9	
		Material	Bezeichnung	Werkstoff	Fischbox - Setup	
		MPI für Hirnforschung			SIZE	DWG NO
					Scale	Gewicht
					Fischbox-setup.dft	
					SHEET 10 OF 1	



Alle Maße in mm Toleranzen nach DIN ISO 2768-1 sofern nicht anders angegeben		Zeichner Auftraggeber	NAME Fabian Boyer 02/12/10	DATUM Abteilung	Spiegelhalter Pos. 9	
		Material	Bezeichnung	Werkstoffnr.	SIZE	REV
					A4	
				Fischbox - Setup		
				Fischbox-setup.dft		
				Scale	Gewicht	SHEET 11 OF 1
MPI für Hirnforschung						

APPENDIX C

Matlab scripts

testFish.m

```

1      % testFish
2      -   clc
3      -   clear all
4      -   close all
5
6
7      -   v = get(0,'MonitorPosition');
8      -   x =get(0,'ScreenSize');
9
10
11
12      -   Screen('Preference', 'SkipSyncTests', 1);
13      -   screenNum=0;
14      -   wPtrA=Screen('OpenWindow',screenNum,[120 120 120],...
15      [1681 1 2528 240]);
16      -   pause(1);
17      -   wPtrB=Screen('OpenWindow',screenNum,[230 230 230],...
18      [1681 241 2528 480]);
19      -   pause(5);
20
21
22      -   LoopTime=15*60; % [seconds]
23      -   CatchFrames=10; % [seconds]
24      -   NLoops=LoopTime/CatchFrames;
25      -   dirOut=[pwd filesep 'CycleFrames_' date];
26      -   if ~isdir(dirOut)
27      -       mkdir(dirOut);
28      -   end
29
30      -   Experiment=2; % Experiment
31      -   k=0;
32      -   HideCursor;
33      -   for k=1:NLoops
34      -       tic
35      -       fOut=sprintf('%s%s%s_Exp%d_Frame%d.jpg',dirOut,filesep,date,Experiment,k);
36      -       robo = java.awt.Robot;
37      -       t = java.awt.Toolkit.getDefaultToolkit();
38      -       rectangle = java.awt.Rectangle(t.getScreenSize());
39      -       image = robo.createScreenCapture(rectangle);
40      -       filehandle = java.io.File(fOut);
41      -       javax.imageio.ImageIO.write(image,'jpg',filehandle);
42      -       T=toc;
43      -       pause(CatchFrames-T);
44      -   end % End of Loop
45      -   ShowCursor;
46      -   Screen('CloseAll');
47

```

trainFish.m

```
1   % trainFish
2 -   clc
3 -   clear all
4
5 -   TrainTime=45; %[min];
6 -   TrainTime=TrainTime*60; % [sec];
7
8 -   Screen('Preference', 'SkipSyncTests', 1);
9 -   screenNum=0;
10 -  wPtrA=Screen('OpenWindow',screenNum,[120 120 120],...
11     [1681 1 2528 240]);
12 -  pause(1);
13 -  wPtrB=Screen('OpenWindow',screenNum,[230 230 230],...
14     [1681 241 2528 480]);
15
16 -  pause(TrainTime);
17
18 -  Screen('CloseAll');
19
```

APPENDIX D

Protein identification list

Accession	Description	# Unique Peptides	# Peptides	MW [kDa]	calc. pI
110005909	titin a [Danio rerio]	200	238	3646.1	6.55
110005908	titin b [Danio rerio]	169	206	3198.2	6.33
169259784	myosin, heavy polypeptide 1, skeletal muscle [Danio rerio]	7	175	222.0	5.67
220941698	novel myosin family protein [Danio rerio]	5	173	222.1	5.69
50512294	myosin, heavy polypeptide 2, fast muscle specific [Danio rerio]	13	168	221.7	5.69
189540216	PREDICTED: wu:fd14a01 [Danio rerio]	3	109	221.5	5.74
189520343	PREDICTED: similar to myosin heavy chain fast skeletal muscle [Danio rerio]	10	102	222.1	5.92
117582129	slow myosin heavy chain 1 [Danio rerio]	46	96	222.8	5.66
169158649	novel protein similar to vertebrate nebulin (NEB) [Danio rerio]	78	81	709.7	9.35
71834286	hypothetical protein LOC321166 [Danio rerio]	75	77	412.3	5.24
44890667	Krt4 protein [Danio rerio]	20	42	54.0	5.39
55741944	ATPase, Ca ⁺⁺ transporting, fast twitch 1 [Danio rerio]	22	42	108.7	5.19
220672991	myosin, heavy polypeptide 6, cardiac muscle, alpha [Danio rerio]	2	40	222.7	5.68
39645432	Krt5 protein [Danio rerio]	10	37	57.8	5.34
41388915	Type I cytokeratin, enveloping layer [Danio rerio]	2	32	46.5	5.21
130504059	type I cytokeratin, enveloping layer, like [Danio rerio]	3	31	46.6	5.21
45387533	actinin alpha 3b [Danio rerio]	6	31	102.9	5.33
56118264	actinin alpha 3a [Danio rerio]	9	31	103.5	5.20
190338031	Pc protein [Danio rerio]	28	29	129.9	6.90
190337430	Clathrin, heavy polypeptide a (Hc) [Danio rerio]	5	27	191.7	5.69
18858249	actin, alpha 1, skeletal muscle [Danio rerio]	12	27	41.9	5.39
42560193	RecName: Full=Actin, cytoplasmic 1; AltName: Full=Beta-actin	10	26	41.7	5.48
117606266	ATPase, Ca ⁺⁺ transporting, cardiac muscle, fast twitch 1 [Danio rerio]	4	25	108.9	5.15
120537710	Zgc:109868 protein [Danio rerio]	8	25	47.1	5.34
116325975	ATP synthase, H ⁺ transporting, mitochondrial F1 complex, alpha subunit [Danio rerio]	24	24	59.7	9.03
38488747	tubulin, beta 5 [Danio rerio]	5	24	49.6	4.89
18858295	Na ⁺ /K ⁺ -ATPase alpha 1 subunit [Danio rerio]	8	24	113.3	5.33
28278942	Eukaryotic translation elongation factor 2, like [Danio rerio]	24	24	95.4	6.70
189528657	PREDICTED: hypothetical protein LOC503600 [Danio rerio]	2	23	191.5	5.72
239582731	tubulin, beta 2c [Danio rerio]	2	23	49.8	4.89
18859505	alpha-tropomyosin [Danio rerio]	23	23	32.7	4.74
123229625	creatine kinase, muscle [Danio rerio]	12	23	42.8	6.80
29335502	keratin 8 [Danio rerio]	8	22	55.5	5.08
157787181	muscle creatine kinase b [Danio rerio]	12	22	42.8	6.77
94732413	novel protein similar to type I cytokeratin, enveloping layer [Danio rerio]	5	21	49.7	5.43
68402816	PREDICTED: wu:fb37a10 isoform 1 [Danio rerio]	12	20	50.1	5.06
82658236	tubulin, beta, 2 [Danio rerio]	4	20	49.7	4.92
160333682	heat shock protein 8 [Danio rerio]	17	20	71.1	5.47
41282137	ATPase, Na ⁺ /K ⁺ transporting, alpha 3a polypeptide [Danio rerio]	9	20	112.5	5.38
27545251	solute carrier family 25 alpha, member 5 [Danio rerio]	12	19	32.7	9.76
169146331	ATPase, Na ⁺ /K ⁺ transporting, alpha 1b polypeptide [Danio rerio]	2	19	112.7	5.35
57526509	propionyl-Coenzyme A carboxylase, alpha polypeptide [Danio rerio]	19	19	77.8	7.21
158253775	Zgc:165344 protein [Danio rerio]	18	19	52.8	5.94
189525553	PREDICTED: hypothetical protein LOC336197 [Danio rerio]	18	18	55.1	5.27
11067034	Na ⁺ /K ⁺ ATPase alpha subunit isoform 8 [Danio rerio]	3	18	112.4	5.47
3212009	heat shock protein hsp90beta [Danio rerio]	9	18	83.3	5.01
41282194	glutamate dehydrogenase 1 [Danio rerio]	17	17	59.9	8.27
167234796	si:dkeyp-113d7.4 [Danio rerio]	12	17	49.9	5.02
131888757	hypothetical protein LOC100034647 [Danio rerio]	1	17	46.3	5.49
41054603	actinin alpha 4 [Danio rerio]	7	17	103.7	5.16
41054651	isocitrate dehydrogenase 2 (NADP ⁺), mitochondrial [Danio rerio]	16	17	50.4	8.12
53933236	ribosomal protein S4, X-linked [Danio rerio]	16	16	29.7	10.17
47550717	solute carrier family 25 (mitochondrial carrier; adenine nucleotide carrier) [Danio rerio]	9	16	32.7	9.73
27545193	brain creatine kinase b [Danio rerio]	12	16	42.9	5.80
189524989	PREDICTED: neurobeachin-like 2 [Danio rerio]	16	16	165.2	8.19

153792263	matrilin 1 [Danio rerio]	15	16	53.3	7.33
60688481	Ribosomal protein L3 [Danio rerio]	15	15	46.2	10.18
189532484	PREDICTED: similar to crystallin B1 protein isoform 10 [Danio rerio]	15	15	26.8	6.87
47086117	ribosomal protein S2 [Danio rerio]	14	14	30.3	10.20
18858587	elongation factor 1-alpha [Danio rerio]	14	14	50.0	9.09
198282117	hypothetical protein LOC572199 [Danio rerio]	13	14	60.2	6.15
148596963	spectrin alpha 2 [Danio rerio]	14	14	284.8	5.24
169403947	glyceraldehyde-3-phosphate dehydrogenase [Danio rerio]	12	14	35.8	8.12
47551317	enolase 3, (beta, muscle) [Danio rerio]	11	14	47.4	6.70
41152461	ribosomal protein L7a [Danio rerio]	13	13	30.0	10.56
54261775	ribosomal protein L4 [Danio rerio]	12	13	42.5	11.12
62202562	Ribosomal protein L6 [Danio rerio]	13	13	30.5	11.06
41054601	voltage-dependent anion channel 2 [Danio rerio]	11	13	30.3	8.82
37595356	ribosomal protein S3 [Danio rerio]	12	12	26.9	9.66
42415539	ribosomal protein S9 [Danio rerio]	12	12	22.5	10.51
152013098	Guanine nucleotide binding protein (G protein), beta polypeptide [Danio rerio]	12	12	35.1	7.69
189516653	PREDICTED: myosin, heavy chain 9, non-muscle like-1, isoform 1 [Danio rerio]	11	12	204.1	5.48
51011067	pyruvate kinase, muscle, b [Danio rerio]	10	12	58.3	7.28
47550793	nicotinamide nucleotide transhydrogenase [Danio rerio]	12	12	112.7	6.84
38707983	aconitase 2, mitochondrial [Danio rerio]	12	12	84.8	7.68
47086477	ribosomal protein L13a [Danio rerio]	11	11	23.7	10.86
157787167	histone 1, H4, like [Danio rerio]	11	11	11.4	11.36
41393119	valosin containing protein [Danio rerio]	11	11	89.4	5.26
28277619	Ldhd protein [Danio rerio]	7	11	36.2	6.89
37362304	tubulin, alpha 2 [Danio rerio]	3	11	50.0	5.15
18859297	parvalbumin 2 [Danio rerio]	10	11	11.6	4.68
18859049	myosin, light polypeptide 2, skeletal muscle [Danio rerio]	5	11	18.9	4.73
66472494	muscle glycogen phosphorylase [Danio rerio]	8	11	96.9	7.12
169158744	keratin 15 [Danio rerio]	2	11	48.8	5.22
41152175	ribosomal protein S7 [Danio rerio]	11	11	22.2	10.10
123916361	RecName: Full=Betaine-homocysteine S-methyltransferase [Danio rerio]	11	11	44.0	7.09
127799604	Ribosomal protein L7 [Danio rerio]	10	10	28.4	10.80
47550881	ribosomal protein S8 [Danio rerio]	10	10	24.1	10.52
41107591	Tnnt3b protein [Danio rerio]	9	10	27.3	9.60
182890016	Tkt protein [Danio rerio]	9	10	68.0	7.20
40363541	S-adenosylhomocysteine hydrolase [Danio rerio]	10	10	47.9	6.79
113681112	heat shock protein 90-alpha 2 [Danio rerio]	1	10	84.6	5.01
115496720	insulin-like growth factor 2 mRNA binding protein 1 [Danio rerio]	8	10	65.5	8.76
213385251	alpha-2 macroglobulin-like [Danio rerio]	10	10	159.7	5.45
62902024	beta A1-2-crystallin [Danio rerio]	10	10	24.5	6.87
47085833	glyceraldehyde-3-phosphate dehydrogenase, spermatogonia [Danio rerio]	8	10	36.1	7.03
148886613	RecName: Full=Keratin, type I cytoskeletal 18; AltName: Full=Keratin 18 [Danio rerio]	7	10	48.6	5.64
51010939	crystallin, gamma N2 [Danio rerio]	10	10	21.7	6.27
169234746	tenascin W [Danio rerio]	10	10	102.4	6.42
41053385	fast skeletal myosin alkali light chain 1 [Danio rerio]	7	10	20.9	4.77
41152457	ribosomal protein S3A [Danio rerio]	9	9	30.2	9.73
51010975	ribosomal protein L15 [Danio rerio]	9	9	24.0	11.53
47087057	ribosomal protein S11 [Danio rerio]	9	9	18.4	10.46
37700241	ribosomal protein L13 [Danio rerio]	9	9	24.3	11.60
169146764	novel protein similar to H.sapiens VDACC3, voltage-dependent anion channel 3 [Danio rerio]	7	9	33.9	9.33
41053780	adenosine monophosphate deaminase 1 (isoform M) [Danio rerio]	8	9	82.9	6.83
47550699	synaptotagmin binding, cytoplasmic RNA interacting protein [Danio rerio]	9	9	69.9	8.65
156523287	ryanodine receptor 1b (skeletal) [Danio rerio]	9	9	574.4	5.12
50539834	hypothetical protein LOC436656 [Danio rerio]	4	9	49.8	5.50
123232728	creatine kinase, mitochondrial 2 (sarcomeric) [Danio rerio]	4	9	44.4	6.74
157954508	hypothetical protein LOC100126134 [Danio rerio]	7	9	21.2	7.84

47086021	aldolase a, fructose-bisphosphate, b [Danio rerio]	4	9	39.5	8.24
18858353	hemoglobin beta embryonic-1 isoform 1 [Danio rerio]	9	9	16.2	7.44
110626137	crystallin, beta A4 [Danio rerio]	9	9	23.0	6.73
122890758	novel protein (zgc:63516) [Danio rerio]	9	9	68.3	5.58
45501385	Pkm2a protein [Danio rerio]	7	9	58.1	6.80
70887615	H2A histone family, member Y-like [Danio rerio]	9	9	39.8	9.83
220672954	transferrin-a [Danio rerio]	9	9	73.2	6.95
42542943	Eef1g protein [Danio rerio]	9	9	50.2	7.30
47085883	mitochondrial malate dehydrogenase [Danio rerio]	9	9	35.4	8.15
29124621	Heterogeneous nuclear ribonucleoprotein A/B [Danio rerio]	5	9	37.0	6.04
154426250	hypothetical protein LOC560055 [Danio rerio]	6	9	25.9	6.96
189528287	PREDICTED: hypothetical protein LOC553473 [Danio rerio]	6	9	25.6	7.24
50344752	crystallin, beta A2a [Danio rerio]	6	9	23.8	6.87
29124460	Rplp0 protein [Danio rerio]	8	8	34.4	5.99
51010947	ribosomal protein L18 [Danio rerio]	7	8	21.0	11.82
41152307	ribosomal protein L8 [Danio rerio]	8	8	28.0	10.89
50344812	ribosomal protein S13 [Danio rerio]	8	8	17.2	10.70
18858959	L-lactate dehydrogenase A [Danio rerio]	4	8	36.2	7.30
122891425	KH domain containing, RNA binding, signal transduction	6	8	40.2	8.78
220673290	oxoglutarate (alpha-ketoglutarate) dehydrogenase (lipoa	7	8	115.6	6.95
52219166	myosin light chain, phosphorylatable, fast skeletal muscle	2	8	19.1	4.69
238550183	myomesin 1a [Danio rerio]	8	8	166.2	6.60
157423409	Zgc:113984 protein [Danio rerio]	8	8	15.3	11.40
229606068	tyrosine 3-monooxygenase/tryptophan 5-monooxygenase	5	8	27.6	4.78
122890545	DEAD (Asp-Glu-Ala-Asp) box polypeptide 39a [Danio rerio]	3	8	48.9	5.59
47085711	DEAD (Asp-Glu-Ala-Asp) box polypeptide 39 [Danio rerio]	3	8	48.9	5.59
189525434	PREDICTED: im:7157373 [Danio rerio]	8	8	59.4	9.77
29242793	cytosolic malate dehydrogenase A [Danio rerio]	8	8	36.2	7.42
41053399	acidic (leucine-rich) nuclear phosphoprotein 32 family, member	2	8	29.1	4.08
37590349	Enolase 1, (alpha) [Danio rerio]	5	8	47.0	6.58
112363126	cytoplasmic dynein 1 heavy chain 1 [Danio rerio]	8	8	532.9	6.47
114158708	acidic (leucine-rich) nuclear phosphoprotein 32 family, member	2	8	29.5	4.03
189538569	PREDICTED: similar to myomesin 2 [Danio rerio]	8	8	67.2	5.97
125855691	PREDICTED: similar to predicted protein [Danio rerio]	8	8	13.6	10.37
41053595	nucleoside diphosphate kinase B [Danio rerio]	5	8	17.1	7.28
189527317	PREDICTED: similar to myomesin 2, partial [Danio rerio]	8	8	91.8	7.37
7649818	fast skeletal myosin light chain 3 [Danio rerio]	5	8	16.5	4.55
56797871	matrilin-4 [Danio rerio]	7	8	70.9	5.16
94732818	novel protein similar to vertebrate carboxylesterase precursor	2	8	60.6	5.66
49257533	Zgc:153863 protein [Danio rerio]	2	8	60.6	5.85
38198643	eukaryotic translation initiation factor 4A, isoform 1A [Danio rerio]	7	8	46.2	5.41
166158222	hypothetical protein LOC100135346 [Xenopus (Silurana)]	6	7	28.7	11.09
47086525	ribosomal protein S15a [Danio rerio]	7	7	14.8	10.13
50344868	ribosomal protein L5 [Danio rerio]	7	7	34.0	9.69
41393117	ADP-ribosylation factor 1 like [Danio rerio]	7	7	20.6	6.80
39645428	Heat shock protein 5 [Danio rerio]	4	7	71.9	5.14
193788703	procollagen-proline, 2-oxoglutarate 4-dioxygenase (proline	7	7	56.6	4.65
157422722	Rpl14 protein [Danio rerio]	7	7	16.1	10.33
18859497	troponin T3a, skeletal, fast [Danio rerio]	6	7	27.8	9.44
47086115	splicing factor proline/glutamine rich (polypyrimidine tract	7	7	69.8	9.52
47085781	ubiquitin-like modifier activating enzyme 1 [Danio rerio]	7	7	118.1	5.68
68391583	PREDICTED: hypothetical protein [Danio rerio]	7	7	41.2	10.87
63100850	Serpina1 protein [Danio rerio]	7	7	44.8	6.42
22671688	aldolase A [Danio rerio]	2	7	39.7	8.05
34194032	Hnrpa0 protein [Danio rerio]	6	7	32.0	7.93
68448507	syntaxin binding protein 1 [Danio rerio]	7	7	67.1	6.67

45433533	eukaryotic translation initiation factor 3, subunit 10 (the	7	7	151.2	7.87
46329565	Lmnb1 protein [Danio rerio]	5	7	66.6	5.21
52219178	high-mobility group box 2, like [Danio rerio]	6	7	24.2	5.91
45709105	Agxt protein [Danio rerio]	7	7	45.9	8.78
38541222	Pabpc1a protein [Danio rerio]	7	7	37.4	8.81
20977259	glial fibrillary acidic protein [Danio rerio]	2	7	42.1	5.10
112419426	LOC572200 protein [Danio rerio]	7	7	46.9	5.10
18858197	glutathione S-transferase pi [Danio rerio]	7	7	23.5	8.03
47085861	ribosomal protein L26 [Danio rerio]	6	6	17.3	10.62
47086479	solute carrier family 25, member 12 [Danio rerio]	6	6	75.3	8.47
41053337	ribosomal protein L10 [Danio rerio]	6	6	24.6	10.17
53749651	peptidylprolyl isomerase B [Danio rerio]	5	6	23.9	9.22
45387573	parvalbumin isoform 1d [Danio rerio]	3	6	11.4	4.64
49402291	heterogeneous nuclear ribonucleoprotein A1 [Danio rerio]	5	6	42.6	8.84
47087069	heterogeneous nuclear ribonucleoprotein L2 [Danio rerio]	6	6	53.3	6.60
37497110	ribophorin I [Danio rerio]	6	6	67.6	6.81
5731215	t-complex polypeptide 1 [Danio rerio]	6	6	50.3	8.00
41055022	ribosomal protein L18a [Danio rerio]	6	6	20.7	11.15
47086935	heterogeneous nuclear ribonucleoprotein A/B [Danio rerio]	2	6	34.2	7.28
50540230	hypothetical protein LOC436855 [Danio rerio]	4	6	21.3	7.84
189529246	PREDICTED: hypothetical protein [Danio rerio]	6	6	14.0	6.60
18858657	fatty acid binding protein 7, brain, a [Danio rerio]	6	6	14.9	5.60
189532165	PREDICTED: keratin, type 1, gene 19d [Danio rerio]	3	6	45.4	6.89
63101968	LOC553451 protein [Danio rerio]	6	6	113.8	6.34
38488694	creatine kinase, mitochondrial 1 [Danio rerio]	3	6	46.7	7.91
41054193	hypothetical protein LOC327506 [Danio rerio]	3	6	20.5	8.85
47086533	2-peptidylprolyl isomerase A [Danio rerio]	6	6	17.4	8.59
157888752	novel protein similar to vertebrate dihydropyrimidinase-li	6	6	58.2	6.27
50540044	ribosomal protein L35a [Danio rerio]	6	6	12.5	11.12
48597017	heterogeneous nuclear ribonucleoprotein U isoform 1 [D	6	6	73.1	4.88
41054527	proteasome (prosome, macropain) 26S subunit, non-ATP	6	6	99.4	5.40
47086959	hypothetical protein LOC406277 [Danio rerio]	6	6	38.2	9.28
112807244	histone 2A family member ZA [Danio rerio]	5	6	13.6	10.58
18858539	desmin [Danio rerio]	3	6	54.0	5.69
220673308	high-mobility group box 2 [Danio rerio]	6	6	19.8	9.89
160774198	Acadvl protein [Danio rerio]	6	6	71.0	8.41
47271422	triosephosphate isomerase 1 [Danio rerio]	6	6	26.8	7.33
51571925	adenylate kinase 1 [Danio rerio]	6	6	21.4	8.00
50540234	crystallin, beta A2b [Danio rerio]	3	6	23.6	6.39
118150590	periostin isoform 1 [Danio rerio]	6	6	82.9	7.83
37748736	ATPase, H+ transporting, lysosomal, V1 subunit B, mem	6	6	56.0	5.57
50539878	arrestin 3, retinal (X-arrestin), like [Danio rerio]	6	6	39.5	6.47
50540238	crystallin, beta A1b [Danio rerio]	6	6	23.3	6.39
158534025	zgc:171710 [Danio rerio]	5	5	15.8	10.49
29124464	Rpl12 protein [Danio rerio]	5	5	17.7	9.29
115529347	ribosomal protein S16 [Danio rerio]	5	5	16.3	10.14
41152199	ribosomal protein S26 [Danio rerio]	5	5	13.0	10.99
50344934	ribosomal protein L11 [Danio rerio]	5	5	20.4	9.86
38016165	heat shock protein 90kDa beta, member 1 [Danio rerio]	4	5	91.2	4.86
189533598	PREDICTED: similar to ribosomal protein S18 [Danio rerio]	5	5	11.4	9.99
47087315	guanine nucleotide binding protein (G protein), beta pol	4	5	37.3	6.00
41282078	ribosomal protein L23 [Danio rerio]	5	5	14.9	10.51
18858981	lamin b2 [Danio rerio]	4	5	65.9	5.26
41053347	mitochondrial trifunctional protein, beta subunit [Danio r	5	5	49.9	9.20
37595366	ubiquitin C [Danio rerio]	5	5	26.5	8.24
41152375	mitochondrial ATP synthase gamma-subunit [Danio rerio]	5	5	32.1	9.39

47777306	Voltage-dependent anion channel 1 [Danio rerio]	4	5	30.6	6.70
113195584	vesicle-fusing ATPase [Danio rerio]	5	5	82.5	6.84
41152181	retinal pigment epithelium abundant protein RPE65 [Danio rerio]	5	5	60.8	6.30
41054677	H1 histone family, member 0 [Danio rerio]	4	5	21.2	10.86
220673387	novel protein (sb:cb26) [Danio rerio]	4	5	183.1	6.57
47086051	KH domain containing, RNA binding, signal transduction	3	5	39.0	7.59
47085769	fibrinogen gamma polypeptide [Danio rerio]	5	5	48.8	5.27
50540432	casein kinase 2 [Danio rerio]	5	5	47.3	4.21
56744251	catalase [Danio rerio]	5	5	59.7	8.07
55741912	acidic (leucine-rich) nuclear phosphoprotein 32 family, member 1	5	5	28.1	3.98
47085983	phosphoenolpyruvate carboxykinase [Danio rerio]	4	5	69.7	8.44
18858613	ELAV (embryonic lethal, abnormal vision, Drosophila)-like protein 1	3	5	35.9	8.97
28502787	Ilf3 protein [Danio rerio]	5	5	68.0	8.98
50539876	hypothetical protein LOC436681 [Danio rerio]	4	5	21.2	7.99
189517833	PREDICTED: envoplakin, partial [Danio rerio]	5	5	196.7	7.61
29477118	Aldolase b, fructose-bisphosphate [Danio rerio]	4	5	39.2	8.51
50539808	aldehyde dehydrogenase 6A1 [Danio rerio]	5	5	57.1	8.03
18858571	insulin-like growth factor 2 mRNA binding protein 3 [Danio rerio]	3	5	63.3	8.79
33504513	staphylococcal nuclease domain containing 1 [Danio rerio]	5	5	100.0	7.28
182890966	Ywhai protein [Danio rerio]	2	5	26.2	4.96
42542740	Vat1 protein [Danio rerio]	5	5	52.3	6.81
81294186	Aldh2b protein [Danio rerio]	5	5	52.7	5.81
71834408	calcium/calmodulin-dependent protein kinase (CaM kinase) delta	5	5	62.5	7.09
169154685	novel protein similar to vertebrate DEAH (Asp-Glu-Ala-His) domain	5	5	139.9	7.42
41054351	ribosomal protein L27 [Danio rerio]	5	5	15.8	10.62
41054047	elastase 2 like [Danio rerio]	4	5	28.5	7.08
41393077	flotillin 1b [Danio rerio]	5	5	47.2	6.73
31044489	heat shock 60 kD protein 1 [Danio rerio]	5	5	61.2	5.72
41387118	ubiquinol-cytochrome c reductase core protein I [Danio rerio]	5	5	52.1	6.64
33416409	Nme2 protein [Danio rerio]	2	5	17.2	7.96
41053395	glutamate oxaloacetate transaminase 2 [Danio rerio]	3	5	47.4	8.76
41053909	solute carrier family 1 (glial high affinity glutamate transporter) member 1	5	5	61.2	5.74
18859437	stomatolysin [Danio rerio]	5	5	31.6	5.44
56606106	liver glycogen phosphorylase [Danio rerio]	2	5	111.5	5.73
61806490	NADH dehydrogenase (ubiquinone) 1 alpha subcomplex, 1	5	5	34.4	9.76
61651684	crystallin, gamma MX [Danio rerio]	5	5	20.6	7.06
37362224	GDP dissociation inhibitor 2 [Danio rerio]	5	5	50.6	5.85
51230582	hypothetical protein LOC445282 [Danio rerio]	5	5	28.8	8.10
189532330	PREDICTED: similar to Epiplakin [Danio rerio]	5	5	422.1	7.39
41152439	ribosomal protein L10a [Danio rerio]	3	4	24.6	9.94
190337988	Copa protein [Danio rerio]	4	4	138.0	7.59
41055138	ribosomal protein L34 [Danio rerio]	4	4	13.4	11.47
41388972	Pgk1 protein [Danio rerio]	4	4	44.7	6.93
47086529	hypothetical protein LOC336641 [Danio rerio]	4	4	21.4	10.11
218546780	RecName: Full=Dolichyl-diphosphooligosaccharide--protein transferase	3	4	48.5	5.48
41152494	prohibitin 2 [Danio rerio]	4	4	33.3	9.91
27545227	ribosomal protein L24 [Danio rerio]	4	4	17.9	11.25
47086505	fibrinogen, B beta polypeptide [Danio rerio]	4	4	54.4	7.84
60551107	Rpl9 protein [Danio rerio]	4	4	21.6	9.95
47086001	ribosomal protein S20 [Danio rerio]	4	4	13.3	9.94
50344966	ribosomal protein L21 [Danio rerio]	4	4	18.5	10.62
56118789	parvalbumin isoform 1c [Danio rerio]	1	4	11.6	4.88
125835118	PREDICTED: im:7145503 [Danio rerio]	3	4	111.9	6.27
115313778	Zgc:152810 [Danio rerio]	4	4	74.9	4.73
220678446	novel protein similar to vertebrate phosphoglycerate mutase	4	4	28.8	6.65
125829720	PREDICTED: collagen, type VI, alpha 1 [Danio rerio]	3	4	106.6	6.20

220672696	succinate-CoA ligase, GDP-forming, alpha subunit [Danio rerio]	4	4	34.2	9.14
94536703	C-terminal binding protein 1 [Danio rerio]	4	4	48.1	6.77
18858877	HuG [Danio rerio]	2	4	35.5	8.97
157502233	ribosomal protein L37a [Danio rerio]	4	4	10.2	10.30
35902900	fructose-bisphosphate aldolase C [Danio rerio]	3	4	39.2	6.64
56090186	far upstream element (FUSE) binding protein 3 [Danio rerio]	3	4	62.1	7.53
41152400	peptidylprolyl isomerase A, like [Danio rerio]	3	4	17.5	8.07
54261767	succinate-CoA ligase, ADP-forming, beta subunit [Danio rerio]	4	4	50.0	6.92
50726890	guanine nucleotide binding protein (G protein), beta polypeptide [Danio rerio]	3	4	36.5	6.16
189527793	PREDICTED: wu:fb05a01 [Danio rerio]	4	4	641.8	6.06
197247219	Rpl28l protein [Danio rerio]	4	4	15.6	12.12
169646741	pre-mRNA processing factor 8 [Danio rerio]	3	4	274.2	8.84
41152179	ribosomal protein S19 [Danio rerio]	4	4	15.9	10.23
45709332	Solute carrier family 25 (mitochondrial carrier; phosphate carrier) 2 [Danio rerio]	4	4	39.4	8.88
55962783	novel protein similar to vertebrate dihydropyrimidinase-like protein 1 [Danio rerio]	4	4	61.3	6.77
213021179	elastase 2 [Danio rerio]	3	4	28.8	8.02
125808587	PREDICTED: similar to histone cluster 2, H2ab [Danio rerio]	3	4	13.6	10.89
47086131	ribosomal protein L36 [Danio rerio]	4	4	12.2	11.50
183075544	serine hydroxymethyltransferase 2 (mitochondrial) [Danio rerio]	4	4	54.4	8.59
148726396	profilin 2 like [Danio rerio]	4	4	15.0	6.55
47087061	glutamic-oxaloacetic transaminase 2a, mitochondrial (aspartate aminotransferase) [Danio rerio]	2	4	47.6	9.17
27881906	Glucose phosphate isomerase a [Danio rerio]	4	4	62.0	6.95
47085773	glutamic-oxaloacetic transaminase 1, soluble [Danio rerio]	4	4	46.0	7.01
169158963	propionyl Coenzyme A carboxylase, beta polypeptide [Danio rerio]	4	4	60.6	7.84
18858765	guanine nucleotide binding protein (G protein), alpha transducin-like [Danio rerio]	3	4	40.2	5.53
12751181	reggie 1a [Danio rerio]	4	4	43.5	5.25
220679252	glutathione S-transferase M [Danio rerio]	4	4	26.0	6.38
34784843	Nop56 protein [Danio rerio]	4	4	52.8	9.00
41054573	hydroxysteroid dehydrogenase like 2 [Danio rerio]	4	4	44.4	7.47
16565980	alcohol dehydrogenase [Danio rerio]	4	4	40.0	7.18
41055823	hypothetical protein LOC393488 [Danio rerio]	3	4	20.9	4.92
157423081	Zgc:77517 protein [Danio rerio]	2	4	44.1	5.02
49902906	Zgc:110216 protein [Danio rerio]	4	4	16.9	10.92
122891384	novel protein similar to vertebrate threonyl-tRNA synthetase [Danio rerio]	4	4	82.8	7.01
47087305	cullin-associated and neddylation-dissociated 1 [Danio rerio]	4	4	135.9	5.82
83415094	hypothetical protein LOC553283 [Danio rerio]	4	4	24.9	9.23
51467909	ATP synthase, H+ transporting, mitochondrial F1 complex, c subunit [Danio rerio]	4	4	22.5	9.82
41152028	prohibitin [Danio rerio]	4	4	29.7	5.40
158254352	Proteasome (prosome, macropain) 26S subunit, ATPase, alpha [Danio rerio]	4	4	49.1	6.13
29165686	Adaptor-related protein complex 2, beta 1 subunit [Danio rerio]	3	3	105.6	5.35
18858453	coatamer protein complex, subunit gamma 2 [Danio rerio]	3	3	97.5	5.67
48597012	ribosomal protein L23a [Danio rerio]	3	3	17.6	10.39
41152464	ribosomal protein S14 [Danio rerio]	3	3	16.2	9.99
27881963	Sb:cb825 protein [Danio rerio]	3	3	54.7	6.76
27545223	ribosomal protein S5 [Danio rerio]	3	3	22.9	9.60
148224245	mitochondrial trifunctional protein, alpha subunit [Danio rerio]	3	3	82.8	9.01
41053327	ribosomal protein L27a [Danio rerio]	3	3	16.6	10.76
148725413	novel protein similar to ARP2 actin-related protein 2 homolog 1 [Danio rerio]	2	3	27.7	6.81
50417157	Srl protein [Danio rerio]	3	3	55.0	8.15
41053816	heterogeneous nuclear ribonucleoprotein A1 [Danio rerio]	3	3	38.4	8.73
51230594	proteasome (prosome, macropain) 26S subunit, ATPase, beta [Danio rerio]	2	3	45.6	7.55
224496086	UDP-glucose pyrophosphorylase 2 [Danio rerio]	3	3	56.8	8.46
56207617	novel protein similar to vertebrate splicing factor, arginine [Danio rerio]	3	3	16.0	10.15
125829873	PREDICTED: similar to transketolase [Danio rerio]	2	3	69.3	7.49
220678038	novel protein similar to vertebrate carnitine palmitoyltransferase 1 [Danio rerio]	3	3	67.4	7.43
189519626	PREDICTED: similar to dynamin 2 [Danio rerio]	2	3	86.5	6.86

189529439	PREDICTED: similar to plectin 1 isoform 2 [Danio rerio]	3	3	516.5	6.37
28278640	Heat shock protein 9 [Danio rerio]	2	3	73.8	7.40
55742595	protein phosphatase 2A, catalytic subunit, beta isoform [Danio rerio]	3	3	35.5	5.43
189518709	PREDICTED: wu:fi22e08 [Danio rerio]	3	3	37.1	6.54
169145723	novel protein (zgc:56036) [Danio rerio]	3	3	41.8	8.15
37362194	chaperonin containing TCP1, subunit 8 (theta) [Danio rerio]	3	3	59.3	5.35
220678527	fibrinogen alpha chain [Danio rerio]	3	3	75.2	6.10
41393103	aldehyde dehydrogenase 9A1a [Danio rerio]	3	3	55.2	6.55
41393063	TAR DNA binding protein [Danio rerio]	3	3	44.4	6.02
113681126	topoisomerase (DNA) II beta [Danio rerio]	3	3	182.4	7.72
114216750	fast muscle troponin I [Danio rerio]	3	3	20.1	8.81
40850963	Hnrpa0l protein [Danio rerio]	2	3	31.7	7.78
37362210	dihydropyrimidinase [Danio rerio]	3	3	53.6	7.52
47087630	splicing factor, arginine/serine-rich 1, like [Danio rerio]	3	3	26.8	10.05
8395615	cytochrome c oxidase subunit II [Danio rerio]	3	3	26.0	4.72
41053941	eukaryotic translation elongation factor 1 beta 2 [Danio rerio]	3	3	24.5	4.65
56797851	matrilin-3a [Danio rerio]	3	3	32.8	7.66
50344770	SUMO1 activating enzyme subunit 1 [Danio rerio]	3	3	39.1	5.16
169158718	novel protein similar to eukaryotic translation initiation factor 4E [Danio rerio]	3	3	14.1	6.54
50344790	hypothetical protein LOC415158 [Danio rerio]	3	3	11.4	9.44
189538686	PREDICTED: similar to heterogeneous nuclear ribonucleoprotein A2 [Danio rerio]	3	3	66.7	4.92
181331982	activating signal cointegrator 1 complex subunit 3-like 1 [Danio rerio]	3	3	243.8	6.07
45387527	SET and MYND domain containing 1 [Danio rerio]	3	3	54.5	7.40
237874200	casein kinase II-like [Danio rerio]	3	3	63.8	3.69
41393109	high density lipoprotein-binding protein (vigilin) [Danio rerio]	3	3	134.6	6.74
157073897	ubiquinol-cytochrome c reductase, Rieske iron-sulfur polypeptide [Danio rerio]	3	3	29.7	8.29
45387789	hypothetical protein LOC402985 [Danio rerio]	2	3	36.8	7.09
41055646	ribosomal protein S10 [Danio rerio]	3	3	18.9	10.04
51230650	acetyl-Coenzyme A acetyltransferase 1 [Danio rerio]	3	3	44.3	8.85
156739307	hypothetical protein LOC795883 [Danio rerio]	3	3	34.3	5.74
41054557	hypothetical protein LOC322453 [Danio rerio]	3	3	26.4	5.12
126540854	novel protein similar to vertebrate histone 1, H1d (HIST1D) [Danio rerio]	3	3	20.7	11.24
157422742	Ezrl protein [Danio rerio]	3	3	52.2	7.83
50539954	opsin 1 (cone pigments), long-wave-sensitive, 2 [Danio rerio]	3	3	39.5	8.07
169158157	isocitrate dehydrogenase 1 (NADP+), soluble [Danio rerio]	2	3	32.1	7.11
41152046	chaperonin containing TCP1, subunit 6A (zeta 1) [Danio rerio]	3	3	57.6	7.12
189535578	PREDICTED: fetuin B [Danio rerio]	3	3	56.6	6.79
47087353	heterogeneous nuclear ribonucleoprotein D-like [Danio rerio]	3	3	33.2	5.82
41053583	proteasome, 26S, non-ATPase regulatory subunit 6 [Danio rerio]	3	3	45.3	6.73
47086795	chymotrypsin B1 [Danio rerio]	3	3	28.2	7.34
190337264	Zgc:194528 protein [Danio rerio]	3	3	145.6	6.96
156739303	cystatin B [Danio rerio]	3	3	11.2	6.37
41055708	proteasome (prosome, macropain) 26S subunit, non-ATPase [Danio rerio]	3	3	57.9	8.76
190684659	amine oxidase, copper containing 3 [Danio rerio]	3	3	86.3	6.90
91176310	hypothetical protein LOC677758 [Danio rerio]	3	3	14.3	10.54
30141105	TPA: TPA_exp: glutamine synthetase [Danio rerio]	3	3	41.5	5.90
41393153	4-aminobutyrate aminotransferase [Danio rerio]	3	3	45.5	7.17
51230625	NADH dehydrogenase ubiquinone flavoprotein 1 precursor [Danio rerio]	3	3	53.7	8.38
41054748	RAS related protein 1b [Danio rerio]	3	3	20.8	6.70
41055100	reticulon 3 [Danio rerio]	3	3	24.5	8.97
47086749	heterogeneous nuclear ribonucleoprotein A0 [Danio rerio]	3	3	32.0	8.50
32401412	annexin A4 [Danio rerio]	3	3	35.6	6.46
134024899	Zgc:162944 protein [Danio rerio]	3	3	24.0	6.30
41387190	guanine nucleotide binding protein (G protein), alpha class 1 [Danio rerio]	2	3	40.0	5.43
42542468	Setb protein [Danio rerio]	3	3	31.0	4.30
38511590	Opsin 1 (cone pigments), short-wave-sensitive 1 [Danio rerio]	3	3	37.2	6.93

162139026	hypothetical protein LOC566702 [Danio rerio]	3	3	56.5	6.47
183986405	Citrate synthase [Danio rerio]	3	3	51.8	7.85
2558533	putative RNA helicase (DEAD box) [Danio rerio]	3	3	75.7	7.93
28422327	Calrl protein [Danio rerio]	3	3	48.2	4.46
160773274	Acyl-Coenzyme A dehydrogenase, C-4 to C-12 straight ch	3	3	46.1	8.05
27545249	chaperonin containing TCP1, subunit 3 (gamma) [Danio	3	3	60.3	5.90
24119230	proteasome (prosome, macropain) subunit, alpha type, c	3	3	25.9	8.43
22651403	cathepsin D precursor [Danio rerio]	3	3	43.1	6.68
41055130	eukaryotic translation initiation factor 4A, isoform 3 [Dan	2	3	46.4	6.71
162329921	Chain A, Crystal Structure Of Zebrafish Ape	3	3	31.9	5.74
41053961	serpin peptidase inhibitor, clade B (ovalbumin), member	3	3	42.6	5.31
115495185	hypothetical protein LOC767682 [Danio rerio]	3	3	55.5	7.77
169146129	myelin expression factor 2 [Danio rerio]	3	3	60.0	6.93
189534181	PREDICTED: leucyl-tRNA synthetase, partial [Danio rerio	3	3	92.8	6.55
21105454	chaperonin-containing TCP-1 complex beta chain [Danio	3	3	54.8	6.39
41053339	hypothetical protein LOC336637 [Danio rerio]	3	3	12.0	4.91
41055788	lectin, galactoside-binding, soluble, 1 (galectin 1)-like 3	3	3	13.3	6.87
44890302	Ribophorin II [Danio rerio]	3	3	69.0	5.39
18859495	troponin C, fast skeletal [Danio rerio]	3	3	18.2	4.08
220679245	ATP synthase, H+ transporting, mitochondrial F0 comple	3	3	28.2	9.35
28502924	Zgc:85653 [Danio rerio]	2	2	49.7	9.55
914049	casein kinase 2 alpha subunit; CK2 alpha [Danio rerio]	2	2	34.6	8.29
50344884	actin related protein 2/3 complex, subunit 3 [Danio rerio	2	2	20.4	8.59
61806482	hypothetical protein LOC541327 [Danio rerio]	2	2	15.4	9.85
41152459	ribosomal protein S12 [Danio rerio]	2	2	14.5	7.24
32401408	annexin A11b [Danio rerio]	2	2	51.4	7.65
45387521	actin related protein 2/3 complex subunit 4 [Danio rerio]	2	2	19.7	8.43
160773369	Anxa5b protein [Danio rerio]	2	2	35.1	5.64
61806512	peroxiredoxin 1 [Danio rerio]	2	2	22.0	6.92
45767805	Si:dkey-16k6.1 protein [Danio rerio]	2	2	32.4	5.44
83415112	ribosomal protein L22 [Danio rerio]	2	2	14.7	9.32
4506645	ribosomal protein L38 [Homo sapiens]	2	2	8.2	10.10
189524015	PREDICTED: similar to Tricarboxylate transport protein, i	2	2	34.3	9.58
41054984	ribosomal protein S24 isoform 2 [Danio rerio]	2	2	12.2	9.99
189517144	PREDICTED: similar to adaptor-related protein complex 3	2	2	103.2	7.27
189539129	PREDICTED: similar to Ras-related C3 botulinum toxin su	2	2	18.9	8.88
66910271	Actr3 protein [Danio rerio]	2	2	45.7	5.78
50540198	ras-related GTP-binding protein RAB10 [Danio rerio]	2	2	22.6	8.37
49227325	ribosomal protein S15 [Danio rerio]	2	2	17.0	10.39
41053331	ribosomal protein L30 [Danio rerio]	2	2	13.0	9.63
27545279	nascent polypeptide-associated complex alpha subunit [I	2	2	23.4	4.56
226958509	40S ribosomal protein S27-like [Danio rerio]	2	2	9.5	9.52
115528116	Protein kinase, cAMP-dependent, regulatory, type II, alpi	2	2	44.7	4.82
47087453	eukaryotic translation initiation factor 3, subunit C [Danio	2	2	106.3	5.62
27545275	ribosomal protein L36A [Danio rerio]	2	2	12.5	10.54
91176292	hypothetical protein LOC677748 [Danio rerio]	2	2	15.8	11.47
55925442	3-oxoacid CoA transferase 1a [Danio rerio]	1	2	57.2	8.25
205831554	RecName: Full=Succinate dehydrogenase [ubiquinone] f	2	2	72.0	6.60
125840569	PREDICTED: similar to synaptic vesicle glycoprotein 2 a	2	2	83.4	6.04
171222380	plasma membrane calcium ATPase 4 [Danio rerio]	2	2	129.7	5.78
52219010	EH-domain containing 1 [Danio rerio]	2	2	60.0	6.38
40555832	Hdac1 protein [Danio rerio]	2	2	51.9	5.59
53749653	pyruvate dehydrogenase E1 alpha 1 [Danio rerio]	2	2	43.7	7.96
66472750	dihydropyrimidinase-like 3 [Danio rerio]	2	2	61.5	6.44
220678632	novel protein similar to vertebrate asparaginyl-tRNA synt	2	2	63.8	6.13
159570628	calreticulin, like 2 [Danio rerio]	2	2	48.9	4.51

41053367	coactosin-like 1 [Danio rerio]	2	2	15.9	5.40
149773502	hypothetical protein LOC795095 [Danio rerio]	2	2	19.2	5.19
45768686	Purb protein [Danio rerio]	2	2	32.5	5.67
41053814	transmembrane protein 38A [Danio rerio]	2	2	32.9	8.35
57222259	talin 1 [Danio rerio]	2	2	270.5	6.20
18858919	junction plakoglobin [Danio rerio]	2	2	80.0	6.33
189520462	PREDICTED: similar to glucose transporter 1A [Danio rerio]	2	2	50.3	8.21
54261753	fibrillarlin [Danio rerio]	2	2	33.6	10.20
50344982	hypothetical protein LOC415253 [Danio rerio]	2	2	13.6	8.60
49903114	Syntaxin1b protein [Danio rerio]	2	2	25.7	5.14
51010945	zgc:92726 [Danio rerio]	2	2	29.2	6.68
47085923	pyruvate dehydrogenase (lipoamide) beta [Danio rerio]	2	2	39.3	6.11
33089399	embryonic globin beta e3 [Danio rerio]	2	2	16.1	8.46
50540540	small nuclear ribonucleoprotein polypeptides B and B1 [Danio rerio]	2	2	24.4	11.19
189517050	PREDICTED: glycine C-acetyltransferase [Danio rerio]	2	2	49.6	8.18
189527563	PREDICTED: similar to mitogen-activated protein kinase [Danio rerio]	2	2	43.6	6.70
148725418	caspase b [Danio rerio]	2	2	46.0	6.29
108742052	Pdia4 protein [Danio rerio]	2	2	72.4	5.21
239048085	SMT3 suppressor of mif two 3 homolog 3 [Danio rerio]	2	2	10.7	5.50
50540060	ubiquinol-cytochrome c reductase, complex III subunit V [Danio rerio]	2	2	9.6	9.44
158517994	pancreatic carboxypeptidase B1 [Danio rerio]	2	2	29.8	6.86
47085959	RCC1-like [Danio rerio]	2	2	54.1	8.34
37595360	WD repeat domain 1 [Danio rerio]	2	2	66.4	7.09
161612168	Dmgdh protein [Danio rerio]	2	2	97.4	7.01
125828761	PREDICTED: similar to zinc finger protein 9 [Danio rerio]	2	2	13.7	8.48
47085687	heterogeneous nuclear ribonucleoprotein K [Danio rerio]	2	2	46.4	8.06
113674446	hypothetical protein LOC692317 [Danio rerio]	2	2	91.5	5.38
66773084	gamma crystallin-like [Danio rerio]	2	2	21.2	7.97
47086023	A kinase (PRKA) anchor protein 8-like [Danio rerio]	2	2	69.4	6.07
123230120	eukaryotic translation initiation factor 3, subunit 7 zeta [Danio rerio]	2	2	63.9	6.43
189515541	PREDICTED: desmoplakin a [Danio rerio]	2	2	273.2	6.84
18859307	ras-related nuclear protein [Danio rerio]	2	2	24.4	7.09
41054972	ribosomal protein SA [Danio rerio]	2	2	34.0	4.84
68372438	PREDICTED: similar to es1 protein [Danio rerio]	2	2	24.1	7.24
52218988	calpain 3 [Danio rerio]	2	2	83.8	5.45
32766415	Sept2 protein [Danio rerio]	2	2	38.9	6.86
161611562	Aprt protein [Danio rerio]	2	2	19.3	7.91
39752649	kelch repeat and BTB (POZ) domain containing 10 [Danio rerio]	2	2	68.6	5.19
32308153	annexin A2a [Danio rerio]	2	2	38.1	7.71
134133294	aldehyde dehydrogenase 18 family, member A1 [Danio rerio]	2	2	85.3	7.08
28277505	Retinoblastoma binding protein 4 [Danio rerio]	2	2	47.5	4.83
220678866	calpain 2, (m/II) large subunit a [Danio rerio]	2	2	67.4	5.02
5833459	proteasome subunit beta 5 [Danio rerio]	2	2	28.0	6.40
48762654	cystathionase (cystathionine gamma-lyase) [Danio rerio]	2	2	43.8	7.03
47550713	Obg-like ATPase 1 [Danio rerio]	2	2	44.9	7.74
148726383	5'-3' exoribonuclease 2 [Danio rerio]	2	2	109.2	7.25
147905490	hypothetical protein LOC100037379 [Danio rerio]	2	2	11.8	10.33
71480064	U2 small nuclear RNA auxiliary factor 2a [Danio rerio]	2	2	52.3	8.82
55742246	glioblastoma amplified sequence [Danio rerio]	2	2	33.6	9.11
9857942	chaperonin 10 [Danio rerio]	2	2	9.9	8.10
45786121	Taldo1 protein [Danio rerio]	2	2	37.9	6.44
126632812	novel protein (zgc:55818) [Danio rerio]	2	2	106.5	5.29
45709024	Pdlim7 protein [Danio rerio]	2	2	23.4	7.50
50539816	ferritin heavy chain [Danio rerio]	2	2	20.3	5.45
71834518	zgc:114044 [Danio rerio]	2	2	28.4	5.06
56693257	N-myc downstream-regulated gene 2 [Danio rerio]	2	2	40.4	5.66

182891892	Fah protein [Danio rerio]	2	2	38.8	6.74
189517072	PREDICTED: ubiquitin specific peptidase 7 (herpes virus-	2	2	129.2	5.64
94733942	novel protein similar to vertebrate myelin expression fac	2	2	55.8	8.13
62955689	complement component 1, q subcomponent binding pro	2	2	30.0	4.78
56790262	superoxide dismutase 1, soluble [Danio rerio]	2	2	15.9	6.61
41387146	peroxiredoxin 6 [Danio rerio]	2	2	25.0	6.57
45501264	Hexokinase 1 [Danio rerio]	2	2	102.7	6.35
62531021	Try protein [Danio rerio]	2	2	26.5	7.49
166157561	F-box only protein 2 [Danio rerio]	2	2	20.0	4.44
44917595	alcohol dehydrogenase 8b [Danio rerio]	2	2	40.8	7.62
41054643	eukaryotic translation initiation factor 2, subunit 1 alpha	2	2	36.2	5.03
47085885	fructose-1,6-bisphosphatase 1b [Danio rerio]	2	2	36.8	7.30
47086523	ictacalcin [Danio rerio]	2	2	10.4	5.21
47086169	acyl-CoA dehydrogenase-like [Danio rerio]	2	2	47.8	8.51
68448530	vitellogenin 5 [Danio rerio]	2	2	148.9	8.60
41055247	protein arginine methyltransferase 1 [Danio rerio]	2	2	39.3	5.72
56090174	visinin-like 1 [Danio rerio]	2	2	22.2	5.05
61806580	Tu translation elongation factor, mitochondrial [Danio rer	2	2	49.2	6.92
37606175	novel protein similar to vertebrate synaptophysin (SYP) [2	2	32.1	5.14
51011113	hydroxyacyl-Coenzyme A dehydrogenase [Danio rerio]	2	2	33.3	8.59
170784871	wu:fk52f12 [Danio rerio]	2	2	24.5	6.80
148226835	nucleosome assembly protein 1-like 4a [Danio rerio]	2	2	40.2	4.72
41151992	nucleosome assembly protein 1, like 1 [Danio rerio]	2	2	44.4	4.50
41152406	FK506 binding protein 1A, 12kDa [Danio rerio]	2	2	11.7	7.99
50540382	ubiquinol-cytochrome c reductase core protein II [Danio	2	2	49.1	7.53
47087003	ras homolog gene family, member Ac [Danio rerio]	2	2	21.8	6.10
47086597	aldehyde dehydrogenase 7 family, member A1 [Danio rer	2	2	55.6	6.32
148726015	novel protein (zgc:101083) [Danio rerio]	2	2	36.8	6.57
41054081	methionine adenosyltransferase I, alpha [Danio rerio]	2	2	43.3	6.80
50344930	hypothetical protein LOC415227 [Danio rerio]	2	2	18.2	4.56
47271384	cofilin 2, like [Danio rerio]	2	2	18.8	7.33
28279681	High-mobility group box 1 [Danio rerio]	2	2	23.7	6.23
47087055	protein phosphatase 2 (formerly 2A), regulatory subunit	2	2	53.1	4.96
193788711	proteasome beta 3 subunit [Danio rerio]	2	2	23.1	5.47
116284149	Zgc:123103 [Danio rerio]	2	2	35.9	5.88
189519911	PREDICTED: hypothetical protein LOC337820 [Danio rer	2	2	33.8	9.07
50370310	Zgc:112160 protein [Danio rerio]	2	2	28.1	5.91
237681177	malic enzyme 2, NAD(+)-dependent, mitochondrial [Dar	2	2	64.9	7.02
161611630	Wu:fd12d03 protein [Danio rerio]	2	2	121.8	7.46
94732607	novel protein similar to vertebrate proteasome (prosome	2	2	23.9	9.63

APPENDIX E

Publications

Noncanonical Amino Acid Labeling in Vivo to Visualize and Affinity Purify Newly Synthesized Proteins in Larval Zebrafish

Flora I. Hinz,^{†,‡} Daniela C. Dieterich,[§] David A. Tirrell,^{||} and Erin M. Schuman^{*,†,‡}

[†]Division of Biology, California Institute of Technology, Pasadena, California 91125, United States

[‡]Max Planck Institute for Brain Research, D-60528 Frankfurt am Main, Germany

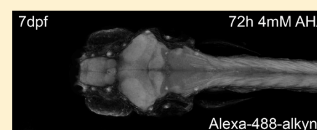
[§]Emmy Noether Research Group Neuralomics, Leibniz Institute for Neurobiology, D-39118 Magdeburg, Germany

^{||}Division of Chemistry and Chemical Engineering, California Institute of Technology, Pasadena, California 91125, United States

Supporting Information

ABSTRACT: Protein expression in the nervous system undergoes regulated changes in response to changes in behavioral states, in particular long-term memory formation. Recently, methods have been developed (BONCAT and FUNCAT), which introduce noncanonical amino acids bearing small bio-orthogonal functional groups into proteins using the cells' own translational machinery. Using the selective "click reaction", this allows for the identification and visualization of newly synthesized proteins in vitro. Here we demonstrate that noncanonical amino acid labeling can be achieved in vivo in an intact organism capable of simple learning behavior, the larval zebrafish. We show that azidohomoalanine is metabolically incorporated into newly synthesized proteins, in a time- and concentration-dependent manner, but has no apparent toxic effect and does not influence simple behaviors such as spontaneous swimming and escape responses. This enables fluorescent labeling of newly synthesized proteins in whole mount larval zebrafish. Furthermore, stimulation with a GABA antagonist that elicits seizures in the larval zebrafish causes an increase in protein synthesis throughout the proteome, which can also be visualized in intact larvae.

KEYWORDS: Protein synthesis, larval zebrafish, noncanonical amino acid tagging, click chemistry, pentyltetrazol



Both chemical stimuli and changes in behavioral states alter protein expression in the nervous system. In particular, studies in many different model organisms have shown that protein synthesis, during or shortly after learning, is an essential step in the formation of long-term memory.¹ In 1964, Agranoff and co-workers showed that the protein synthesis inhibitor (PSI) puromycin injected intracranially into the goldfish produces impairment of memory for a shock avoidance task and that this impairment is time- and PSI concentration-dependent.^{2,3} Since then, protein synthesis has been shown to be necessary for long-term memory formation in a variety of learning paradigms, including appetitively and shock-motivated discrimination learning, passive and active avoidance learning, shuttle box learning, and long-term habituation [reviewed in ref 1].

While it is now clear that long-term memory requires new protein synthesis, the identification of newly synthesized proteins has been sparse and limited to individually identified candidate proteins. Advances in mass spectrometry based approaches now permit the characterization and quantification of proteins, especially when paired with approaches such as stable isotope labeling with amino acids in cell culture (SILAC),⁴ which allow for comparative quantification between proteomes of differentially stimulated cell populations. However, the proteome of the nervous system is complex and without a chemical handle to enable affinity purification of the newly synthesized proteins specifically, proteins of low abundance will likely be missed.

In addition, the identification of cells or neural circuits that show increased protein synthesis in response to memory

formation would allow us to understand the components of memory circuits that undergo long-term modifications after learning. Genetically encoded fluorescent tags, such as GFP, have revolutionized cell biology by permitting visualization of fusion proteins of interest in vivo.⁵ However, the size of GFP and the requirement for genetic manipulation of the target protein may interfere with its endogenous function, while at the same time only permitting investigation of a small number of candidates at once.

Recently, new techniques for labeling a variety of molecules based on the principle of bio-orthogonal metabolic labeling have been developed.⁶ Here, small functional groups that are commonly absent in the cellular environment, most prominently ketones and azides or alkynes, are introduced using the cells' own synthetic machinery. Using this approach, sugars,⁷ lipids,⁸ virus particles,⁹ DNA, and RNA¹⁰ have been labeled and subsequently visualized using fluorescent dyes or enriched and identified using affinity reagents. Bertozzi and co-workers, in particular, have demonstrated in vivo labeling of glycans in living organisms ranging from rodents^{11,12} to larval zebrafish^{13–15} and *C. elegans*.¹⁶

Using a similar approach, bio-orthogonal noncanonical amino acid tagging (BONCAT)^{17,18} and fluorescent non-canonical amino acid tagging (FUNCAT)¹⁹ have been used to

Received: September 21, 2011

Accepted: November 7, 2011

Published: November 7, 2011

tag and identify or visualize newly synthesized proteins. BONCAT and FUNCAT utilize noncanonical methionine derivatives, such as the azide-bearing azidohomoalanine (AHA), to bio-orthogonally label newly synthesized proteins. AHA can cross cell membranes and be charged onto methionine tRNAs by the endogenous methionyl-tRNA synthetase (MetRS). During protein synthesis, AHA is introduced in place of methionine, resulting in the introduction of azide groups into the newly synthesized proteins. These azide groups can be used to tag proteins with either an alkyne affinity tag (BONCAT) or an alkyne fluorescent tag (FUNCAT) via selective Cu(I)-catalyzed or strain-promoted [3 + 2] azide-alkyne cycloaddition.^{20–22} Affinity tagged proteins can be quantified using immunoblot analysis or separated from the preexisting proteome by affinity purification and identified by tandem mass spectrometry. Fluorescent tags can be used to visualize newly synthesized proteins, including those proteins of interest whose identities may not be known. Alternatively, the alkyne moiety may also be introduced into newly synthesized proteins by replacing methionine with the noncanonical amino acid homopropargylglycine (HPG) and subsequently labeled using azide bearing affinity or fluorescent tags. Azides and alkynes are small, so light labeling with AHA or HPG is likely to only cause modest, perhaps even insignificant, perturbations of protein folding, localization,¹⁷ and therefore function of the labeled protein *in vivo*. Furthermore, azides and alkynes are stable under biological conditions and essentially absent from vertebrate cells, which makes the azide-alkyne ligation (“click chemistry”) very selective.

BONCAT and FUNCAT techniques have already successfully been applied to study the proteome of HEK293 cells during a 2 h time window,¹⁷ as well as investigate local protein synthesis in dissociated hippocampal cultures.¹⁹ Furthermore, metabolic AHA incorporation has been used to identify regions of the *Drosophila* genome that show high levels of histone turnover,²³ show that *Chlamydia* co-opt the functions of the lysosomes of their host cells to acquire essential amino acids,²⁴ as well as demonstrate that treatment of primary sensory

neurons with the cytokine interleukin-6 or the neurotrophin nerve growth factor (NGF) increases nascent protein synthesis in axons.²⁵ Recently, these techniques have also been used to indicate that the transmembrane receptor DCC may regulate protein synthesis in a localized manner within the cells as DCC was found to overlap with areas of new protein synthesis at the tips of filopodia in commissural neurons.²⁶ However, these studies have only used the techniques *in vitro*. Given the role of protein synthesis in learning and memory, developing BONCAT and FUNCAT for use in an intact organism in which simple forms of learning may be investigated is the essential next step.

In this study, we describe the application of these techniques *in vivo*, in the 7-day-old larval zebrafish. The larval zebrafish is an excellent model organism as it is a genetically tractable, simple vertebrate, which is transparent and therefore ideal for imaging. Furthermore, zebrafish larvae have a well-defined behavioral repertoire,²⁷ and the range of experimental paradigms to test this has recently been expanded to include associative conditioning.²⁸ Larval zebrafish can absorb small chemical compounds directly from their surrounding medium, all of which make them not only amenable to chemical screens and an emerging human disease model but also an excellent system to study the applicability of bio-orthogonal metabolic labeling of newly synthesized proteins *in vivo*.

Here we show that AHA is metabolically incorporated into newly synthesized proteins, in a time- and concentration-dependent manner, but has no apparent toxic effects and does not influence simple behaviors. This enables fluorescent labeling of newly synthesized proteins in whole mount larval zebrafish. Furthermore, we find that stimulation with the GABA antagonist, pentylenetetrazole (PTZ), causes an increase in protein synthesis throughout the proteome, which can also be visualized in intact larvae.

RESULTS AND DISCUSSION

The BONCAT and FUNCAT protocols were adapted to larval zebrafish (Figure 1a). All larvae, unless otherwise noted, were

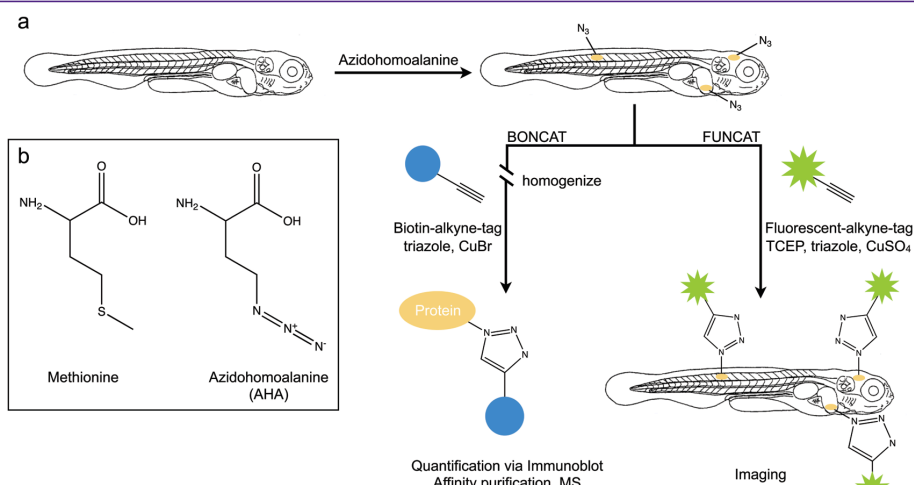


Figure 1. Labeling of newly synthesized proteins for identification (BONCAT) and visualization (FUNCAT) in larval zebrafish. (a) Scheme depicting metabolic labeling of newly synthesized proteins in 7-day-old larval zebrafish using AHA incorporation and Cu(I)-catalyzed [3 + 2] azide-alkyne cycloaddition. TCEP, tris(2-carboxyethyl)phosphine. (b) Chemical structures of methionine and azidohomoalanine (AHA).

analyzed at 7dpf. We incubated larvae in E3 embryo medium supplemented with the methionine surrogate AHA (Figure 1b) for a period of 0–72 h immediately prior to harvesting, with the aim of incorporating the azide group into newly synthesized proteins throughout the zebrafish proteome. To quantify successful incorporation of AHA into protein, larvae were washed, anesthetized, and homogenized and the resulting lysate was reacted with biotin-alkyne in the presence of CuBr and the triazole ligand (see Methods). This allowed for detection and quantification of newly synthesized biotin-labeled proteins using immunoblot analysis or for affinity purification of the newly synthesized proteins (BONCAT). To visualize newly synthesized proteins following AHA exposure, larvae were washed, anesthetized, fixed, and permeabilized. Whole mounted larval zebrafish were reacted with AlexaFluor-488-alkyne in the presence of CuSO₄, the reducing agent tris(2-carboxyethyl)-phosphine (TCEP), and the triazole ligand, before imaging using a confocal microscope (FUNCAT). This allowed for visualization of new protein synthesis, in the intact larval zebrafish.

Previously, Dieterich et al. showed that metabolic labeling of mammalian cell culture with AHA does not alter global protein synthesis rates or promote ubiquitin-mediated degradation, indicating that AHA incorporation does not cause severe protein misfolding or degradation.¹⁷ To ensure that incubation and incorporation of AHA into newly synthesized proteins is not toxic for the living animal, larvae were exposed to E3 embryo medium supplemented with 0–20 mM AHA, or 10 mM methionine, for 6–72 h. Larvae were scored as healthy, if after incubation they were still responsive to light touch. No significant toxic effects were observed when larvae were incubated with 1–10 mM AHA, even after 72 h incubations (Figure 2a). Only incubations with extremely high (20 mM) concentrations of AHA were toxic beginning around 24 h after onset of incubation. This indicates that incubation with low to moderate concentrations of AHA, even over extended periods of time is not toxic to the living animal. In the remainder of the studies reported here, concentrations of ≤ 4 mM AHA were used.

Next, we explored whether incorporation of AHA causes changes in simple behaviors. We conducted a series of behavioral tests after incubation in E3 medium supplemented with 4 mM AHA, for 0–48 h. First we investigated spontaneous swimming behavior. 7-day-old larval zebrafish were incubated in 4 mM AHA for 0–48 h prior to observation, and then placed individually into a 1 cm by 7.5 cm swimming chamber (Supporting Information Figure S1) and their spontaneous swimming bouts were recorded for a period of 15 min. Sample traces of spontaneous swimming behavior are depicted in Supporting Information Figure S1. There was no significant difference in the number of individual spontaneous swimming bouts initiated between 48 h AHA incubated, 24 h AHA incubated and control larvae, although there was a small, not significant decrease in the 48 h and 24 h AHA groups as compared to the control group (Figure 2b). There was also no difference in the number of AHA incubated and control larvae that failed to exhibit spontaneous swimming bouts during the 15-min trial period (Figure 2b).

To study whether AHA incubation causes deficits in visual tracking, 7-day-old larvae were tested for the optokinetic response²⁹ after incubation in 4 mM AHA for 24–48 h. Larvae were immobilized in 0.4% low-melting point agarose in a circular array of LEDs, which delivered a spot of white light that

moved in a horizontal plane around the immobilized larvae. Similar to control larvae, AHA incubated larvae were able to track the light stimulus, producing smooth tracking eye movements and rapid saccades (Figure 2c, Supporting Information video), indicating that neither visual acuity nor neural circuits underlying visual tracking behavior seem to be affected by prolonged incubation with 4 mM AHA. To further test whether AHA incubation altered visual acuity and simple reflexive behaviors, we tested the animal's startle response to light flash and dark flash. Larvae were placed in a circular array of LEDs, which delivered either a light flash or a dark flash while the response of the larva was monitored. Figure 2d shows a representative startle response to a light flash in an animal following a 24 h incubation with 4 mM AHA. The larva is clearly exhibiting a stereotypical C-bend escape response,³⁰ indicating that AHA has no effect on the motor function associated with escape behavior. Furthermore, incubation with 4 mM AHA for 24–48 h did not alter the percentage of larval zebrafish that responded to either light or dark flash (Figure 2e) nor did it affect the delay in response to either light or dark flash (Figure 2f). Therefore, we conclude that AHA incorporation is not toxic and has no effects on simple behaviors at low concentrations (4 mM), even over prolonged incubation periods, making it suitable for labeling newly synthesized proteins *in vivo*.

To determine whether AHA is metabolically incorporated into newly synthesized proteins, we tagged lysates prepared from larval zebrafish incubated for 0–72 h with 4 mM AHA with biotin-alkyne in the presence of the Cu(I) catalyst. Subsequent dot blot analysis with a biotin antibody revealed successful incorporation of AHA into proteins in an incubation-time-dependent manner. A sample dot blot is shown in Figure 3a, along with quantification of several experiments. After only a 6 h incubation period with E3 embryo medium supplemented with 4 mM AHA, statistically significant ($p < 0.005$) AHA incorporation could be detected. After 24, 48, and 72 h incubations, approximately 140 ng (± 8 ng), 375 ng (± 34 ng), and 699 ng (± 72 ng) of biotinylated protein were detected per homogenized larva, respectively. The total soluble protein per larva under the experimental conditions we used was 6.38 μg (± 0.53 μg). From this, we can estimate that 24, 48, or 72 h incubation with 4 mM AHA leads to labeling and tagging of approximately 2.2%, 5.9%, and 10.9%, respectively, of the total soluble protein per larval zebrafish. However, as different proteins may show different levels of AHA incorporation, and therefore different biotin signal strength, the analysis given here should be regarded as semiquantitative.

To verify the specificity of AHA incorporation into newly synthesized proteins, we incubated larval zebrafish in E3 embryo medium supplemented with AHA along with low concentrations of the protein synthesis inhibitor puromycin. These very low concentrations of PSI did not have a toxic effect on larval zebrafish (data not shown). Although abundant biotin signal was detected in lysates of larval zebrafish incubated with AHA only, no signal was detected when larval zebrafish were incubated without AHA, and a significantly lower signal was detected when larval zebrafish were incubated in AHA in the presence of puromycin (Figure 3b). Furthermore, when the concentration of PSI in the incubation medium was increased from 2.5 to 5 $\mu\text{g}/\text{mL}$, a significant decrease in AHA labeled and biotinylated proteins was observed. However, no further decrease was observed when the PSI concentration was further increased to 10 $\mu\text{g}/\text{mL}$.

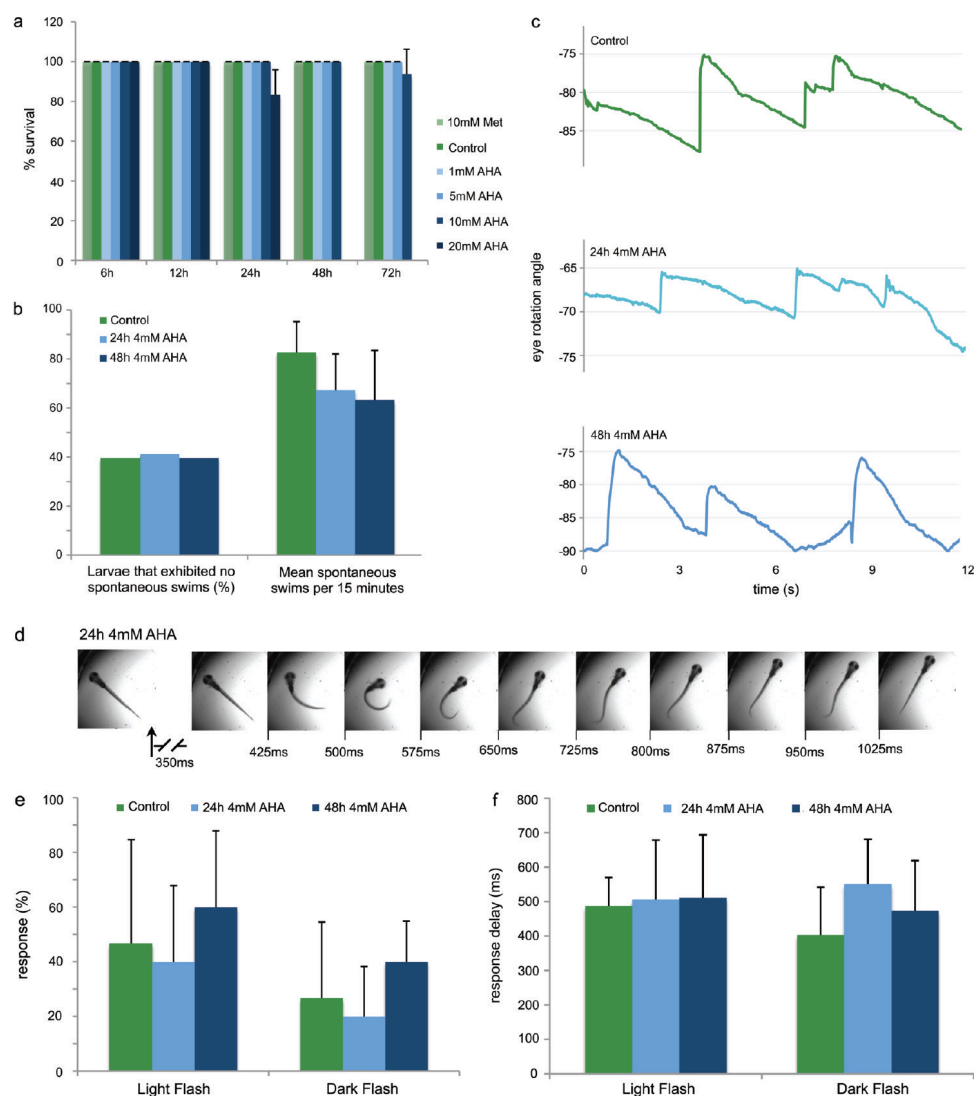


Figure 2. At low concentrations, AHA exposure is not toxic and does not significantly alter simple behaviors. (a) Survival rate of 7-day-old larval zebrafish when incubated with AHA (0–20 mM, 6–72 h) or methionine (10 mM, 6–72 h), $n = 20$. (b) Quantification of spontaneous swimming behavior of larval zebrafish after AHA incubation (4 mM, 0–48 h). Percentage of larvae that show no spontaneous swimming behavior per 15 min interval. Mean swimming bursts per 15 min interval, $n = 10$ –12. Differences are not statistically significant. (c) Traces depicting the angle of eye rotation during a typical optokinetic response after AHA incubation (4 mM, 0–48 h). (d) Sample startle response upon light flash after AHA incubation (4 mM, 24 h). (e) Mean response percentage to light or dark flash after AHA incubation (4 mM, 0–48 h), $n = 5$ larvae, flashed three times each. Error bars represent standard deviation of response percentage. Differences are not statistically significant. (f) Mean delay in response to light or dark flash after AHA incubation (4 mM, 0–48 h), $n = 5$ larvae, flashed three times each. Error bars represent standard deviation of response time. Differences are not statistically significant.

The above results confirm that BONCAT labels newly synthesized proteins with high specificity in the larval zebrafish. In addition, we observed that AHA incorporation in larval zebrafish scales nonlinearly with incubation time (Figure 3a) and we assume that an incorporation plateau would be reached after even longer incubation periods. Also, labeling was AHA concentration-dependent (Supporting Information Figure S2). While no signal was detected when 4-day-old larval zebrafish were incubated with 0 mM AHA,

increasing the concentration of AHA in the incubation medium from 1 to 4 mM resulted in a detectable signal increase. Furthermore, AHA was incorporated not only into a few select proteins, but into a large variety of newly synthesized proteins throughout the proteome over time, as is shown by the abundance of protein bands on the Western blot of affinity purified biotinylated proteins from whole larval zebrafish lysates reacted with the biotin-alkyne and probed against biotin (Supporting Information Figure S3a). Biotin

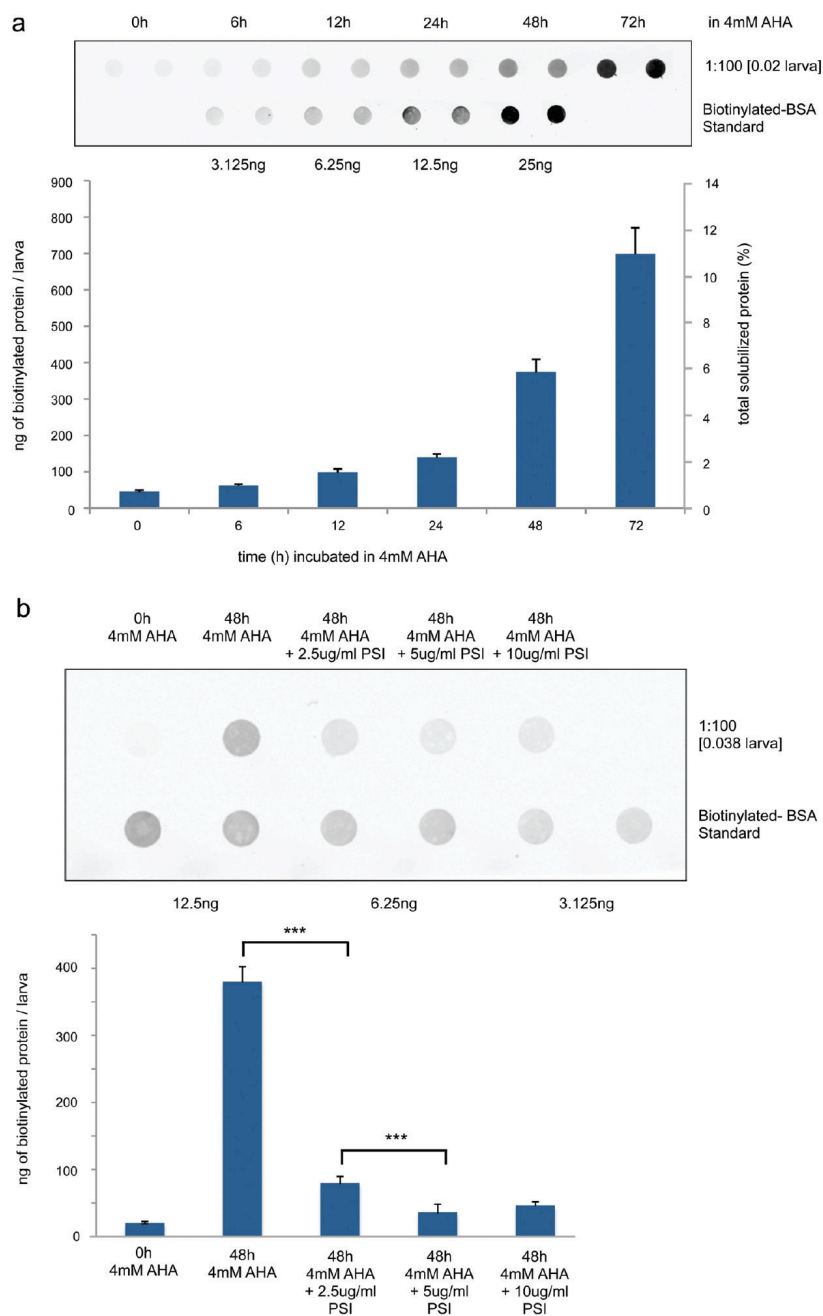


Figure 3. AHA is metabolically incorporated into larval zebrafish proteins in vivo. Sample immunoblot and quantification of immunoblots of lysates from AHA-treated 7-day-old larval zebrafish reacted with biotin-alkyne ($10 \mu\text{M}$) for 12 h, probed with antibody against biotin. (a) Larval zebrafish were incubated with 4 mM AHA for 0–72 h, $n = 4$. (b) Larval zebrafish were incubated with AHA (0 or 4 mM) or 4 mM AHA in the presence of puromycin (2.5–10 $\mu\text{g}/\text{mL}$) for 48 h, $n = 3$. *** $p < 0.001$.

signal detected in the samples not incubated with AHA are likely a result of endogenous biotinylation.

To examine whether AHA is also incorporated into newly synthesized proteins in deeper structures such as the nervous system, we incubated 4-day-old transgenic HuC::GFP larval

zebrafish with 4 mM AHA for 48 h. HuC encodes an RNA-binding protein that serves as an excellent early marker for differentiating neurons and the HuC::GFP line is a stable zebrafish transgenic line in which GFP is expressed specifically in neurons.³¹ With the exception of a few cells in the olfactory

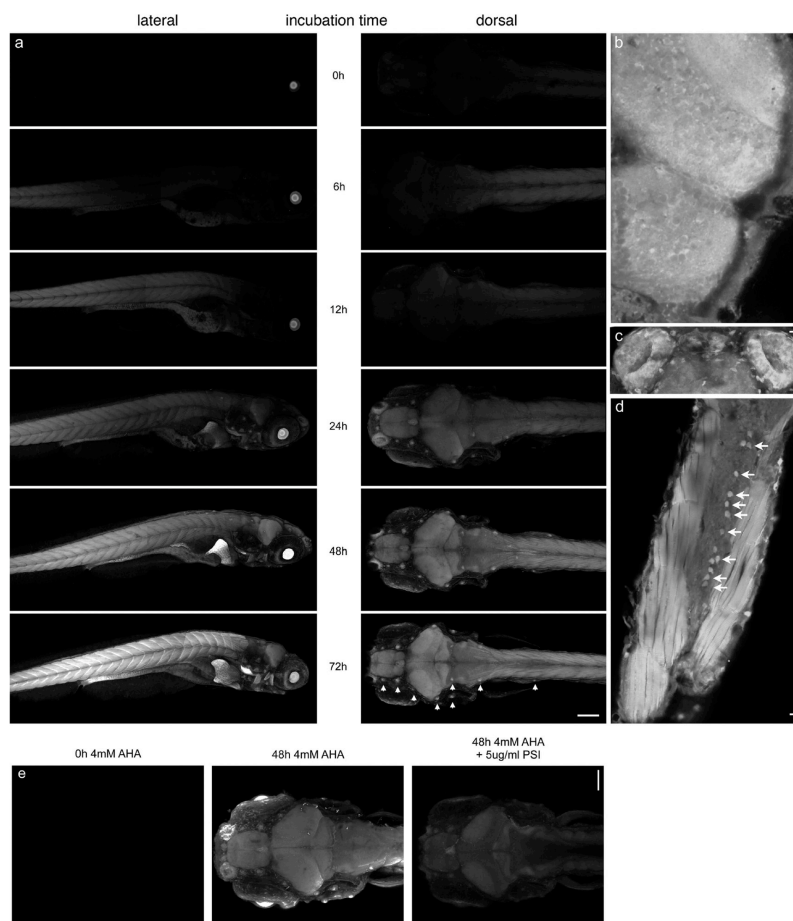


Figure 4. Imaging of newly synthesized proteins after *in vivo* labeling. (a) 7 dpf larval zebrafish were metabolically labeled with 4 mM AHA for 0–72 h prior to fixation and reacted with 5 μ M AlexaFluor-488-alkyne tag for 12 h. Left panel, lateral view; right panel, dorsal view. Arrow heads indicate neuromasts of the lateral line. (b, d, e) 7-day-old larval zebrafish labeled with 4 mM AHA for 48 h imaged at higher magnification. Dorsal views of (b) optic tectum and cerebellum, (c) olfactory pits, (d) horizontal cross-section of tail, showing tail muscles and spinal cord. Arrows indicate potential Rohon-Beard neurons. Scale bar in (a), 150 μ m; in (b, d, e), 20 μ m. (e) Larval zebrafish were metabolically labeled with 4 mM AHA for 0, 48, or 48 h in the presence of 5 μ g/mL puromycin. Dorsal view; scale bar is 100 μ m; $n = 5$.

pit and the lateral line, the majority of these neurons are not surface structures. As before, whole zebrafish lysates were labeled with the biotin-alkyne, affinity purified, and then analyzed using Western blot probed against GFP. Only in the sample that was incubated in 4 mM AHA for 48 h were we able to affinity purify AHA-labeled, biotin-tagged GFP, indicating that AHA is not only incorporated into newly synthesized proteins in surface structures of the larval zebrafish, but also in the nervous system, the sole area of GFP expression in the HuC::GFP transgenic line (Supporting Information Figure 3b).

We next optimized the labeling and reaction conditions to maximize specific visualization of newly synthesized proteins (FUNCAT) in the intact larval zebrafish. For this purpose, we used the mutant zebrafish line *nacre*, which lacks melanophores throughout development³² and thus is relatively transparent and ideal for imaging. Larval zebrafish were, as before, incubated in E3 medium supplemented with 4 mM AHA for 0–72 h. Larvae were anesthetized, fixed, and permeabilized,

before whole mount samples were reacted with 5 μ M AlexaFluor-488-alkyne, in the presence of CuSO_4 , TCEP, and the triazole ligand, at room temperature overnight. After several washes in PBDTT buffer, samples were immobilized in 0.4% agarose and imaged using a confocal microscope.

Incubation of larval zebrafish with 4 mM AHA followed by reaction with Alexa-488-alkyne resulted in an incubation-time dependent fluorescent labeling of newly synthesized proteins throughout the larval zebrafish (Figure 4a). Low fluorescent signals, especially in the muscles of the tail, could be detected after as little as 12 h incubation with AHA. Other structures, including the brain, spinal cord, liver, intestines, and heart, could be readily visualized after 24 h incubation with AHA. Specifically, sensory organs such as the neuromasts of the lateral line (indicated by arrow heads in Figure 4a, 72 h incubation dorsal view panel) and the olfactory pit (Figure 4c) seem to be areas of especially high levels of fluorescence. Furthermore, deeper structures such as the optic tectum,

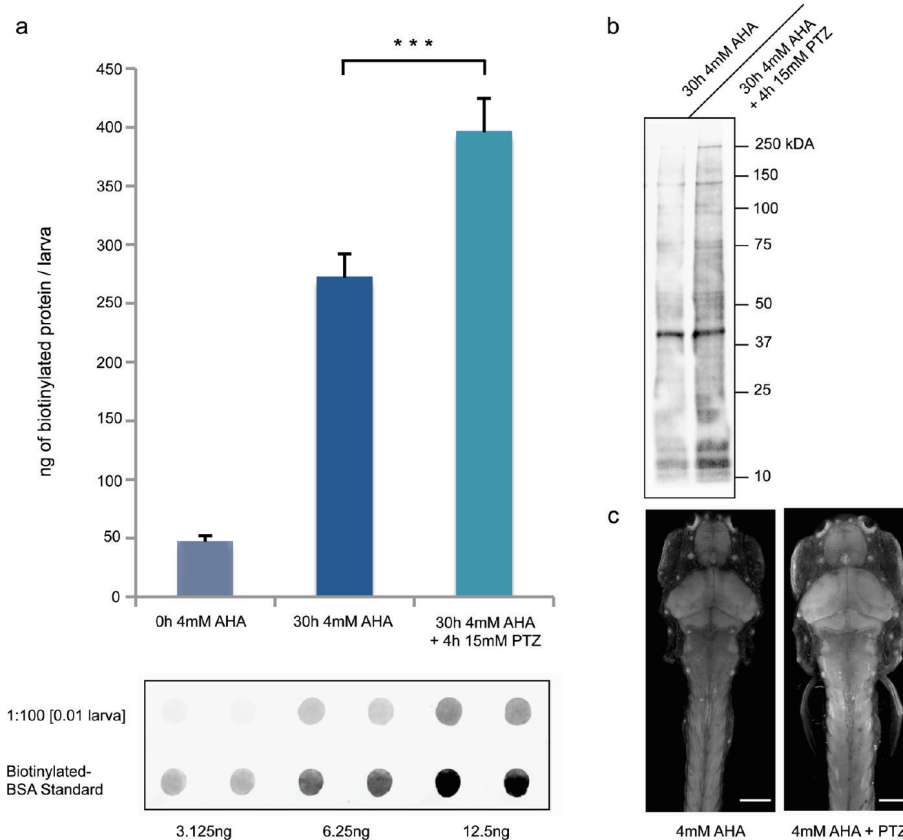


Figure 5. GABA antagonist PTZ induces increased protein synthesis in larval zebrafish. (a) Sample immunoblot and quantification of immunoblots of lysates from 7-day-old larval zebrafish reacted with biotin-alkyne tag ($10 \mu\text{M}$) for 12 h, probed with antibody against biotin. Zebrafish were incubated with 4 mM AHA (0 or 30 h) or with 4 mM AHA for 30 h as well as 15 mM PTZ for two periods of 2 h, 20 and 6 h before harvesting, $n = 3$. $***p < 0.001$. (b) Western blot of biotin affinity-purified lysates of zebrafish incubated with 4 mM AHA for 30 h with or without 4 h 15 mM PTZ exposure. (c) Imaging of 7-day-old larval zebrafish after 48 h 4 mM AHA incubation with or without 4 h 15 mM PTZ exposure, reacted with AlexaFluor-488-alkyne ($5 \mu\text{M}$, 12 h); dorsal view. Scale bar is $150 \mu\text{m}$; $n = 6$.

cerebellum (Figure 4b), and the spinal cord (Figure 4d) are not only readily labeled and tagged using the AlexaFluor-488 alkyne but show differences in fluorescence intensity on the cellular level. In the case of the spinal cord, we believe this population of brightly labeled cells corresponds to Rohon-Beard neurons³³ (Figure 4d, as indicated by arrows). To verify that the fluorescent signal observed in the above experiments represents incorporation of AHA into newly synthesized proteins, larval zebrafish were incubated in E3 medium containing 4 mM AHA in the presence of $5 \mu\text{g}/\text{mL}$ puromycin (Figure 4e). In agreement with previously described results from lysates, abundant fluorescent signal was detected in whole mounts of larval zebrafish incubated with AHA only, while no signal was detected when larval zebrafish were incubated without AHA, and only background signal was detected when larval zebrafish were incubated in AHA in the presence of puromycin. These results suggest that FUNCAT may be used to identify regions of protein synthesis, specific cells, or groups of cells that are metabolically active, during the AHA incubation window in intact larval zebrafish.

To further investigate whether BONCAT and FUNCAT can be used to identify changes in protein synthesis in vivo, larval zebrafish were exposed PTZ, a GABAergic receptor antagonist that induces epileptic-like neuronal discharges and seizure-like behaviors in rodents and zebrafish.^{34–36} It has been shown that exposure to PTZ induces expression of immediate early genes in larval zebrafish³⁴ and leads to changes in postsynaptic GABA receptor expression³⁷ and hilar neurogenesis³⁸ in rodents.

Larval zebrafish were exposed to 15 mM PTZ for two 2 h periods, 24 and 8 h before anesthesia while being incubated in 4 mM AHA for 30 h. The amount of biotinylated protein per larva was detected using dot blot analysis, as previously described. We observed a significant increase in the amount of biotinylated protein in larval zebrafish exposed to PTZ during AHA incubation, as compared to larvae that were not exposed to PTZ (Figure 5a), indicating that PTZ induces an increase in protein synthesis. This increase in biotinylated protein signal is not specific to one or a few protein bands, but it seems to be the result of a general increase of protein synthesis throughout the proteome as detected by Western blot analysis of affinity purified samples (Figure 5b). Furthermore, using the FUNCAT

technique, we were able to visualize an increase in fluorescent signal in the brain and tail muscles in larval zebrafish that had been incubated in 4 mM AHA for 48 h and exposed to 15 mM PTZ for two 2 h periods (Figure 5c). These results indicate that chemical stimulation with the GABAergic receptor antagonist PTZ induces an increase in protein synthesis, which can be quantified and localized using the BONCAT and FUNCAT techniques in larval zebrafish.

In this study we have shown that the BONCAT and FUNCAT techniques, which introduce bio-orthogonal chemical groups into newly synthesized proteins using the endogenous cellular translation machinery, can be applied to live, 7-day-old larval zebrafish. This enables the enrichment and quantification of newly synthesized proteins, when using an affinity tag such as the biotin-alkyne, and the visualization of protein synthesis, when using fluorescent-alkyne tags, such as the AlexaFluor-488-alkyne. Furthermore, we have shown that chemical stimulation with the proconvulsant PTZ increases protein synthesis, which can be detected using the methods developed in this study.

BONCAT and FUNCAT techniques enable labeling of newly synthesized proteins only when methionine is substituted by noncanonical amino acids during translation. However, AHA competes with endogenous methionine for charging onto methionine tRNA by the somewhat promiscuous MetRS. Previous work by the Tirrell group has shown that the charging rate of AHA relative to that of methionine onto methionine tRNA in bacterial cells is 1/390, as indicated by the specificity constant k_{cat}/K_m ,³⁹ suggesting that not all newly synthesized proteins may incorporate AHA in the presence of endogenous methionine. Furthermore, only proteins that contain at least one methionine residue can be labeled. This, however, is not an important factor in zebrafish, as 97.97% of zebrafish proteins contain at least one nonterminal methionine. Only two of 27 014 currently annotated zebrafish proteins contain no methionine at all (NCBI *Danio rerio* protein database, 5.17.2011).

Recent work using bacterial cells has opened the door to increasing the specificity of these techniques. A different noncanonical amino acid, azidonorleucine (ANL), can be used for the BONCAT/FUNCAT reaction.⁴⁰ ANLs' azide bearing side-chain is too bulky to fit into the binding pocket of wild-type MetRS and can therefore not be charged onto methionine tRNA in wild-type cells. However, introducing specific point mutations into the MetRS sequence enables charging of ANL. This permits genetic restriction of the tagging techniques by selective expression of the mutant MetRS in cell populations of interest. We are currently constructing transgenic fish in which the mutant MetRS is placed under the control of a specific promoter. Subsequent incubation with ANL will enable us to observe labeling and downstream identification of newly synthesized proteins in specific cell populations, as oppose to the whole organism.

Recently, the larval zebrafish has become a model organism for small molecule screens, permitting identification of small neuroactive molecules, which alter motor activity⁴¹ or circadian rhythm.⁴² In the future, the FUNCAT and BONCAT techniques can be paired with different chemical stimuli that cause behavioral changes to investigate underlying adjustments of the proteome in distinct regions of the nervous system. Even complex tasks known to be protein synthesis-dependent, such as long-term memory formation, can now be tackled with these techniques to elucidate which neurons and neuronal circuits are affected or involved.

METHODS

Reagents. All chemical reagents were of analytical grade, obtained from Sigma unless otherwise noted, and used without further purification. We prepared AHA as described previously.⁴³ The AlexaFluor-488 alkyne was purchased from Invitrogen (catalog number A10267), while the biotin-alkyne tag was purchased from Jena Biosciences (catalog number TA105).

Zebrafish Stocks and Husbandry. Adult fish strains AB, HuC::GFP and *nacre* were kept at 28 °C on a 14 h light/10 h dark cycle. Embryos were obtained from natural spawnings and were maintained in E3 embryo medium (5 mM NaCl, 0.17 mM KCl, 0.33 mM CaCl₂, 0.33 mM MgSO₄⁴⁴).

Toxicity and Behavioral Tests. To test AHA toxicity, larvae were placed five at a time in a 24-well Falcon culture dish well. Each well contained approximately 2 mL of embryo medium. Medium was replaced with embryo medium supplemented with 0–20 mM AHA or 10 mM methionine at the appropriate time point. Larvae were checked for response to light touch at 7 dpf.

For other behavioral tests, larvae were incubated in 10 mL of embryo medium or embryo medium supplemented with 4 mM AHA for 24–48 h in a 6 cm Petri dish. To monitor spontaneous swimming bouts, larvae were placed individually in a 1 cm by 7.5 cm behavioral chamber and spontaneous swimming was recorded using a webcam for 15 min. Subsequently, swimming bouts were scored. The optokinetic response was measured by immobilizing 7dpf larval zebrafish in a drop of 0.4% low melting point agarose (Promega) in embryo medium. Immobilized larvae were placed in a circular array of LEDs, which delivered a spot of white light that moved in a horizontal plane around the immobilized larvae. The optokinetic response was recorded using a high-speed camera (Redlake MotionScope M3), and eye movements were analyzed using Matlab. The startle response was measured by placing larval zebrafish in 5 cm Petri dish in a circular array of LEDs. LEDs delivered 50 ms light or dark flashes, while a high-speed camera mounted above the arena recorded responses. Response onset was scored.

Copper-Catalyzed [3 + 2] Azide–Alkyne Cycloaddition Chemistry and Detection of Tagged Proteins. Zebrafish larvae were incubated in embryo medium supplemented with AHA after which larvae were washed three times in 25 mL of embryo medium. Larvae were moved into a 1.5 mL Eppendorf tube in ~1 mL of embryo medium and anesthetized on ice for 1 h. Remaining medium was removed, and anesthetized fish were washed once with 1 mL of ice cold PBS + protease inhibitor (PI; Roche, complete ULTRA Tablets, Mini, EDTA-free Protease Inhibitor cocktail tablets). PBS+PI was removed and replaced with 100 μ L of fresh PBS+PI. Zebrafish larvae were homogenized using a Kontes pellet pestle motor. Then 1% SDS and 1 μ L of benzonase (≥ 500 U) were added and the lysate vortexed and heated at 95 °C for 10 min. Lysate was allowed to cool to room temperature, before 400 μ L of PBS+PI and 0.2% triton X-100 were added. Then, lysates were centrifuged at 15 000g at 4 °C for 10 min. Supernatant was transferred to a new 1.5 mL Eppendorf tube. For BONCAT, samples were reacted with 10 μ M biotin-alkyne in the presence of 200 μ M triazole ligand (tris[(1-benzyl-1H-1,2,3-triazol-4-yl)methyl]amine, 97%) and 5 mg/mL CuBr suspension and incubated at 4 °C with agitation overnight. Samples were then centrifuged at 4 °C for 5 min at 5000g to pellet CuBr. Supernatant was moved into a new 1.5 mL Eppendorf tube. To remove excess, unligated biotin-alkyne, samples were applied to a PD MiniTrap G-25 size exclusion column (GE Healthcare). Samples were then analyzed using "dot blots" and affinity purified as described in ref 18. For Western blot analysis of affinity purified samples, 25 μ L of washed NeutrAvidin beads (Thermo Scientific) previously incubated with sample were heated at 95 °C for 5 min in 50 μ L of LDS sample buffer (Invitrogen) containing reducing agent (Invitrogen). Proteins were separated on precast NuPAGE 4–12% Bis-Tris gels (Invitrogen) and transferred to PVDF membranes and blocked in PBST (PBS+0.1% Tween-20) containing 5% milk. For detection, membranes were probed with goat anti-biotin (Biomol) and mouse anti-goat LI-COR-IR 800 secondary antibody and analyzed using the Odyssey Infrared Imaging system (LI-COR).

To image AHA labeled proteins, larval zebrafish were incubated in embryo medium supplemented with AHA, washed, and anesthetized as described above. Remaining embryo medium was removed and replaced with ~1 mL of fixation solution (4% PFA, 88 mM sucrose in PBS). Larvae were fixed at room temperature for 3 h, dehydrated in 100% methanol, and stored at -20°C overnight. Larvae were rehydrated through successive 5 min washes with 75% methanol in PBST, 50% methanol in PBST, 25% methanol in PBST, and finally PBST. This was followed by two washes in PBDTT (PBST + 1% DMSO and 0.5% Triton X-100) and 1 h permeabilization in Protease K (10 $\mu\text{g}/\text{mL}$ in PBST). After permeabilization, larvae were briefly washed with PBST and then immediately postfixed for 20 min. Larvae were washed twice for 5 min with PBST and three times for 5 min with PBDTT, before blocking (5% BSA, 10% goat serum in PBDTT) for at least 3 h at 4°C . Larvae were washed three times in PBST (pH 7.8), before being conjugated to the probe by addition of 200 μM triazole ligand, 5 μM AlexaFluor-488-alkyne, 200 μM CuSO_4 , and 400 μM TCEP at room temperature overnight with gentle agitation. Samples were washed four times for 30 min in PBDTT + 0.5 mM EDTA, and twice for 1 h in PBDTT, before being rinsed in PBST and immobilized on Matek dishes using 0.4% low melting point agarose. Images were obtained using a Zeiss LSM780 laser scanning confocal microscope with 10 \times or 20 \times air lens. AlexaFluor-488 was excited with the 488 nm line of an argon ion laser, and the emitted light was detected between 510 and 550 nm. We performed all postacquisition processing and analysis with ImageJ (NIH). Significance was tested for using the two-tailed *t* test and error bars represent standard deviation.

■ ASSOCIATED CONTENT

● Supporting Information

S1. Tracking spontaneous swimming behavior of 7-day-old larval zebrafish with AHA incubation (4 mM, 0–48 h). 15 min interval; frame captured every 10 s. S2. AHA incorporation is AHA concentration-dependent. Immunoblot of lysates from 4-day-old larval zebrafish reacted with biotin-alkyne (10 μM) for 12 h, probed with an antibody against biotin. Larval zebrafish were incubated with 0–4 mM AHA for 48 h. S3. AHA incorporation occurs throughout the proteome. (a, b) Western blot analysis of biotin affinity purified lysates of zebrafish incubated with 4 mM AHA for 0 to 72 h. (a) Probed with an antibody against biotin. (b) HuC::GFP larval zebrafish lysates probed with an antibody against GFP. Supplementary video. Optokinetic response of 7-day-old larval zebrafish with 48 h 4 mM AHA incubation. This material is available free of charge via the Internet at <http://pubs.acs.org>.

■ AUTHOR INFORMATION

Notes

The authors declare no competing financial interest.

Funding Information

This work was supported by the Max-Planck Society. D.A.T. acknowledges support from NIH (GM62523). F.I.H. acknowledges support from NIH/NRSA Institutional training grant 5T32 GM07616.

■ ACKNOWLEDGMENTS

The authors would like to thank Mark Aizenberg for his help with behavioral tests, Georgi Tushev for his help with calculations of zebrafish proteome methionine content, Jennifer Hodas and John Ngo for general discussions and Stefanie Bunse and Susanne tom Dieck for comments on the manuscript.

■ REFERENCES

- (1) Davis, H. P., and Squire, L. R. (1984) Protein Synthesis and Memory: A Review. *Psychol. Bull.* 96, 518–559.

- (2) Agranoff, B. W., and Klinger, P. D. (1964) Puromycin Effect on Memory Fixation in the Goldfish. *Science* 146, 952–953.
- (3) Agranoff, B. W., Davis, R. E., and Brink, J. J. (1966) Chemical Studies on Memory Fixation in Goldfish. *Brain Res.* 1, 303–309.
- (4) Ong, S. E., Blagoev, B., Kratchmarova, I., Kristensen, D. B., Steen, H., Pandey, A., and Mann, M. (2002) Stable isotope labeling by amino acids in cell culture, SILAC, as a simple and accurate approach to expression proteomics. *Mol. Cell Proteomics* 5, 376–386.
- (5) Tsien, R. Y. (1998) The green fluorescent protein. *Annu. Rev. Biochem.* 67, 509–544.
- (6) Best, M. D. (2009) Click chemistry and bioorthogonal reactions: unprecedented selectivity in the labeling of biological molecules. *Biochemistry* 28, 6571–6584.
- (7) Laughlin, S. T., and Bertozzi, C. R. (2009) Imaging the glycome. *Proc. Natl. Acad. Sci. U.S.A.* 1, 12–7.
- (8) Kho, Y., Kim, S. C., Jiang, C., Barma, D., Kwon, S. W., Cheng, J., Jaunbergs, J., Weinbaum, C., Tamanoi, F., Falck, J., and Zhao, Y. (2004) A tagging-via-substrate technology for detection and proteomics of farnesylated proteins. *Proc. Natl. Acad. Sci. U.S.A.* 34, 12479–12484.
- (9) Bruckman, M. A., Kaur, G., Lee, L. A., Xie, F., Sepulveda, J., Breitenkamp, R., Zhang, X., Joralemon, M., Russel, T. P., Emrick, T., and Wang, Q. (2008) Surface modification of tobacco mosaic virus with “Click” chemistry. *ChemBioChem* 9, 519–523.
- (10) Weisbrod, S. H., and Marx, A. (2008) Novel strategies for the site-specific covalent labeling of nucleic acids. *Chem. Commun.*, 5675–5658.
- (11) Prescher, J. A., Dube, D. H., and Bertozzi, C. R. (2004) Chemical remodeling of cell surfaces in living animals. *Nature* 7002, 873–877.
- (12) Chang, P. V., Prescher, J. A., Sletten, E. M., Baskin, J. M., Miller, L. A., Agard, N. J., Lo, A., and Bertozzi, C. R. (2010) Copper-free click chemistry in living animals. *Proc. Natl. Acad. Sci. U.S.A.* 5, 1821–1826.
- (13) Laughlin, S. T., Baskin, J. M., Amacher, S. L., and Bertozzi, C. R. (2008) In vivo imaging of membrane-associated glycans in developing zebrafish. *Science* 5876, 664–667.
- (14) Baskin, J. M., Dehnert, K. W., Laughlin, S. T., Amacher, S. L., and Bertozzi, C. R. (2010) Visualizing enveloping layer glycans during zebrafish early embryogenesis. *Proc. Natl. Acad. Sci. U.S.A.* 23, 10360–10365.
- (15) Dehnert, K. W., Beahm, B. J., Huynh, T. T., Baskin, J. M., Laughlin, S. T., Wang, W., Wu, P., Amacher, S. L., and Bertozzi, C. R. (2011) Metabolic labeling of fucosylated glycans in developing zebrafish. *ACS Chem Biol.* 6, 547–552.
- (16) Laughlin, S. T., and Bertozzi, C. R. (2009) In vivo imaging of Caenorhabditis elegans glycans. *ACS Chem Biol.* 12, 1068–1072.
- (17) Dieterich, D. C., Link, A. J., Graumann, J., Tirrell, D. A., and Schuman, E. M. (2006) Selective identification of newly synthesized proteins in mammalian cells using bioorthogonal noncanonical amino acid tagging (BONCAT). *Proc. Natl. Acad. Sci. U.S.A.* 103, 9482–9487.
- (18) Dieterich, D. C., Lee, J. J., Link, A. J., Graumann, J., Tirrell, D. A., and Schuman, E. M. (2007) Labeling, detection and identification of newly synthesized proteomes with bioorthogonal non-canonical amino-acid tagging. *Nat. Protoc.* 2, 532–540.
- (19) Dieterich, D. C., Hodas, J. J., Gouzer, G., Shadrin, I. Y., Ngo, J. T., Triller, A., Tirrell, D. A., and Schuman, E. M. (2010) In situ visualization and dynamics of newly synthesized proteins in rat hippocampal neurons. *Nat. Neurosci.* 7, 897–905.
- (20) Rostovtsev, V. V., Green, L. G., Fokin, V. V., and Sharpless, K. B. (2002) A stepwise huisgen cycloaddition process: copper(I)-catalyzed regioselective “ligation” of azides and terminal alkynes. *Angew. Chem.* 14, 2596–2599.
- (21) Tornøe, C. W., Christensen, C., and Meldal, M. (2002) Peptidotriazoles on solid phase: [1,2,3]-triazoles by regioselective copper(I)-catalyzed 1,3-dipolar cycloadditions of terminal alkynes to azides. *J. Org. Chem.* 9, 3057–3064.
- (22) Agard, N. J., Prescher, J. A., and Bertozzi, C. R. (2004) A strain-promoted [3 + 2] azide-alkyne cycloaddition for covalent modification of biomolecules in living systems. *J. Am. Chem. Soc.* 126, 15046–15047.

- (23) Deal, R. B., Henikoff, J. G., and Henikoff, S. (2010) Genome-wide kinetics of nucleosome turnover determined by metabolic labeling of histones. *Science* 5982, 1161–1164.
- (24) Ouellette, S. P., Dorsey, F. C., Moshiah, S., Cleveland, J. L., and Carabeo, R. A. (2011) Chlamydia species-dependent differences in the growth requirement for lysosomes. *PLoS One* 3, 16783.
- (25) Melemedjian, O. K., Asiedu, M. N., Tillu, D. V., Peebles, K. A., Yan, J., Ertz, N., Dussor, G. O., and Price, T. J. (2010) IL-6- and NGF-induced rapid control of protein synthesis and nociceptive plasticity via convergent signaling to the eIF4F complex. *J. Neurosci.* 45, 15113–15123.
- (26) Tcherkezian, J., Brittis, P. A., Thomas, F., Roux, P. P., and Flanagan, J. G. (2010) Transmembrane receptor DCC associates with protein synthesis machinery and regulates translation. *Cell* 4, 632–644.
- (27) Tierney, K. B. (2011) Behavioural assessments of neurotoxic effects and neurodegeneration in zebrafish. *Biochim. Biophys. Acta* 3, 381–389.
- (28) Aizenberg, M., and Schuman, E. M. (2011) Cerebellar-dependent learning in larval zebrafish. *J. Neurosci.* 24, 8708–8712.
- (29) Huang, Y. Y., and Neuhauss, S. C. (2008) The optokinetic response in zebrafish and its applications. *Front Biosci.* 13, 1899–1916.
- (30) Kimmel, C. B., Patterson, J., and Kimmel, R. O. (1974) The development and behavioral characteristics of the startle response in the zebra fish. *Dev. Psychobiol.* 1, 47–60.
- (31) Park, H. C., Kim, C. H., Bae, Y. K., Yeo, S. Y., Kim, S. H., Hong, S. K., Shin, J., Yoo, K. W., Hibi, M., Hirano, T., Miki, N., Chitnis, A. B., and Huh, T. L. (2000) Analysis of upstream elements in the HuC promoter leads to the establishment of transgenic zebrafish with fluorescent neurons. *Dev. Biol.* 2, 279–293.
- (32) Clarke, J. D., Hayes, B. P., Hunt, S. P., and Roberts, A. (1984) Sensory physiology, anatomy and immunohistochemistry of Rohon-Beard neurones in embryos of *Xenopus laevis*. *J. Physiol.* 348, 511–525.
- (33) Lister, J. A., Robertson, C. P., Lepage, T., Johnson, S. L., and Raible, D. W. (1999) *nacre* encodes a zebrafish microphthalmia-related protein that regulates neural-crest-derived pigment cell fate. *Development* 17, 3757–3767.
- (34) Baraban, S. C., Taylor, M. R., Castro, P. A., and Baier, H. (2005) Pentylentetrazole induced changes in zebrafish behavior, neural activity and *c-fos* expression. *Neuroscience* 3, 759–768.
- (35) Baraban, S. C., Dinday, M. T., Castro, P. A., Chege, S., Guyenet, S., and Taylor, M. R. (2007) A large-scale mutagenesis screen to identify seizure-resistant zebrafish. *Epilepsia* 6, 1151–1157.
- (36) Naumann, E. A., Kampff, A. R., Prober, D. A., Schier, A. F., and Engert, F. (2010) Monitoring neural activity with bioluminescence during natural behavior. *Nat. Neurosci.* 4, 513–520.
- (37) Brooks-Kayal, A. R., Shumate, M. D., Jin, H., Rikhter, T. Y., and Coulter, D. A. (1998) Selective changes in single cell GABA(A) receptor subunit expression and function in temporal lobe epilepsy. *Nat. Med.* 10, 1166–1172.
- (38) Parent, J. M., Yu, T. W., Leibowitz, R. T., Geschwind, D. H., Sloviter, R. S., and Lowenstein, D. H. (1997) Dentate granule cell neurogenesis is increased by seizures and contributes to aberrant network reorganization in the adult rat hippocampus. *J. Neurosci.* 10, 3727–3738.
- (39) Küick, K. L., Saxon, E., Tirrell, D. A., and Bertozzi, C. R. (2002) Incorporation of azides into recombinant proteins for chemoselective modification by the Staudinger ligation. *Proc. Natl. Acad. Sci. U.S.A.* 1, 19–24.
- (40) Ngo, J. T., Champion, J. A., Mahdavi, A., Tanrikulu, I. C., Beatty, K. E., Connor, R. E., Yoo, T. H., Dieterich, D. C., Schuman, E. M., and Tirrell, D. A. (2009) Cell-selective metabolic labeling of proteins. *Nat. Chem. Biol.* 10, 715–717.
- (41) Kokel, D., Bryan, J., Laggner, C., White, R., Cheung, C. Y., Mateus, R., Healey, D., Kim, S., Werdich, A. A., Haggarty, S. J., Macrae, C. A., Shoichet, B., and Peterson, R. T. (2010) Rapid behavior-based identification of neuroactive small molecules in the zebrafish. *Nat. Chem. Biol.* 3, 231–237.
- (42) Rihel, J., Prober, D. A., Arvanites, A., Lam, K., Zimmerman, S., Jang, S., Haggarty, S. J., Kokel, D., Rubin, L. L., Peterson, R. T., and Schier, A. F. (2010) Zebrafish behavioral profiling links drugs to biological targets and rest/wake regulation. *Science* 5963, 348–351.
- (43) Link, J. A., Vink, M. K. S., and Tirrell, D. A. (2007) Preparation of the functionalizable methionine surrogate azidohomoalanine via copper-catalyzed diazo transfer. *Nat. Protoc.* 8, 1879–1883.
- (44) Brand, M., Granato, M., and Nüsslein-Volhard, C. (2002) Keeping and Raising Zebrafish, in *Zebrafish. A Practical Approach* (Nüsslein-Volhard, C. and Dahm, R., Eds.), Oxford University Press, Oxford.



Metabolic Labeling with Non-canonical Amino Acids and Visualization by Chemoselective Fluorescent Tagging

Journal:	<i>Current Protocols</i>
Manuscript ID:	Draft
Wiley - Manuscript type:	Protocol
Date Submitted by the Author:	n/a
Complete List of Authors:	tom Dieck, Susanne; MPI Brain Research, Synaptic Plasticity Mueller, Anke; LIN, Research Group Neuralomics; OvG University, Institute for Pharmacology and Toxicology Nehring, Anne; MPI Brain Research, Synaptic Plasticity Hinz, Flora; MPI Brain Research, Synaptic Plasticity Bartnik, Ina; MPI Brain Research, Synaptic Plasticity Schuman, Erin Dieterich, Daniela; LIN, Research Group Neuralomics; OvG University, Institute for Pharmacology and Toxicology
Keywords:	FUNCAT, click chemistry, copper(I)-catalyzed [3+2]azide-alkyne cycloaddition, AHA, HPG, protein synthesis
Abstract:	Fluorescent labeling of proteins by genetically encoded fluorescent protein tags has enabled an enhanced understanding of cell biological processes but is restricted to the analysis of a limited number of identified proteins. This approach does not permit, for example, the unbiased visualization of a full proteome in situ. We describe here a fluorescence-based method to follow proteome-wide patterns of newly synthesized proteins in cultured cells, tissue slices and a whole organism. This technique is compatible with immunohistochemistry and in situ hybridization. Key to this method is the introduction of a small bio-orthogonal reactive group by metabolic labeling. This is accomplished by replacing the amino acid methionine by the azide-bearing methionine surrogate azidohomoalanine (AHA) in a step very similar to classical radioisotope labeling. Subsequently an alkyne-bearing fluorophore is covalently attached to the group by 'click chemistry' – a copper(I)-catalyzed [3+2]azide-alkyne cycloaddition. By similar means, metabolic labeling can also be performed with the alkyne-bearing homopropargylglycine (HPG) and clicked to an azide-functionalized fluorophore.



PROTOCOL UNIT

Metabolic Labeling with Non-canonical Amino Acids and Visualization by Chemoselective Fluorescent Tagging

Susanne tom Dieck¹, Anke Müller^{2,3}, Anne Nehring¹, Flora I. Hinz¹, Ina Bartrik¹, Erin M. Schuman^{1*}, Daniela C. Dieterich^{2,3*}

¹Max Planck Institute for Brain Research, Department of Synaptic Plasticity, Max-von-Laue-Str.3, 60438 Frankfurt/Main, Germany

²Leibniz Institute for Neurobiology, Research Group Neuralomics, Brenneckestr. 6, 39118 Magdeburg, Germany

³Otto-von-Guericke-University Magdeburg, Medical Faculty, Institute for Pharmacology and Toxicology, House 20, Leipziger Str. 44, 39120 Magdeburg, Germany

*to whom correspondence should be addressed

Erin Schuman
phone +49 69 506820 1000
fax +49 69 506820 1002
erin.schuman@brain.mpg.de

or

Daniela Dieterich
phone +49 391 6715875
fax +49 391 6715869
Daniela.Dieterich@med.ovgu.de

ABSTRACT

Fluorescent labeling of proteins by genetically encoded fluorescent protein tags has enabled an enhanced understanding of cell biological processes but is restricted to the analysis of a limited number of identified proteins. This approach does not permit, for example, the unbiased visualization of a full proteome *in situ*. We describe here a fluorescence-based method to follow proteome-wide patterns of newly synthesized proteins in cultured cells, tissue slices and a whole organism. This technique is compatible with immunohistochemistry and *in situ* hybridization. Key to this method is the introduction of a small bio-orthogonal reactive group by metabolic labeling. This is accomplished by replacing the amino acid methionine by the azide-bearing methionine surrogate azidohomoalanine (AHA) in a step very similar to classical radioisotope labeling. Subsequently an alkyne-bearing fluorophore is covalently attached to the group by 'click chemistry' – a copper(I)-catalyzed [3+2]azide-alkyne cycloaddition. By similar means, metabolic labeling can also be performed with the alkyne-bearing homopropargylglycine (HPG) and clicked to an azide-functionalized fluorophore.

Keywords: FUNCAT, click chemistry, copper(I)-catalyzed [3+2]azide-alkyne cycloaddition, AHA, HPG, protein synthesis

INTRODUCTION

This unit describes Fluorescent Non-Canonical Amino acid Tagging (FUNCAT), a recently developed fluorescent labeling method to visualize proteome-wide spatio-temporal patterns of newly synthesized proteins (Beatty and Tirrell, 2008; Dieterich et al., 2010; Hinz et al., 2012; Roche et al., 2009; Tcherkezian et al., 2010). This method complements its non-fluorescent sister technology BONCAT (Bio-orthogonal Non-Canonical Amino acid Tagging) that enables the tagging of newly synthesized proteins for selective isolation and identification (Dieterich et al., 2006; for detailed BONCAT protocol see Dieterich et al., 2007).

FUNCAT is based on the introduction of small bio-orthogonal, chemically reactive alkyne or azide groups into proteins by means of metabolic labeling with the non-canonical amino acid analogs azidohomoalanine (AHA, azide-bearing) or homopropargylglycine (HPG, alkyne-bearing). Both amino acid analogs are surrogates for methionine and are incorporated into nascent proteins when applied to the extracellular medium and taken up by the cells (Dieterich et al., 2006). Thus, the metabolic labeling step is very similar to classical radioisotope labeling and can be combined with or follow drug treatment or electrophysiological stimulation (Figure 1). To increase the fraction of replaced methionine, a methionine depletion step prior to AHA or HPG addition is advisable and methionine must be absent from the medium during the metabolic labeling reaction. The incorporated azide or alkyne groups, as non-biological reactive "handles", serve to distinguish newly synthesized proteins from the pre-existing protein fraction

before metabolic labeling. Following AHA (or HPG) treatment cells are fixed and a fluorophore is covalently and chemoselectively attached to the introduced functional groups by means of 'click chemistry' – a copper(I)-catalyzed [3+2]azide-alkyne cycloaddition (for details and chemistry see commentary/background).

Strategic planning

The **basic protocol** describes FUNCAT with AHA metabolic labeling of cultured cell lines and primary cells (COS cells, hippocampal neurons, glial cells) plated on cover slips or glass bottom dishes, visualization of newly synthesized proteins in fixed cells by chemoselective reaction with a fluorophore-alkyne and subsequent immunolabeling (Figure 1).

Three **alternate protocols** are provided in the following sections to describe differences in the protocol when applying FUNCAT to hippocampal slices (**alternate protocol 1**), to a whole organism – larval zebrafish – (**alternate protocol 2**) and to hippocampal neurons cultured in microfluidic chamber devices (**alternate protocol 3**) (Figure 1). The first and second approach visualize protein synthesis in tissue with intact circuitries, thus they are perfectly suited to combine them with electrophysiology or, as in the case of zebrafish larvae, with behavioral studies. The FUNCAT procedure described in **alternate protocol 3** is designed to allow compartment-specific treatment of neurons – an approach to study aspects of local protein synthesis or local pharmacological manipulation. Since the method is compatible with immunohistochemistry all protocols include a section describing post-hoc antibody labeling. The **support protocol** provides a guide to combine FUNCAT with high-resolution fluorescence *in situ* hybridization (FISH, Figure 1). This will be of relevance when bridging the gap between *in situ* localization of mRNAs, translation and the newly translated proteome.

The decision about which tissue or cell line to use, which protocol, and the exact conditions to carry out the FUNCAT labeling obviously depends on the biological question of interest. In the protocols provided we give recommendations for appropriate concentrations and incubation times to use - these serve as good starting points as these conditions typically yield robust labeling. In the protocols we indicate the importance of the biological question and discuss several parameters to consider. We also discuss the limitations of this method in the commentary section. Figure 1 gives an overview of the protocols and shows additional options for further extending experiments e.g. to live imaging studies.

BASIC PROTOCOL

Basic Protocol title: FUNCAT IN CELL LINES AND PRIMARY CELLS

Introductory paragraph

This protocol describes the metabolic labeling of cultured standard cell lines or cultured primary cells with the azide-bearing non-canonical amino acid azidohomoalanine (AHA) or alternatively the alkyne-bearing amino acid homopropargylglycine (HPG) and the subsequent visualization of labeled proteins using chemoselective fluorescence tagging based on 'click-chemistry'. It is applicable for the examination of new protein synthesis on a cellular level within a specified time frame and specified conditions. Since the fluorescence tagging procedure is performed with fixed and permeabilized cells, newly synthesized proteins of all cell compartments can be visualized.

The protocol is divided into three parts including the metabolic labeling of cells, the FUNCAT-reaction allowing visualization of labeled proteins and an optional additional immunocytochemistry procedure. Included are basic recommendations and relevant observations for the procedure. This procedure is easy to perform and allows robust and reproducible results in a time frame of about two days.

Materials

Reagents and solutions

adherent cells from primary cell preparation or cell lines grown on
glass coverslips (18 mm) in a 12-well culture plate or
glass coverslips (12 mm) in a 24-well culture plate or
Matek glass bottom dishes
(densities 10 – 40 K for hippocampal neurons in MatTek dishes or 24-well plate,
cell lines and glial cells 80 % confluency)

methionine-free media
HBS (see recipe) or
methionine-free DMEM with supplements (see recipe) or
methionine-free Hibernate A with B27 (see recipe)

100 mM AHA (see recipe)

100 mM methionine (see recipe)

40 mM anisomycin (see recipe)

PBS-MC (see recipe)

Fixation solutions

*PFA-sucrose (see recipe) or
PLP (see recipe)*

B-Block (see recipe) or
C-Block (see recipe)
PBS pH 7.8 (see recipe)
500 mM TCEP in H₂O (see recipe)
200 mM CuSO₄ in H₂O (see recipe)
200 mM TBTA in DMSO, triazole ligand (see recipe)
2 mM fluorophore-alkyne-tag in DMSO (see recipe)
FUNCAT wash buffer (see recipe)
PBS pH 7.4 (see recipe)
Primary antibody
Secondary antibody, fluorophore-coupled
1 mg/ml DAPI (see recipe)
mounting medium
*Mowiol or
Fluoromount or
Aquapolymount*
microscopic slides

Equipment

Horizontal shaker
Vortex
FUNCAT incubation plate (see special equipment, Figure 2A) or
MatTek overhead incubation support (see special equipment, Figure 2B)

Protocol steps FUNCAT in cell lines and primary cells

Labeling of newly synthesized proteins with AHA

Day 1

1. Wash cells with HBS or methionine-free medium prewarmed to 37°C

Choose labeling medium according to cell type and duration of labeling time. For cell lines methionine-free DMEM and for primary neuronal cultures the methionine-free Hibernate A medium can be used. Supplementing the medium with serum or similar additives will not reduce labeling efficiency. For labeling times up to one hour HBS is sufficient. Longer labeling procedures demand methionine-free medium to supply cells with additional nutrients. Incubate neurons preferentially with methionine-free Hibernate A supplemented with B27.

2. Incubate cells with HBS or methionine-free medium for 20-30 min using appropriate culture conditions for the cell type used.
3. Dilute AHA from the stock solution to a final concentration of 4 mM AHA in methionine-free medium and add any other desired stimulus/drug. Incubate cells for 2 hrs (or any other appropriate time) using culture conditions according to the cell type. To evaluate background labeling treat control cells with 4 mM methionine and/or 4 mM AHA in presence of a protein synthesis inhibitor (e.g. 40 μ M anisomycin).

AHA is relatively expensive but can easily be synthesized (Link et al., 2007) using a standard rotary evaporator. Make sure that there are no precipitates or filter fibers in the stock solution when using self-synthesized AHA since they lead to fluorescent precipitate signal later. Centrifugation or filtration clears the stock solution.

Depending on the biological question, use AHA at other concentrations. We suggest 4 mM AHA as an initial concentration as it leads to robust labeling in a time frame of minutes to hours. When adjusting incubation conditions to the question of interest first vary incubation times and as a second step vary concentrations.

Alternatively AHA can be replaced by HPG (or added in a second incubation phase). In this case an azide-bearing fluorescent tag has to be used in the click reaction step (step 10d).

4. Optional: Incubate with HBS or methionine-free medium with 4 mM methionine for 15 min.

A chase of AHA with methionine reduces background when expected integration of AHA is low and the signal after fluorescent tagging is weak.

5. Place dishes on ice. Wash 2x briefly with ice-cold PBS-MC.
6. Fix with PFA-sucrose for 20 min at RT or PLP for 2 min at 37 °C and 20 min on ice.

Gentle agitation assures even fixation.

7. Wash 3x with PBS pH 7.4 for 10 min at RT.

At this point, coverslips can be stored in PBS pH 7.4 at 4 °C for several days.

Chemo-selective fluorescent tagging

8. Incubate in B-Block with Triton X-100 for 1.5 hours at RT to permeabilize cells and block unspecific binding sites.

Make sure that B-Block is supplemented with Triton X-100 for this step. Alternatively incubate the cells with PBS-Tx for 15 min and block before immunocytochemistry.

Use the following volumes for incubation steps and washes: 500 μ l for 12mm coverslips/ 24-well plate and MatTek dishes, 1 ml for 18 mm coverslips/ 12-well plate.

9. Wash 3x with PBS pH 7.8 for 10 min.

During the washing steps prepare the TCEP and CuSO₄ solutions and prewarm aliquots of TBTA and fluorescent tag to RT.

10. Assemble the FUNCAT reaction protected from light and without interruption at RT in the following order:

Example is given for 5 ml FUNCAT reaction mix and needs to be scaled up or down according to the experimental needs.

- a. 5 ml PBS pH 7.8.

The PBS pH 7.8 should be at RT to prevent precipitation of the TBTA. Use freshly diluted PBS from the 10x PBS stock solution.

- b. Add 5 μ l of 200 mM TBTA stock solution (1:1000), vortex at high speed for 10 seconds.

After addition of TBTA the solution will turn milky.

- c. Add 5 μ l of 500 mM TCEP stock solution (1:1000), vortex at high speed for 10 seconds.

- d. Add 0.5 μ l – 1 μ l of 2 mM fluorophore-alkyne-tag (1:5000-1:10 000), vortex at high speed for 10 seconds.

After addition of the fluorophore-alkyne-tag, the solution sometimes clears slightly.

- e. Add 5 μ l of the 200 mM CuSO₄ stock solution (1:1000), vortex at high speed for 30 seconds.

The solution turns clear. If precipitates from the fluorescent tag are observed on the coverslips, filter the FUNCAT reaction mix through 0.22 μ m pore size filters at this point.

11. Incubate cells upside-down in FUNCAT reaction mix overnight at RT with gentle agitation. Protect from light in all subsequent steps.

We strongly recommend to carry out the incubation in the FUNCAT reaction mix upside-down since otherwise the reaction solution will form fluorescent precipitates on the coverslips.

For overhead incubation of coverslips the reaction mix is added to the FUNCAT incubation plate (Figure 2A) and coverslips are placed on the paraffin dots with the cells facing the solution. Make sure that the coverslip is completely covered with the reaction mix. Prevent air bubbles.

For overhead incubation of MatTek dishes apply a thin layer of silicone grease to the edge of the MatTek incubation support. Fill the support with 300 μ l reaction mix to yield a positive meniscus of the solution and place the MatTek dish carefully on top with cells facing down (Figure 2B). Gently press and turn in order to seal the chamber with the grease.

Day 2

12. Wash 3x with FUNCAT wash buffer for 10 min at RT.

For washing steps turn coverslips so that the cells are facing up again.

13. Wash 2x with PBS pH 7.4 for 10 min at RT.

Immunocytochemistry

14. Incubate with primary antibody in B-Block or C-Block for 1-2 hours at RT or overnight at 4°C.

Overall fluorescence background might be increased due to CuSO_4 in the FUNCAT reaction. If experiments include weakly overexpressed GFP or RFP fusion proteins it is advisable to enhance the fluorescence signal by using immunocytochemistry.

15. Wash 3x with PBS pH 7.4 for 10 minutes each.
16. Incubate with secondary antibody in B-Block or C-Block for 0.5-2 hours at RT
17. Wash 2x with PBS pH 7.4 for 10 min
18. Optional: to label nuclei dilute DAPI stock 1:1000 in PBS and incubate cells for 3 min at RT
19. Wash 3x with PBS pH 7.4
20. Mount on microscope slide using mounting medium. Store at 4°C until imaged

ALTERNATE PROTOCOL 1

ALTERNATE PROTOCOL 1 TITLE: FUNCAT IN HIPPOCAMPAL SLICES

FUNCAT labeling is applicable to intact tissues such as acute hippocampal slices. The protocol summarizes steps for fluorescence detection of proteins in acute hippocampal slices that are newly synthesized during an incubation period of up to several hours after dissection. This protocol uses AHA metabolic labeling and immunohistochemistry in acute hippocampal slices and is accomplished within 3 days. The same protocol can be used to label organotypic slice cultures.

Materials***Reagents and solutions***

acute 450 μ m hippocampal slices sectioned on a vibratome or tissue slicer (for protocol see Madison & Edson, 2001)

Ringer solution, carbogenated (see recipe)

carbogen

100 mM AHA (see recipe)

100 mM methionine (see recipe)

40 mM anisomycin (see recipe)

PBS-MC (see recipe)

Fixation solutions

PFA-sucrose (see recipe) or

PLP (see recipe)

superglue

B-Block (see recipe)

PBS pH 7.8 (see recipe)

3% Agarose solution (see recipe)

500 mM TCEP in H₂O (see recipe)

200 mM CuSO₄ in H₂O (see recipe)

200 mM TBTA in DMSO, triazole ligand (see recipe)

2 mM fluorophore-alkyne-tag in DMSO

FUNCAT wash buffer (see recipe)

PBS-T pH 7.4 (see recipe)

Primary antibody

Secondary antibody, fluorophore-coupled

1 mg/ml DAPI (see recipe)

mounting medium

Mowiol or
Fluoromount or
Aquapolymount

microscopic slides

coverslips

Equipment

Vibratome Leica VT1200S

Tissue slicer (optional)

Interface recovery chamber (Madison and Edson, 2001)

Whatman filter paper #1

Submerged incubation chamber (tissue slice chamber, Harvard Apparatus)

Water bath

Hot plate magnetic stirrer

Artist brushes

Stereomicroscope

Scalpel

Forceps

Horizontal shaker

Vortex

Protocol steps: **FUNCAT in hippocampal slices**

Metabolic labeling of newly synthesized proteins in slices with AHA

Day 1

1. Incubate acute hippocampal slices on Whatman filter paper (#1) moistened with Ringer's solution on a 35 mm tissue culture dish in an interface recovery chamber for 1.5 h at RT.
2. Dilute AHA from stock solution to 4 mM AHA in Ringer. Transfer slices into a submerged chamber filled with oxygenated 4 mM AHA and incubate for 4 hrs (or any other desired time) at 32°C. Use 4 mM methionine and 4 mM AHA/ 40 µM anisomycin in Ringer's solution as controls.

*Incubation times of 1 to 4 hrs lead to increased labeling with the indicated concentration in this protocol. Vary time and concentration as needed.
Place the submerged incubation chamber in water bath to maintain a temperature of 32 °C*

HPG can be used instead of or to chase AHA. Note that in this case an azide-bearing fluorescent tag must be used in step 13.d.

3. Wash 1x with PBS-MC
4. Fix with PFA-sucrose for 20 min at RT.
5. Wash 1x with PBS-MC.
6. Embed fixed slices in 3% agarose.

Prepare 3% low gelling temperature agarose in PBS, pH 7.8. Keep the agarose liquid by stirring it on a hot plate magnetic stirrer at 50 °C. Pour some of the agarose into a prewarmed glass dish. Briefly wash slices in agarose to get rid of excess PBS from the washing steps. Add a few drops of agarose into the lid of a 1.5 ml microcentrifuge tube. Quickly transfer one slice into the agarose while it is still liquid using fine brushes. Straighten the slice in the agarose under a stereo microscope. Place agarose embedded slice on ice for 5 min.

7. Cut agarose block containing the slice.

Remove the agarose block from the lid and cut a small cuboid along the 6 planes of the slice using a fine scalpel and fine forceps to hold the agarose block. Make sure that there is enough agarose left around the slice (500 µm) to glue the agarose block to the support in the next step.

8. Mount agarose embedded slice.

*Paste a little bit of superglue to the stage of the vibratome and immediately place the agarose-embedded slice on top using fine forceps. Let the glue harden for 10 sec.
Place the stage with the mounted block in the vibratome chamber filled with PBS, pH 7.8.*

9. Prepare 50 µm vibratome sections from agarose embedded slices

Use vibratome settings of 0.01 mm/sec speed and 0.8 mm amplitude.

10. Transfer re-sectioned slices into 24-well plates filled with PBS, pH 7.8.
11. Permeabilize slices with 0.5% Triton X-100 in B-Block at 4 °C overnight

Chemo-selective fluorescence tagging

Day 2

12. Wash slices 3x with 0.1% Triton X-100 in PBS, pH 7.8

13. Assemble FUNCAT reaction, protected from light, without interruption in the following order in a 15 ml Falcon tube:

Example is given for 5 ml FUNCAT reaction mix and needs to be scaled according to the experimental needs.

- a. 5 ml PBS pH 7.8.

The PBS pH 7.8 should have RT to prevent precipitation of the TBTA. Use freshly diluted PBS from the 10x PBS stock solution.

- b. Add 5 μ l of 200 mM TBTA stock solution (1:1000), vortex at high speed for 10 seconds.

After addition of TBTA the solution will turn milky.

- c. Add 5 μ l of 500 mM TCEP stock solution (1:1000), vortex at high speed for 10 seconds.

- d. Add 5 μ l of 2 mM fluorophore-alkyne-tag (1:1000), vortex at high speed for 10 seconds.

After addition of the fluorophore-alkyne-tag the solution sometimes clears slightly.

- e. Add 5 μ l of the 200 mM CuSO₄ stock solution (1:1000), vortex at high speed for 30 seconds.

The solution turns clear. If precipitates from the fluorescent tag are observed at later steps, filter the FUNCAT reaction mix through 0.22 μ m pore size filters at this point.

14. Incubate each slice in 250 μ l of FUNCAT reaction mix at RT overnight. Protect from light in all subsequent steps.

Free-floating slices can be incubated in multi-well dishes and do not need overhead incubation. Cu(I) precipitates predominantly adhere to coated dishes.

Immunohistochemistry

Day 3

15. Wash slices 3x with FUNCAT wash buffer for 20 min.
16. Wash slices 2x with PBS-T for 10 min.
17. Incubate with primary antibody in B-Block for 2 hrs.
18. Wash slices 3x with PBS-T for 15 min.
19. Incubate with secondary antibody in B-Block including DAPI 1:1000 for 1 hr.
20. Wash slices 3x with PBS-T for 15 min.

21. Wash slices 2x with PBS pH 7.4 for 10 min.
22. Mount on microscopic slides with MOWIOL or Fluoromount and cover with coverslip. Store at 4°C until imaged.

ALTERNATE PROTOCOL 2

ALTERNATE PROTOCOL 2 TITLE: FUNCAT IN LARVAL ZEBRAFISH

Metabolic labeling with AHA to visualize areas of new protein synthesis is also applicable to the larval zebrafish. Nacre zebrafish lack melanophores and, therefore, enable direct imaging e.g. of the nervous system without prior dissection. AHA has been found not to be toxic to the live organism at the concentration described here (Hinz et al., 2012), however longer incubations than compared to cell culture and hippocampal slices are necessary to allow for diffusion of AHA into the tissue and incorporation into newly synthesized proteins. High levels of fluorescence have been found especially in the tail muscles and the liver, however visualization of differential protein synthesis was also possible in the spinal cord and nervous system. The protocol is accomplished within approximately 1 week.

Materials

Reagents and solutions

4-6 days post fertilization (dpf) larval zebrafish
E3 embryo medium (see recipe)
100 mM AHA (see recipe)
5 mg/ml puromycin (see recipe)
PFA-sucrose (see recipe)
PBS-T (pH 7.4 and 7.8) (see recipe)
Methanol
PBDDT (see recipe)
Proteinase K (10 µg/ml)
Z-Block (see recipe)
500 mM TCEP in H₂O (see recipe)

200 mM CuSO₄ in H₂O (see recipe)
200 mM TBTA in DMSO, triazole ligand (see recipe)
2 mM fluorophore-alkyne-tag in DMSO (see recipe)
0.5 M EDTA
Primary antibody
Secondary antibody, fluorophore-coupled
0.6% agarose
MatTek dish

Equipment

Stereo microscope
Vortex
Rotary shaker
Microwave

Protocol steps: **FUNCAT in larval zebrafish**

Metabolic labeling of newly synthesized proteins in larval zebrafish with AHA

Day 1

1. Incubate 4-6 dpf larval zebrafish in E3 embryo medium (pH 7.0-7.6) or E3 embryo medium (pH 7.0-7.6) containing 4 mM AHA at 26 - 28°C in a petri dish.

Incubation times of 24 hrs or more lead to prominent labeling. Incubation times of more than 72 hrs are not recommended. Puromycin (5 µg/ml, dilute from 1000x stock) controls can be carried out for up to 48 hrs.

Day 2

2. Wash larval zebrafish 3x 5 min with 25 ml E3 embryo medium at RT.
3. Transfer larvae to 1.5 ml Eppendorf tube and anesthetize for 30 min to 1 hr on ice.
Do not use more than ~5 larvae in each tube.
4. Remove remaining E3 embryo medium and replace with RT PFA-sucrose fixative. Incubate at RT for 3 hr and invert the tube every 30 min.
5. Wash larval zebrafish briefly in 100% methanol at RT.

6. Incubate in 100% methanol at -20°C overnight.

At this step, samples can be stored for prolonged time periods.

Chemo-selective fluorescence tagging

Day 3

7. Rehydrate larvae by successive 5 min washes in 75% methanol in PBS-T, 50% methanol in PBS-T, 25% methanol in PBS-T and PBS-T pH 7.4.
8. Wash 2x for 5 min with PBDTT.
9. Permeabilize sample by incubating in 10 µg/ml Proteinase K in PBS-T pH 7.4 for 1 hr at RT.

Do not exceed 1 hr incubation, as tissue will deteriorate rapidly.

10. Wash briefly in PBS-T pH 7.4 and immediately post-fix for 20 min in PFA-sucrose at RT.
11. Wash 2x in PBS-T pH 7.4.
12. Wash 3x in PBDTT for 5 min.
13. Incubate in Z-Block for 3 hrs at 4°C
14. Wash 3x in PBS-T pH 7.8 for 10-15 minutes.
15. Assemble FUNCAT reaction mix, protected from light, without interruption in the following order in a 1.5 ml Eppendorf tube:
 - a. 1 ml PBS-T pH 7.8.

The PBS-T pH 7.8 should have RT to prevent precipitation of the TBTA. Use freshly diluted PBS from the 10x PBS stock solution.
 - b. Add 1 µl of 200 mM TBTA stock solution (1:1000), vortex at high speed for 10 seconds.

After addition of TBTA the solution will turn slightly milky but TBTA should not precipitate.
 - c. Add 1 µl of 500 mM TCEP stock solution (1:1000), vortex at high speed for 10 seconds.
 - d. Add 2.5 µl of 2 mM fluorophore-alkyne-tag (1:400), vortex at high speed for 10 seconds.

After addition of the fluorophore-alkyne-tag the solution sometimes clears slightly.

- e. Add 1 μ l of the 200 mM CuSO₄ stock solution (1:1000), vortex at high speed for 30 seconds.

The solution turns clear. If precipitates from the fluorescent tag are observed at later stages, filter the FUNCAT reaction mix through 0.22 μ m pore size filters at this point.

16. Incubate each set of 5 larvae in 0.5 ml of FUNCAT reaction mix overnight at RT with agitation.

Immunohistochemistry

Day 4

17. Wash 4x in PBDTT + 0.5 mM EDTA for 30 min at RT.
18. Incubate in primary antibody in 20% Z-Block overnight at 4°C.

Day 5

19. Wash 4x in PBDTT for 30 min.
20. Incubate in secondary antibody in 20% Z-Block overnight at 4°C.

Day 6

21. Wash 2x in PBDTT for 1 hr.
22. Wash 4x in PBDTT for 30 min.
23. Wash in PBS pH 7.4 for 15 min.
24. Mount in 0.6% agarose in E3 embryo medium on MatTek dishes. Store at 4°C until imaged.

When mounting larvae, place area of interest directly against the glass area of the Matek dish.

ALTERNATE PROTOCOL 3**ALTERNATE PROTOCOL 3 TITLE: FUNCAT IN MICROFLUIDIC CHAMBERS**

In order to approach visualization of newly synthesized proteins in combination with either compartmentalized labeling or compartment specific treatment of neurons we use FUNCAT in microfluidic chamber devices (Taylor et al., 2010). The use of the chambers allows the compartment specific addition of the amino acid surrogate and/or drugs. This protocol describes the variations made to the basic protocol to investigate sub-compartments.

This alternate protocol describes metabolic labeling of hippocampal neurons with AHA via different compartments of a standard microfluidic or μ LP (microfluidic Local Perfusion) chamber (Figure 2C,D) and indicates putative changes, manipulations with drugs and pitfalls. Of note, due to potential intracellular diffusion of AHA and some drugs, time scales have to be figured out individually. Experiments designed to study local protein synthesis might need laser assisted transection of dendrites and axons. This method is under development and the protocol serves as a basis to approach visualization of local protein synthesis.

Materials***Reagents and solutions***

Primary hippocampal neurons cultured in microfluidic chambers (Taylor et al., 2010)
Microfluidic chambers (Taylor et al., 2010) (Figure 2C,D; available from Xona Microfluidics LLC: SDN900 or μ LP)
methionine free Hibernate A (Brain Bits) with B27 (see recipe)
100 mM AHA (see recipe)
100 mM methionine (see recipe)
40 mM anisomycin (see recipe)
PBS-MC (see recipe)
Fixation solutions
 PFA-sucrose (see recipe) or
 PLP (see recipe)

PBS-Tx (see recipe)
C-Block (see recipe)

PBS pH 7.8 (see recipe)
500 mM TCEP in H₂O (see recipe)
200 mM CuSO₄ in H₂O (see recipe)
200 mM TBTA in DMSO, triazole ligand (see recipe)
2 mM fluorophore-alkyne-tag in DMSO
spacer (approximately 3x1x1 mm³)
humidified chamber
PBS pH 7.4 (see recipe)
Primary antibody
Secondary antibody, fluorophore-coupled
1 mg/ml DAPI (see recipe)
mounting medium
 Mowiol or
 Fluoromount or
 Aquapolymount
microscopic slides

Equipment

Syringe pump
Vortex

Protocol steps: **FUNCAT in microfluidic chambers**

Metabolic labeling of newly synthesized proteins in microfluidic chambers

Day 1

1. Wash cell body chamber 2x with 300 µl prewarmed methionine-free Hibernate A.

Aspirate medium from both connected cell body wells (wells 1 in Figure 2C,D) carefully with a pipet. To achieve full replacement of the standard culture medium and to avoid clogging by air bubbles immediately apply washing solution to only one of the connected wells and allow for flow through. Remove first wash from both wells and repeat. Use the same procedure also for axon wells (next step, wells 2 in Figure 2C,D) and all subsequent solution replacements.

2. Wash axon chamber 2x with 300 μ l prewarmed methionine-free Hibernate A.
3. Replace medium in all perfusion channel wells by 75 μ l of prewarmed (37°C) methionine-free Hibernate A.
4. Connect syringe pump tubing to channel outlet. Set pump to withdrawal mode with 0.1ml/hr.

The perfusion channel needs 5 minutes to be filled with the respective solutions with these settings. For incubations place chambers back into the incubator and pump constantly otherwise in this chamber type solutions will diffuse extracellularly to other compartments. Fluidic isolation can be checked by adding different fluorescent dyes, such as Alexa 488 hydrazide to the various compartments (e.g. Taylor et al., 2010).

5. Incubate cells with methionine-free Hibernate A for 20-30 minutes in the incubator for methionine depletion.
6. Prepare prewarmed solutions with AHA in methionine-free Hibernate A and drug solutions if applicable and replace in the desired wells.

The concentration of AHA depends on the purpose of the experiment as does the incubation time. We recommend 4 mM AHA for 2 hrs as starting conditions as those give robust labeling in cell bodies no matter where AHA is applied. Control experiments with 4 mM methionine and 4 mM AHA and 40 μ M anisomycin are recommended to estimate the extent of background labeling.

Replace solutions by the method indicated above in the desired compartment. In all other compartments keep methionine-free Hibernate A. The design of the experiment might require replacements in several wells e.g. addition of AHA to the axon wells, addition of a protein synthesis inhibitor to the cell body chamber and a glutamate receptor antagonist to the perfusion channel. Preferably do not stop perfusion when changing incubation solutions. Replace solutions quickly in the respective wells. To prevent diffusion by differences in hydrostatic pressure load wells 1 and 2 (Figure 2) with similar volumes.

7. Incubate for the desired time (starting point 2 hrs) with chambers placed in the incubator with constant pumping and perfusion.

Adjust time and drug/ AHA concentrations to the biological question.

8. Place dishes on ice and gently remove PDMS part of the chamber without displacing dendrites (Figure 2E).
9. Wash coverslips immediately two times with ice-cold PBS-MC.
10. Wash once with 0.5 ml fixation solution, then fix for 20 minutes at RT with 0.5 ml PFA-sucrose or PLP.
11. Wash 1x with 0.5 ml PBS-Tx and then permeabilize with 0.5 ml PBS-Tx 15 min at RT.

If preferentially newly synthesized membrane proteins are intended to be labeled this step can be omitted. Note that this reduces the signal obtained later significantly. For this purpose blocking buffer in the next step has to be without detergent and cells have to be permeabilized with PBS-Tx and blocked before immunocytochemistry and after FUNCAT reaction.

Chemo-selective fluorescence tagging

12. Incubate in C-Block for 1 hr at RT.
13. Wash 2x 5 min with PBS pH 7.8
14. Prepare 1 ml FUNCAT reaction mix per coverslip as described in the basic protocol (step 10a-d).
15. Incubate coverslip upside down in click reaction mix overnight at RT.

Pipet 1 ml of FUNCAT reaction mix on parafilm in a humidified chamber, position a small spacer (made from silicone or any other inert material) next to the drop and place the coverslip upside down with one edge on the parafilm and one resting on the spacer (Figure 2E). This way the solution evenly distributes under the cover slip, the cells are covered but not destroyed. Protect from light.

Immunohistochemistry

Day 2

16. Wash with PBS-Tx 2 x 5 min
17. Wash with PBS 1 x 5 min
18. Proceed with DAPI staining or immunohistochemistry section of basic protocol

SUPPORT PROTOCOL

SUPPORT PROTOCOL TITLE: Combination of FUNCAT with high resolution FISH

Introductory paragraph

This support protocol describes the steps necessary to combine FUNCAT with high- resolution fluorescence *in situ* hybridization using the Affymetrix QG ViewRNA method based on branched DNA *in situ* hybridization (Player et al., 2001).

Materials

Reagents and solutions

Cells (see basic protocol/alternate protocol 3)

Affymetrix QG ViewRNA HC Screening Assay Kit containing stock solutions for buffers, prepare the following buffers according to the manufacturer's recommendations:

Working detergent solution
Working protease stop buffer
Working probe set diluent
RNAView wash buffer
Working storage buffer
Working amplifier diluent
Working label probe diluent

Affymetrix QG ViewRNA Probe set for mRNA of interest

Affymetrix QG ViewRNA HC Screening Signal Amplification Kit; aliquot in 10 µl-aliquots when thawing for the first time and use aliquots up to 3 times.

Preamplifier
Amplifier
Label probe

RNAse free water

PLP

RNAse free PBS

Equipment

Thermomixer, heating block (40 °C)

Hybridization oven (40 °C)

Humidified chamber

Protocol steps: **Combination of FUNCAT with high resolution FISH**

Day 1

Metabolic labeling with AHA

1. Perform metabolic labeling with AHA as described in basic protocol steps 1-3 or alternate protocol 3 steps 1-9.
2. Wash 2x with PBS pH 7.4 to stop metabolic labeling.
3. Fix with PLP for 30 min at RT.

Avoid RNAse contamination of the samples. Wear gloves, change them frequently and use RNAse free water and PBS.

For washing steps in 24-well plates or MatTek dishes use $\geq 300 \mu\text{l}$, for incubation steps $150 \mu\text{l}$.

Hybridize probe set

4. Wash 3x with PBS at RT.
5. Permeabilize 3 min with $150 \mu\text{l}$ working detergent solution at RT.
6. Wash 3x with PBS at RT.

The manufacturer recommends a proteinase K digestion step that is not performed in this protocol to avoid degradation of the newly synthesized proteins.

7. Equilibrate in $150 \mu\text{l}$ working protease stop buffer up to 30 minutes until probe set is prepared at RT.

Dilute probe set 1:100 in working probe set diluent prewarmed to 40°C .

8. Wash cells 1x with PBS at RT.
9. Incubate with $150 \mu\text{l}$ probe set mixture for 3 hrs at 40°C in an hybridization oven.

Create an humidified chamber to avoid evaporation: seal 24-well plates with parafilm before placing into the oven. Place Matek dishes on a tray with tissues soaked in water, slip it into a plastic bag and seal it before transfer to 40°C .

10. Wash 3x with RNAView wash buffer at RT.
11. (Optional:) store in working storage buffer at 4°C overnight.

Day 2

Amplify hybridized probe set

12. Wash 2x with RNAView wash buffer at RT.
13. Incubate with PreAmp mixture 1 hr at 40°C in humidified chamber.

Dilute PreAmp 1:100 in working amplifier diluent prewarmed to 40°C .

14. Wash 3x with RNAView wash buffer at RT.
15. Incubate with Amp mixture 1 hr at 40°C in humidified chamber.

Dilute Amp 1:100 in working amplifier diluent prewarmed to 40°C .

16. Wash 3x with RNAView wash buffer at RT.
17. Incubate with Label Probe mixture 1 hr at 40°C in humidified chamber.

Dilute label probes 1:100 in working label probe diluent prewarmed to 40 °C.

Choose the label probe fluorophore appropriate for combination with the fluorophores used to be clicked to AHA and coupled to the antibodies used for immunocytochemistry. Protect from light.

18. Wash 3x with RNAView wash buffer at RT.

Chemo-selective fluorescence tagging

19. Wash 3x with PBS-MC at RT.

20. Block 1 hr with C-Block at RT.

21. Prepare FUNCAT reaction mix and proceed at step 10 of basic protocol.

It is possible to perform both chemoselective labeling and immunohistochemistry after FISH. Use RNase free reagents and shortest possible incubation times. If the signal to noise ratio allows, shorten the click reaction to 2 hrs.

REAGENTS AND SOLUTIONS

Agarose solution

Dissolve low gelling temperature agarose in 1x PBS, pH 7.8, to a final concentration of 3% by heating on a hot plate magnetic stirrer.

AHA or HPG or methionine

Dissolve AHA (L-Azidohomoalanine, Invitrogen) or HPG (L-Homopropargylglycine, Invitrogen) or methionine in HBS or in methionine-free medium to a final concentration of 100 mM.

Store at 4 °C up to 1 week

Anisomycin stock solution

Dilute Anisomycin (Tocris) to a final concentration of 40 mM in DMSO.
Store aliquots at -20 °C for up to 1 month.

B-Block

Dissolve in 1x PBS pH 7.4

10% normal horse serum

5% sucrose

2% BSA

Filter with 0.22 µm pore size sterile filters

Store 6-12 months at -20 °C

Before use: add Triton X-100 to 0.1% for cell permeabilization when needed

C-Block

Dissolve in 1x PBS pH 7.4
4% normal goat serum
Filter with 0.22 µm pore size sterile filters
Store 6-12 month at -20°C

Z-Block

Dissolve in PBDTT:
5% BSA
10% normal goat serum

CuSO₄ solution

Dissolve CuSO₄ to a final concentration of 200 mM in distilled water
Prepare solution fresh directly before use

DAPI stock solution (1000x)

Dissolve DAPI 1 mg/ml distilled water.
Store in aliquots at -20°C for 1 year. Use aliquots at 4°C for 1 month.
Dilute directly before use 1:1000 in PBS or respective incubation solution.

E3 embryo medium

5 mM NaCl
0.17 mM KCl
0.33 mM CaCl₂,
0.33 mM MgSO₄

Fluorescent tag

fluorophore-alkyne or -azide tags are commercially available from Invitrogen or Click Chemistry Tools (e.g. AlexaFluor for 488 nm, 555 nm, 594 nm and 647 nm excitation wavelength from Invitrogen)

Dissolve tag in DMSO to final concentration of 2 mM

Dispense in 20 µl aliquots

Store 6-12 month at -20°C

Working aliquot can be stored at 4°C for up to 3 month, protected from light

FUNCAT-wash buffer

Dissolve in PBS pH 7.8
0.5 mM EDTA
1% Tween-20

2x HBS

238 mM NaCl
10 mM KCl

4 mM CaCl₂ (from 1M stock solution)
4 mM MgCl₂ (from 1M stock solution)
60 mM glucose
20 mM Hepes
Adjust pH to 7.35 with a few drops of 1N NaOH.
Filter through sterile 0.22 µm pore size filters.
Store at 4°C for up to 2 month, alternatively aliquot and store at -20°C for up to 6 months. For 1x HBS mix 1 + 1 with deionized water

Methionine-free medium

For DMEM minus methionine, minus Cysteine, minus glutamine, add L-Cysteine to a final concentration of 0.201 mM, add glutamine, serum and other supplements necessary for cultivation of cell culture lines.
Filter through 0.22 µm pore size sterile filters.
For Methionine-free Hibernate A add supplements necessary for cultivation of primary cell cultures. The use of B27 (Invitrogen, 1:50) for cultivation of neuronal cultures is advisable. Filter through 0.22 µm pore size sterile filters

1x PB, pH 7.4

21.71 g Na₂HPO₄ x 7 H₂O
2.62 g NaH₂PO₄ x H₂O
ad 1 l with distilled water

10x PBS

1.37 M NaCl
27 mM KCl
43 mM Na₂HPO₄·7H₂O
14 mM KH₂PO₄
Distilled water up to 900 ml
Adjust pH with a few drops of 1N NaOH
ad 1l with distilled water
For 1x PBS use 1 part of 10x PBS and 9 parts of distilled water, adjust pH if necessary

1x PBS-MC

Dissolve in 1x PBS pH 7.4
1 mM MgCl₂
0.1 mM CaCl₂
Dilute MgCl₂ and CaCl₂ from 1M stock solutions

PBS-DTT

Dissolve 1% DMSO, 0.5% Triton X-100 and 0.1% Tween-20
in 1x PBS pH 7.4

PBS-T

Dissolve 0.1% Tween-20 in 1x PBS
Adjust pH to 7.4 or 7.8 with a few drops of 1 N NaOH

PBS-Tx

Dissolve 0.1% Triton X-100 in 1x PBS

PFA-Sucrose

PBS-MC supplemented with
4% PFA (Stock: 16% w/v, Alfa Aesar)
and 4% (w/v) sucrose

PFA-Sucrose for larval zebrafish

1x PBS, pH 7.4 supplemented with
4% PFA (Stock: 16% w/v, Alfa Aesar)
3% (w/v) sucrose

PLP-Fix

Solution A: Lysine Phosphate Buffer
3.66 g Lysine hydrochloride ad 100 ml distilled water
adjust pH to 7.4 by adding 0.1M Na₂HPO₄
double the volume of the solution by adding the appropriate amount of 1x
PB

Solution B: Paraformaldehyde
0.54 g Glucose
10 ml 16% w/v Paraformaldehyde solution (Alfa Aesar)

mix 3 parts of Solution A with 1 part of Solution B
add Sodium-m-periodate to a final concentration of 0.01 M (0.21 g/100 ml)
use solution for 1 week, store at 4°C

Puromycin (1000x stock)

Dissolve puromycin 5 mg/ml in distilled water, aliquot and store at -20°C for up to 1
month.

Ringer's solution

119 mM NaCl
2.5 mM KCl
1.3 mM MgSO₄
2.5 mM CaCl₂
1.0 mM NaH₂PO₄
26.2 mM NaHCO₃
11.0 mM glucose
adjust pH to 7.35 with 1 N NaOH
Make sure that CaCl₂ is completely dissolved before the next compounds are added.
Store the solution for one week at 4°C. Start carbogenating the solution 10-15 min
before perfusion of hippocampal slices.

TBTA

Dissolve TBTA (tris[(1-benzyl-1H-1,2,3-triazol-4-yl)methyl]amine) in anhydrous, freshly opened DMSO to a final concentration of 200 mM. Store aliquots up to 6 months at -20°C. Avoid repeated freezing and thawing of aliquots (no more than 3 times).

TCEP

Dissolve TCEP-HCl (Tris-(2-carboxyethyl)phosphine hydrochloride) to a final concentration of 500 mM in distilled water. Prepare solution fresh directly before use.

Preparation of special equipment***FUNCAT incubation plate***

To prepare FUNCAT incubation plates use a 12 well or 24 well culture plate according to the coverslip size used. Heat paraffin (e.g. Granopent "P", Carl Roth) in a glass beaker on a hot plate with a temperature of 150°C. Dip a glass pipette into the fluid paraffin and make four paraffin dots of the size of a pin per well. The plates can be cleaned easily and reused many times (Figure 2A).

MatTek overhead incubation support

Fill a lid of a 5 ml round bottom tube with toy modeling clay. Leave 2-3 mm space to the edge and seal the surface with a layer made from two-component epoxy glue. The created well should hold 300 µl of solution (Figure 2B).

COMMENTARY**Background Information*****Comparison with other methods***

Fluorescent labeling of proteins by genetically encoded fluorescent protein tags pioneered by GFP opened a new era in understanding cell biological processes by visualization of spatio-temporal patterns in protein distribution (Chalfie et al., 1994; Heim et al., 1994). One drawback of this approach is the relatively big size of the tag, which in some cases affects the folding and behavior of the proteins of interest. Another limitation became obvious with the focus of studies turning to a systems biological point of view. With the genetically-encoded fluorescent tagging approach the analysis is restricted to a limited number of known proteins at a given time.

Metabolic labeling of the proteome with either radioisotope- or stable isotope-tagged amino acids are powerful methods to quantify or identify and compare proteome-wide changes in combination with biochemistry and mass spectrometry, respectively (Cox and Mann, 2011; Hu et al., 2004). Since the nature of the label doesn't influence biological processes, it is perfectly suited to reflect physiological conditions. In contrast, these methods are not well-suited for either the purification of the newly synthesized protein pool or the *in situ* visualization within the cell. The conversion of radioactivity into a visual signal by exposure to film emulsion is time-consuming, difficult to combine with other imaging methods and can't be extended to live imaging. BONCAT and FUNCAT fill these gaps. FUNCAT is a fluorescence-based method to follow proteome-wide patterns of newly synthesized proteins *in situ* and is compatible with immunohistochemistry and *in situ* hybridization. Introduction of non-canonical amino acids with small, bioorthogonal chemical handles enables a multitude of ligation options (Fig 3 A,B) e. g. to fluorophores for visualization (FUNCAT), biotin for purification and mass spec (BONCAT) but is not limited to those. Thus the elegance in this approach lies in the versatility of the method.

Mechanism and chemistry

As described above, the introduction of a small bio-orthogonal reactive handle is accomplished by metabolic labeling similar to classical radioisotope labeling. Methionine is replaced in the medium by the azide- or alkyne-bearing methionine surrogates AHA or HPG (Figure 3A). Both non-canonical amino acids are taken up by cellular amino acid transporters – mainly by LAT1 (Figure 3C, (Kanai et al., 1998)). Key to this methodology is that not only transporters but also endogenous methionyl tRNA synthetase (MetRS) - the enzyme charging methionine onto its tRNA – accepts AHA and HPG as substrates although with lower efficiency than methionine (Kiick et al., 2002). Once charged onto the tRNA, incorporation of the amino acid analogs into nascent proteins is straight-forward. Thus, during metabolic labeling newly synthesized proteins are endowed with new functionalities, namely azide (AHA) or alkyne (HPG) groups that differentiate them from the pre-existing protein pool (Fig 3C). If AHA and HPG are applied sequentially (or potentially also at two distinct places) two different subpopulations of proteins are labeled (Dieterich et al., 2010).

After incorporation into newly synthesized proteins the functional groups are visualized by fluorophores in a reaction based on 'click chemistry' - a copper(I)-catalyzed [3+2]azide-alkyne cycloaddition (Figure 3B,C) (Rostovtsev et al., 2002; Tornøe et al., 2002). To this end the fluorophore has to be functionalized by the respective counterpart. AHA reacts with alkyne-

bearing fluorescent tags, HPG is clicked to azide carriers. The catalyzing Cu(I) is produced directly in the reaction from TCEP and Cu(II) and the triazole ligand TBTA serves the dual purpose of both activating the Cu(I) ion for catalysis and protecting it from disproportionation, thus improving the kinetics of the bioconjugation and also allowing for long reaction times required in some applications (Dieterich, 2010; Dieterich and Link, 2009; Prescher and Bertozzi, 2005)(for further details see Prescher and Bertozzi, 2005, Dieterich, 2010; Dieterich and Link, 2009).

Limitations and extensions

Beside the versatility of the method in general, the introduction of bioorthogonal groups by AHA and HPG have the advantage of minimal interference with protein folding, trafficking and function (Dieterich et al., 2006) due to the small size chemical tags and, thus, the likely close reflection of physiological conditions. The conditions given in the protocols give robust labeling (Figure 4,5) but may need adaptation to the cell type or question of – see the critical parameters and troubleshooting section.

A prerequisite for a protein to be labeled by this method is the presence of at least one naturally occurring methionine in the protein and secondly, that this is replaced by the surrogate amino acid during protein synthesis. Even if the number of potential replacement sites is not a severe limitation since e.g. for the zebrafish genome a fraction of 99.99 % percent of proteins was calculated to fulfill this prerequisite and 99.98% of all protein entries of a human protein database contain at least a single methionine (Dieterich et al., 2006; Hinz et al., 2012), the replacement fraction sometimes is. The factors influencing most prominently the fraction of methionine replacement are the competition with the internal methionine pool and the incubation time. With long incubation periods eventually a steady state level will be reached but never full replacement. The shorter the metabolic labeling time the more important it will be to reduce competition by methionine. Methionine depletion prior to the AHA metabolic labeling decreases competition by methionine for charging onto it's tRNA but also provides a non-physiological situation to the cell. Long metabolic labeling times might become an issue when cells, in particular neurons, do not tolerate or react to long incubations in artificial medium or when intended local applications are counteracted by intracellular distribution or diffusion of the amino acids or drugs. In microfluidic chambers we find that after 1 hr - regardless from which compartment AHA is loaded - the non-canonical amino acid reached the cell body even when fluidic isolation is intact (Figure 5B,C).

The advantage that FUNCAT labels newly synthesized proteins on a proteome-wide level might turn into a disadvantage when for instance only a subpopulation of cells is of interest and the signal in other cell types creates a 'background'. New developments aim to restrict the metabolic labeling. Expression of mutant MetRS versions that accept a longer-chain homolog of AHA – ANL (Azidonorleucine) – that in turn is not a substrate of the endogenous MetRS, are a potential way to genetically control the metabolic labeling (Ngo et al., 2009). Genetic manipulation of the MetRS instead of directly the protein of interest as in fluorescent protein-tagged approaches rules out problems and restrictions due to overexpression and the limited capacity for genetically encoding several tags at the same time.

The fact that CuSO_4 is toxic to cells limits the use of the protocols described here to manipulations that are analyzed after fixation of the cells or tissue of interest. Recent developments to apply this technique also in live cells make use of the fact that [3+2]azide-alkyne cycloaddition can not only be catalyzed by Cu(I) but also is achieved by strain promotion (Agard et al., 2004). The embedding of the alkyne moiety into a cyclooctene structure with sidechains that promote strain as in DIBO (Dibenzocyclooctyne) or DIFO (Difluorinated cyclooctyne) thus enables a copper-free click reaction. To date the poor membrane permeability of the reagents limit the application to labeling of newly synthesized membrane proteins (Dieterich et al., 2010) but efforts to extend the repertoire of reagents to enable the live visualization of intracellular proteins are in progress (Beatty et al., 2010; Beatty et al., 2011).

Critical Parameters & Troubleshooting

The conditions given in the protocols should lead to robust labeling (Figures 4 & 5). Problems that could arise and their possible solutions are listed in table 1. However, the starting times and concentrations suggested here might not be optimal for all biological questions. Adaptations of parameters in the protocol should consider the following: protein synthesis rates differ between cell types. Incorporation of the amino acid surrogates into postmitotic cells like neurons is lower than in dividing cells. The choice of the labeling medium should also be considered. The ideal labeling medium with respect to cell health and physiological state would be the respective fully complemented and conditioned culturing medium free of methionine. Unfortunately this is not possible in most cases. While cell lines usually tolerate an incubation in HBS or unsupplemented media well this is certainly not the case for neurons. We use methionine-free Hibernate A supplemented with B27 for neurons and found that leaving out B27 already for short incubations compromises the neurons. We recommend to test if cells tolerate the incubation conditions of choice before performing a metabolic labeling experiment.

When adjusting the incubation conditions for FUNCAT experiments in microfluidic chambers, factors that might be critical and have to be controlled for are e.g. extracellular and intracellular diffusion of drugs or amino acid analogs, uptake capacity of the respective cellular compartment for AHA (neurites of different neuron types might have different amino acid transporter densities) and the time needed for newly synthesized proteins to reach their final destination. From our experience it is crucial to control every microfluidic chamber for the quality of the cultured neurons and assure that dendrites and axons populate the microgrooves evenly without any cell debris clogging the microgrooves.

When combining this protocol with FISH any source of RNase contamination should be avoided after the fixation step. Click reaction time, blocking steps and antibody incubation steps can be shortened. Of note, we do not use proteinase K treatment in this FISH protocol (in contrast to the manufacturer's recommendation). We avoid proteinase K in order to preserve the integrity of newly synthesized proteins and enable the combination with immunocytochemistry. The procedure leads to clear and highly localized *in situ* signals with every antisense probe set we used so far.

Anticipated Results

Application of the protocols should result in fluorescent labeling of cells and tissue that is clearly distinguishable from background labeling as assessed with a methionine-incubated control or when compared to a sample treated with AHA in presence of a protein synthesis inhibitor. Typical example results with immunostaining are shown in Figures 4 and 5. In our experience we face detection limits in hippocampal neurons when we lower concentrations of AHA to less than 100 μM or limit incubation times to less than 10 minutes. These limits depend on the cell types used and should be analyzed by comparison with the respective controls.

Time Considerations

The basic protocol is usually accomplished within 2 days. One day is needed for metabolic labeling with the exact length depending on the incubation time. Fixation, blocking and preparation for the FUNCAT reaction need approximately 2 hrs. The click reaction itself is carried out overnight but can – with concomitant loss of signal intensity - be shortened to few hours. The next day optional immunocytochemistry requires an additional ~5 hrs. If FISH (support protocol) is included in the procedure the first day includes after metabolic labeling (depending on desired time), fixation and permeabilization (approximately 1 hr in total) a 3 hr probe set hybridization. Next, the protocol has an overnight storage step that can be omitted. The remainder of the FISH protocol is accomplished in 4 hrs (3 hrs of them incubation time) before switching back to the FUNCAT basic protocol (FUNCAT reaction mix incubation).

The alternate protocol 1 (FUNCAT in hippocampal slices) is carried out within 3 days. The most time-consuming part compared to the other protocols is the re-sectioning of the agarose-embedded slices on day 1 which takes approximately 1 hour per slice.

Alternate protocol 2 (FUNCAT in larval zebrafish) needs longer incubations to assure penetration of reagents into the whole organism. The whole protocol from metabolic labeling to immunohistochemistry needs one week.

Alternate protocol 3 (FUNCAT in microfluidic chambers) is comparable in time to the basic protocol.

Acknowledgement

Research is supported by the German Research Foundation DFG, DFG DI1512/1-1 and DFG DI1512/2-1 to DCD.

Literature Cited

- Agard, N.J., J.A. Prescher, and C.R. Bertozzi. 2004. A strain-promoted [3 + 2] azide-alkyne cycloaddition for covalent modification of biomolecules in living systems. *Journal of the American Chemical Society*. 126:15046-15047.
- Beatty, K.E., J.D. Fisk, B.P. Smart, Y.Y. Lu, J. Szychowski, M.J. Hangauer, J.M. Baskin, C.R. Bertozzi, and D.A. Tirrell. 2010. Live-cell imaging of cellular proteins by a strain-promoted azide-alkyne cycloaddition. *Chembiochem : a European journal of chemical biology*. 11:2092-2095.
- Beatty, K.E., J. Szychowski, J.D. Fisk, and D.A. Tirrell. 2011. A BODIPY-cyclooctyne for protein imaging in live cells. *Chembiochem : a European journal of chemical biology*. 12:2137-2139.
- Beatty, K.E., and D.A. Tirrell. 2008. Two-color labeling of temporally defined protein populations in mammalian cells. *Bioorg Med Chem Lett*. 18:5995-5999.
- Chalfie, M., Y. Tu, G. Euskirchen, W.W. Ward, and D.C. Prasher. 1994. Green fluorescent protein as a marker for gene expression. *Science*. 263:802-805.
- Cox, J., and M. Mann. 2011. Quantitative, High-Resolution Proteomics for Data-Driven Systems Biology. *Annu Rev Biochem*. 80:273-299.
- Dieterich, D.C. 2010. Chemical reporters for the illumination of protein and cell dynamics. *Curr Opin Neurobiol*. 20:623-630.

- Dieterich, D.C., J.J. Hodas, G. Gouzer, I.Y. Shadrin, J.T. Ngo, A. Triller, D.A. Tirrell, and E.M. Schuman. 2010. In situ visualization and dynamics of newly synthesized proteins in rat hippocampal neurons. *Nat Neurosci.* 13:897-905.
- Dieterich, D.C., J.J. Lee, A.J. Link, J. Graumann, D.A. Tirrell, and E.M. Schuman. 2007. Labeling, detection and identification of newly synthesized proteomes with bioorthogonal non-canonical amino-acid tagging. *Nat Protoc.* 2:532-540.
- Dieterich, D.C., and A.J. Link. 2009. Click Chemistry in Protein Engineering, Design, Detection and Profiling. *In Click Chemistry for Biotechnology and Materials Science.* J. Lahann, editor. John Wiley & Sons. 309-325.
- Dieterich, D.C., A.J. Link, J. Graumann, D.A. Tirrell, and E.M. Schuman. 2006. Selective identification of newly synthesized proteins in mammalian cells using bioorthogonal noncanonical amino acid tagging (BONCAT). *Proc. Natl. Acad. Sci.* 103:9482-9487.
- Heim, R., D.C. Prasher, and R.Y. Tsien. 1994. Wavelength mutations and posttranslational autooxidation of green fluorescent protein. *Proc Natl Acad Sci U S A.* 91:12501-12504.
- Hinz, F.I., D.C. Dieterich, D.A. Tirrell, and E.M. Schuman. 2012. Noncanonical Amino Acid Labeling in Vivo to Visualize and Affinity Purify Newly Synthesized Proteins in Larval Zebrafish. *Acs Chem Neurosci.* 3:40-49.
- Hu, Y., X. Huang, G.Y. Chen, and S.Q. Yao. 2004. Recent advances in gel-based proteome profiling techniques. *Molecular biotechnology.* 28:63-76.
- Kanai, Y., H. Segawa, K. Miyamoto, H. Uchino, E. Takeda, and H. Endou. 1998. Expression cloning and characterization of a transporter for large neutral amino acids activated by the heavy chain of 4F2 antigen (CD98). *The Journal of biological chemistry.* 273:23629-23632.
- Klick, K.L., E. Saxon, D.A. Tirrell, and C.R. Bertozzi. 2002. Incorporation of azides into recombinant proteins for chemoselective modification by the Staudinger ligation. *P Natl Acad Sci USA.* 99:19-24.
- Link, A.J., M.K. Vink, and D.A. Tirrell. 2007. Preparation of the functionalizable methionine surrogate azidohomoalanine via copper-catalyzed diazo transfer. *Nat Protoc.* 2:1879-1883.
- Madison, D., and E.B. Edson. 2001. Preparation of Hippocampal Brain Slices. *In Current Protocols in Neuroscience.* John Wiley & Sons.
- Ngo, J.T., J.A. Champion, A. Mahdavi, I.C. Tanrikulu, K.E. Beatty, R.E. Connor, T.H. Yoo, D.C. Dieterich, E.M. Schuman, and D.A. Tirrell. 2009. Cell-selective metabolic labeling of proteins. *Nat Chem Biol.* 5:715-717.

- Player, A.N., L.P. Shen, D. Kenny, V.P. Antao, and J.A. Kolberg. 2001. Single-copy gene detection using branched DNA (bDNA) in situ hybridization. *J Histochem Cytochem.* 49:603-612.
- Prescher, J.A., and C.R. Bertozzi. 2005. Chemistry in living systems. *Nat Chem Biol.* 1:13-21.
- Roche, F.K., B.M. Marsick, and P.C. Letourneau. 2009. Protein synthesis in distal axons is not required for growth cone responses to guidance cues. *J Neurosci.* 29:638-652.
- Rostovtsev, V.V., L.G. Green, V.V. Fokin, and K.B. Sharpless. 2002. A stepwise Huisgen cycloaddition process: copper(I)-catalyzed regioselective "ligation" of azides and terminal alkynes. *Angew Chem Int Ed Engl.* 41:2596-2599.
- Taylor, A.M., D.C. Dieterich, H.T. Ito, S.A. Kim, and E.M. Schuman. 2010. Microfluidic local perfusion chambers for the visualization and manipulation of synapses. *Neuron.* 66:57-68.
- Tcherkezian, J., P.A. Brittis, F. Thomas, P.P. Roux, and J.G. Flanagan. 2010. Transmembrane receptor DCC associates with protein synthesis machinery and regulates translation. *Cell.* 141:632-644.
- Tornøe, C.W., C. Christensen, and M. Meldal. 2002. Peptidotriazoles on solid phase: [1,2,3]-triazoles by regioselective copper(I)-catalyzed 1,3-dipolar cycloadditions of terminal alkynes to azides. *The Journal of organic chemistry.* 67:3057-3064.

Figure Legends

Fig 1 FUNCAT strategy and protocol overview. The flow chart summarizes the steps of the protocols provided and indicates protocol choice points. Alternatives and options mentioned in the text, but not extensively described, are included to indicate potential extensions (light gray).

Fig 2 Special reagents and materials described in the FUNCAT protocols. (A) FUNCAT incubation plate made from a 24-well cell culture plate with paraffin drops for upside-down incubation of circular coverslips. (B) Tube-lid support filled with modeling clay and sealed with two-component epoxy glue for upside-down incubation of MatTek glass-bottom dishes. (C) Standard microfluidic chamber for compartmentalized neuron incubation. Neurons are plated on the cell body chamber side through the connected wells 1. They extend axons and dendrites into the microgrooves but only axons grow the whole 900 μm distance through the microgrooves and reach the axon chamber that is accessible via the connected wells 2. Dendrites usually stop growing at a 200-300 μm distance within the microgrooves. The cell body and axon chamber can be fluidically isolated and, therefore, compartments can be incubated with different solutions. (D) The microfluidic Local Perfusion (μLP) version of the microfluidic chamber has a perfusion channel perpendicular to the microgrooves (Taylor et al., 2010). It is located at a distance from the cell body chamber where dendrites still populate the microgrooves. Thus, perfusion via the perfusion channel allows one to manipulate selectively a proportion of dendrites and axons. (E) The microfluidic chambers are assembled on coverslips where the cells attach. After metabolic labeling, the PDMS part of the chamber is removed and the cells are fixed and processed further on the coverslip. Upside-down incubation for the click reaction is performed on Parafilm with unilateral silicone spacer support in a humidified chamber.

Fig 3 FUNCAT – chemistry and principle. (A) The chemical structures of the non-canonical amino acids AHA (azide-bearing) and HPG (alkyne-bearing) are similar to Methionine (Met). A variety of azide- or alkyne-functionalized fluorophores (A) are available to covalently ligate a fluorophore to the non-canonical amino acids by Cu(I)-catalyzed azide + alkyne [3+2]-cycloaddition (B). The Cu(I) catalyst is produced in the reaction mixture from Cu(II) and TCEP and is stabilized by the triazole ligand. (C) Explanation of FUNCAT procedure steps during metabolic labeling and click reaction.

Fig 4 Example results. Representative FUNCAT experiments in (A) COS7 cells, (B) glial cells, (C) cultured hippocampal neurons and (D) acute hippocampal slices using different fluorescent

tags. (A) COS cells incubated with 4 mM AHA for 1 hr, clicked to Alexa594-alkyne, labeled for actin with Alexa488-phalloidin and DAPI to stain nuclei. In the presence of the protein synthesis inhibitor anisomycin (40 μ M) the FUNCAT signal is significantly reduced (present only at low levels in the nucleus) and when AHA is replaced by Met no FUNCAT signal is visible. (B) Primary astrocytes treated with 4mM AHA, clicked to TxRed-alkyne and stained for GFAP (2 left panels) and the respective anisomycin control (two right panels). (C) Increasing the duration of 4 mM AHA incubation increases the FUNCAT signal (AHA, Tamra-alkyne and Met control) in hippocampal neurons stained for the neuron marker MAP2 and the presynaptic protein synaptophysin. FUNCAT signal (as fire lookup table in lower panel) is clearly visible in soma and dendrites after 2 hrs. After 6 hrs there is also ample labeling of synaptic sites. (D) Micrograph of area CA1 from a FUNCAT experiment in an acute hippocampal slice incubated for 4 hrs with 4 mM AHA (left panel) and clicked to Alexa488-alkyne and the respective Met control (right panel). For better visual orientation slices are stained with the neuron marker MAP2. DAPI labeling in the AHA slice shows that the FUNCAT signal in pyramidal cells is higher than in other cells dispersed in the neuropil layer. Scale bars 20 μ m (A), 10 μ m (B,C), 100 μ m (D).

Fig 5 Expected results. (A) FUNCAT in whole 7 dpf zebrafish larvae after 72 hrs AHA labeling was combined with antibody labeling for parvalbumin. A dorsal view of the head of larvae incubated without (ctrl) and with 4 mM AHA, clicked to Alexa594-tag and stained for parvalbumin shows the specificity and low background of the FUNCAT labeling (A, left panel). Higher magnifications of different regions – a lateral view of the spinal cord (s, Alexa594-tag), dorsal view of the cerebellum (cb, Alexa488-tag) and a lateral view of the pectoral fin (pf, Alexa488-tag) show that within the tissue cell populations show differences in FUNCAT signal and can be identified by antibody staining. (B,C) Application of 4 mM AHA for 2 hr via the perfusion channel (pc) in a μ LP chamber (B) or 1 hr via the axon chamber (ax) of a microfluidic chamber without perfusion channel (C). Both conditions lead to signal in the cell body compartment (cb) in the soma of cells (cb) that send neurites to the respective compartment indicating that axons and dendrites are capable of AHA uptake. MAP2 positive cells (B) that do not extend dendrites through the microgrooves (mg) to the perfusion channel (pc) are not intensely labeled. In a well-grown chamber culture usually around 30 - 50 % of the neurons in a distance of 150 μ m from the microgrooves are labeled when AHA is loaded from the perfusion channel. (D) High resolution FISH for Rab1 mRNA combined with FUNCAT in a hippocampal neuron. After FISH the click reaction was performed for only 2 hrs instead of overnight for

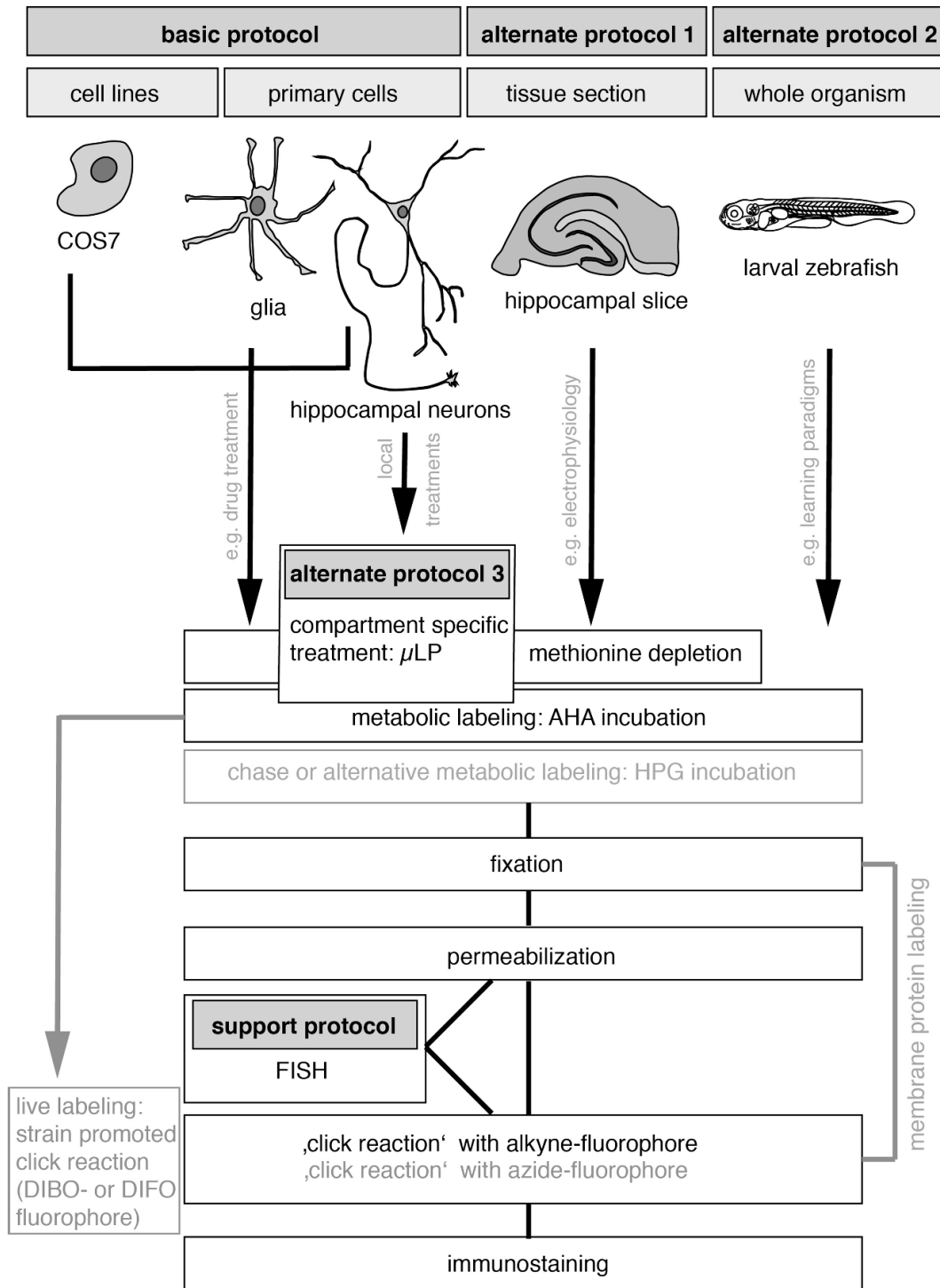
maximal preservation of the FISH signal. (E) Fluorescent precipitates (arrow) appear in the samples and make analysis difficult when the FUNCAT click reaction is not performed overhead or grease from sealing the MatTek dishes on the incubation support during overhead click reaction spills to the sample. Scale bars 100 μm (A, left panel), 25 μm (A, other panels), 20 μm (B, D), 50 μm (C).

Tables

Table 1 Troubleshooting

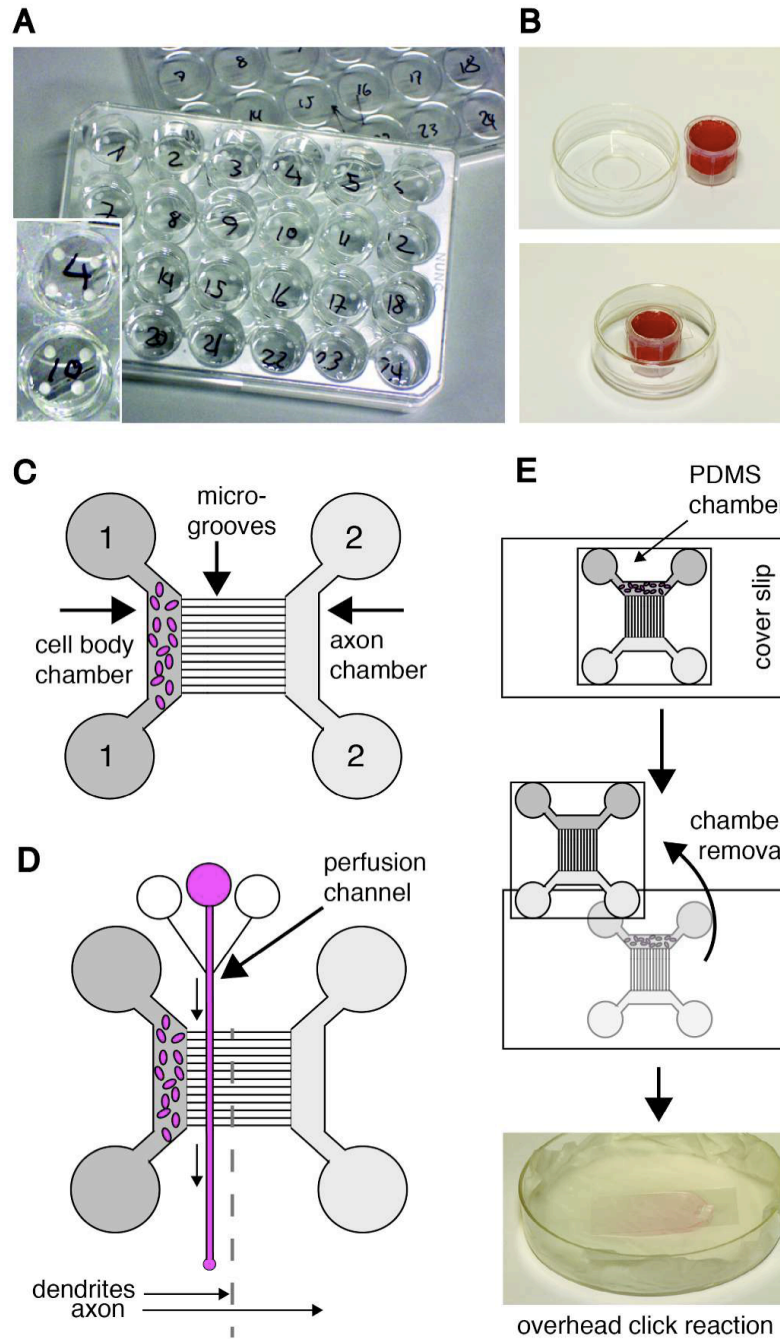
problem	cause	potential solution
no or low FUNCAT signal	no alkyne-azide reaction	<i>make sure that you use an alkyne-bearing fluorophore for ligation to AHA and azide-bearing fluorophores for ligation to HP</i>
	pH of click reaction mix	<i>click reaction works best with a slightly basic pH of 7.6-7.8</i>
	click reaction reagents added in the wrong order to the reaction mix	<i>it is critical to add the reagents in the correct order, quickly and with vigorous vortexing</i>
	fluorophore bleaching	<i>starting with the assembly of the FUNCAT reaction mixture, protect both the mixture and samples from light</i>
	TCEP not working, no Cu(I) formation	<i>dissolve TCEP immediately prior to reaction assembly – if this doesn't help purchase a new batch of TCEP</i>
	fluorescent tag stock solution not properly dissolved	<i>always use fresh and preferably unopened DMSO to prepare the fluorescent tag stock solution. If the solution is not immediately clear upon dissolving in DMSO it is unusable</i> <i>store tag in aliquots at -20 °C, don't freeze-thaw more than 3 times</i>
	triazole ligand not working	<i>always use fresh and preferably unopened DMSO to prepare the ligand stock solution. The ligand solution should become clear and with a light yellow color after vortexing.</i> <i>store small aliquots of the dissolved ligand at -20 °C, don't freeze-thaw more than 3 times</i>
high background signal in methionine or protein synthesis inhibitor controls	non-specific binding of fluorescent tag	<i>block unreacted aldehyde groups from PFA fixation with 0.1M glycine in PBS</i> <i>block other unspecific binding sites with a BSA-containing blocking buffers prior to FUNCAT reaction</i> <i>increase the number and duration of washing steps</i> <i>try a different fluorescent tag</i> <i>synthesize the fluorescent tag with water soluble polyethylene glycole linker</i>
	protein synthesis inhibitor not working	<i>store in aliquots at -20 °C, don't freeze-thaw more than 3 times, if this doesn't help use new batch</i>
	autofluorescence of tissue/cells	<i>try a different fluorescent tag</i>
fluorescent precipitates form	copper/tag precipitate from click reaction	<i>it is critical to add the reagents in the correct order, quickly and with vigorous vortexing; also prewarm the reagents to RT</i> <i>carry out click reaction upside down at RT</i> <i>filter reaction mix through 0.22 µm filter</i> <i>decrease CuSO₄ concentration (perform dilution series)</i>
	Leaking grease from sealing support chambers	<i>take care that no excess grease is used to seal the Matek dish on the support and avoid spills into the incubation solution, use less or no grease, incubate instead in humidified chamber</i>

FISH signal not visible	RNA degradation	<i>use RNase free reagents</i> <i>shorten incubation times, e.g. perform click reaction for only 2 hrs instead of overnight</i>
	background from FUNCAT signal	<i>change combination of fluorophores for FISH and fluorescent tag</i>



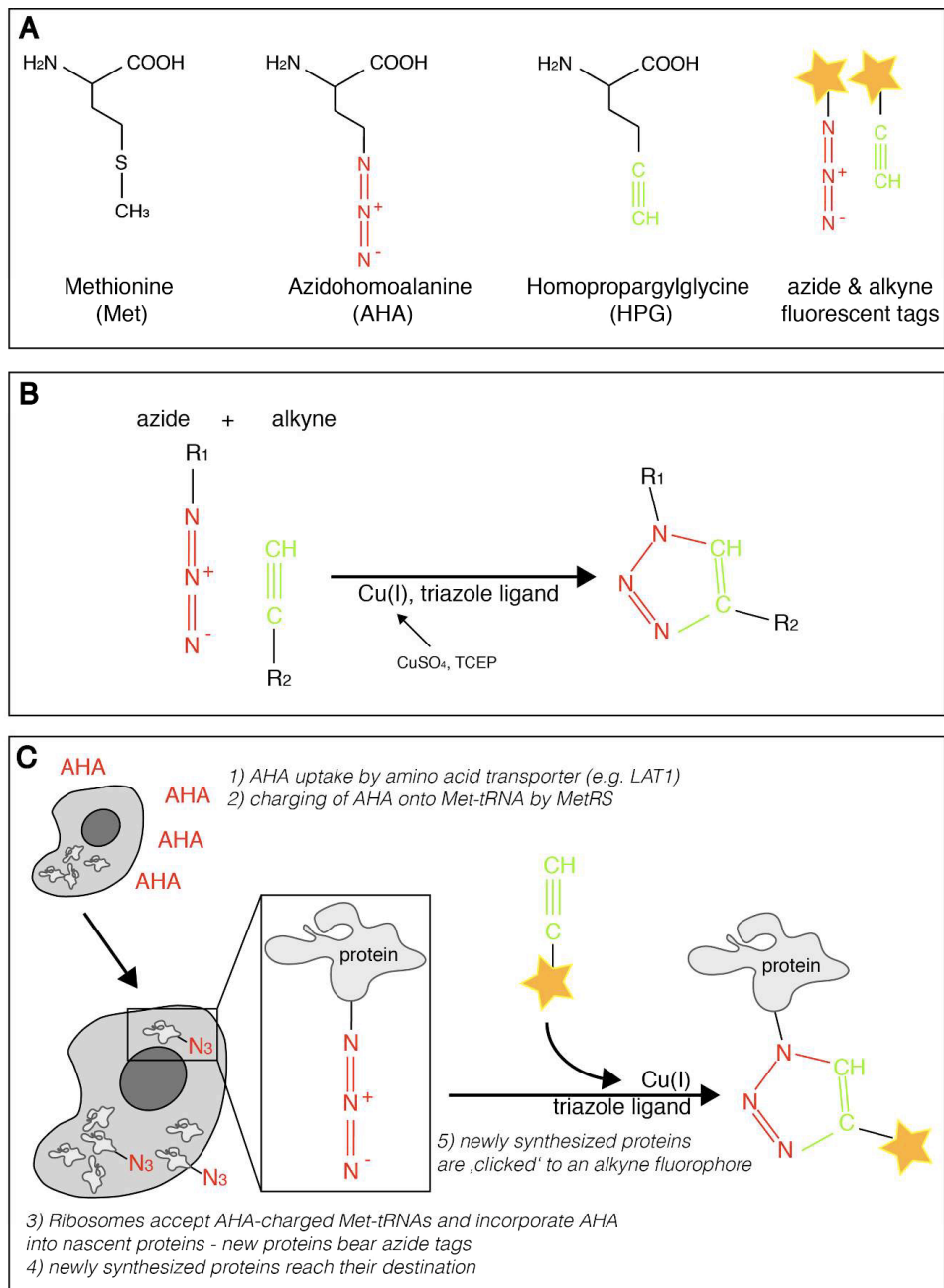
FUNCAT_Fig1_overview-strategic planning

835x1198mm (72 x 72 DPI)



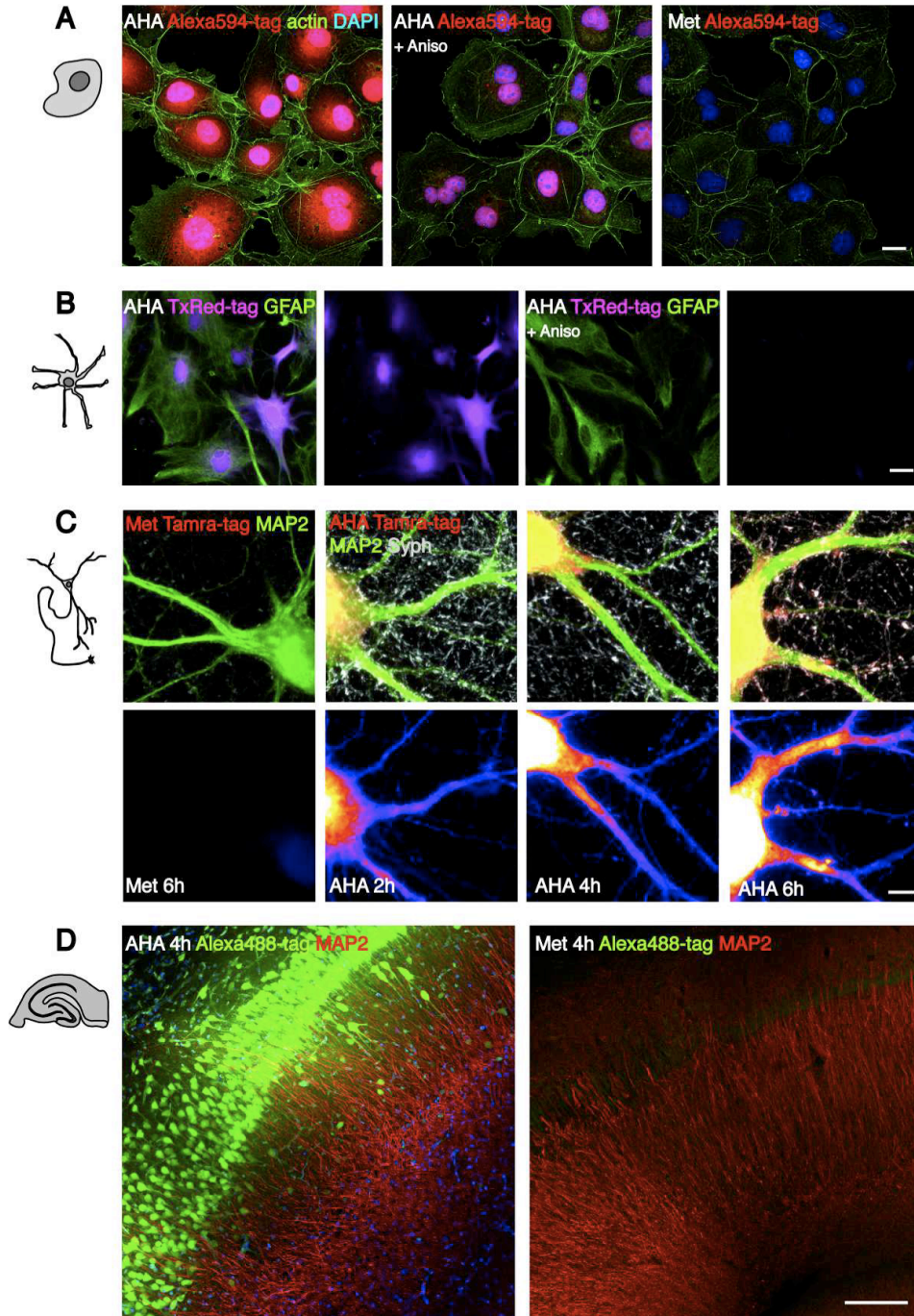
Funcat_Fig_2 material

699x1168mm (72 x 72 DPI)



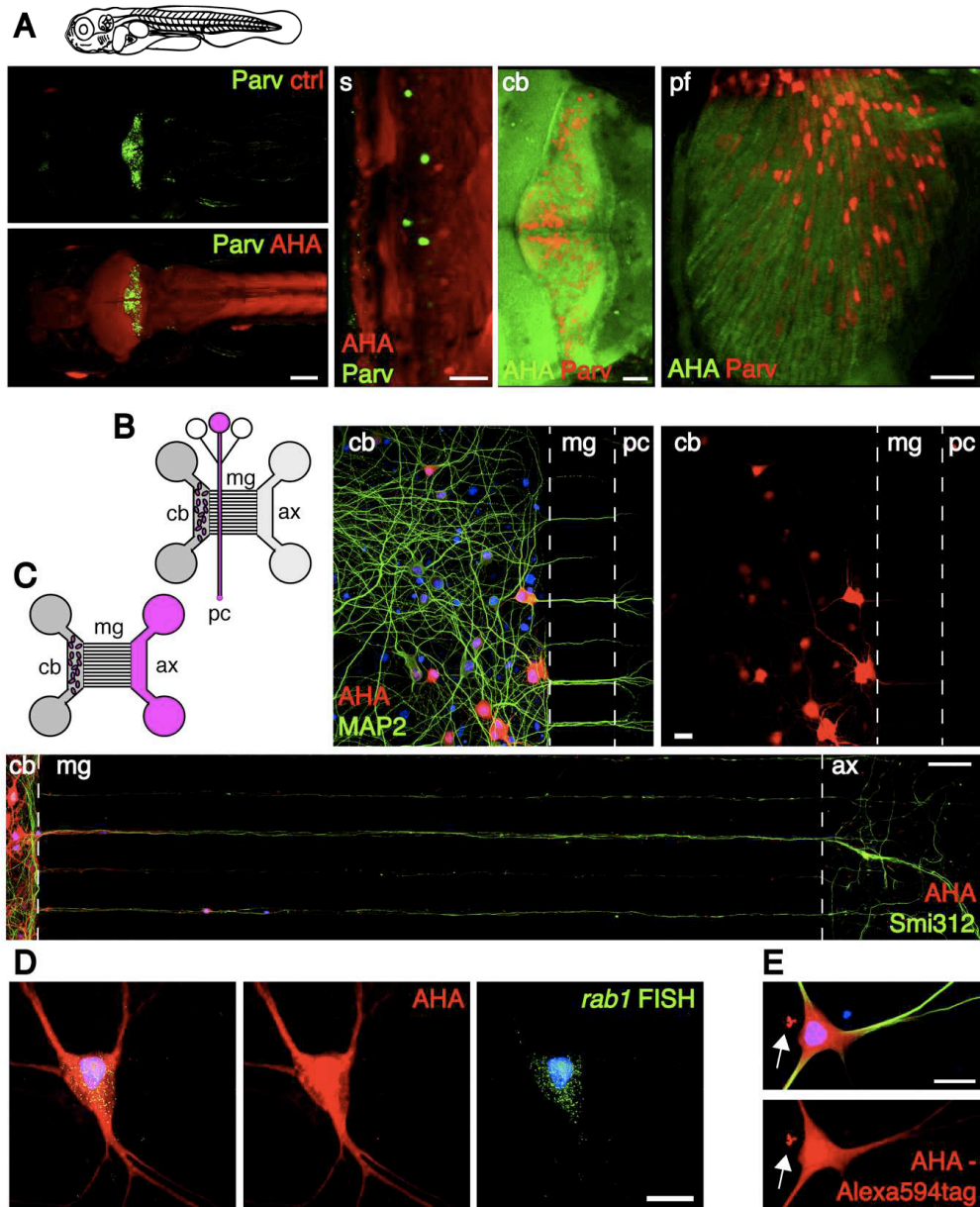
FUNCAT_Fig 3_chemistry-background

868x1233mm (72 x 72 DPI)



FUNCAT_Fig4_examples

180x278mm (300 x 300 DPI)



Funcat_Fig_5 expected results and trouble shooting

180x237mm (300 x 300 DPI)